Preparation and Characterisation of Alginate Composite Beads and Investigations into their Potential Use in Environmental Applications

A thesis submitted to the National University of Ireland in fulfillment of

the requirements for the degree of

Doctor of Philosophy

By

Louise Ann Gallagher

NUI MAYNOOTH

Ollscoil na hÉireann Má Nuad

Department of Chemistry,
Faculty of Science and Engineering,
National University of Ireland Maynooth,
Maynooth,
Co. Kildare,
Ireland.

August 2012

Research Supervisors: Dr. Denise Rooney and Prof. Carmel Breslin

Head of Department: Dr. John Stephens

Table of Contents

Declaration of Authorship

I hereby certify that this thesis has not been submitted before, in whole or in part, to this or any other university for any degree and is, except were stated, the original work of the author.

Signed: _____ Date: _____

Louise Gallagher, B.Sc.

Acknowledgements

The completion of this thesis would not have been possible without the guidance and the help of several individuals who in one way or another contributed and extended their valuable assistance in the preparation and completion of this study. I therefore take this opportunity to thank the many people who have helped me along this journey.

First and foremost I would like to sincerely thank my two supervisors, Dr. Denise Rooney and Professor Carmel Breslin. Thank you both for your patience and encouragement throughout my study in NUIM. Special thanks to Denise for your never-ending help, advice and friendship on a daily basis over the past number of years, without which, this thesis would not have been possible. I would also like to thank Dr. Malachy McCann and Dr. Kevin Kavanagh for the use of their biological labs and also for their expert help and time spent working with me on this project.

I would like to express my sincere gratitude to Dr. John Stephens, the current head of Department and also to Professor John Lowry, the former head of Department for giving me the opportunity to pursue my Ph.D. Also, I would like to thank Sligo County Council and the Department of Agriculture, Fisheries and Food for financial support.

I also must thank all of the staff of the Chemistry Department, particularly to the technicians and the Executive Administrators, for their assistance at all stages of this project. In particular I would like to thank Ollie for all her help with the SEM. A special mention must go to Noel for making my bead producing machine without which this project would not have been possible, and also for keeping me and my 'prehistoric' laptop going throughout the last few years, you have always been there to help despite the hassle and extra work I must have caused.

Thanks to all the postgrads and postdocs, both past and present (there are too many of you to name!). You have all provided a friendly work environment and I have thoroughly enjoyed the many conversations, laughs and nights out that we have had together. Special thanks to the girls in the synthesis lab: Trish, Carol, Alanna Niamh and Laura, and also to the girls in the electrochemistry lab: Urusla, Orla and Emer for their friendship, support, encouragement over the last few years. I would also

like to say thanks to Collette and Catherine for all the proof reading!! An extra special mention goes to Wayne, for the unending cups of tea!!!, the chats, the frights, the countless number of shots we shared on nights out. My life has been a constant rollercoaster since we met and without a doubt you have been a great source of entertainment and a great friend, and for that I thank you.

To Pauraic, thank you for your patience and encouragement over the last number of years but especially through-out my thesis writing period, I know it hasn't been easy!! You have been a great support and I would have been lost without you. Thank you for always finding some way to make me laugh and distract me when I was stressed and for that I genuinely thank you.

Outside my life in Maynooth I have also received support and help along the way which I must mention. To my parents, Gerard and Geraldine and my grandmother, Nora, I thank you from the bottom of my heart as none of this would have been possible without you. To my brothers Gerard and Anthony, and my sisters Lisa, Claire and Yvonne, thanks for all your support over the last few years. A special mention to Lisa, whom I am especially grateful, you were always there to listen to me, offer encouragement and most importantly keep me sane. Thanks for all the laughs, shopping and babysitting over the years, I wouldn't be where I am today without all of your help. To my nephew Keelan and niece Chelesa, who have the constant ability to always make the world seem like a brighter place, thank you!!! To my friends from home: Sandra, Martina and Anne Maire, thanks for always been there for me over the years. Special thanks goes to Sandra, who never let a Christmas go by without remembering us and I also want to thank the friends I made as an undergrad especially Theo who deserves a special thanks for always being there to listen to me complain. Thank you.

Last but by no means least I must thank my sons, Jordan and Jamie. You have been with me from the start of this journey, you have put up with me through thick and thin, in good times and in bad and I thank you wholeheartedly for all the love and support, for always making me smile and giving me hope when things seemed impossible. It is because of both of you that I am where I am today and to you I dedicate this thesis.

To Jordan and Jamie,

I dedicate this to you,

Thank You.

List of Abbreviations

µl	Microlitre
Ag	Silver
Alg	Alginate
ANOVA	Analysis of Variance
Ca^{2+}	Calcium Ions
$CaCl^2$	Calcium Chloride
CNBr	Cyanogen Bromide
COOH	Carboxylic Acid
Cu(II)	Copper Ions
DCC	N,N'-dicyclohexylcarbodiimide
DMAP	4-(N,N-dimethylaminopyridine)
EDC	1-ethyl-3-(3-dimethylaminopropyl) carbodiimide
EDC-HCl	1-ethyl-3-(3-dimethylaminopropyl) carbodiimide Hydrochloride
EDX	Energy-Dispersive X-ray Spectroscopy
ESD	Equilibrium Swelling
$FeCl_3$	Iron(III) Chloride
FTIR	Fourier Transform Infrared Spectroscopy
G	Guluronic acid
H	Hydrogen
H_2O	Water
HAS	Human Serum Albumin
HCl	Hydrochloric Acid
HPLC	High-Performance Liquid Chromatography
M	Mannuronic Acid
Min	Minute
Ml	Milliliter
mM	Millimolar

Mn(II)	Manganese Ions
N_2O	Nitrous Oxide
NaCl	Sodium Chloride
$NaIO_4$	Sodium Periodate
NaOH	Sodium Chloride
NBPT	N-(n-butyl) thiophosphoric triamide
NBPTO	N-(n-butyl)phosphorictriamide
NH_3	Ammonia
NH_4^+	Ammonium
NHS	N-Hydroxysuccinimide
NMR	Nuclear Magnetic Resonance
NO_3^-	Nitrate
O_3	Ozone
OD	Optical Density
OH-	Hydroxide Ions
Pd	Palladium
PEG	Polyethylene Glycol
PGA	Propylene Glycol Alginate
SEM	Scanning Electron Microscope
TSA	3-(trimethoxysilyl)alky
UV/Vis	Ultraviolet-Visible Spectroscopy
W*d*	Dry Weight
W*s*	Swollen Weight
YEPD	Yeast Extract Peptone Dextrose

Abstract

The present research is concerned with the polymer sodium alginate, a naturally occurring biocompatible and biodegradable polysaccharide.

The first objective was to prepare, characterise and monitor the release properties of a urease inhibitor (NBPT) from different calcium alginate hydrogel beads. Four bead types were chosen for this study, calcium alginate, charcoal-loaded and bentonite-loaded calcium alginate, and polypyrrole-coated calcium alginate beads. The surface morphology of the beads was investigated using SEM. The swelling studies on the beads showed that the polypyrrole-coated calcium alginate beads showed the lowest amount of swelling in all media tested. The stability of the NBPT as a function of pH was investigated using NMR spectroscopy, which showed that NBPT decomposes at acidic and highly basic pH values. The release of NBPT into aqueous solutions was monitored using UV/Vis spectroscopy. Release was uncontrolled if beads were agitated and was significantly slowed down when they were not agitated. The bentonite-loaded and polypyrrole-coated calcium alginate beads showed the most promising results for developing a controlled release system for NBPT.

The second objective was to assess the ability of alginate beads, which contained silver(I) and silver(0), to inactivate pathogenic microorganisms in a water treatment process. The three different bead supports used were sodium alginate beads (Alg), propylene glycol alginate composite beads (PGA) and alginate beads functionalised with propyloctadecyldimethylammonium groups (TSA beads). Atomic absorption spectroscopy was used to assess the amount of silver encapsulated in the beads. Swelling studies in water indicate that the TSA beads were resistant to swelling. The beads were studied for their ability to inhibit the growth or kill one strain of fungi and five strains of bacteria. The TSA beads that contained silver(I) showed the greatest antimicrobial activity against the six micro-organisms studied, making them the most attractive polymer support, for use in materials for water disinfection.

Chapter 1:

Introduction and Literature Review

1.1 Introduction

The Industrial Revolution resulted in a significant change in the daily lives of humans and this has led to a modern society that is heavily dependent on fossil fuels for transportation, and energy. The fossil fuel of particular importance to modern society is oil. Oil is primarily used as a transportation fuel and most countries are now highly dependent upon oil. Moreover, as well as being a source of energy, oil forms the basis of the petrochemical industry.[1] Due to rapid economic growth in the developing world and modern society's high reliance upon motor transportation, demand for oil has grown and is likely to continue. This causes problems in providing sufficient quantities of oil. Oil is not considered to be a renewable resource, it takes millions of years to form and there are a finite number of oilfields. In recent years the discovery rates of new oilfields have been falling, resulting in reserves being quickly depleted and it is predicted that oil will run out in about 70 years.[1]

There are a number of problems associated with converting fossil fuels to energy, such as air and water-pollution. One major problem with fossil fuels is that burning them has led to large emissions of greenhouse gases.[2] There is much scientific evidence to suggest that these greenhouse gases have led to global warming.[3-5] When coal is burned it releases nitrous oxide and carbon dioxide, both of which are greenhouse gases.[6] The impact of global warming on the environment is extensive and affects many areas.

Chemistry's response to the reliance of the chemical industry on oil as a starting material is to look to sustainable chemistry. Sustainable chemistry involves the design of products and processes that minimise the use and generation of hazardous substances.[7] This fulfils one of the principles of Green Chemistry as outlined in the book Green Chemistry: Theory and Practice.[8] "*A raw material feedstock should be renewable rather than depleting whenever technically and economically practical*". In particular, chemistry is looking at chemical processes based on renewable resources such as biopolymers and chemical products that enhance the efficiency of synthesis of the products.[9] Chemicals from renewable resources have attracted an increasing amount of attention over the past two decades predominantly due to two major reasons: firstly environmental concerns, and

secondly the realisation that our petroleum resources are limited.[9] As a major component of petroleum consumption is used to form synthetic polymers, this has led to an increase in research to discover new polymer material based on biological feed stocks.

Research is now focused on renewable resources to produce natural polymers for applications in which synthetic polymers have previously been used.[9-11] A major disadvantage with using polymers from natural resources is their fast degradation rate which is not always desirable. Yu *et al.* discuss the use of polymer blends to overcome some of the disadvantages associated with using biodegradable polymers obtained from natural resources alone.[9] Starch and cellulose are two examples of important natural polymers that are receiving a lot of attention. Khalili *et al.* demonstrate the ability of cellulose to replace man-made fibres as reinforcement to make environmentally friendly green products.[11] Another important natural polymer is chitosan, which is a renewable abundant material. Chitosan already has many applications such as controlled-release agents, ingredients in cosmetics and personal care products, and biodegradable food packaging. Chitosan has the ability to be used as an environmental friendly starting material for packaging in which water resistance is necessary, as shown by Cui *et al.*[10] Alginate is an abundant material which is readily available in nature. It is found as a structural component of brown algae and it is also isolated from some bacterial species.[12] Alginate offers many advantages over synthetic polymers as it forms hydrogels and it is non-toxic, biocompatible, biodegradable, less expensive and freely available. All these advantages make alginate a very useful material for biomedical application, especially for controlled delivery of drugs[13] and other biologically active compounds.[14]

1.2 Biopolymers

Polymers are compounds with a high molecular weight consisting of up to millions of repeated linked units that are relatively light and simple. They are built up from simple 'monomers' or single parts.[15] Carbohydrates are organic compounds that consist only of carbon hydrogen and oxygen. Carbohydrates (saccharides) are divided into four chemical groups: monosaccharaides, disaccharides,

oligosaccharides and polysaccharides. In general monosaccharaides and disaccharides which are smaller carbohydrates are referred to as sugars.[16] Monosaccharaides can be linked together by glycosidic bonds to form polysaccharides. Most polysaccharides have hundreds or thousands of simple sugar units linked together to form long polymer chains. They are a class of biopolymer, or naturally occurring polymers.[15] Biopolymers are polymers produced by living organisms that have unique structures, multidimensional properties, highly sophisticated functions and wide ranging applications in biomedical and industrial areas.[17,18] To exploit the unique properties and to realise the full potential of these versatile polymers, research and development work on biopolymers has reached a status of intense activity in many parts of the world.[19] Some important examples of carbohydrate biopolymers are outlined below.

Cellulose (Figure 1.1), a polymer of D-glucose, is the world's most abundant organic material. It is a straight chain polymer composed of D-glucose units linked by equatorial β-(1,4')-glycosidic bonds which are rigid and very stable, giving cellulose desirable properties for a structural material in organisms.[16]

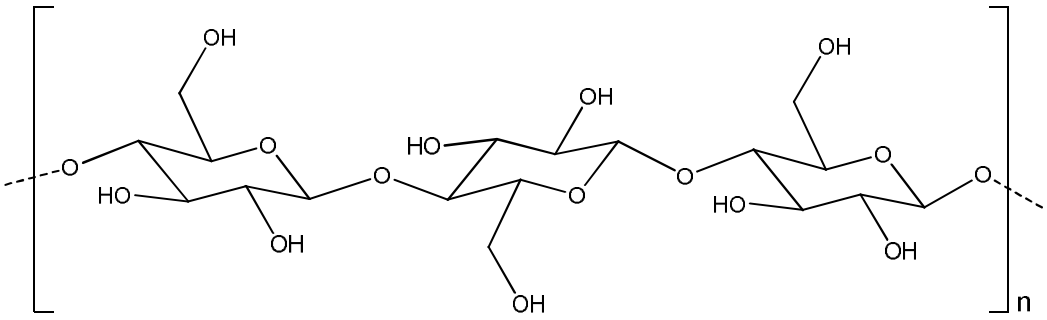

Figure 1.1: Structure of cellulose.

Cellulose is abundant in trees and other plants as a structural material to support the weight of the plant. Wood and straw consist of 50% of the polysaccharide. Cellulose is biodegradable but is insoluble in water and most organic solvents which limit its potential applications. However, functionalised cellulose derivatives have been studied and utilised for a long time. Cellulose nitrate has long been one of the world's most popular explosives. The properties of cellulose derivatives are determined primarily by the type of functional group they

contain. They can be modified by adjusting the degree of functionalisation and the degree of polymerisation of the polymer backbone.[20]

Starch (Figure. 1.2) is a polymeric carbohydrate consisting of anhydroglucose units linked together primarily through α-D-(1,4')-glycosidic bonds.[21] The anhydroglucose unit consists of two types of molecules; amylose (normally 20–30%) and amylopectin (normally 70–80%). In amylose these are α-D-(1,4')-glycosidic bonds whereas, in amylopectin about one residue in every twenty or fifty is also α-D-(1,6') glycosidic bonds forming a branch point.[22] Starch granules are synthesised by many plant tissues and act as an energy store. Different plants produce variations in starch granule parameters such as shape, size and composition. In addition, starch may be chemically, enzymatically or physically modified to induce novel characteristics.[23] Starch has proven popular in sustainable chemistry as it is versatile, cheap and has many uses as a thickener, water binder, emulsion stabiliser and a gelling agent.[22]

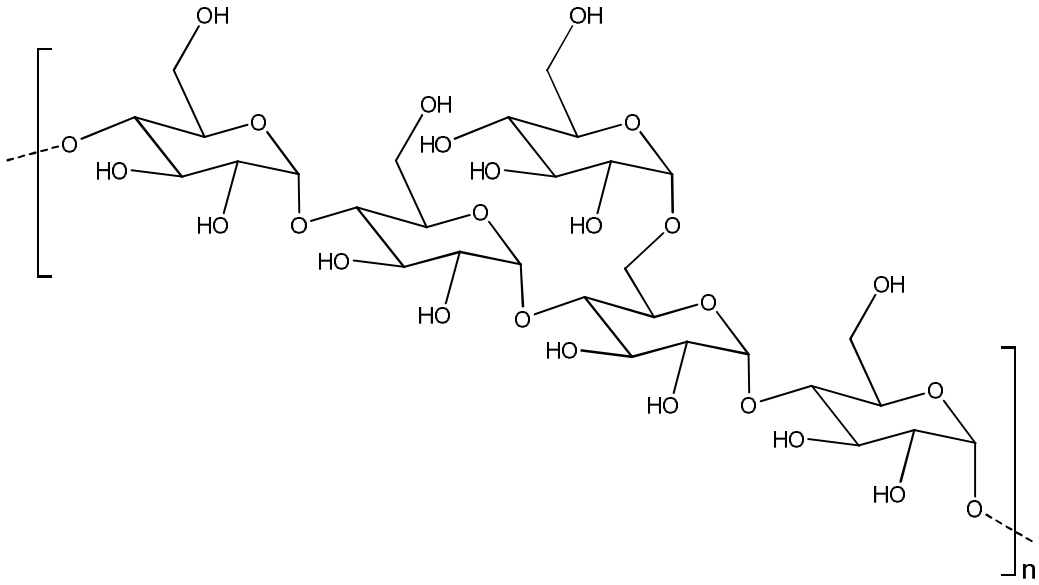

Figure 1.2: Structure of starch.

Dextran is a water-soluble polysaccharide produced by bacteria from sucrose. Dextran consists mainly of α-(1,6') linked D-glucopyranose residues with a low percentage of α-(1,2'), α-(1,3') and α-(1,4') linked side chains.[24] The degree of branching depends on the source of dextran and may vary from 0.5 to 60%. Furthermore, the source of dextran determines the molecular weight distribution of

the polymers. Increasing the branching of the macromolecules decreases the water solubility of dextran.[25] Dextran is non-toxic and is therefore useful in medical applications as a blood plasma substitute.[24]

Chitin (Figure 1.3) is the second most abundant natural biopolymer in the world. It is held together by β-(1,4')glycosidic bonds. It is a polymer of *N*-Acetylglucosamine. *N*-Acetylglucosamine is an amino sugar that is common in living organisms. Chitin forms in the exoskeletons of insects such as butterflies and spiders.[26,27] In crustaceans, chitin forms a matrix that binds calcium carbonate crystals into the exoskeleton.[28] The glycosidic bonds in chitin give it a structural rigidity, strength and stability that exceed even that of cellulose.[15,] Owing to the semi-crystalline structure of chitin with extensive hydrogen bonding, the cohesive energy density, and hence the solubility parameters are very high and therefore causing it to be insoluble in all the usual solvents including deionised water.[29]

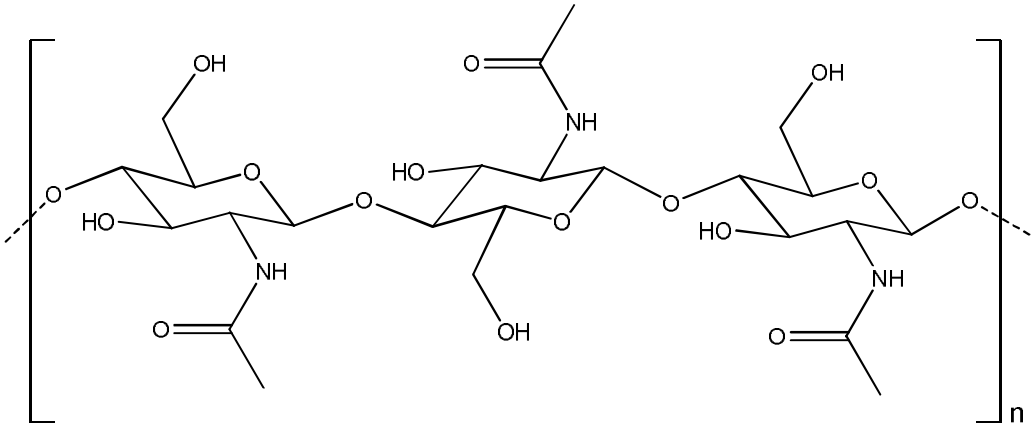

Figure 1.3: Structure of chitin.

However, chitosan (Figure 1.4) is produced by the de-acetylation of chitin and is readily soluble in dilute acid solutions below pH 6. At a low pH, chitosan becomes protonated and positively charged, which makes it a water-soluble cationic polyelectrolyte. On the other hand, as the pH increases above 6, the glucosamine units of chitosan become deprotonated and the polymer loses its charge and becomes insoluble. The ability to dissolve chitosan in dilute acid aqueous solutions, its properties such as biodegradability, low toxicity and good biocompatibility have led to a great deal of interest for its use in agricultural, medical and pharmaceutical applications.[30,31]

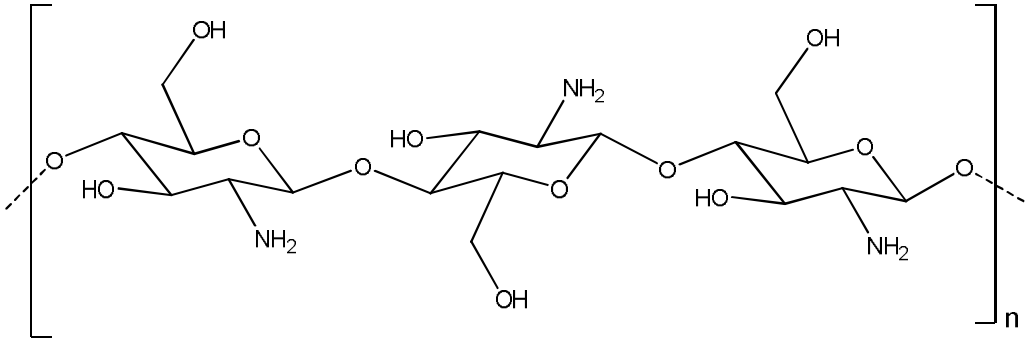

Figure 1.4: Structure of chitosan.

Alginate (Figure. 1.5) is a natural polymer extracted from the cell walls of brown algae. Alginate is also isolated from some bacterial species such as *Pseudomonas aeruginosa* and *Pseudomonas syringae.*[12] It is known to be biocompatible, non-toxic, non-immunogenic and biodegradable.[32] Alginic acid is a natural linear, anionic block co-polymer hetero-polysaccharide. Its structure contains monomers of β-D-mannuronic acid (M) and its C-5 epimer, α-L-guluronic acid (G) residues joined together by α-(1,4')-glycosidic linkages.[12] The G and M units are joined together in blocks and three types of blocks are found. It can be composed of homopolymeric blocks M–M or G–G, and blocks with an alternating sequence of M–G blocks. Sodium alginate salt has a unique property of cross-linking in the presence of multivalent cations, such as calcium ions in aqueous media which complex to form insoluble calcium alginate. Depending on the degree of cross-linking, alginate will significantly reduce its swelling in the presence of the solvent which it is in, generally resulting in a reduction of the permeability of different solutes. As a consequence, the release of embodied drugs from alginate matrices will be delayed, allowing these systems to be used in controlled drug release.[13]

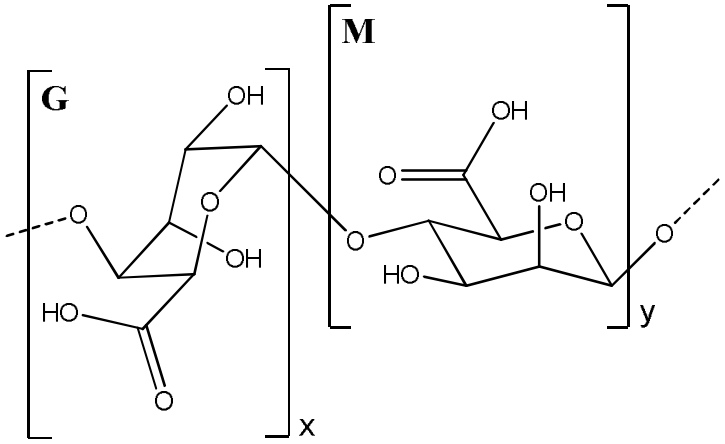

Figure 1.5: Structure of alginate.

1.3 Alginate Hydrogels

Hydrogels belong to a class of polymer that can swell to a large extent in water while maintaining their dimensional network structure in the swollen state.[33,34] Hydrogels are three-dimensional polymer networks composed of water-soluble polymers which are crosslinked to form a water-insoluble hydrogel.[35] They can swell and retain a significant portion of water when placed in an aqueous solution.[14] A superabsorbent hydrogel is defined as a gel which swells over 95% of its composition.[36] Superabsorbent hydrogels have high biocompatibility due to their large degree of water retention and their physiochemical similarity with the native extracellular matrix both compositionally and mechanically. Hydrogels are often divided into three classes depending on the nature of their network, namely entangled networks, covalently crosslinked networks and networks formed by physical interactions.

Hydrogels possess a degree of flexibility very similar to natural tissue due to their significant water content. A xerogel is a solid formed from the hydrogel by evaporating the pore liquid at relatively low temperature and at ordinary pressure. Xerogels usually retain high porosity and enormous surface area along with small pore size.[37] Hydrogels have been extensively researched and have found applications in a wide variety of fields including medical application,[33] wound

dressing,[38] drug delivery,[39] agriculture and food industries,[40,41,42] water treatment [43, 44] and catalysis.[45,46]

1.3.1 Formation and Properties of Alginate Hydrogles

Alginate hydrogels can be formed using a variety of different ionic or covalent crosslinkers. The properties of the hydrogels, such as swelling, and mechanical strength are dependent on the degree and type of crosslinking.[33,47-50]

1.3.1.1 Ionic Crosslinking

Ionic crosslinking or physically crosslinking is where a physical interaction occurs between different polymer chains. This is the preferred method of crosslinking as it avoids the use of toxic compounds, which generally have to be removed before the gel can be used. This method of crosslinking is mainly used throughout the research presented here in. One of the most important properties of alginates is their ability to form gels on addition of di- and trivalent metal ions such as bivalent Group 2 metals (Ca^{2+}, Sr^{2+} and Ba^{2+}) or trivalent (Fe^{3+} and Al^{3+}) ions.[12,38,51] The formation of the gel is due to ionic interactions between the carboxylate groups located on the polymer backbone and the cations present in the crosslinking solution (Figure 1.6).[52]

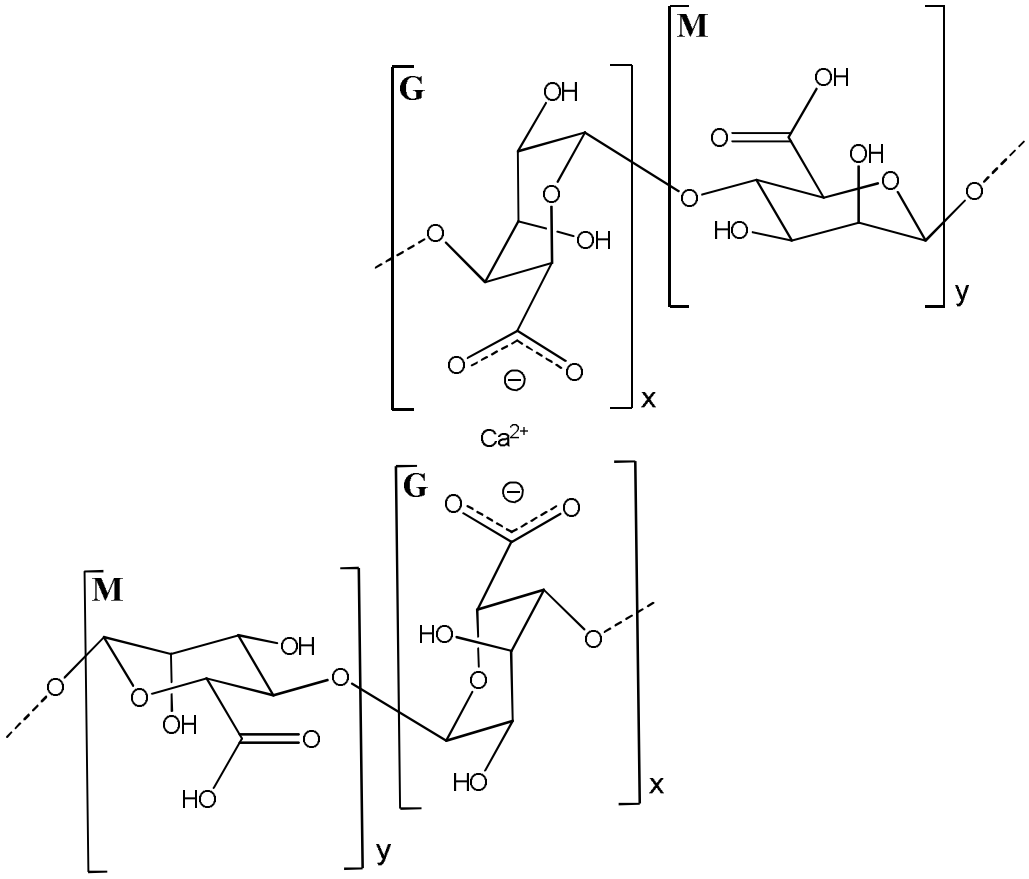

Figure 1.6: Structure of alginate showing ionic crosslinking between the alginate chains and the calcium ion.

The gelation of alginate can be carried out in an extremely mild environment. Due to the shapes of the monomers and their modes of linkage in the polymer, sodium alginate is a particularly attractive material for forming hydrogels. The geometries of the G and M block regions are substantially different from each other. The G-block is buckled while the M-block has a ribbon shape. When two G-block units are aligned side by side they have the ability to crosslink with a calcium ion, forming a link between two strands of alginate. Binding of the calcium to the alginate occurs preferentially at the guluronic units.[53-55] Thus, alginates with high numbers of guluronic units yield stronger gels. The calcium from the crosslinking solution is ionically substituted at the carboxylate site of the sodium alginate chain. This results in a chain of calcium-linked alginates that forms a solid gel. The Ca^{2+} ions fit into electronegative cavities like eggs in a box (Figure 1.7) and this is the

source of the term 'egg box structure'.[12,54] Crosslinking of sodium alginate is generally done using calcium chloride, resulting in the formation of calcium alginate hydrogel beads.

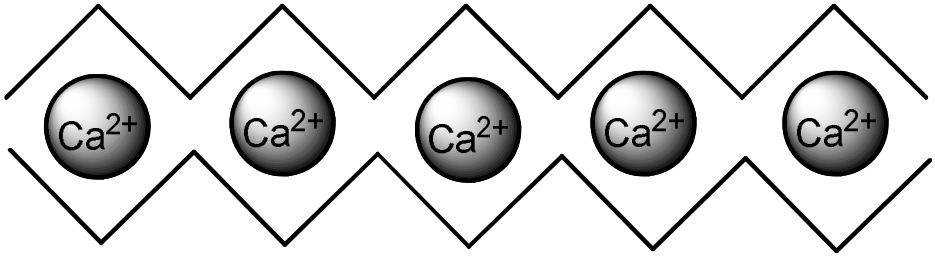

Figure 1.7: 'Egg-box' structure of the calcium ions binding in alginate.

1.3.1.2 Covalent Crosslinker

The use of covalent crosslinkers results in covalent bonds being formed between different polymer chains. Each uronic unit in an alginic acid chain contains two types of functional groups, OH and COOH, which are used for crosslinking. Covalent crosslinking of alginates is advantageous as it leads to hydrogels with improved mechanical strength. Ionic alginate hydrogels are known to have limited stability when in contact with solutions containing monovalent ions, as these cause destabilisation of the hydrogel and can lead to the gel rupturing. Covalent crosslinking can create more stable and robust networks. Alginates are often used for dehydration of ethanol-water mixtures due to the ability of the alginate to incorporate water into the hydrophilic membrane.[56] Excess hydrophilicity is disadvantageous in this procedure as it can cause low selectivity and poor membrane stability. Covalently crosslinked alginates are readily used for this process as they improve the membrane properties.

- Covalent crosslinking at the Hydroxyl Group

Glutaraldehyde is a commonly used covalent crosslinker and it crosslinks at the OH group of the alginate chain (Scheme 1.1).[57] Kulkarni *et al.* reported the successful encapsulation of a natural liquid pesticide in sodium alginate beads after crosslinking with glutaraldehyde.[57] These beads were used to control the release of the pesticide into soil, and the extent of crosslinking was studied in order to find the optimum amount of crosslinking required. They observed that an increase in the

degree of crosslinking resulted in a decrease of the pesticide being released from the beads. Yeom and co-workers also used glutaraldehyde to covalently crosslink the sodium alginate membranes to enhance the stability of the membranes against water.[58] It was observed that crosslinking with glutaraldehyde could reduce both the solubility of water in the membrane and the selectivity of the membrane towards water.

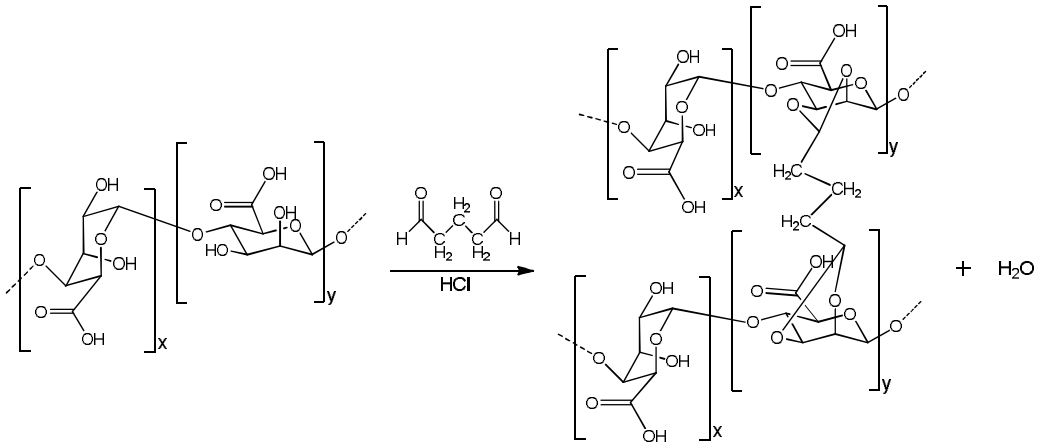

Scheme 1.1: Reaction scheme for covalent crosslinking of sodium alginate using glutaraldehyde.

Gotok and co-workers used the hydroxyl groups on the alginate to add covalent crosslinks to calcium alginate beads.[52] They first reacted a number of the hydroxyl groups with cyanobromide in the presence of base and then crosslinked the polymer chains upon addition of hexane-1, 6-diamine as given in Scheme 1.2.

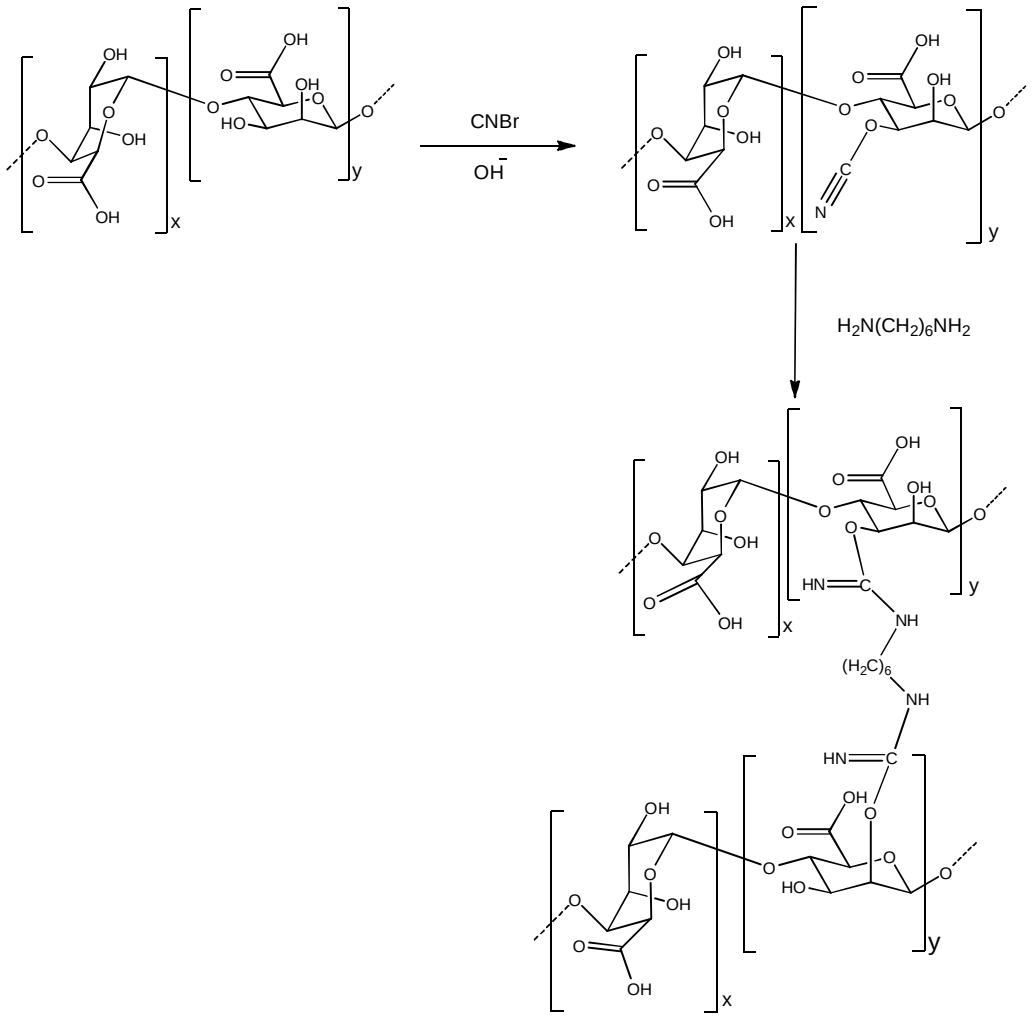

Scheme 1.2: Crosslinking of alginate with hexane-1, 6-diamine.

- Covalent crosslinking at the Carboxyl Groups

Covalent crosslinking can be achieved by reaction at the carboxyl groups with diamines to form diamide links. Auguste and co-workers reacted pre-formed calcium alginate beads with either ethylene diamine, butane-1,4-diamine or hexane-1,6-diamine using 1-ethyl-3-(3-dimethylaminopropyl)carbodiimide as the coupling agent.[59] In addition, Eiselt *et al.* used this reaction to crosslink sodium alginate with (poly(ethylene glycol))PEG-diamines of different chain lengths (Scheme 1.3). Hydrogels formed rapidly with each PEG-diamines crosslinkers, and the mechanical properties and swelling behaviour can be modified by using the chain length of the cross-linking molecules.[33]

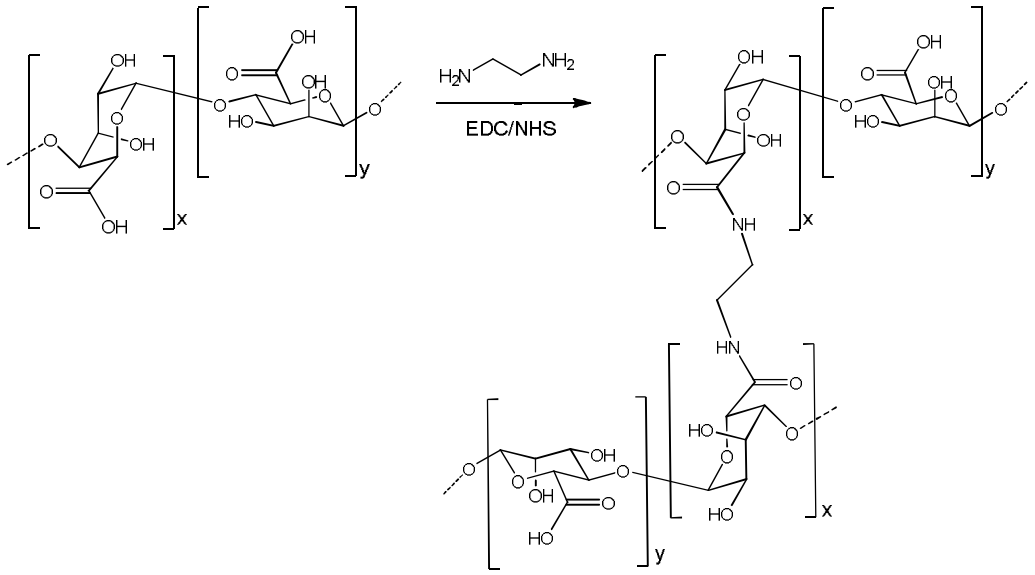

Scheme 1.3: Reaction of alginic acid with ethylene diamine.

Gattas-Asfura *et al.* carried out a reaction with sodium alginate and a PEG linker which was functionalised with an amine at one end and an azide group at the other.[60] The amine reacted with the carboxylate group to form an amide group (Scheme 1.4). The azide groups were then reacted with PEG chains containing 1-methyl-2-diphenylphosphino-terephthalate end groups via the Staudinger reaction (Scheme 1.4) to form a covalently crosslinked hydrogel.

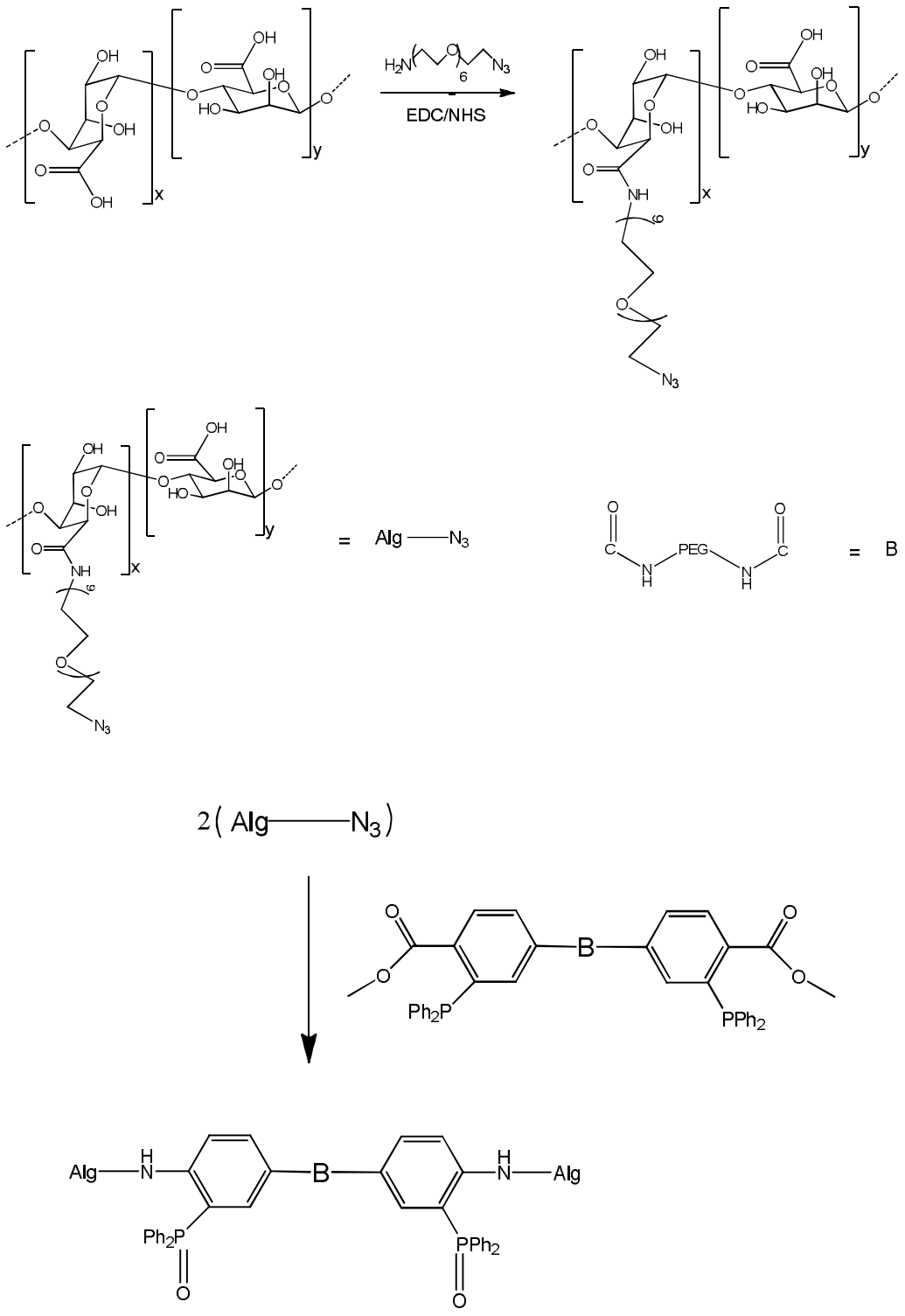

Scheme 1.4: Reaction scheme for covalent crosslinking alginate via amide bonding with a H_2N-PEG-N_3 followed by the Staudinger reaction.

1.3.1.3 Preparation of Ionically Crosslinked Alginate Beads

There are many different techniques available to produce beads, each with their own advantages and disadvantages. One of the main requirements for all beads production is that the beads should be homogeneous with a narrow size distribution range.

- Dripping

This is the simplest method for producing beads and the most common way of preparing alginate beads.[61] The alginate solution is placed in a syringe with or without a needle attached. The alginate solution passes through the syringe and/or needle into a solution containing the divalent/trivalent ion. The size of the beads depends on the size of the needle or syringe.[62] The alginate solution sticks to the edge of the syringe or needle until the gravitational force is high enough to overcome the surface tension resulting in the release of a drop. Dripping depends on gravitational forces alone to remove the adhering drop from the syringe or needle. This method is used mainly for small scale productions in laboratories, as it is not practical for large scale production due to difficulties that can be encountered such as blockage of the needle and low quantities of beads are produced. The dripping method was used throughout the research presented here.

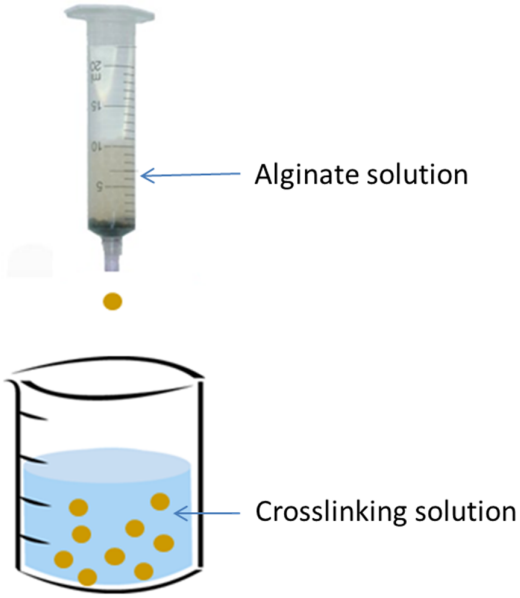

Figure 1.8: Schematic diagram for the production of calcium alginate hydrogel beads using the dripping method.

- Electrostatic Dripping and Coaxial Air-flow

Electrostatic dripping and coaxial air-flow are based on the formation of single droplets at the tip of a syringe or needle. Both these techniques work under the same principle as dripping but there is acceleration of the normal droplet formation. For the electrostatic dipping there are electrostatic forces used to pull the droplets off the needle at a considerably faster rate.[63,64] The polymer solution is usually passed through a needle with a charge applied and the drops fall into a solution which has been earthed or held at the opposite charge. Coaxial air-flow uses a stream of compressed air to pull the liquid droplets from the nozzle at a faster rate compared to the normal gravitational force.[62,65] Both of these techniques result in beads with diameters within a smaller range compared to dripping alone.

- Atomisation

Syringe based units are not practical for large scale production because of the large number of needles required and operational problems such as needle blockage, cleaning and sanitation. Atomisation is a method of making alginate hydrogel beads on a large scale. Atomisation is a process in the making of a colloidal suspension of

fine solid particles or liquid droplets in a high velocity gas stream. Atomisation is a method of preparing micron sized capsules with a very narrow size distribution. Air atomisation[66] and electrostatic atomisation[67] are two of the main types of atomisation used to make alginate capsules. Air atomisation sprays the sodium alginate solution into the calcium chloride solution to form hydrogel capsules.[66,68] An air blast atomiser uses compressed air to spray the sodium alginate into a solution of the calcium chloride which induces gelation. Herrero *et al*. reported that this method of making hydrogels resulted in capsules with a diameter of 1-50 μm.[66] Electrostatic atomisation is where the liquid is dispersed into fine droplets by an electrostatic force working on the surface of the liquid. Watanabe *et al*. prepared alginate gel beads using the electrostatic atomisation technique, whereby an aqueous sodium alginate solution containing an enzyme to be encapsulated was dispersed into an aqueous solution of calcium chloride as small droplets by applying a high voltage.[67]

- Emulsification

This method of forming alginate beads is only used for stable drugs because it involves the use of harsh chemical reagents to remove oil at the end of the process. The size of the micro-beads produced depends on stirring speed and the rate of the addition of the crosslinking solution. Emulsification is mainly used to encapsulate bioactive materials into small beads and the main advantage of this method is the generation of beads with a small diameter.[69] There are different emulsification techniques. One commonly used technique is to form an emulsion of an aqueous alginate solution in oil, which is then added to a calcium chloride solution to form beads. Hurteaux *et al.* used the emulsification techniques in the making of their propylene glycol alginate beads to encapsulate peptides which readily degrade. An aqueous solution of alginate and propylene alginate were placed in an oil into which an aqueous solution of calcium chloride was mixed.[70] The disadvantage of this method is that the bead size cannot be easily controlled. A more efficient technique was the one used by Ponclelet *et al.* whereby the formation of beads was achieved through the rapid release of calcium ions from an insoluble dispersed calcium complex.[69] The addition of an oil soluble acid frees up the calcium ions via acidification thus forming beads when it comes into contact with the alginate. All of

their beads formed were less than 1 mm in diameter and this method is a viable method for large scale production of beads.

1.3.2 Forming Alginate Beads using Functionalised Alginates

1.3.2.1 Reactions to Functionalise Alginate

From the structure of alginate given in Figure 1.5 it can be seen that each uronic unit has two secondary hydroxyl and one carboxylate groups present which make it an ideal candidate for functionalisation in order to change the characteristics of the parent alginate. There are a wide variety of reactions which have been used to derivitise alginate in the literature,[55] so this review will only concentrate on a number of reactions which increase the hydrophobic properties of the polymer. The hydrophilic nature of alginate polymers can be reduced by covalently attaching long chained alkyl chains or aromatic molecules. Common reactions used to derivatise the hydroxyl groups of the alginate backbone in this manner are oxidation and reductive-amination. Functionalisation of the carboxyl groups can be performed through esterification or amidation. The extent to which each of the reactions proceeds depends on the reaction conditions, so generally in order to characterise the products the degree of substitution of the derivitised alginate needs to be determined.

- Oxidation of the Hydroxyl Group

Oxidation of the alginate at the hydroxyl groups leads to alginates that have more reactive groups attached which also leads to improvement in the biodegradability. Oxidation of the alginate is usually carried out using sodium periodate as shown in Scheme 1.5.[71] The aldehyde groups can then be used as sites for the covalent attachment of crosslinkers, hydrophobic moieties, or from which to graft polymer chains.

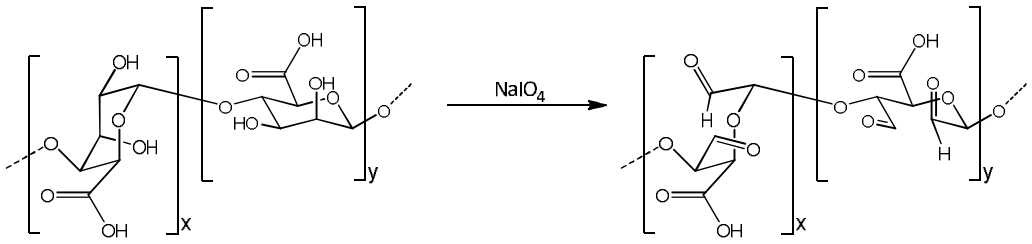

Scheme 1.5: Partial oxidation of alginate by $NaIO_4$.

- Reductive Amination Reaction on Partially Oxidised Alginate

When the partially oxidised alginate formed in Scheme 1.5 is reacted with a primary amine in the presence of a reducing agent, such as sodium cyanoborohydride, the aldehyde groups can be converted to amines. Sodium cyanoborohydride is used as the reducing agent as at pH values of approximately 6 it will selectively reduce the imine groups of the reaction intermediate. Duval *et al.* have used this reaction to modify sodium alginate with short polyether chains (Scheme 1.6).[72] Gelation of the alginate in the presence of divalent cations can still be performed since the carboxyl groups are still present on the alginate backbone.

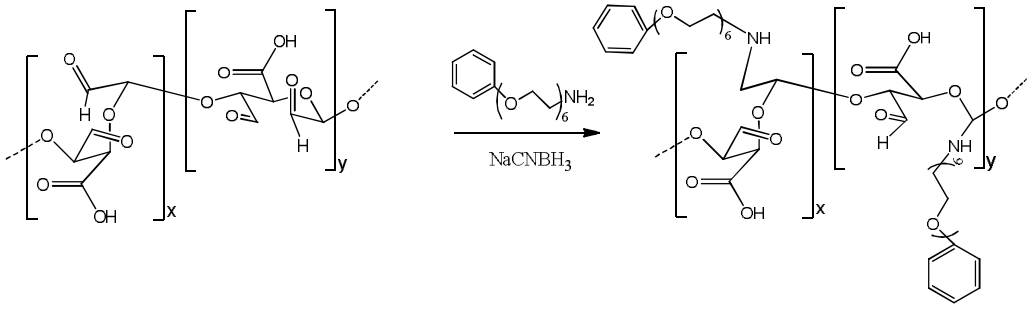

Scheme 1.6: Reaction of partially oxidised alginate with an amine.

- Reaction of the Hydroxyl Groups with 3-(trimethoxysilyl)alkyl derivatives

A number of studies have shown that sodium alginate reacts with 3-(trimethoxysilyl)-propyloctadecyldimethylammonium (TSA) chloride (Scheme 1.7) in acid solution. This reaction anchors the TSA group to the polymer backbone by a covalent non-hydrolysable bond.[73-75,76]

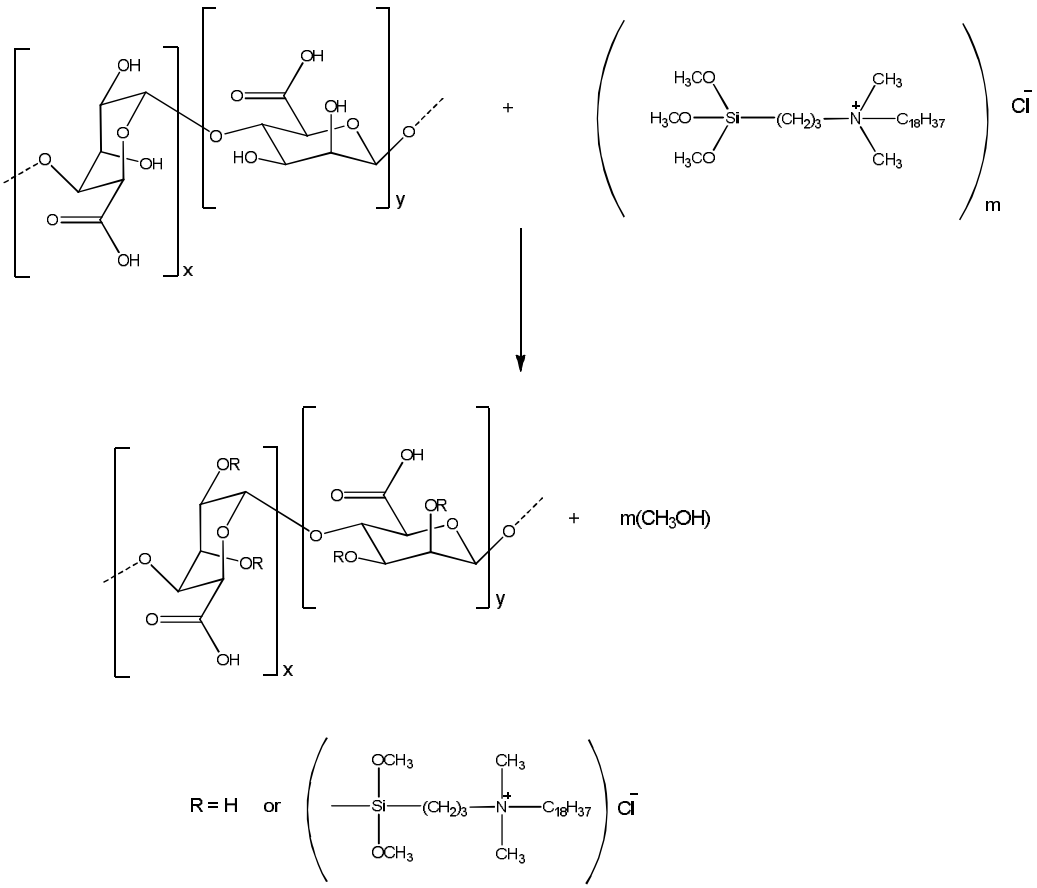

Scheme 1.7: Reaction of 3-(trimethoxysilyl)-propyloctadecyldimethylammonium with alginate.

- Esterification of the Carboxylate Groups

Esterification can be carried out using alkyl bromides (Scheme 1.8) by first converting the sodium alginate to alginic acid and then neutralising this with the tetrabutyl ammonium (TBA) hydroxide. The TBA alginate is carefully dried and dissolved in an organic solvent (DMSO) to which the alkyl bromide with the chosen chain length is added.[77,78,76] After the reaction has taken place the TBA cation is exchanged for Na^+ using NaCl.

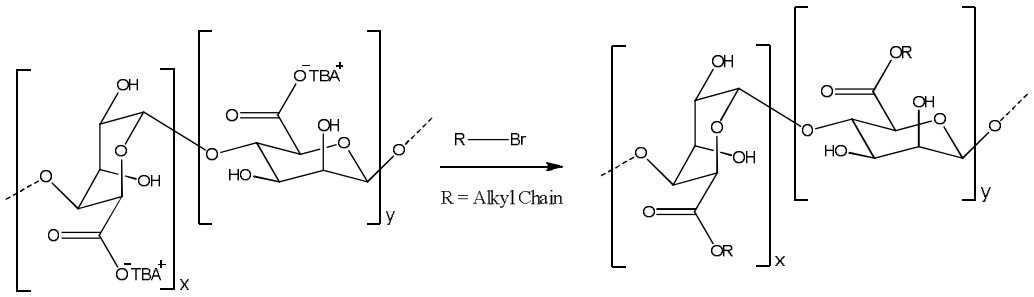

Scheme 1.8: Esterification of TBA alginate with an alkyl bromide.

Alternatively, the carboxyl groups of partially protonated sodium alginate can be converted to ester groups by reaction with the appropriate alcohol in the presence of the coupling agent *N*,*N*'-dicyclohexylcarbodiimide (DCC) and the base 4-(*N*,*N*'-dimethylaminopyridine) (DMAP). Yang *et al*. used this synthesis to form a soluble amphiphilic sodium alginate derivative by covalently attaching a cholesterol unit to the backbone of the alginate (Scheme 1.9).[79] The cholesterol unit was attached at the carboxylate group on the sodium alginate backbone and had the ability to encapsulate the hydrophobic compound pyrene.

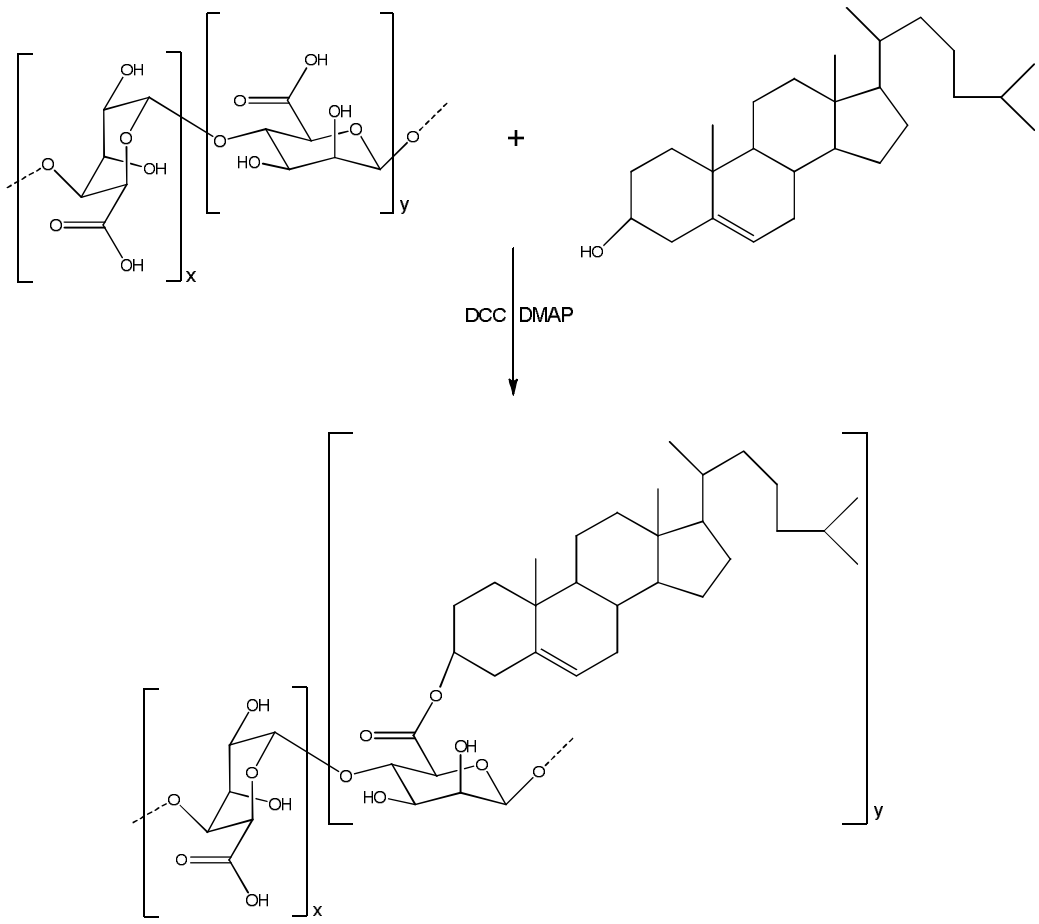

Scheme 1.9: Reaction of cholesterol with alginate.

Alginic acid will react with epoxides to form esters by the reaction given in Scheme 1.10. This reaction has been used to form propylene glycol alginate which is a partially esterified derivative of alginate which is commercially available,[80] in which approximately 70% of the carboxylic groups are esterified with propylene glycol.[81]

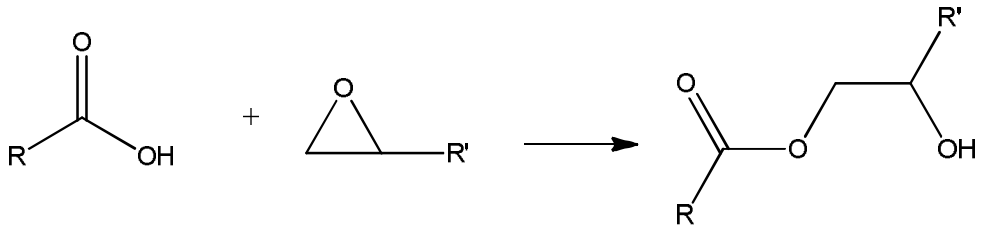

Scheme 1.10: Reaction between alginic acid and alkylene oxide R' represents an alkyl chain and R represents the rest of the alginic acid chain.

- Formation of Alginate Amides

A common method of forming alginate amide derivatives is to first form an alginate ester and then react this with the appropriate amine. Sinquin *et al*. used this reaction to form a C_8-C_{14}-linked alginate amide derivative starting from propylene glycol esters of alginate.[82] This reaction is given in Scheme 1.11.

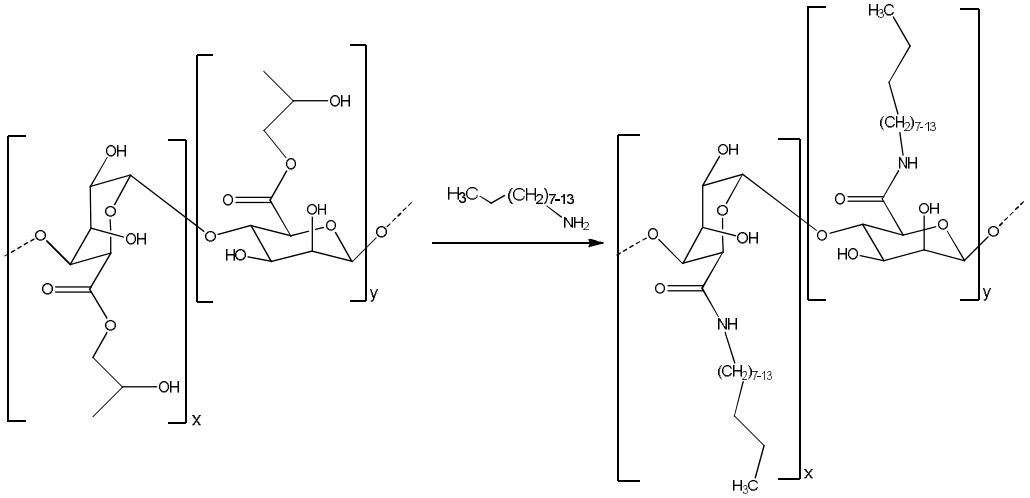

Scheme 1.11: Reaction of propylene glycol alginate with an amine.

Alternatively Galant *et al.* synthesised the C_8-linked alginate amide from alginate acid using n-octylamine and 1-ethyl-3-(3-dimethylaminopropyl)carbodimide hydrochloride (EDC-HCl) as an activating agent.[83]

1.3.2.2 Bead Formation using Functionalised Alginates

Two derivitised alginates have been used in the research associated with this project. The first involved the reaction to derivitise the OH group using a 3-(trimethoxysilyl)alkyl compound (Scheme 1.7) to add a quaternary ammonium group to the alginate polymer. The second was propylene glycol alginate which is commercially available. When the alginate is derivatised at the hydroxyl groups the carboxylate groups are still available for a crosslinking reaction, and as long as the polymer has sufficient water solubility, bead formation can take place by ionic gelation using calcium ions. A study had shown that, when alginate was functionalised with a quaternary ammonium group using the reaction given in Scheme 1.7, beads were then formed through calcium ion crosslinks.[84] However, if

the derivatised alginate contains only a low amount of unreacted carboxylate groups then ionic gelation no longer will result in the formation of structurally stable beads. One way to circumvent this problem is to form composite bead materials. Propylene glycol alginate (PGA) is a partially (70%) esterified derivative of alginate. Esterification of the alginate leads to a polymer which is more hydrophobic, leading to a polymer which has many uses in industrial applications such as the ability to stabilise foams in drinks and ice creams.[80] Researchers have developed calcium crosslinked composite PGA/alginate beads which they showed could be used to encapsulate proteins for slow release systems.[70] In order to give the beads more mechanical strength in addition to the calcium crosslinks, human serum albumin (HSA) was used to form a coating over the beads by the reaction between the ester group and the amino groups of the protein.[85] The HSA is linked to the alginate via an amide bond. Studies have showed that propylene glycol alginate is bio-compatible.[70,86] which makes it an ideal candidate for drug delivery. It has been observed in the literature that composite propylene glycol/alginate beads offer better resistance towards freezing, lyophilisation, sterilisation and increased mechanical strength compared to ionically crosslinked alginate beads.[86,70,81]

1.3.3 Composite Alginate Polymer Beads

Another way of altering the properties of the beads such as swelling, mechanical strength, hydrophobicity is to make composite materials in which the two or more components of the beads are simply mixed together without the involvement of covalent bonds.

1.3.3.1 Hybrid Co-Polymer Beads

Chitosan is commonly used to form hybrid composite materials with alginate as at the appropriate pH the polymers can be held together by electrostatic attractions. There has been an increasing interest in the study of alginate-chitosan hydrogels for controlled release of protein drugs. Several reports have shown that coating the surface of alginate, which is a polyanionic copolymer, with chitosan, which is a cationic polymer, provides stability to the hydrogel material.[87,88] Large pores present in the alginate polymer are responsible for the leaching of encapsulated materials from the hydrogel. Chitosan has limited ability for controlling the release

of encapsulated compounds due to its hydrophilic nature and easy solubility in acidic medium. Together these polymers make favourable drug delivery vehicles as together they can prevent excess leaching and are more stable under the harsh acidic conditions of the stomach.[88] Composite magnetic alginate-chitosan beads containing Fe_3O_4 were prepared by Wu and co-workers, for the adsorption of lanthanum from aqueous solutions.[89] These composite beads showed high adsorption capacity and selectivity for lanthanum. The lanthanum was selectively separated from metal based ions such as Pb(II) and Cu(II) through mechanisms of cation exchange, electrostatic interactions and surface complexation with the oxygen atoms being the main binding sites.

Composite beads have also been prepared with alginate and other biopolymers. For example, Saha *et al.* have shown that co-polymer beads have the potential to be used for health care purposes such as drug delivery, by using two biopolymers, sodium alginate and gelatin.[90] They then showed the anti-microbial properties of these hybrid co-polymer beads against a number of different microbes and how efficient they are at inhibiting the growth. Another well used biopolymer is carboxymethyl cellulose which is an anionic derivative of cellulose. The advantage of using carboxymethyl cellulose for drug delivery is its solubility in water and the reactive groups on its backbone which can be easily modified by chemical reaction, which can change the characteristics of the polymer. Wang *et al.* used carboxymethyl cellulose-alginate composite beads, and modified them to control the release of diclofenac sodium at different pH values.[91] At a pH of 1.2 the beads did not swell and the drug was not released, whereas when the pH was increased to 6.8 the beads began to swell and the drug was released. This system is ideal for getting the drug past the harsh conditions of the stomach and into the intestine where it can be released.

1.3.3.2 Alginate Beads Containing Inorganic-Fillers

Typical inorganic fillers that can be trapped within a polymer bead are powdered activated charcoal, carbon fibres, carbon nanotubes, clays and zeolites. The advantage of these materials is that they have a high surface area and therefore can act as highly effective adsorbent materials. In the current research we investigated two types of fillers activated charcoal and the clay bentonite.

Activated charcoal is also referred to as activated carbon, it is a natural substance derived from raw materials such as vegetables and wood. Chemical manufacturers produce activated charcoal by exposing carbon powder to oxygen contained in steam at high temperatures. This process increases the surface area of the material, making it highly absorptive. The structure of activated charcoal consists of short stacks of small graphite-like sheets arranged in a highly disordered fashion to form a poorly interconnected micro porous network.[92] Activated charcoal is fine in texture and has a significant binding power making it an effective adsorbent. Due to these good adsorbent properties, activated charcoal has been utilised in a range of applications including the removal of pollutants, hydrogen storage and as catalytic supports.[93] Activated charcoal is often used to treat people who have ingested poisonous materials or have taken a drug over-dose.[94] Charcoal is also widely used for the controlled release of liquid pesticides.[95] A number of studies have involved entrapping activated charcoal in polymer beads or membranes.[93,96-99] Of particular relevance to the research described herein, alginate-activated charcoal beads were studied as a controlled release system for a number of pesticides.[95] The beads were formed by dissolving the sodium alginate and charcoal in water. These mixtures were vigorously stirred for 1 h. The mixtures were then added drop wise into a bath of calcium chloride. Garrido-Herrer and co-workers found that the addition of the activated charcoal led to larger and heavier beads that were more spherical. Another function of the activated charcoal is the removal of organic liquids from water. Aminabhavi *et al.* have shown that activated charcoal can be successfully incorporated into sodium alginate membranes and that the membranes can successfully separate liquid organic molecules from water.[92]

Bentonite is a naturally occurring impure clay and is a hydrated aluminium silicate made up mostly of montmorillonite. Bentonite contains a number of exchangeable cations which are mainly calcium or sodium. Figure 1.9 shows a representation of the structure of bentonite.

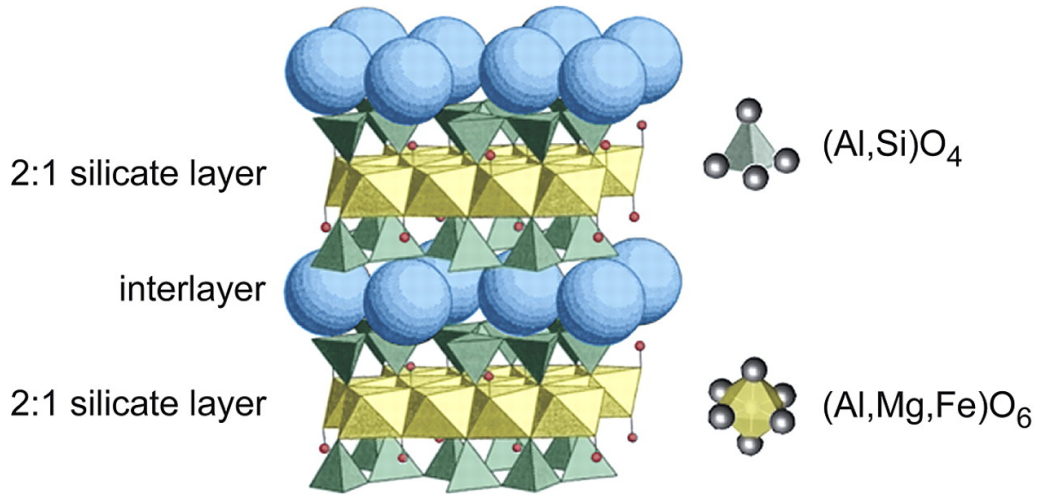

Figure 1.9: Schematic diagram showing the structure of bentonite. Within each layer a layer of cations bound to 6 oxygens (octahedra) are sandwiched between two layers containing cation bound to 4 oxygens (tetrahedra). Between each layer there are hydrated sodium or calcium ion (blue spheres) Hydrogen atoms are denoted by red spheres.[100]

Bentonite because of its high surface area and ion exchange properties has been used in a range of applications, including as an adsorbent (cat litter), in agrochemical delivery systems and as a binder in animal feed.[101] A number of studies have looked at different applications of bentonite loaded calcium alginate beads. The addition of clays to hydrogels can overcome the drawback of using clay or alginate, such as the low mechanical strength of the alginate or the ease of removal of the bentonite. Bentonite loaded calcium beads have been investigated in a number of applications such as adsorbents[102-104] and in delivery systems.[95,105,106] In general the beads are formed by mixing the alginate and the bentonite together and dropping them into a calcium chloride solution. Gerrido-Herrera found that the beads were larger in size and encapsulated more of the pesticide than the alginate beads themselves.[95]

1.4 Applications of Alginate Beads

1.4.1 Drug Delivery

Controlled release delivery systems represent an important area of health care which is rapidly growing and there has been a significant interest in investigating the use of alginate beads in drug delivery systems.[107,108] This method of drug delivery offers many advantages over conventional methods, as the delivery of the drugs from within the alginate polymer can be controlled through varying the properties of the alginate polymer. One of the advantages of using alginate is that it is biodegradable which means it can degrade within the body during or after drug release without any toxic side effects, and there is no need for surgical removal after the drug is used within the body. The preferred method for delivery of drugs is orally, but due to the harsh environment of the stomach many drugs, particularly protein-based formulations, get destroyed at this stage. Alginate has attracted a lot of attention for oral delivery and is now widely used to deliver acid sensitive drugs as it can pass through the stomach without being destroyed because it is stable under acidic conditions. When it gets to the intestines, where the pH increases the beads swell and release the encapsulated drug in its active form.[107] Murata *et al*. studied the release of the model drug hydrocortisone from coated calcium alginate beads into simulated gastrointestinal conditions.[51] They found that the rate of release of the hydrocortisone was much slower when the beads were placed in the solution with pH 1.2 (simulating stomach conditions) than when they were placed in the solution at a pH of 6.8 (simulating intestinal conditions). Bentonite loaded alginate beads have been used in drug delivery systems for the controlled release of vitamins B_1 and B_6.[109]

1.4.2 Agrochemical Delivery

Sodium alginate beads are also used in the agricultural sector as a controlled release polymer. Kulkarni *et al.* have used sodium alginate beads crosslinked with glutaraldehyde to encapsulate and slowly release the encapsulated pesticide.[57] When the beads are applied to the soil they release the pesticide in a slow and sustained manner and this prevents excess pesticide being applied to the soil and being washed away before it has any effect on the pests present in the soil. A number of studies

have employed bentonite-loaded calcium alginate beads as delivery systems for pesticides.[41,95,105] In addition to being used as a delivery system for pesticides, calcium alginate beads have been also used to entrap bacteria for agriculture and horticulture applications. Wu *et al.* used bentonite-loaded calcium alginate beads to encapsulate the plant growth-promoting bacteria *Raoultella planticola* in order to develop a controlled release system.[110] In a different study researchers encapsulated an atrazine degrading bacteria *Rhodococcus erythroplis* into these beads to develop a system to remove this pollutant from soils.[111]

1.4.3 Water Treatment and Disinfection

Alginate gels have been used to remove heavy metal ions and organic pollutants from very dilute waste water streams. Alginate beads have many advantages, for example reusability. Gotoh *et al.* showed that alginate beads could successfully adsorb metal ions such as Cu(II) and Mn(II) from water.[52] Bentonite loaded calcium alginate beads have been investigated as adsorbents for a range of chemicals including phenol,[104] Cu(II) ions and nitrophenol[102,103] and uranyl ions.[112] In terms of water disinfection alginate was used to anchor quaternary ammonium groups onto the backbone of the polymer.[73] Quaternary ammonium compounds are known to have antimicrobial activity. Once the quaternary ammonium group is linked covalently to the alginate chain it prevents leaching of the material and the polymer is active without releasing the reactive agent. Hydrogel beads have been made using this polymer which results in an insoluble polymer that has antimicrobial activity when it comes into contact with water.[73]

1.4.4 Catalysis

Immobilisation of catalytic species onto solid supports, such as calcium alginate, offers easy recycling of the catalyst and allows the substrates and products to be easily separated. Alginate is a popular biopolymer for heterogeneous catalysis due to its unlimited availability as a renewable resource and the fact that it is biodegradable. Calcium alginate gel matrixes have been widely used to encapsulate enzymes which are then used as biocatalysts.[45,113] Jamal *et al.* presented work using enzymes supported onto calcium alginate matrix which was then used efficiently for the removal of synthetic dyes from industrial effluents.[45] Alginates have also been

used to immobilise ionic liquids to prepare catalytic materials.[114,115] The combination of the polymer with ionic liquids provides a support for binding a wide variety of metals including those used for catalysis such as Pd. For example Jouannin *et al.* prepared palladium immobilised ionic liquid supported on alginates, which were tested for the hydrogenation of 4-nitroaniline.[115]

1.5 Urease Inhibitors

An objective of this research was to develop biodegradable hydrogel beads as a potential delivery system for the urease inhibitor *N*-(*n*-butyl) thiophosphoric triamide (NBPT) as shown in Figure 1.10.

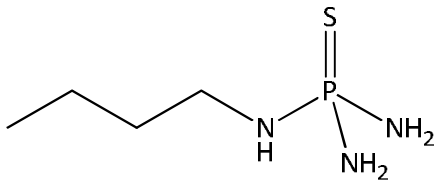

Figure 1.10: Structure of NBPT

Urease is an enzyme that catalyses the hydrolysis of urea to ammonia and carbon dioxide.[116] Urea is one of the main sources of nitrogen used in fertilisers. Once the urea is applied to soils as fertilisers or urine it undergoes a catalytic reaction converting it to ammonia which is mainly lost to the atmosphere due to volatilisation. In agriculture, high urease activity causes significant environmental and economic problems by releasing large amounts of ammonia into the atmosphere during urea fertilisation. It also induces plant damage by depriving plants of essential nutrients and secondarily by ammonia toxicity, increasing the pH of the soil. Nitrogen losses through NH_3 volatilisation are a major cause of environmental pollution and this also results in lower efficiency of fertilisers, which is a major cost to agriculture.[116] Therefore, inhibitors such as NBPT are applied to the soil in order to slow down the rate of hydrolysis of urea, so as to reduce these losses and so there is a more efficient uptake of nitrogen which has originated from urea by the plants.

Inhibitors are compounds that have the ability to interact with the active sites of enzymes and block their normal activity toward natural substrates. There are many known urease inhibitors available in both medicine and agriculture. Overall urease inhibitors are divided into three groups according to their structure of binding capacities with the urease enzyme.[117,118] The first group blocks the sulphydryl groups of the active sites on the enzyme; these are usually reactive organic or inorganic compounds such as metal ions, e.g., Ag^{+} or Cu^{2+}. The second group of inhibitors are metal chelating compounds that cause inhibition due to complex formation with one of the Ni ions at the active site of the urease enzyme. The third group are competitive inhibitors which are structural analogues of urea like thiourea and methyl urea.[118] This third class has been the most extensively studied for agriculture use and it is in this group that some of the best known inhibitors are classified for example NBPT and PPDA (phenylphosphorodiamidate) and CHPT (cyclohexylphosphoric triamide).

NBPT is well documented in the literature as an efficient urease inhibitor.[119,120] NBPT itself is not an active urease inhibitor, because after application to soils the NBPT is converted to its oxygen analogue, *N*-(*n*-butyl) phosphoric triamide (NBPTO) (Figure 1.11), and it is this molecule that is the active inhibitor. NBPTO has the ability to bind to the two nickel units present in the active site of the urease inhibitor.[121,122] Once it is bound there it blocks the urea from entering the active site and therefore prevents the conversion of some of the urea to volatile ammonia. NBPT is widely used to minimise the leaching of nitrates from the soils and to limit the loss of nitrogen through gaseous emissions in agriculture. Gill *et al.* showed that when NBPT was applied with urea to different soil that the hydrolysis of urea was delayed for up to 16 days resulting in reduced NH_3 volatilisation[119] and Varel *et al.* concluded from their study that the NBPT reduces ammonia emissions from animal waste thus preventing environmental damage.[123]

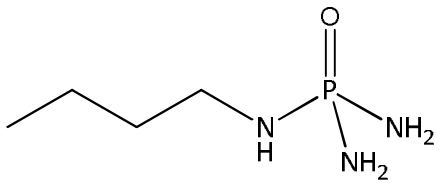

Figure 1.11: Structure of NBPTO

A delivery system is required for the inhibitor NBPT so that it can be released in a slow and sustained manner so as it will be readily available in its active form over longer periods of time. Having the inhibitors encapsulated in hydrogel beads could also shield the compounds from heavy rainfall, therefore keeping them in the soils for longer.

1.6 Antimicrobial Activity of Silver Impregnated Beads

The other aspect of this research was to investigate alginate bead supports impregnated with silver(I) and silver(0) which could be used in water disinfection systems. Ionic silver is known to have the largest antimicrobial capacity of all metals. It is recognised for its long term biocidal properties, its low volatility and low toxicity to eukaryotic cells. Silver (Ag^{+}) is effective against a broad range of micro-organisms such as yeast and bacteria including MRSA.[124]

Clean drinking water is necessary for the survival of the human race; however, bacterial contaminations from drinking water are a very common cause of ill health, especially in developing countries. Removal or inactivation of these pathogenic microorganisms in a safe manner is a demanding task in any water treatment process. Silver has been used for water disinfectant since ancient Greek times.[125] In the past decade research has started to focus the use of polymers containing silver for water disinfection.[126] Rivas *et al.* showed the use of co-polymer alginate hydrogels which have silver attached as successful antibacterial agents.[127] Silver based technologies have proved to be superior to other methods of water purification, for example purification using heating and/or chloride.[128] Metallic silver is inert in the presence of human and bacteria cells, it is the silver ion that is biologically active and readily binds to cell surface receptors and metal carrier proteins like albumins. The anti-microbial properties of alginate beads loaded with silver is based on a slow and

sustained release of silver ions from the polymer network. With the current widespread use of silver increasing in areas such as water purification, humans will be exposed to silver in the food chains and through drinking water. Higher levels of biological silver are to be expected in humans, but there is no evidence to suggest that silver exhibits any physiological function and are therefore of no clinical or toxicological significance. European legislation does not regulate the use of silver concentrations in water. The Drinking Water Directive (80/778/EEC) identified water quality indicators and classified silver in Group C which indicates that it may be toxic in large amounts. The World Health Organisation (WHO) does not regulate silver in drinking water.[128]

Research into the antimicrobial properties of silver has continued to grow rapidly over the last number of years due to the emergence of a large number of antibiotic resistant strains of microbes.[89,129] Therefore, the focus of the current research is based on developing new cost effective antimicrobial agents, which are effective against a broad range of these multi-drug resistant bacteria. One area of this research is to develop antimicrobial polymers as they have shown promise to enhance the chemical stability and efficacy of some existing antimicrobial agents.[130] In addition, if the agent is covalently linked to the solid support the risk of the antimicrobial agent being released into the water system is reduced. Of the metal based compounds, silver based materials have proved the most promising as they exhibit a broad range spectrum activity.[131] Moreover, silver impregnated polymer supports, like the biopolymer-metal combinations studied here, are attracting much attention because of their long term biocidal activity, chemical stability and their relative low cost.

The overall aim of this part of the project was to make polymer supports with antimicrobial properties, which would have the potential to be used in water disinfection systems. The different alginate polymer supports were encapsulated with silver(I) and silver(0) and were then assessed for their ability to slowly release silver over time, with the intention of inactivating pathogenic microorganism.

1.7 References

(1) McLaren, J. S. *Trends in Biotechnology* **2005**, *23*, 339-342.
(2) Song, C. S. *Catalysis Today* **2006**, *115*, 2-32.
(3) Dikshit, V.; Yueh, F.-Y.; Singh, J. P.; McIntyre, D. L.; Jain, J. C.; Melikechi, N. *Spectrochim Acta Part B: Atomic Spectroscopy* **2012**, *68*, 65-70.
(4) Rawat, M.; Ramanathan, A. *Journal of Environmental Protection* **2011**, *2*, 399-407.
(5) Rasmussen, J.; Harrison, A. *ISRN Veterinary Science* **2011**, 613172, 613110 pp.
(6) Huttunen, J. T.; Alm, J.; Liikanen, A.; Juutinen, S.; Larmola, T.; Hammar, T.; Silvola, J.; Martikainen, P. J. *Chemosphere* **2003**, *52*, 609-621.
(7) http://www.epa.gov/greenchemistry/.
(8) Anastas, P.; Warner, J. *Green Chemistry: Theory and Practice* Oxford University Press, **1998**.
(9) Yu, L.; Dean, K.; Li, L. *Progress in Polymer Science* **2006**, *31*, 576-602.
(10) Cui, Z.; Beach, E. S.; Anastas, P. T. *Green Chemistry Letters and Reviews* **2011**, *4*, 35-40.
(11) Khalil, H. P. S. A.; Bhat, A. H.; Yusra, A. F. I. *Carbohydrate Polymers* **2012**, *87*, 963-979.
(12) Shilpa, A.; Agrawal, S. S.; Ray, A. R. *Journal of macromolecular science* **2003**, *43*, 187-221.
(13) Wang, Q.; Hu, X.; Du, Y.; Kennedy, J. F. *Carbohydrate Polymers* **2010**, *82*, 842-847.
(14) Deligkaris, K.; Tadele, T. S.; Olthuis, W.; Van den Berg, A. *Sensors and Actuators B: Chemical* **2010**, *147*, 765-774.
(15) Denniston, K. C., R; Topping, J; *General, Organic and Biochemistry*; 6th ed.; McGraw-Hill, **2007**.
(16) Wade, L. G. *Organic Chemistry*; 4th ed.; Addidon Wesley Longman, **1999**.
(17) Tirrell, J. G.; Tirrell, D. A. *Current Opinion in Solid State and Materials Science* **1996**, *1*, 407-411
(18) Vallee, F.; Muller, C.; Durand, A.; Schimchowitsch, S.; Dellacherie, E.; Kelche, C.; Cassel, J. C.; Leonard, M. *Carbohydrate Research* **2009**, *344*, 223-228.
(19) Vollhardt, P.; Schore, N. *Organic Chemisrty Structure and Function, p 392*; 6th ed.; W.H. Freeman and Company, **2011**.
(20) Wiegand, C.; Heinze, T.; Hipler, U.-C. *Wound Repair and Regeneration* **2009**, *17*, 511-521.
(21) Liu, H.; Xie, F.; Yu, L.; Chen, L.; Li, L. *Progress in Polymer Science* **2009**, *34*, 1348-1368
(22) Al-Karawi, A. J. M.; Al-Daraji, A. H. R. *Carbohydrate Polymers* **2010**, *79*, 769-774.
(23) Tester, R. F.; Karkalas, J.; Qi, X. *Journal of Cereal Science* **2004**, *39*, 151-165.
(24) Stenekes, R. J. H.; Talsma, H.; Hennink, W. E. *Biomaterials* **2001**, *22*, 1891-1898.
(25) Mehvar, R. *Journal of Controlled Release* **2000**, *69*, 1-25.
(26) Ingram, A. L.; Deparis, O.; Boulenguez, J.; Kennaway, G.; Berthier, S.; Parker, A. R. *Arthropod Structure and Development* **2011**, *40*, 21-25.

(27) Schröder-Turk, G. E.; Wickham, S.; Averdunk, H.; Brink, F.; Fitz Gerald, J. D.; Poladian, L.; Large, M. C. J.; Hyde, S. T. *Journal of Structural Biology* **2011**, *174*, 290-295.
(28) Falini, G.; Fermani, S.; Ripamonti, A. *Journal of Inorganic Biochemistry* **2002**, *91*, 475-480.
(29) Pillai, C. K. S.; Paul, W.; Sharma, C. P. *Progress in Polymer Science* **2009**, *34*, 641-678.
(30) Berger, J.; Reist, M.; Mayer, J. M.; Felt, O.; Peppas, N. A.; Gurny, R. *European Journal of Pharmaceutics and Biopharmaceutics* **2004**, *57*, 19-34.
(31) Araújo, M. M.; Teixeira, J. A. *International Biodeterioration and Biodegradation* **1997**, *40*, 63-74.
(32) Yang, J.-S.; Xie, Y.-J.; He, W. *Carbohydrate Polymers* **2011**, *84*, 33-39.
(33) Eiselt, P.; Lee, K. Y.; Mooney, D. J. *Macromolecules* **1999**, *32*, 5561-5566.
(34) Bursali, E. A.; Coskun, S.; Kizil, M.; Yurdakoc, M. *Carbohydrate Polymers* **2011**, *83*, 1377-1383.
(35) Panic, V.; Adnadjevic, B.; Velickovic, S.; Jovanovic, J. *Chemical Engineering Journal* **2010**, *156*, 206-214.
(36) Alupei, I. C.; Popa, M.; Hamcerencu, M.; Abadie, M. J. M. *European Polymer Journal* **2002**, *38*, 2313-2320.
(37) Andrade-Espinosa, G.; Escobar-Barrios, V.; Rangel-Mendez, R. *Colloid and Polymer Science* **2010**, *288*, 1697-1704.
(38) Goh, C. H.; Heng, P. W. S.; Chan, L. W. *Carbohydrate Polymers* **2012**, *88*, 1-12.
(39) Matricardi, P.; Di Meo, C.; Coviello, T.; Alhaique, F. *Expert Opinion on Drug Delivery* **2008**, *5*, 417-425.
(40) Singh, B.; Sharma, D. K.; Kumar, R.; Gupta, A. *Journal of Hazardous Materials* **2010**, *177*, 290-299.
(41) Singh, B.; Sharma, D. K.; Kumar, R.; Gupta, A. *Applied Clay Science* **2010**, *47*, 384-391.
(42) Champagne, C. P. *Cl and CEO* **2006**, *12*, 11-17.
(43) Abou Taleb, M. F.; Hegazy, D. E.; Ismail, S. A. *Carbohydrate Polymers* **2012**, *87*, 2263-2269.
(44) Singh, S. K.; Bansal, A.; Jha, M. K.; Dey, A. *Bioresource Technology* **2012**, *104*, 257-265.
(45) Jamal, F.; Qidwai, T.; Singh, D.; Pandey, P. K. *Journal of Molecular Catalysis B-Enzymatic* **2012**, *74*, 125-131.
(46) Saha, S.; Pal, A.; Kundu, S.; Basu, S.; Pal, T. *Langmuir* **2010**, *26*, 2885-2893.
(47) Barbucci, R.; Consumi, M.; Magnani, A. *Macromolecular Chemistry and Physics* **2002**, *203*, 1292-1300.
(48) Benavides, S.; Villalobos-Carvajal, R.; Reyes, J. E. *Journal of Food Engineering* **2012**, *110*, 232-239.
(49) Lee, K. Y.; Mooney, D. J. *Progress in Polymer Science* **2012**, *37*, 106-126.
(50) Lekka, M.; Sainz-Serp, D.; Kulik, A. J.; Wandrey, C. *Langmuir* **2004**, *20*, 9968-9977.
(51) Murata, Y.; Jinno, D.; Liu, D.; Isobe, T.; Kofuji, K.; Kawashima, S. *Molecules* **2007**, *12*, 2559-2566.
(52) Gotoh, T.; Matsushima, K.; Kikuchi, K.-I. *Chemosphere* **2004**, *55*, 57-64.
(53) Kong, H. J.; Kaigler, D.; Kim, K.; Mooney, D. J. *Biomacromolecules* **2004**, *5*, 1720-1727.

(54) Rees, D. A. *Pure and Applied Chemistry* **1981**, *53*, 1-14.
(55) Pawar, S. N.; Edgar, K. J. *Biomaterials* **2012**, *33*, 3279-3305.
(56) Yeom, C. K.; Jegal, J. G.; Lee, K. H. *Journal of applied polymer science* **1996**, *62*, 1561-1576.
(57) Kulkarni, A. R.; Soppimath, K. S.; Aminabhavi, T. M.; Dave, A. M.; Mehta, M. H. *Journal of Controlled Release* **2000**, *63*, 97-105.
(58) Yeom, C. K.; Lee, K. H. *Journal of applied polymer science* **1998**, *67*, 209-219.
(59) You, J.-O.; Rafat, M.; Auguste, D. T. *Langmuir* **2011**, *27*, 11282-11286.
(60) Gattas-Asfura, K. M.; Stabler, C. L. *Biomacromolecules* **2009**, *10*, 3122-3129.
(61) Patil, J. S.; Kamalapur, M. V.; Marapur, S. C.; Kadam, D. V. *Digest Journal of Nanomaterials and Biostructures* **2010**, *5*, 241-248.
(62) Pruesse, U.; Bilancetti, L.; Bucko, M.; Bugarski, B.; Bukowski, J.; Gemeiner, P.; Lewinska, D.; Manojlovic, V.; Massart, B.; Nastruzzi, C.; Nedovic, V.; Poncelet, D.; Siebenhaar, S.; Tobler, L.; Tosi, A.; Vikartovska, A.; Vorlop, K.-D. *Chemical Papers* **2008**, *62*, 364-374.
(63) Bugarski, B.; Li, Q. L.; Goosen, M. F. A.; Poncelet, D.; Neufeld, R. J.; Vunjakg *Aiche Journal* **1994**, *40*, 1026-1031.
(64) Nedovic, V.; Manojlovic, V.; Prusse, U.; Bugarske, B.; Vorlop, K. **2006**, *12*, 53-57.
(65) Anilkumar, A. V.; Lacik, I.; Wang, T. G. *Biotechnology and Bioengineering* **2001**, *75*, 581-589.
(66) Herrero, E. P.; Del, V. E. M. M.; Galan, M. A. *Chemical Engineering Journal* **2006**, *117*, 137-142.
(67) Watanabe, H.; Matsuyama, T.; Yamamoto, H. *Biochemical Engineering Journal* **2001**, *8*, 171-174.
(68) Kwok, K. K.; Groves, M. J.; Burgess, D. J. *Pharmaceutical Research* **1991**, *8*, 341-344.
(69) Poncelet, D.; Babak, V.; Dulieu, C.; Picot, A. *Colloids and Surfaces A: Physicochemical and Engineering Aspects* **1999**, *155*, 171-176.
(70) Hurteaux, R.; Edwards-Levy, F.; Laurent-Maquin, D.; Levy, M. C. *European Journal of Pharmaceutical Sciences* **2005**, *24*, 187-197.
(71) Gomez, C. G.; Rinaudo, M.; Villar, M. A. *Carbohydrate Polymers* **2007**, *67*, 296-304.
(72) Duval, J. M.; Delestre, C.; Carre, M. C.; Hubert, P.; Dellacherie, E. *Carbohydrate Polymers* **1991**, *15*, 233-242.
(73) Kim, Y. S.; Kim, H. W.; Lee, S. H.; Shin, K. S.; Hur, H. W.; Rhee, Y. H. *International Journal of Biological Macromolecules* **2007**, *41*, 36-41.
(74) Kim, H. W.; Kim, B. R.; Rhee, Y. H. *Carbohydrate Polymers* **2010**, *79*, 1057-1062.
(75) Krysinski, J.; Placzek, J.; Skrzypczak, A.; Blaszczak, J.; Predki, B. *QSAR and Combinatorial Science* **2009**, *28*, 995-1002.
(76) Pelletier, S.; Hubert, P.; Lapicque, F.; Payan, E.; Dellacherie, E. *Carbohydrate Polymers* **2000**, *43*, 343-349.
(77) Valle, F. D.; Romeo, A.; Fidia S.p.A: United States, **1990**; Vol. 4965353.
(78) Ghahramanpoor, M. K.; Najafabadi, S. A. H.; Abdouss, M.; Bagheri, F.; Eslaminejad, M. B. *Journal of Materials Science-Materials in Medicine* **2011**, *22*, 2365-2375.

(79) Yang, L. Q.; Zhang, B. F.; Wen, L. Q.; Liang, Q. Y.; Zhang, L. M. *Carbohydrate Polymers* **2007**, *68*, 218-225.
(80) Sarker, D. K.; Wilde, P. J. *Colloids and Surfaces B-Biointerfaces* **1999**, *15*, 203-213.
(81) Sinquin, A.; Hubert, P.; Marchal, P.; Choplin, L.; Dellacherie, E. *Colloids and Surfaces a-Physicochemical and Engineering Aspects* **1996**, *112*, 193-200.
(82) Sinquin, A.; Hubert, P.; Dellacherie, E. *Polymer* **1994**, *35*, 3557-3560.
(83) Galant, C.; Kjoniksen, A. L.; Nguyen, G. T. M.; Knudsen, K. D.; Nystrom, B. *Journal of Physical Chemistry B* **2006**, *110*, 190-195.
(84) Andreeva, D. V.; Gorin, D. A.; Shchukin, D. G.; Sukhorukov, G. B. *Macromolecular Rapid Communications* **2006**, *27*, 931-936.
(85) Edwards-Levy, F.; Levy, M. C. *Biomaterials* **1999**, *20*, 2069-2084.
(86) Callewaert, M.; Laurent-Maquin, D.; Edwards-Levy, F. *International Journal of Pharmaceutics* **2007**, *344*, 161-164.
(87) Dai, Y.-N.; Li, P.; Zhang, J.-P.; Wang, A.-O.; Wei, Q. *Journal of Biomedical Materials Research Part B-Applied Biomaterials* **2008**, *86B*, 493-500.
(88) George, M.; Abraham, T. E. *Journal of Controlled Release* **2006**, *114*, 1-14.
(89) Wu, D.; Zhang, L.; Wang, L.; Zhu, B.; Fan, L. *Journal of Chemical Technology and Biotechnology* **2011**, *86*, 345-352.
(90) Saha, N.; Saarai, A.; Roy, N.; Kitano, T.; Saha, P. *Journal of Biomaterials and Nanobiotechnology*, **2011**, *2*, 85-90.
(91) Wang, Q.; Wang, W.; Wu, J.; Wang, A. *Journal of applied polymer science* **2012**, *124*, 4424-4432.
(92) Aminabhavi, T. M.; Patil, M. B.; Bhat, S. D.; Halgeri, A. B.; Vijayalakshmi, R. P.; Kumar, P. *Journal of applied polymer science* **2009**, *113*, 966-975.
(93) Chan, W.-C.; Chang, S.-C. *Journal of applied polymer science* **2011**, *120*, 1782-1787.
(94) Mikhalovsky, S. V.; Nikolaev, V. G. *Interface Science and Technology* **2006**, *7*, 529-561.
(95) Garrido-Herrera, F. J.; Gonzalez-Pradas, E.; Fernandez-Perez, M. *Journal of Agricultural and Food Chemistry* **2006**, *54*, 10053-10060.
(96) Surdo, E. M.; Khan, I. A.; Choudhury, A. A.; Saleh, N. B.; Arnold, W. A. *Journal of Hazardous Materials* **2011**, *188*, 334-340.
(97) Sokker, H. H.; Gad, Y. H.; Ismail, S. A. *Journal of applied polymer science* **2009**, *114*, 149-156.
(98) Hsieh, M.-F.; Wen, H.-W.; Shyu, C.-L.; Chen, S.-H.; Li, W.-T.; Wang, W.-C.; Chen, W.-C. *Journal of Biomedical Materials Research Part A* **2010**, *94A*, 1133-1140.
(99) Khoder, M.; Tsapis, N.; Huguet, H.; Besnard, M.; Gueutin, C.; Fattal, E. *International Journal of Pharmaceutics* **2009**, *379*, 251-259.
(100) Williams, L. B.; Haydel, S. E.; Ferrell, R. E., Jr. *Elements* **2009**, *5*, 99-104.
(101) Murray, H. H. *Acta Geodynamica et Geomaterialia* **2005**, *2*, 127-134.
(102) Ely, A.; Baudu, M.; Basly, J.-P.; Kankou, M. O. S. A. O. *Journal of Hazardous Materials* **2009**, *171*, 405-409.
(103) Ely, A.; Baudu, M.; Kankou, M. O. S. A. O.; Basly, J.-P. *Chemical Engineering Journal* **2011**, *178*, 168-174.
(104) Cornelia, M.; Maicaneanu, A.; Indolean, C.; Burca, S.; Stanca, M. *Studia Universitatis Babes-Bolyai Chemia* **2010**, *55*, 115-123.

(105) Fernández-Pérez, M.; González-Pradas, E.; Villafranca-Sánchez, M.; Flores-Céspedes, F. *Chemosphere* **2001**, *43*, 347-353.
(106) Gonzalez-Pradas, E.; Fernandez-Perez, M.; Villafranca-Sanchez, M.; Martinez-Lopez, F.; Flores-Cespedes, F. *Pesticide Science* **1999**, *55*, 546-552.
(107) Yurdasiper, A.; Sevgi, F. *Journal of Chemical and Pharmaceutical Research* **2010**, *2*, 704-721.
(108) Tonnesen, H. H.; Karlsen, J. *Drug Development and Industrial Pharmacy* **2002**, *28*, 621-630.
(109) Kevadiya, B. D.; Joshi, G. V.; Patel, H. A.; Ingole, P. G.; Mody, H. M.; Bajaj, H. C. *Journal of Biomaterials Applications* **2010**, *25*, 161-177.
(110) Wu, Z.; Guo, L.; Qin, S.; Li, C. *Journal of Industrial Microbiology Biotechnology* **2012**, *39*, 317-327.
(111) Vancov, T.; Jury, K. *Advances Environmental Research* **2012**, *6*, 377-398.
(112) Tayyebi, A.; Khanchi, A.; Ghofrani, M. B.; Outokesh, M. *Separation Science and Technology* **2010**, *45*, 288-298.
(113) Vorlop, K. D.; Steinert, H. J.; Klein, J. *Annals of the New York Academy of Sciences* **1987**, *501*, 339-342.
(114) Chtchigrovsky, M.; Lin, Y.; Ouchaou, K.; Chaumontet, M.; Robitzer, M.; Quignard, F.; Taran, F. *Chemistry of Materials* **2012**, *24*, 1505-1510.
(115) Jouannin, C.; Dez, I.; Gaumont, A. C.; Taulemesse, J. M.; Vincent, T.; Guibal, E. *Applied Catalysis B: Environmental* **2011**, *103*, 444-452.
(116) Amtul, Z.; Kausar, N.; Follmer, C.; Rozmahel, R. F.; Rahman, A. U.; Kazmi, S. A.; Shekhani, M. S.; Eriksen, J. L.; Khan, K. M.; Choudhary, M. I. *Bioorganic & Medicinal Chemistry* **2006**, *14*, 6737-6744.
(117) Naidu, R. *Chemical Bioavailability in Terrestial Environments, p.342-343*; Elsevier, **2008**; Vol. 32.
(118) Borlaug, N.; Krishnamurthy, V. N.; Gowariker, S.; Dhanorkar, M.; paranjape, K. *The Fertilizer Encyclopedia, p.712*; Wiley, **2009**.
(119) Gill, J. S.; Bijay, S.; Khind, C. S.; Yadvinder, S. *Nutrient Cycling in Agroecosystems* **1999**, *53*, 203-207.
(120) Douglass, E. A.; Hendrickson, L. L. *Journal of Agricultural and Food Chemistry* **1991**, *39*, 2318-2321.
(121) Font, M.; Dominguez, M. J.; Sanmartin, C.; Palop, J. A.; San-Francisco, S.; Urrutia, O.; Houdusse, F.; Garcia-Mina, J. M. *Journal of Agricultural and Food Chemistry* **2008**, *56*, 8451-8460.
(122) Manunza, B.; Deiana, S.; Pintore, M.; Gessa, C. *Soil Biology & Biochemistry* **1999**, *31*, 789-796.
(123) Varel, V. H.; Nienaber, J. A.; Freetly, H. C. *Journal of Animal Science* **1999**, *77*, 1162-1168.
(124) Lara, H. H.; Garza-Trevino, E. N.; Ixtepan-Turrent, L.; Singh, D. K. *Journal of Nanobiotechnology* **2011**, *9*, 30.
(125) Gangadharan, D.; Harshvardan, K.; Gnanasekar, G.; Dixit, D.; Popat, K. M.; Anand, P. S. *Water Research* **2010**, *44*, 5481-5487.
(126) Liu, Y.; Liu, X.; Wang, X.; Yang, J.; Yang, X.-J.; Lu, L. *Journal of applied polymer science* **2010**, *116*, 2617-2625.
(127) Rivas, B. L.; Pereira, E. D.; Moreno-Villoslada, I. *Progress in Polymer Science* **2003**, *28*, 173-208.

(128) Lansdown, A. B. *Silver in Healthcare its Antimicrobial Efficacy and Safety in Use*, **2012**.
(129) Dutta, S.; Shome, A.; Kar, T.; Das, P. K. *Langmuir* **2011**, *27*, 5000-5008.
(130) Sawada, I.; Fachrul, R.; Ito, T.; Ohmukai, Y.; Maruyama, T.; Matsuyama, H. *Journal of Membrane Science* **2012**, *387-388*, 1-6.
(131) Jun, B.-H.; Byun, J.-W.; Kim, J. Y.; Kang, H.; Park, H.-J.; Yoon, J.; Lee, Y.-S. *Journal of Materials Science* **2010**, *45*, 3106-3108.

Chapter 2:

Experimental

2.1 Introduction

The experimental techniques and procedures employed in this study are outlined in this Chapter. The various materials and methods used throughout this work are described in detail. A range of analytical techniques were used to obtain data on each of the polymers. A brief description of the theoretical background for each of the different experimental techniques is also provided. Firstly, a description of how alginate beads can be used to encapsulate and release the inhibitor *N*-(*n*-butyl)thiophosphoric triamide (NBPT) will be discussed. The techniques used in the preparation of the polymer samples are introduced in this chapter and general information about the characterisation of the samples is presented. Secondly, the preparation of different calcium alginate beads to make polymer supports in which silver can be incorporated; resulting in beads with antimicrobial properties will be discussed.

The present research is concerned with the polymer sodium alginate, a naturally occurring biocompatible and biodegradable polysaccharide, which is soluble in aqueous solution and in the presence of $CaCl_2$ has the ability to form hydrogels.[1] For these reasons sodium alginate was chosen to form the hydrogel beads. Hydrogels are three dimensional polymer networks capable of absorbing large amounts of fluid.[2] When hydrogels absorb water the pores in the polymer network expand allowing encapsulated molecules to diffuse out through them. The ability of molecules of different size to diffuse into and out of hydrogels permits the use of hydrogels as delivery systems. In the present study beads were crosslinked with an ionic or covalent crosslinker and loaded with either (a) silver in the +1 or 0 oxidation state or (b) the urease inhibitor, NBPT.

The first part of this research was concerned with the preparation, characterisation and monitoring the release properties of NBPT from different calcium alginate beads. The urease inhibitor, NBPT can reduce ammonia losses from livestock waste by restricting the conversion of urea and urine to ammonium.[3] Four different polymeric beads were studied in this section namely (a) sodium alginate beads, which were crosslinked with calcium ions, (b) sodium alginate beads, which were crosslinked with calcium ions and loaded with charcoal, (c) sodium alginate beads, which were crosslinked with calcium ions and loaded with bentonite

and (d) sodium alginate beads, which were crosslinked with calcium ions and coated with a layer of polypyrrole. The properties of the beads such as their surface morphology, pore size and swelling behaviour was investigated. Each type of bead was loaded with the urease inhibitor, NBPT. The stability of the NBPT as a function of pH and within the bead matrices was investigated using NMR spectroscopy. The release of NBPT into aqueous solution was monitored using UV/Vis spectroscopy.

The second part of this study was a study of the antimicrobial activity of silver impregnated polymer beads. The three different polymeric bead supports used in the antimicrobial study were (a) sodium alginate beads, which were crosslinked with calcium ions, (b) propylene glycol alginate/ sodium alginate composite (PGA) beads which were crosslinked with calcium ions and additionally covalently crosslinked with human serum albumin (HSA) (c) alginate functionalised with propyloctadecyldimethylammonium groups/sodium alginate composite (TSA) beads, which were ionically crosslinked with calcium ions. Ionic silver was first encapsulated into the different types of alginate beads, and then the silver ions were reduced to metallic silver to obtain a second oxidation state of silver. The antimicrobial activity derives from two possible mechanisms of action; firstly, silver can be released from the polymer support and secondly, the polymer can kill microbes which come into contact with it.[4] The polymer beads were then assessed for their ability to encapsulate silver(I) and silver(0) and to slowly release them over time. The amount of silver incorporated into the different polymeric networks varied with the concentration of silver nitrate solution the beads were immersed in and the nature of polymers. The surface morphology and swelling behaviour of the different polymeric beads was also examined. All polymers were assessed for their ability to inhibit the growth or kill of one species of fungi *Candida albicans* (ATCC 10231) and they were also tested against five different strains of bacteria, namely (a) *Staphyloccoccus aureus*, (b) methicillin resistant *Staphyloccoccus aureus* (MRSA) (c) *Pseudonomas aeruginosa* (ATCC 27853), (d) *Pseudonomas aeruginosa* (ATCC 10145), and (e) *Escherichia coli* (*E.coli).*

2.2 Chemicals and Preparation of Beads

2.2.1 Chemicals for Preparation of a Delivery System for Agrochemicals

Unless otherwise stated, all chemicals and solvents used in this work were purchased from Sigma Aldrich. Reagents and solvents were reagent grade and used without further purification and supplied from commercial sources. The alginic acid (sodium salt) with a viscosity of 20-40 cps 1% in H_2O was purchased from Sigma Aldrich. Pyrrole was purchased from Sigma Aldrich, it was distilled under vacuum and stored in the freezer at -20°C. *N*-(*n*-butyl)thiophosphoric triamide (NBPT) was purchased from Apollo Scientific and stored in the fridge at -4°C. Propylene glycol alginate was purchased from Wako chemicals. The sodium alginate gelling, crosslinking and release solutions were prepared in Millipore deionised water.

2.2.2 Chemicals for the Preparation of Biological Preparations – *Candida albicans*

Candida ATCC 10231 was obtained from the American Type Culture Collection (ATCC), Manassas, VA, USA. Yeast Extract Peptone Dextrose (YEPD) media was composed of 2% (w/v) glucose, 2% (w/v) bacteriological peptone and 1% (w/v) yeast extract. To solidify the media to make agar plates 2% (w/v) bacteriological agar was added to the above mixture when required. Deionised water was used to make up all media. Silver nitrate (ACS reagent grade) was purchased from Sigma Aldrich and varying concentrations were made up by dissolving the required amount in deionised water. The silver nitrate solutions were kept in the dark at all times. Sodium borohydride (purum grade) was purchased from Sigma Aldrich and this was used as the reducing agent to form silver in the zero oxidation state. Calibration grade silver nitrate (99.9999%) was obtained from Sigma Aldrich for atomic absorption spectroscopy.

2.2.3 Chemicals for the Preparation of Biological Preparations – Bacteria

Chemicals were purchased from commercial sources and were used without further purification. Deionised water was used to make up all media. The nutrient broth medium containing peptone, yeast extract and nutrient agar was purchased from Scharlau Microbiology and made up using the manufacturer's instructions in

sterilised water (13 g in 1 L of deionised water). *Escherichia coli* (*E.coli)* were supplied as a clinical isolate by the Clinical Microbiology Laboratory, St. James' Hospital, Dublin, Ireland and were originally isolated from a Gastro-intestinal tract infection. *Staphylococcus aureus* was supplied as a clinical isolate by the Clinical Microbiology Laboratory, St. James' Hospital, Dublin, Ireland and was originally isolated from a Urinary tract infection. Methicillin resistant *Staphyloccoccus aureus* (MRSA) was obtained as a clinical isolate from Microbiologics, North St. Cloud Mn, USA and was originally isolated from a wound infection. *Pseudonomas aeruginosa* 27853 and 10145 were both obtained from the American Type Culture Collection (ATCC) Marassas, VA, USA.

2.3 Preparation of Hydrogel Beads

The alginate hydrogels were formed as spherical beads. This form was chosen as it is necessary to ensure good uniformity and reproducibility of the size of the hydrogel delivery system. Reproducibility is important in order to quantitatively compare the amount and release rate of the encapsulated compound and to assess the antimicrobial behaviour of the beads.

2.3.1 Preparation of Calcium Alginate Hydrogel Beads

2.3.1 (a) Preparation of Calcium Alginate Hydrogel Beads for release of NBPT

The calcium alginate hydrogel beads were prepared using adaptations of literature procedures.[5-7] Standardly, the beads were prepared by adding alginic acid sodium salt (2 g) slowly, with mixing, to 100 ml of deionised water (2% w/v). This particular concentration of the alginate solution gave the viscosity that was necessary for the production of spherical droplets. If the alginate solution was too viscous, it would adhere onto the tip of the syringe for longer leading to the production of beads with tails. If the alginate solution was not viscous enough, the solution would flow out of the syringe too rapidly, therefore not allowing beads to form. It is necessary for the alginate solution to adhere to the tip of the syringe for the correct amount of time to allow the formation of beads. The resulting viscous solution was placed in a syringe (30 ml), equipped with a needle (0.8 mm diameter), and then added drop

wise into a 100 ml of $CaCl_2$ solution (0.25 M). The smooth and spherical beads were formed under magnetic stirring for 30 min. The Ca^{2+} ions hold the chains of the alginate together through electrostatic attractions to form the hydrogel beads. For optimum bead formation the distance between the $CaCl_2$ solution and the bottom of the needle was fixed at 60 mm and the drop rate was maintained at 0.2 ml/min. Freshly formed beads (n = 500) were kept immersed in $CaCl_2$ solution for 24 h to allow diffusion of more Ca^{2+} ions inside the beads. The beads were removed from the $CaCl_2$ solution by filtration and repeatedly washed with deionised water to remove excess $CaCl_2$ solution. These beads were stored in deionised water for short term storage, and in air tight containers for long term storage.

2.3.1 (b) Preparation of Calcium Alginate Hydrogel Beads for Antimicrobial Testing

To form control beads for comparison with the beads containing the propyloctadecyldimethlyammonium chloride groups, 4 g of sodium alginate was slowly added with mixing to 100 ml of deionised water (4% w/v). The resulting solution was added drop wise from a syringe (30 ml) with no needle attached, into a 100 ml $CaCl_2$ solution (5% w/v). The spherical beads were formed under magnetic stirring for 30 min. The distance between the $CaCl_2$ solution and the bottom of the syringe was fixed at 60 mm and the drop rate was maintained at 0.2 ml/min. Freshly formed beads (n = 500) were kept immersed in $CaCl_2$ solution for 24 h. The beads were removed from the $CaCl_2$ solution by filtration and repeatedly washed with deionised water to remove any excess $CaCl_2$ solution. These beads were stored in deionised water for further use. All other calcium alginate hydrogel beads for antimicrobial testing were formed using the same procedure outlined above with the exception that 2 g of sodium alginate was added to 100 ml of deionised water to make a 2 % w/v solution. No needle was attached to the syringe when beads were been formed.

2.3.2 Preparation of Alginate Hydrogel Beads containing Inorganic Fillers

These beads were formed using variations of published procedures to make alginate beads containing inorganic fillers.[7-11] Formulations were made up in 100 ml of deionised water containing sodium alginate (2% w/v) and bentonite (4 % w/v) or

charcoal (5% w/v). These mixtures were vigorously stirred for 24 h. The resulting viscous mixture was placed in a syringe (30 ml), with no needle attached and then added drop wise into 100 ml of $CaCl_2$ (0.25 M) solution. The spherical beads were formed under magnetic stirring for 30 min. The addition of bentonite or activated charcoal to the alginate formulation led to larger and heavier beads. The distance between the $CaCl_2$ solution and the bottom of the syringe was fixed at 60 mm and the drop rate was maintained at 0.2 ml/min. Freshly formed beads (n = 350) were kept immersed in $CaCl_2$ solution for 24 h. The beads were removed from the $CaCl_2$ solution by filtration and repeatedly washed with deionised water to remove excess $CaCl_2$ solution. These beads were stored in deionised water for further use.

2.3.3 Preparation of Alginate Hydrogel Beads Coated with Polypyrrole

Sodium alginate hydrogel beads (2% w/v) were made as described in Section 2.3.1. The method used to coat the beads with polypyrrole was based on the procedure outlined by Andreeva *et al.*[12] Wet hydrogel beads (n = 20) were placed in an aqueous solution of 0.5 M $FeCl_3$ (10 ml) solution for 15 min, after which they were filtered and washed repeatedly with deionised water to remove any excess of the oxidant. The beads had changed from a yellow colour to a dark orange colour. These beads were then placed into 0.5 ml of a pyrrole solution. The beads turned black immediately on contact with the pyrrole. They were left in this solution for 15 min to allow polymerisation to occur. They were then filtered and washed with deionised water to remove any of the excess polypyrrole from the surface. The beads were stored in their hydrogel state in an air tight stoppered container which was covered with tin foil until further use.

2.3.4 Preparation of Propylene Glycol Alginate beads/ Alginate Composite (PGA) Beads

Propylene glycol alginate is a partially esterified derivative formed from the reaction between propylene oxide and alginic acid in which approximately 70% of the carboxylic groups are esterified with propylene glycol.[13] The beads were formed according to the method developed by Edwards-Levy *et al.*[14] Alginic acid sodium salt (1% w/v) was dissolved in deionised water. Propylene glycol alginate (2% w/v) was added to the alginate solution and then the HSA (5 ml) was added to the mixture

(5% v/v). This mixture was left stirring at room temperature for 24 h. The resulting viscous solution was placed in a syringe (30 ml), and then added drop wise into 100 ml $CaCl_2$ solution (10% w/v). The beads (n = 350) were formed under magnetic stirring for 30 min. For optimum bead formation the distance between the $CaCl_2$ solution and the bottom of the syringe was fixed at 60 mm and the drop rate was maintained at 0.2 ml/min. The beads were filtered and washed repeatedly with deionised water; at this stage they were opaque in appearance. A fresh 0.025 M sodium hydroxide solution was made up. Beads were placed into this solution with constant stirring for 15 min. The beads changed to a white colour instantaneously upon contact with the sodium hydroxide solution, due to the reaction of the HSA with the PGA in the basic solution. The beads were filtered and placed into a pH 7 buffer solution for 15 min. They were then filtered and washed repeatedly with deionised water to remove any excess solution on the surface. The beads were kept in their hydrogel state by storing them in deionised water.

2.3.5 Preparation of Quaternary Ammonium Alginate /Alginate Composite (TSA) Hydrogel Beads

2.3.5 (a) With Chloride as the Counterion

Alginate containing quaternary ammonium groups can be easily prepared by the reaction of sodium alginate with 3-(trimethoxysilyl)-propyloctadecyldimethylammonium chloride in acid solution. This reaction anchors the quaternary ammonium group to the polymer backbone by a covalent non-hydrolysable bond.[12] Alginate beads were prepared according to the method developed by Kim *et al.*[15] Sodium alginate (4 g) was added slowly with mixing to 100 ml of deionised water (4% w/v). 3-(trimethoxysilyl)-propyloctadecyldimethylammonium chloride (0.02 M) was added to the alginate solution, the solution started to change in colour. Acetic acid (0.8M) was added to the mixture to reduce the pH down to a pH of 4 at room temperature. The solution changed from a pale yellow colour to a milky white colour. This solution was left stirring for 24 h. The resulting viscous solution was placed in a syringe (30 ml), with no needle attached and then the solution was dropped in to 100 ml of a $CaCl_2$ solution (5% w/v). The smooth and spherical beads were formed under magnetic

stirring for 30 min. The distance between the $CaCl_2$ solution and the bottom of the syringe was fixed at 60 mm and the drop rate was maintained at 0.2 ml/min for optimum bead formation. Freshly formed beads (n = 350) were kept immersed in $CaCl_2$ solution for 24 h. The beads were removed from the $CaCl_2$ solution by filtration and repeatedly washed with deionised water to remove any excess $CaCl_2$ solution. These beads were stored in deionised water for further use.

2.3.5 (b) With Nitrate as the Counterion

Before silver ions could be incorporated into quaternary ammonium alginate/alginate composite beads the chloride counterions associated with the quaternary ammonium groups were exchanged for nitrate ions to reduce the formation of silver chloride and so enable the silver ions to be incorporated into the beads. The composite beads were placed into an ion exchange tube and washed continuously with nitric acid (0.05 M), until there was no more chloride present. Scanning Electron Microscopy (SEM) and Energy Dispersive X-ray (EDX) analysis were recorded showing the presence and absence of chloride in the beads before and after washing with nitric acid.

Changes in the chemical structure of the TSA beads were investigated using FTIR spectroscopy, CHN and EDX analysis. FTIR spectra, CHN analyses, and EDX spectra were recorded of the starting materials and the dried powdered product. FTIR spectra and elemental analyses were performed on dehydrated samples of the TSA composite alginate beads and the calcium alginate beads (as formed in Section 2.3.1(b)). The hydrogel beads were crushed when wet, and were then dried in an oven at 37 ± 1°C to ensure most of the moisture was removed from the beads.

The FTIR spectrum recorded of the TSA composite beads showed two bands at 908 and 1100 cm^{-1} band which were not present in the spectrum recorded of the calcium alginate beads. These bands were assigned as arising from the Si-O and the Si-O-C stretches respectively.[16] In addition the bands at 2920 and 2851 cm^{-1} which are assigned as arising from the C-H stretching modes of alkyl groups[17] had increased substantially in intensity compared to the analogous bands in the recorded spectrum of the calcium alginate beads. These finding are consistent with the attachment of the 3-(dimethoxysilyl)-propyloctadecyldimethylammonium chloride group to the alginate chain.

The results for the elemental analyses on the samples are given in Table 2.1. The results show that there was no nitrogen present in the alginate beads made in section 2.3.1(b) but there was nitrogen present in the TSA composite beads. Moreover, the %C and %H in the TSA beads had increased compared to that determined the calcium alginate beads. Both these findings are consistent with the attachment of an ammonium group containing a long alkyl chain onto the alginate backbone.

Table 2.1: CHN Analyses on the Calcium Alginate and Quaternary Ammonium Alginate/Alginate Composite Beads

	Element	Experimental Results (%)	
		Run 1	Run 2
Alginate beads	Nitrogen	-	-
	Carbon	21.91	22.13
	Hydrogen	4.29	4.34
Quaternary ammonium alginate/alginate composite beads	Nitrogen	1.62	1.67
	Carbon	41.69	42.30
	Hydrogen	7.65	7.63

2.4 Loading of Beads

2.4.1 Loading of Calcium Alginate Beads with NBPT

(i) Wet hydrogel beads

The prepared polymer beads were carefully removed from the deionised water in which they were stored. The wet beads (n = 100) were then immersed in a 0.05 M solution of the NBPT inhibitor (100 ml). The hydrogel beads were mechanically stirred at a rate of 25 rpm in the solution for a minimum of 24 h before the beads were used as a delivery system.

(ii) Dried hydrogel beads

The prepared polymer beads outlined above were removed from the deionised water in which they were contained. The beads were dried in an oven at 37 ± 1°C for 24 h. The dried beads (n = 100) were then immersed in a 0.05 M solution of the NBPT inhibitor (100 ml). The hydrogel beads were mechanically stirred at a rate of 25 rpm in the solution for a minimum of 24 h. The beads were then dried in an oven at 37 ± 1°C for 24 h before the beads were used as a delivery system.

(iii) Inhibitor incorporated with the polymer before crosslinking.

The sodium alginate (2 g) was mixed in 100 ml of deionised water (2% w/v) for 24 h to ensure the powder was fully dissolved and no clumps remained in the mixture. NBPT powder was then added to the mixture to give a 0.05 M NBPT solution. The resulting solution was placed in a syringe (30 ml), equipped with a needle (0.8 mm diameter), and then added drop wise into 100 ml of $CaCl_2$ solution (0.25 M). The resulting beads were used when wet as a delivery system or dried in the oven at 37 ± 1°C for 24 h before being used as a delivery system.

2.4.1.1 Loading of Alginate Hydrogel Beads Coated with Polypyrrole with NBPT

The alginate polymer beads (2% w/v) were made as described in Section 2.3.1. They were carefully removed from the deionised water they were stored in. The wet beads (n = 100) were then immersed in a 0.05 M solution of the NBPT inhibitor (100 ml). The hydrogel beads were mechanically stirred at a rate of 25 rpm in the solution for a minimum of 24 h. Wet hydrogel beads (n = 20) were placed in an aqueous solution of 0.5 M $FeCl_3$ (10 ml) solution for 15 min, after which they were then filtered and washed with deionised water to remove any excess of the oxidant. The beads had turned orange in colour. These beads were then placed into 0.5 ml of polypyrrole solution. The beads turned black immediately on contact with the polypyrrole. They were left in this solution for 15 min to allow polymerisation to occur. They were then filtered and washed with deionised water to remove any of the excess polypyrrole from the surface. The beads were stored in their hydrogel state in an air tight stoppered container which was covered with tin foil until further use.

2.4.2.1 Loading of Calcium Alginate Beads with Silver(I) Ions

The calcium alginate hydrogel beads were removed from the deionised water in which they were stored in by filtration. Silver nitrate solutions of the required concentration were made up in deionised water. The beads (n = 100) were immersed in a solution of silver nitrate (0.1 M, 0.01 M or 0.001 M) for 3 h. All solutions were kept in the dark and shaken continuously. The uptake of silver from the solution into the beads varied depending on the initial concentration of silver nitrate solution used. The beads were then washed with deionised water to remove any silver ion residues on the surface of the beads. The percentage of silver encapsulated in the calcium alginate beads was estimated using Atomic Absorption (AA) spectroscopy.

2.4.2.2 Loading of Propylene Glycol Alginate /Alginate Composite Beads with Silver(I) Ions

The Propylene glycol alginate /alginate composite hydrogel beads were removed from the deionised water by filtration. Silver nitrate solutions of the required concentration were made up in deionised water. The beads (n = 100) were immersed in solution of silver nitrate (0.1 M or 0.01 M) for 3 h. All solutions were kept in the dark and shaken continuously. The uptake of silver from the solution into the beads varied depending on the initial concentration of silver nitrate solution used. The beads were then washed with deionised water to remove any silver ion residues on the surface of the beads. The percentage of silver encapsulated into the propylene glycol alginate/alginate composite was estimated using atomic AA spectroscopy.

2.4.2.3 Loading of Quaternary Ammonium Alginate/Alginate Composite Hydrogel Beads with Silver(I) Ions

The quaternary ammonium alginate/alginate composite hydrogel beads were filtered from the deionised water that they were stored in. Silver nitrate solutions of the required concentrations were made up in deionised water. The beads (n = 100) were immersed in a solution of silver nitrate (0.1 M or 0.01 M) for 24h with constant shaking. All solutions were kept in the dark. The uptake of silver from the solution into the beads varied depending on the initial concentration of silver nitrate solution used. The beads were then washed with deionised water to remove any silver ion residues on the surface of the beads. The percentage of silver encapsulated in the

quaternary ammonium alginate/alginate composite hydrogel beads was estimated using AA spectroscopy.

2.4.3 Reducing Silver(I) to Silver(0) within the Hydrogel Beads

Silver in its metallic state does not exhibit any antimicrobial activity, but it reacts with the moisture in the skin and the fluid of the wound and becomes ionised. The ionised silver is highly reactive, as it binds to tissue proteins and results in structural changes in micro-organisms.[18-20] Silver(0) particles were prepared via a chemical reduction method using aqueous sodium borohydride. Calcium alginate beads and propylene glycol alginate beads/alginate composite beads containing silver(I) ions were immersed into a solution of 0.1 M sodium borohydride. All solutions were kept in the dark to ensure that the reduction of silver was due to the sodium borohydride and not as a result of sunlight on the beads. Deionised water was used for all solutions. The beads were kept in the sodium borohydride solution for 1 h and were continuously agitated by the generation of the hydrogen bubbles which were formed in the reaction. The beads which had previously been immersed in the 0.1 M silver nitrate solution turned brown indicating that the reduction was successful. The beads which had been immersed in the lower concentrations of silver nitrate darkened in colour and brown speckles were visible throughout the beads which also indicated that reduction of the silver(I) had taken place. The beads were washed with deionised water to remove excess borohydride adhering to the surface of the beads. The beads were subsequently stored in air tight containers to keep them in the hydrogel state.

The quaternary ammonium alginate/alginate composite hydrogel beads containing silver(I) ions were also immersed into a solution of 0.1 M sodium borohydride, under the same conditions as outlined above. However, when the reaction with sodium borohydride to reduce the silver within the beads was attempted, an exothermic process took place and a substantial amount of hydrogen gas was released which caused the beads to disintegrate slowly in solution. Therefore no studies were carried out on these beads containing silver in the zero oxidation state.

2.5 Dehydration of Alginate Hydrogel Beads

2.5.1 Oven drying

In order to remove the deionised water from the interior of the beads, they were placed in an oven set to 37 ± 1°C for a minimum of 24 h. The beads were weighed repeatedly over this time until there was no further reduction in weight.[21,22] At this time, most of the water had left the beads and they were no longer considered 'hydrogels'. The dehydrated alginate beads are referred to as alginate 'xerogel' beads.[23]

2.5.2 Freeze drying

Freeze drying was performed on beads formed in Sections 2.3.1(a) and 2.3.3. The hydrogel beads were filtered out of the water and blotted with filter paper to remove any excess liquid that was adhering to the surface of the beads. The hydrogel beads (n = 30) were placed into a 50 ml round bottom flask. The flask was then placed in liquid nitrogen to freeze the beads instantaneously while keeping them in their swollen state. The flask was then placed into an ice/salt bath which was kept at -20 ± 1°C. The beads were placed under vacuum at a pressure of 2×10^{-2} mBar and maintained at this pressure and temperature (-20 ± 1°C) for 8 h. The freeze dried xerogels were mounted on SEM stubs and the microstructure of the surface of the freeze dried gels was imaged using a scanning electron microscope. SEM micrographs were used to determine pore size of swollen hydrogels and also provide information about the morphology of the gels.

2.6 Analysis of NBPT release from the beads

UV-Visible spectroscopy was used to monitor the rate of release of the inhibitor molecule from the beads. An ultraviolet spectrometer operates by comparing the amount of light transmitted through the sample with the amount of light transmitted through the reference sample. The sample to be tested is placed in a quartz cell, and a sample of the solvent (water) is placed in a reference cell. Passing the reference beam through the reference cell compensates for any absorption of light by the solvent.[24] The wavelength of maximum absorbance is called the λ_{max}. At this fixed wavelength, the absorbance changes in accordance with concentration. From the structure of NBPT (Figure 1.10), it can be seen that the chemical group capable of light absorption i.e. the chromophore is the P=S. The urease inhibitor N-(n-butyl) thiophosphoric triamide (NBPT) has an absorbance band with a λ_{max} value at 212 nm in water (Figure 3.27). To determine the concentration of the inhibitor (NBPT) released for each experiment, a calibration curve was first prepared using NBPT concentrations ranging from 2.42×10^{-4} to 2.08×10^{-5} M. All samples were colourless, thus the absorption measurements were confined to the UV region of 190 – 400 nm. A typical calibration curve is shown in Figure 2.1. Spectra were obtained and analysed to calculate the amount of inhibitor released when beads were placed in aqueous solutions. The amount of the inhibitor released can be determined by measuring the absorbance at a particular wavelength and applying the Beer-Lambert law, Equation 2.1.[25]

$$A=\varepsilon lc \qquad \text{(Equation. 2.1)}$$

Where A is the absorbance, ε is the molar absorbtivity, c is the concentration of the compound in solution and l is the length of cell. From the linear relationship between concentration and absorbance a slope value can be obtained. The data was recorded and analysis was carried out using Microsoft Excel 2007 for Windows.

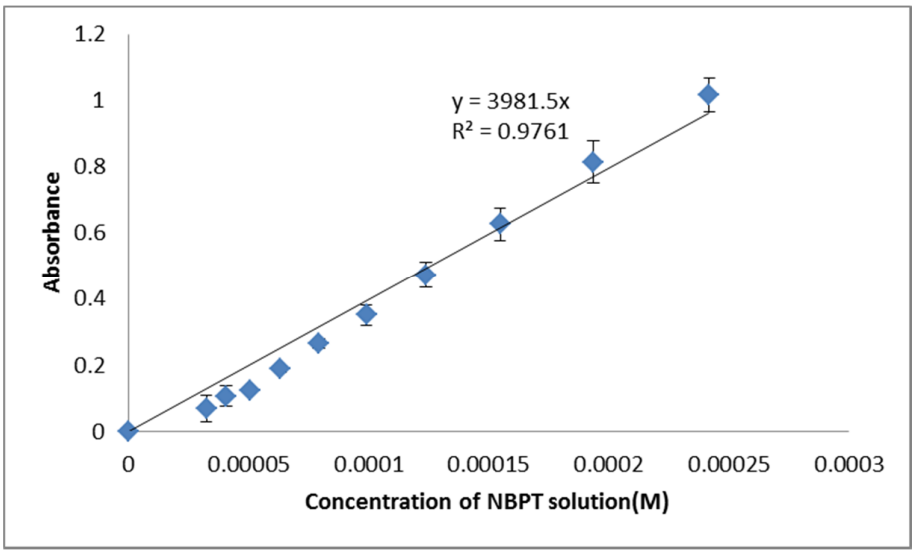

Figure 2.1: Calibration curve for NBPT dissolved in water. Absorbance was measured at λmax = 212 nm. The experiment was repeated in triplicate.

The NBPT release behaviour of the beads was analysed by calculating the amount of NBPT released at different intervals of time from 100 beads in 20 ml of release media (deionised water unless otherwise stated) at a temperature of 20 ± 1°C. To monitor the release of the inhibitor from the beads, 2.5 ml aliquots were sampled from the medium. The aliquots were returned to the solution after the spectrum was recorded to keep the concentration constant throughout. The concentration of the release solution was then calculated using the NBPT calibration curve (Figure 2.1). To examine the effect of agitation on the release behaviour of the inhibitor from the beads, the solution was stirred gently with a stirring bead.

2.7 Swelling Properties of Alginate Xerogel Beads

2.7.1 Determination of the Swelling Ratio (%)

The swelling ratio of the beads was studied by the measurement of the equilibrium swelling degree (ESD) which was calculated according to Equation 2.2.[26]

$$ESD\% = Ws - Wd / Wd \times 100 \qquad \text{(Equation 2.2)}$$

Where W*s* is the weight of swollen beads after filtration and W*d* is the dry weight of the hydrogel beads. ESD values for individual formulations of the beads were determined by measuring the extent of swelling of the beads in the different swelling media at 20 ± 1°C. The different swelling media used are deionised water, sodium chloride (1% w/v), HCl (pH = 4), and NaOH (pH = 9) solutions. Fully dried xerogels (n = 20) were weighed using a 4 figure balance. The water in the water bath was allowed to equilibrate to 20 ± 1°C before the swelling study was conducted. Swelling studies were conducted by placing the beads in 20 ml of swelling media at a temperature of 20 ± 1°C unless otherwise stated. To calculate their weight at a given time the beads were filtered using gravity filtration and extraneous water was removed using filter paper.[26,27] The beads were then weighed using a four figure balance.

2.8 Statistics analysis of results

The statistical significance of the microbe survival rates were analysed using two way anova method utilising GraphPad Prism software (version 5). Three categories of significance were used (***** = $p < 0.05$, ****** = $p < 0.01$, and ******* = $p < 0.001$).

2.9 Experimental Techniques

The analysis and characterisation of synthesised hydrogel beads were carried out using a scanning electron microscopy (SEM) and energy-dispersive X-ray (EDX) analysis. Atomic absorption (AA) spectroscopy was used to quantify both the amount of silver present in the different polymer networks and the amount of silver leached out of the different polymer networks. The NBPT release studies were monitored using a UV/Vis spectrometer. The stability of the NBPT in the alginate beads was monitored using ^{1}H NMR spectroscopy. Fourier transform infrared

spectroscopy (FTIR) and elemental analysis was used to confirm that a reaction between the sodium alginate and the 3-(dimethoxysilyl)-propyloctadecyldimethylammonium chloride had taken place. The size limits of the dried beads were determined using a Gilosonic auto sieve and also measured using an Olympus Microscope.

2.9.1 Scanning Electron Microscopy and Energy-Dispersive X-ray Analysis

Scanning Electron Microscopy (SEM) was carried out on a Hitachi S-3200-N with a tungsten filament electron source, maximum magnification of 300,000 and a resolution of 3.5 nm. This microscope was equipped with an Oxford Instrument INCAx-act EDX system with a silicon drift detector. The surfaces of the hydrogels were examined using SEM.

Scanning Electron Microscopy (SEM) is a type of electron microscope that is used to view and characterise solid materials on a micrometre (μm) to a nanometre (nm) scale.[28,29] Micrographs are formed by scanning a sample with a high energy beam of electrons which interact with atoms of the sample. This interaction emits X-rays, backscattered electrons, and secondary electrons which are collected by the detector and converted into an image.[29] The sample must be free from H_2O as the electrons expelled from the electron gun would vaporise the sample which would have an impact on the micrograph obtained. The SEM itself consists of an electron-optical column mounted on a vacuum chamber. The electron gun is placed on the top of the column and is typically a tungsten thermionic cathode. The electron beam is forced down the column and focused on the sample using magnetic lenses and scan coils. The brightness and contrast of the image generated is directly dependent on the surface topography. To improve the images obtained samples are often sputter coated with a thin layer of a noble metal, e.g. Au, which increases the number of secondary electrons emitted.

Energy Dispersive X-ray (EDX) allows the localised micro-elemental analysis of the top few micrometres of a sample.[30] An EDX spectrum is obtained from the X-ray signals generated when the high-energy electron beam hits the sample surface.[29] Since the orbital energies of each element are characteristic, the X-rays generated by the sample are linked to its chemical composition. Thus, an EDX spectrum consists of a series of peaks at specific energies corresponding to the electronic transitions of

the different elements present in the sample. Although EDX allows for the identification of the elements present in the sample, it is generally not suitable as a quantitative measurement.[29,31]

2.9.2 Optical microscopy

The beads were also examined and optical images were taken on a Leica DMEP DFC-280 and an Olympus BX51M system using Leica application suite and Olympus DP Version 3.2, software. 20 bead diameters were measured using an Olympus BX5IM Microscope, and a similar diameter range was observed to that obtained with the Gilosonic auto sieve.

2.9.3 Gilosonic Auto Sieve

The size limits of the dried beads were determined using a Gilosonic auto sieve. The maximum diameter range of five samples, each containing 100 dried beads, was determined. For the calcium alginate beads five 100 bead samples were measured, greater than 95 beads were found to pass through the 850 µm sieves but were trapped by the 710 µm sieve. This sets a narrow size distribution of 140 µm for this set of beads.

2.9.4 UV/Vis Spectroscopy

The release of the urease inhibitor NBPT from the beads was recorded between 190 and 400 nm on a Unicam UV 500 spectrometer. In all cases, a quartz crystal cuvette with a diameter of 1 cm was used. Deionised water was placed in the reference quartz cuvette and samples to be monitored were placed in quartz cuvette with a volume of approximately 2.5 ml. UV/Vis spectroscopy measures the amount of ultra-violet and visible light transmitted or absorbed by a sample placed in a spectrometer. The wavelength at which a chemical absorbs light is a function of its electronic structure. It is well suited for quantitative study of association constants since the measured absorbance values are proportional to the respective concentration by the Beer-Lambert law[32] (Equation 2.1). The absorption of UV/Vis energy gives rise to the electronic transition of occupied energy levels to unoccupied energy levels. Common UV spectrometers operate in the range 190 to 400 nm

corresponding to photon energies of about 290 to 590 kJ/mol.[33] Spectrometers that also extend into the visible region, from 400 nm to 800 nm, are called UV/Visible spectrometers.

2.9.5 Infra-Red Spectroscopy

In this research infrared spectra (cm^{-1}) were recorded as KBr discs or liquid films between NaCl plates using a Perkin Elmer system 2000 FT-IR spectrometer. Solid samples were finely ground with approximately a tenfold excess of dry potassium bromide and pressed into a disc in a stainless steel pressure die under a pressure of 10 tonnes. Solution samples were placed between two sodium chloride plates.

Infra-red (IR) spectroscopy measures the vibrational excitation of atoms around the bonds that connect them. At energies slightly lower than those of visible radiation, light causes vibrational excitation of the bonds in a molecule.[34] This part of the electromagnetic spectrum is called the infra-red region. Like electronic transitions, these vibrational transitions correspond to distinct energies, and molecules absorb infrared radiation only at certain wavelengths and frequencies. The position of the infrared band is specified by its wavelength (λ), measured in microns (μm) or its reciprocal value called wavenumber (ν). The frequency of the vibrations between two atoms is governed by Hooke's law as the frequency of the stretching vibration depends on two quantities: the masses of the atoms and the stiffness of the bond.[35] Heavier atoms vibrate slower than lighter ones and stronger bonds are generally stiffer, requiring more energy to stretch or compress them. The vibrational bands of many functional groups occur at characteristic wavenumbers which aids interpretation of a spectrum and the entire IR spectrum may be used as a unique fingerprint of a compound.[36]

2.9.6 Nuclear Magnetic Resonance (NMR) Spectroscopy

Nuclear Magnetic Resonance (NMR) spectroscopy is widely used for the determination of the structure of organic compounds. For the purpose of these studies it is the most effective structural tool for investigating the stability of the inhibitor (NBPT) within the sodium alginate beads. ^{1}H NMR and ^{31}P NMR spectra were recorded on a Bruker Avance 300 MHz NMR spectrometer, operating at

300MHz for ^{1}H and 121.48 MHz for ^{31}P, using deuterated (D_2O) unless indicated otherwise. ^{1}H NMR peak protons were reported in ppm relative to internal reference tetramethylsilane (TMS) ($\delta = 0.0$ ppm) and ^{31}P NMR peaks were reported relative to the standard phosphoric acid.

^{1}H NMR spectroscopy is a quantitative technique as the relative number of hydrogen nuclei can be measured by integrating the area under the peak.[37] It also reveals the connectivity of the structure due to the coupling of the protons, and more importantly, for this research, the chemical shifts give a reliable indication of the local chemistry. The chemical shift provides much information and is a measure of the shielding of the nucleus by the electrons around it.[38] Radio waves are used to study the energy level differences of ^{1}H nuclei. Hydrogen nuclei have a nuclear spin of a half and so have two energy levels: they can be aligned either with or against the applied magnetic field.

The ^{31}P NMR experiment is much less sensitive than the ^{1}H NMR experiment but more sensitive that the ^{13}C NMR experiment.[39] The nucleus of ^{31}P is of medium sensitivity, which yields a sharp line and has a wide chemical shift range. Solution ^{31}P-NMR is one of the more routine NMR techniques because ^{31}P has an isotopic abundance of 100% and a relatively high magnetogyric ratio. The ^{31}P nucleus also has a spin of a half, making spectra relatively easy to interpret.[40]

2.9.7 Elemental Analysis

In this research CHN elemental analysis was performed using a Flash EA 1112 Series Elemental Analyser with Eager 300 Operating Software. The major elements of an organic substance namely carbon, hydrogen and nitrogen, are commonly determined using CHN elemental analysis. In this technique the substance under study is combusted under an oxygen stream in a furnace at high temperatures. The end products of the combustion are mostly the oxides of the concerned elements present in the form of gases. These are then separated by mass spectrometry and carried to the detector using inert gases such as helium or argon. The detector then determines the presence of the elements carbon, hydrogen and nitrogen in a given substance and gives the result as percentage amount of these atoms against the total weight.

2.9.8 Atomic Absorption (AA) Spectroscopy

AA spectroscopy was performed using a Perkin Elmer AAnalyst 200 atomic absorption spectrometer. Calibration plots were made using standard solutions of $AgNO_3$ 99.9999% as can be seen in Figure 2.2. From the linear relationship between absorbance and concentration a slope can be obtained. This was then used to calculate the concentration of silver in the solutions tested.

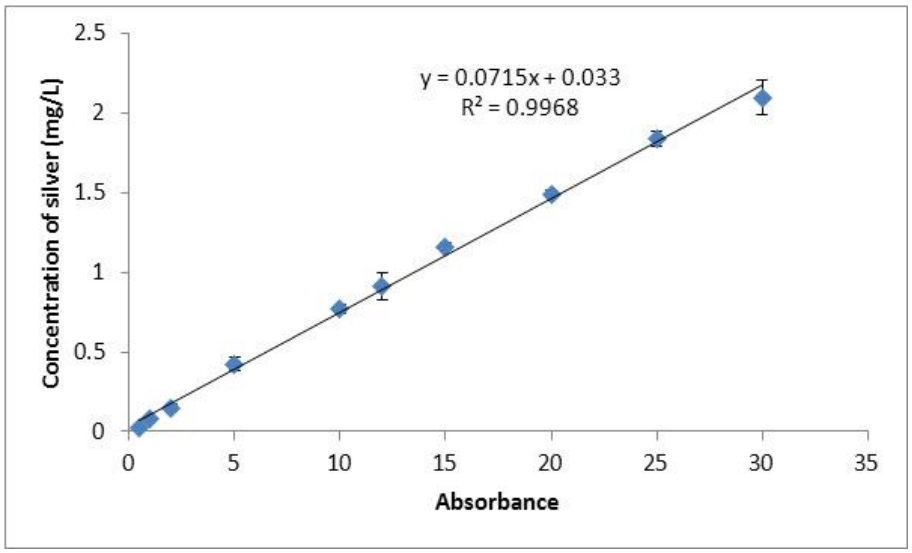

Figure 2.2: Calibration curve for $AgNO_3$ dissolved in water. The experiment was repeated in triplicate.

In atomic absorption spectroscopy light energy (ultraviolet or visible light) is used to cause electronic transitions in atoms. The atoms absorb the light energy and the electrons are promoted to higher energy states. AA spectroscopy requires that the solution species be atoms and in the gas phase, this is achieved using a high temperature flame. A portion of the liquid sample is sucked through a nebuliser tube and into a chamber where it is mixed with a fuel (acetylene) and an oxidant (air). A heterogeneous mixture of fuel air and finely dispersed sample is created. This mixture flows immediately into a burner where it burns and creates gas phase atoms, which absorb some of the light. The amount of absorption is proportional to the concentration of the analyte. The amount of light absorption is calculated by measuring changes in the signal at the detector. The monochromator isolates the

wavelength of the light of the hollow cathode lamp, eliminating any background light due to interferences. Thus, by measuring the signal at the detector with, and without, the sample atoms, the amount of light absorbed by the sample can be calculated.[41] AA spectroscopy was used to quantify the amount of silver released into an aqueous media or contained within the different beads. A hollow cathode silver detection lamp (338 nm wavelength), and air/acetylene burner were used for the determinations. AA standard solutions were prepared by diluting silver atomic absorption standard solutions at appropriate concentrations. Three independent measurements are automatically averaged for each sample.

2.9.9 Sterilisation

Sterilisation of microbiological equipment and media was carried out in a Dixons ST2228 autoclave at 121 ± 2°C and 124 kPa for 20 min. All worktops and benches were sterilised by washing with 70% (v/v) ethanol/water prior to use.

2.9.10 Cell Density

The fungal cell density was measured using a Neubauer hemocytometer under a light microscope at a magnification of × 400. Bacterial cell density was recorded at an optical density of 600nm (OD600) using an Eppendorf Biophotometer

2.9.11 Biological Preparations – Anti *Candida* Testing

*Candida albicans (*ATCC 10231) was grown on Yeast Extract Peptone Dextrose (YEPD) agar plates at 37 ± 1°C and maintained at 4 ± 1°C for short term storage. Deionised water was used to make up all media. Cultures were routinely sub-cultured every 4-6 weeks. Cultures were grown to the stationary phase at 37 ± 1°C and with continuous shaking (2000 rpm) for 24 h in minimal medium (MM) for the three different assays (which are denoted in this thesis as the plate assay, the well assay and the colony count assay). For the plate assay and the well assay the *C. albicans* was plated out on the YEPD plates at a concentration of 1×10^6 cells per ml. The plates were incubated for 1 h at 37 ± 1°C. For the plate assay, 10 polymer beads were placed on the plates in a circle. The plates were incubated for 24 h at 37 ± 1°C, and then the zones of inhibition around the samples were measured. All plate assays experiments were run in triplicate. For the well assay, 30 polymer

beads were placed into tubes containing deionised water (10 ml) at 30 ± 1°C. When the plates had been incubated for 1 h at 37 ± 1°C, wells were dug out using a sterilised cork with a diameter of 3 mm. The test solution (30 µl) was added to the wells and the plates were incubated for 24 h at 37 ± 1°C and the zones of inhibition around the wells were measured. For the colony count test, 10 ml of the medium containing 1×10^6 cells were placed in a sterilised flask containing 10 polymer beads and the flask was held at 30 ± 1°C and continuously shaken at 200 rpm on a rotary shaker. The solution was sampled and the sample was spread onto agar plate. The plates were then incubated for 24 h at 37 ± 1°C and the number of colonies formed on the agar plates was counted and graphed. Photographs of each plate at each time interval were also taken. Each experiment was performed in triplicate and the results are reported as the mean ± the standard error.

2.9.12 Biological Preparations – Anti-Bacteria Testing

The *in vitro* antimicrobial activity of the different hydrogel beads was investigated against pathogenic representatives of both Gram-positive bacteria and Gram negative bacteria. All bacteria were grown on nutrient broth agar plates at 37 ± 1°C and maintained at 4 ± 1°C for short term storage. Cultures were routinely sub-cultured every 4-6 weeks. The five different bacteria were grown overnight to the stationary phase in nutrient broth at 37 ± 1°C and 2000 rpm. The cells were diluted to give an OD600 = 0.05 for the plate and well assays and an OD600 = 0.1 for the colony count assay. For the plate and well assay the bacteria were plated out on the agar plate using the above OD. The plates were incubated for 1 h at 37 ± 1°C. For the plate assay the 10 polymer beads were placed on the plates in a circle. The plates were incubated for 24 h at 37 ± 1°C, and then the zones of inhibition around the samples were measured. For the well assay, 30 polymer beads were placed into tubes containing deionised water (10 ml) at 37 ± 1°C. After the plates were incubated for 1 h at 37 ± 1°C, wells were dug out using a sterilised cork with a diameter of 3 mm. 30 µl of the test solution was added to the wells and the plates were incubated for 24 h at 37 ± 1°C and the zones of inhibition around the wells were measured. For the colony count 10 ml of media (OD600 = 0.1) were placed into a sterilised flask. A sample was taken before the 100 polymer beads were added to the different flasks and this was held at 30 ± 1°C and continuously shaken at 200

rpm on a rotary shaker. The media was sampled every hour for 6 h and the samples were spread onto agar plates. All assays were run in triplicate and the plates were then incubated for 24 h at 37 ± 1°C. The number of colonies formed on the agar plates were counted and graphed. Photographs of each plate at each time interval were also taken. Each experiment was performed in triplicate and the results are reported as the mean ± the standard error.

2.9.13 Measuring zones of inhibitions

To measure zones of inhibition (ZOI), the vertical and horizontal diameters, of the sample, in this case the beads were measured in mm. The vertical and horizontal diameters of the sample and the zone itself were then measured. Then using the formula for the area of a circle, $A = \pi r^2$ the area covered by the beads and the total area of inhibition were calculated. The area under the beads was subtracted from the total area of inhibition to give the area of the zone of inhibition.[42]

2.10 References

(1) Shilpa, A.; Agrawal, S. S.; Ray, A. R. *Journal of Macromolecular Science* **2003**, *43*, 187-221.
(2) Panic, V.; Adnadjevic, B.; Velickovic, S.; Jovanovic, J. *Chemical Engineering Journal* **2010**, *156*, 206-214.
(3) Gill, J. S.; Bijay, S.; Khind, C. S.; Yadvinder, S. *Nutrient Cycling in Agroecosystems* **1999**, *53*, 203-207.
(4) Cui, D.; Szarpak, A.; Pignot-Paintrand, I.; Varrot, A.; Boudou, T.; Detrembleur, C.; Jerome, C.; Picart, C.; Auzely-Velty, R. *Advanced Functional Materials* **2010**, *20*, 3303-3312.
(5) Rousseau, I.; Le Cerf, D.; Picton, L.; Argillier, J. F.; Muller, G. *European Polymer Journal* **2004**, *40*, 2709-2715.
(6) McEntee, M.-K. E.; Bhatia, S. K.; Tao, L.; Roberts, S. C.; Bhatia, S. R. *Journal of Applied Polymer Science* **2008**, *107*, 2956-2962.
(7) Isiklan, N. *Journal of Applied Polymer Science* **2007**, *105*, 718-725.
(8) Garrido-Herrera, F. J.; Gonzalez-Pradas, E.; Fernandez-Perez, M. *Journal of Agricultural and Food Chemistry* **2006**, *54*, 10053-10060.
(9) Fernandez-Perez, M.; Villafranca-Sanchez, M.; Gonzalez-Pradas, E.; Flores-Cespedes, F. *Journal of Agricultural and Food Chemistry* **1999**, *47*, 791-798.
(10) Levy, M. C.; EdwardsLevy, F. *Journal of Microencapsulation* **1996**, *13*, 169-183.
(11) Singh, B.; Sharma, D. K.; Kumar, R.; Gupta, A. *Applied Clay Science* **2009**, *45*, 76-82.
(12) Andreeva, D. V.; Gorin, D. A.; Shchukin, D. G.; Sukhorukov, G. B. *Macromolecular Rapid Communications* **2006**, *27*, 931-936.
(13) Sarker, D. K.; Wilde, P. J. *Colloids and Surfaces B-Biointerfaces* **1999**, *15*, 203-213.
(14) Edwards-Levy, F.; Levy, M. C. *Biomaterials* **2000**, *21*, 645-646.
(15) Kim, Y. S.; Kim, H. W.; Lee, S. H.; Shin, K. S.; Hur, H. W.; Rhee, Y. H. *International Journal of Biological Macromolecules* **2007**, *41*, 36-41.
(16) Lambert, J. B.; Shurvell, H. F.; Lightner, D.; Cooks, R. G. *Introduction to Organic Spectroscopy p.223*; MacMillan, **1987**.
(17) Lambert, J. B.; Shurvell, H. F.; Lightner, D.; Cooks, R. G. *Introduction to Organic Spectroscopy p.169*; MacMillan, **1987**.
(18) Silver, S.; Phung, L. T.; Silver, G. *Journal of Industrial Microbiology & Biotechnology* **2006**, *33*, 627-634.
(19) Rowan, R.; McCann, M.; Kavanagh, K. *Medical Mycology* **2010**, *48*, 498-505.
(20) Wu, J.; Hou, S.; Ren, D.; Mather, P. T. *Biomacromolecules* **2009**, *10*, 2686-2693.
(21) Araújo, M. M.; Teixeira, J. A. *International Biodeterioration and Biodegradation* **1997**, *40*, 63-74.
(22) Solak, E. K.; Asman, G.; Camurlu, P.; Sanli, O. *Vacuum* **2008**, *82*, 579-587.
(23) Andrade-Espinosa, G.; Escobar-Barrios, V.; Rangel-Mendez, R. *Colloid and Polymer Science* **2010**, *288*, 1697-1704.
(24) Wade, L. G., Jr. *Organic Chemistry. p.698*; 8th ed.; Pearson, **2012**.
(25) Wade, L. G., Jr. *Organic Chemistry p.699*; 8th ed.; Pearson, **2012**.
(26) Chen, S.-C.; Wu, Y.-C.; Mi, F.-L.; Lin, Y.-H.; Yu, L.-C.; Sung, H.-W. *Journal of Controlled Release* **2004**, *96*, 285-300.

(27) Abd, E.-G. M. A.; Hashem, M. S.; El-Awady, M. K.; Rabie, A. M. *Carbohydrate Polymers* **2012**, *89*, 667-675.
(28) Goldstein, J. I.; Newbury, D.; Joy, D.; Lyman, C.; Echlin, P.; Lifshin, E.; Sawyer, L.; Micheal, J. *Scanning Electron Microscopy and X-Ray Microanalysis, p108-110*; 3rd ed.; Springer, **2007**.
(29) Vernon-Parry, K. D. *III-Vs Review* **2000**, *13*, 40-44.
(30) Goldstein, J. I.; Newbury, D.; Joy, D.; Lyman, C.; Echlin, P.; Lifshin, E.; Sawyer, L.; Micheal, J. *Scanning Electron Microscopy and X-Ray Microanalysis, p10-12*; 3rd ed.; Springer, **2007**.
(31) Goldstein, J. I.; Newbury, D.; Joy, D.; Lyman, C.; Echlin, P.; Lifshin, E.; Sawyer, L.; Micheal, J. *Scanning Electron Microscopy and X-Ray Microanalysis, p 570*; 3rd ed.; Springer, **2007**.
(32) *http://teaching.shu.ac.uk/hwb/chemistry/tutorials/molspec/beers1.htm*.
(33) Kemp.W. *Organic Spectroscopy, p 1-6*; 2nd ed.; MacMillan, **1987**.
(34) Wade, L. G., Jr. *Organic Chemistry, p701-702*; 8th ed.; Pearson, **2012**.
(35) Kemp.W. *Organic Spectroscopy, p18-19*; 2nd ed.; MacMillan, **1987**.
(36) Coats, J. *Encyclopedia of Analytical Chemistry* **2000**, 10815–10837.
(37) Wade, L. G., Jr. *Organic Chemistry, p 577*; 8th ed.; Pearson, **2012**.
(38) Kemp.W. *Organic Spectroscopy, p 96-99*; 2nd ed.; MacMillan, **1987**.
(39) Kemp.W. *Organic Spectroscopy, p88-89*; 2nd ed.; MacMillan, **1987**.
(40) Vollhardt, P.; Schore, N. *Organic Chemisrty Structure and Function, p 392*; 6th ed.; W.H. Freeman and Company, **2011**.
(41) *http://elchem.kaist.ac.kr/vt/chem-ed/spec/atomic/aa.htm*.
(42) Percival, S. L.; Slone, W.; Linton, S.; Okel, T.; Corum, L.; Thomas, J. G. *International Wound Journal* **2011**, *8*, 237-243.

Chapter 3:

Alginate Beads as potential NBPT Delivery Systems

3.1 Introduction

Nitrogen is a highly dynamic and mobile element in soils, which makes its efficient use as a fertiliser a major challenge in agriculture. Nitrogen losses can occur as a result of nitrate (NO_3^-) leaching, ammonium ion (NH_4^+) run off, and gaseous emissions of ammonia (NH3) and nitrous oxide (N_2O).[1] Urine contains up to 97% urea which is normally lost through volatilization of ammonia. Urea nitrogen is rapidly converted to ammonia by the microbial enzyme urease. The ammonia is then converted to the ammonium ion and it is this form that is necessary for plant use. However, most of the ammonia can be lost to the atmosphere before it is converted to ammonium and used by plants. In agriculture, rapid urease activity releases large amounts of ammonia into the atmosphere during urea fertilization which causes significant environmental and economic problems.[2] This loss of ammonia nitrogen to the atmosphere leads to severe pollution of the environment. Ammonia itself is not a greenhouse gas; however it acts a secondary source of N_2O in the atmosphere and thus contributes to global warming.[1] Nitrous oxide is a greenhouse gas and it is known to deplete ozone (O_3). Due to the rapid expansion of farming and the increased importance of urea fertilisers on farms, there is a need to control the rate at which urea is hydrolysed to ammonium and its subsequent oxidation to NO_3^-. One strategy to conserve nitrogen is to inhibit the urease enzyme that converts urea to ammonia.

Urease is an enzyme found in all microbial and plant species.[3] Urease catalyses the hydrolysis of urea to carbamate and ammonia.[4] The carbamate can then be further broken down to give a second molecule of ammonia and carbon dioxide.[5,6] A unique feature of the urease enzyme is the presence of a bimetallic centre having two nickel ions in its active site (Figure 3.1).[4,7] These nickel ions are essential for the binding of the urea to the enzyme allowing for the conversion of urea into ammonia. Urease inhibitors are the compounds which retard the hydrolysis of urea by inhibiting the urease enzyme in the soil.[8] Urease inhibitors act in a similar binding manner to the urea and bind to the bimetallic centre of the enzyme, thus preventing some of the urea from binding, which in turn slows down the formation of volatile ammonia.

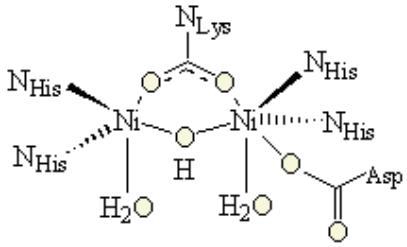

Figure 3.1: Active Site of Urease Enzyme.

Among the urease inhibitors available, *N*-(*n*-butyl) thiophosphoric triamide (NBPT) is regarded as one of the most efficient and it is widely available commercially.[1,7,9] After application to soils, NBPT is quickly converted in soil to its oxygen analogue, *N*-(*n*-butyl) phosphoric triamide (NBPTO), which forms a very stable tridentate ligand with the urease enzyme.[6,7] Effectiveness of NBPT as an urease inhibitor depends greatly on the conversion rate of the NBPT to its oxygen analogue upon contact with the soil. It is this oxygen analogue which is responsible for the decrease in urea hydrolysis.[3] Hendrickson *et al*. observed that the concentration of NBPTO was maintained at a higher concentration than that which was applied to the soil.[10] This suggests that the NBPT is converted into its oxygen analogue in the soil. The effectiveness of both compounds in controlling urea hydrolysis was related to the concentration of the NBPTO in the soil, not the concentration of NBPT applied to the soil. In a related study Francisco *et al*. showed that NBPT urease inhibition is more efficient in alkaline soils.[2]

Hendrickson *et al*.[10] performed a study to examine the reactions of NBPT and NBPTO in soils at different pH values. High performance liquid chromatography (HPLC) was used to monitor the concentrations and to examine the rate of disappearance, of both compounds in soils. They observed that the NBPT disappeared at a greater rate than its oxygen analogue NBPTO. The disappearance of the NBPTO was attributed to its binding to the urease enzyme in soil, while NBPT was converted to the NBPTO. However, in this study it was observed that acidic environments enhanced the rate of degradation of both compounds in comparison to alkaline environments. Additionally, both Douglas *et al*.[9] and Dominguez *et al*.[7] showed that NBPT underwent decomposition when it was put in

slightly acidic (pH 5.5) solutions. Douglas *et al.*[9] reported that both compounds, i.e., NBPT and NBPTO produced *n*-butylamine and ammonia upon acid hydrolysis.

The objective of the research outlined in this chapter was to encapsulate an urease inhibitor into environmentally friendly alginate beads, and then tailor the properties of the hydrogel beads to firstly protect the inhibitors until they were released and secondly to give slow sustained release of the inhibitors. Four types of beads were chosen for this study, calcium alginate, charcoal-loaded calcium alginate, bentonite-loaded calcium alginate, and polypyrrole-coated calcium alginate beads. Bentonite clay and activated charcoal are well-known naturally occurring absorbent materials[11,12] and both have previously been incorporated into alginate polymer supports for applications in controlled release of pesticides,[13-15] in heavy metal remediation[16] and membrane separation systems.[17] Polymeric beads have been previously coated with a layer of polypyrrole in order to attempt to develop capsules which are able to trap low molecular weight water soluble compounds[18] but there are essentially no reports on using polypyrrole-coated alginate bead systems. Each bead type was characterised using SEM and EDX analyses. In each case the average bead size was determined and measurements were carried out to ensure that the beads were formed with a reasonable degree of uniformity. The swelling properties of each type of bead were also determined in a number of media as these are related to the rate at which the beads will release encapsulated compounds. Studies on the stability of NBPT as a function of pH within the beads, and the release of NBPT from the beads were then carried out.

3.2 Results and Discussion

The beads were prepared according to the appropriate methodology outlined in Chapter 2.

3.2.1 Characterisation and Physical Properties of Alginate Beads used in the NBPT Release Studies

3.2.1.1 Surface Morphology of the Beads

3.2.1.1.1 Calcium Alginate Beads

(a) Xerogels Beads

Calcium alginate beads were characterised using SEM microscopy. Generally in this Chapter, unless otherwise stated, the concentration of $CaCl_2$ used in the crosslinking solution to form the calcium alginate beads was 0.25 M. Figure 3.2 shows the SEM micrographs recorded at different magnifications for beads formed using a 0.25 M $CaCl_2$ gelling solution. The micrographs at the lower magnification show that the beads were generally spherical in shape and they had quite a smooth, uniform surface and contained no large pores, as can be seen in Figure 3.2(a). These observations correspond with research carried out by Solak *et al.*[19] and by Hurteaux *et al.*[20] both of whom also reported alginate beads crosslinked with calcium chloride to have a smooth spherical appearance at similar magnifications. The micrographs recorded at a higher magnification (Figure 3.2(b)) showed that cracks, which were due to the shrinkage of the beads during the drying process, were unevenly distributed on the surface of the bead. The micrograph recorded at the highest magnification (Figure 3.2(c)) showed that the morphology of the surface of the xerogels no longer appeared smooth and the cracks were still visible between the wrinkles.

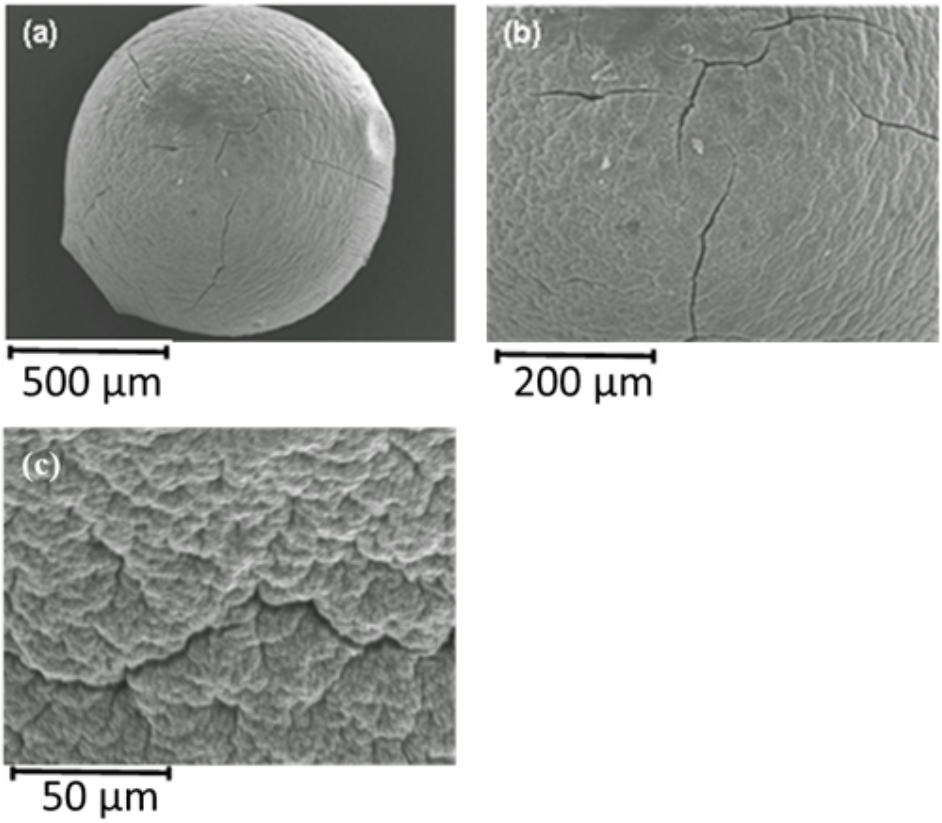

Figure 3.2: SEM micrographs of calcium alginate beads at different magnifications (a), (b) and (c). All beads were dried at room temperature.

A study was then carried out to investigate the influence that the concentration of $CaCl_2$ (0.125 M, 0.25 M, 0.5 M and 1.0 M), in the gelling solution had on the shape and morphology of the beads. The SEM micrographs recorded on each of the four different batches of calcium alginate beads are given in Figure 3.3(a-d).

For each of the four types of calcium alginate beads studied the surface of the beads was smooth with no large pores observed. However, the surface of the beads made using 0.125 M $CaCl_2$ was covered in little white dots (Figure 3.3(d)). As the concentration of the calcium chloride used to form the beads increased, the amount of white speckles increased. For the beads formed using 1.0 M $CaCl_2$, the surface of the beads was completely covered in this white material (Figure 3.3(a)). In order to determine the nature of the white material covering the calcium alginate beads, EDX analyses were carried out on the beads formed using the 0.125 M $CaCl_2$ gelling solution in regions of the surface where it did (Figure 3.4(a)) and it did not appear

(Figure 3.4(b)). The spectrum (Figure 3.4(a)) of the surface containing the white material showed a line at 1.04 keV which is assigned as the Kα line of sodium.[21] This line was not present in the spectrum (Figure 3.4(b)) recorded of a region of the surface which was not covered in the white material. It would appear that the xerogels beads were coated with a layer of NaCl, and that this layer was only removed if the beads were washed in an ultrasonic bath. Studies on the release of NBPT, discussed later in this chapter, showed that the presence of the NaCl layer on the surface of the beads did not influence the rate of its release. Therefore no measures were taken to ensure this layer was completely removed and unless otherwise stated all the beads used in the studies associated with this chapter were simply washed in deionised water.

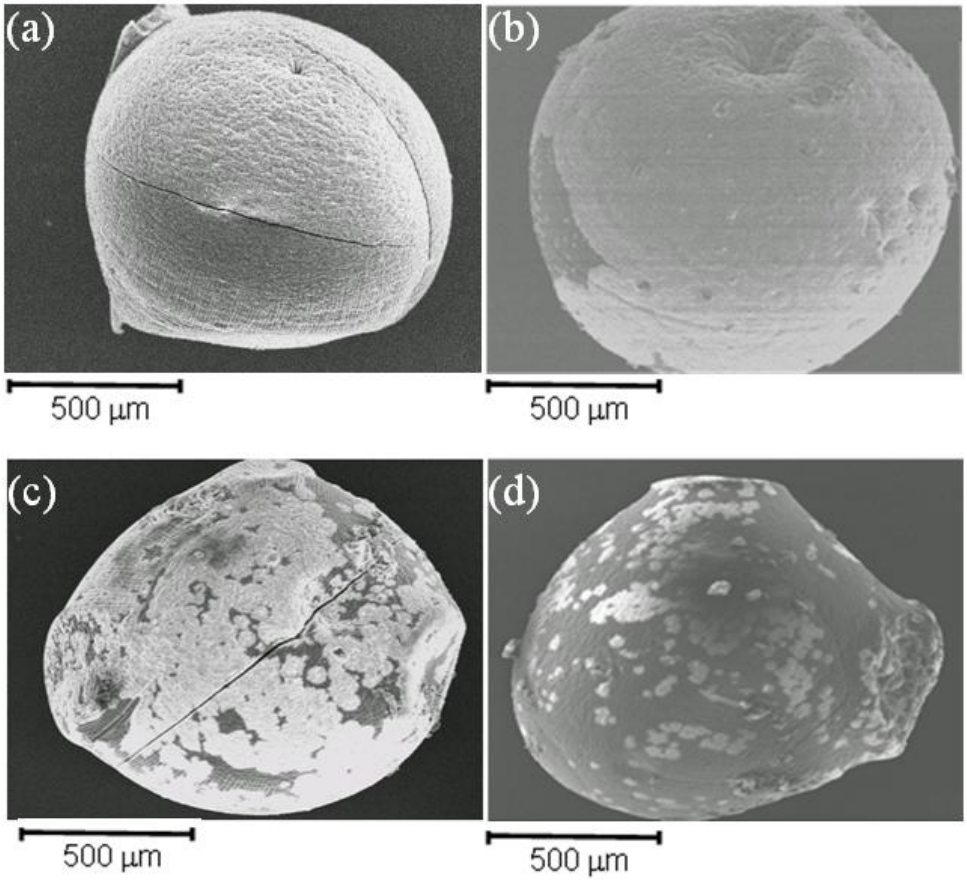

Figure 3.3: SEM micrographs of alginate beads crosslinked with different concentrations of $CaCl_2$, (a) 1.0 M $CaCl_2$ (b) 0.5 M $CaCl_2$ (c) 0.25 M $CaCl_2$ (d) 0.125 M $CaCl_2$.

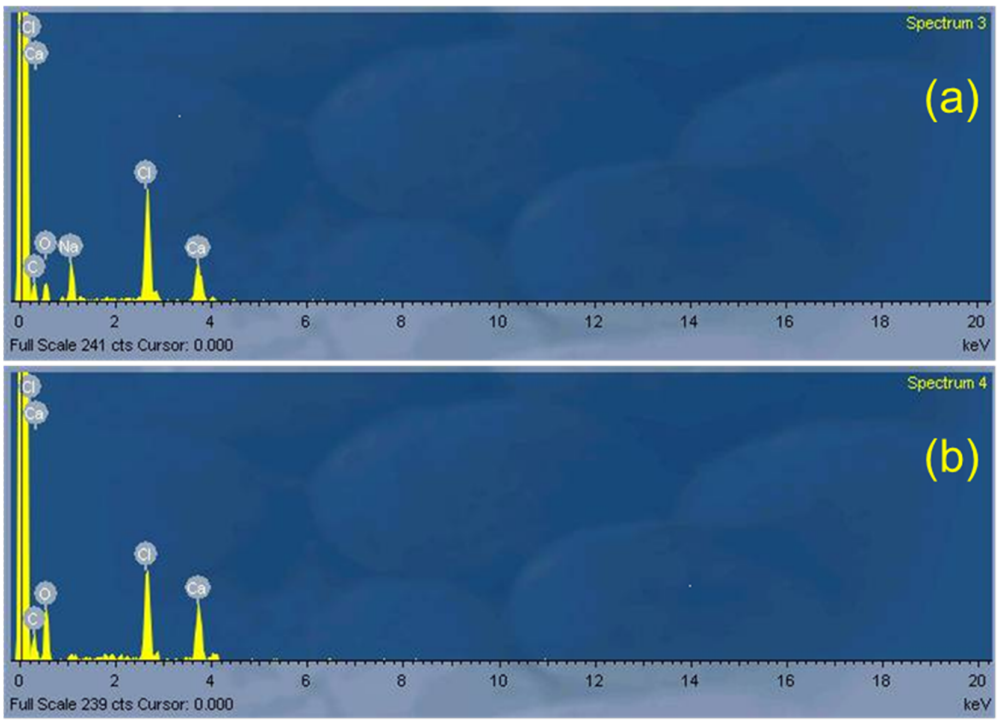

Figure 3.4: EDX spectra recorded of the surface of a calcium alginate bead crosslinked using 0.125 M $CaCl_2$ gelling solution. Spectrum recorded on a region of the surface (a) covered with white material (b) where no white material was present.

(b) Freeze-Dried Beads

The calcium alginate beads crosslinked using the 0.25 M $CaCl_2$ solution were dried under reduced pressure and low temperature in order to minimise the decrease in pore size which occurs when the beads are dried under normal conditions. SEM micrographs, at different magnifications, of the freeze-dried calcium alginate beads are given in Figure 3.5. The shape and surface of the freeze-dried beads were determined using SEM and compared to air-dried beads. The freeze-dried beads completely lost the spherical shape (Figure 3.5(a)) and were substantially larger than the analogous air-dried beads as shown in Figure 3.2(a). In addition, the air-dried beads had a rough surface with cracks present due to the shrinkage of the beads during the drying process. When micrographs were recorded of the freeze-dried beads at higher magnifications (Figure 3.5(b)) it would appear that the surface of the beads was smoother than was the case for the air-dried beads. Tavakol *et al.* recorded similar micrographs for air-dried beads and freeze-dried beads formed from

N,O-carboxymethyl chitosan/alginate crosslinked with calcium ion.[22] They reported that their freeze-dried beads had a rough surface at the higher magnifications and also there were no cracks present in the micrographs of their air-dried beads. The beads formed in this paper were a composite of alginate and *N, O*-carboxymethylchitosan, so this could result in a stronger coating on the beads and could be the reason for the difference observed between both sets of beads. In addition Santagapita *et al.* observed similar differences in the SEM micrographs recorded on freeze-dried and vacuum-dried calcium alginate beads.[23] They stated that the obvious 'folds' on the surface of the freeze-dried beads mean that they have a larger exposed surface area compared to their vacuum- and air-dried analogues. They also noted that the freeze-dried beads were more fragile than their vacuum- or air-dried analogues. This was also the case for the beads formed in our study. Figure 3.5 (c) shows a micrograph of the freeze dried beads recorded at a very high magnification. In contrast to the surface at the lower magnifications which appeared smooth this micrograph showed the surface of the beads to be uneven and rough with lots of indentations present.

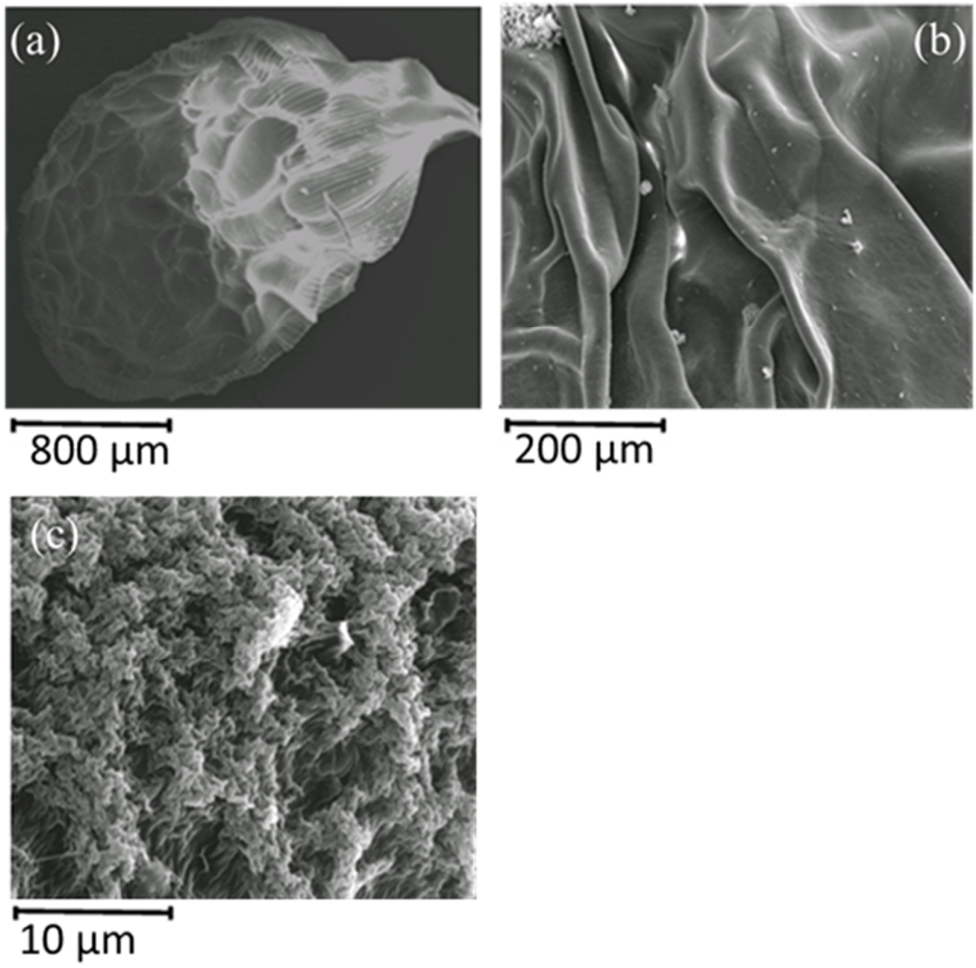

Figure 3.5: SEM micrographs of freeze-dried calcium alginate beads at different magnifications.

3.2.1.1.2 Charcoal-loaded Calcium Alginate Beads

SEM micrographs were recorded of the charcoal-loaded calcium alginate beads to examine the morphology and surface structure of the beads at the required magnification at room temperature. The charcoal-loaded alginate beads were spherical in shape and had a rough surface. (Figure 3.6(a)). At the lower magnifications, (Figure 3.6(a)) there were no major cracks or indentations on the immediate surface of these beads in comparison to the calcium alginate beads in Figure 3.2(a). The lack of cracks present in the charcoal-loaded alginate beads would suggest that these beads were more resistant to the dehydration process and therefore less prone to cracks which were clearly visible on the surface of the

calcium alginate beads. However, at the higher magnifications ((Figure 3.6(b) and Figure 3.6(c)) the charcoal-loaded alginate beads appeared to have a very rough morphology which was substantially different to the morphology of the calcium alginate beads (Figure 3.2(b)). Aminabhavi *et al.* incorporated nanosized activated charcoal into their calcium alginate membranes.[17] Even with the activated charcoal being in the nano range the morphology of these membranes exhibited the same rough surface that was displayed in Figure 3.6. The surface of the beads presented in Figure 3.6 appeared to have the same rough morphology and showed shallow indentations on the surface of the beads.

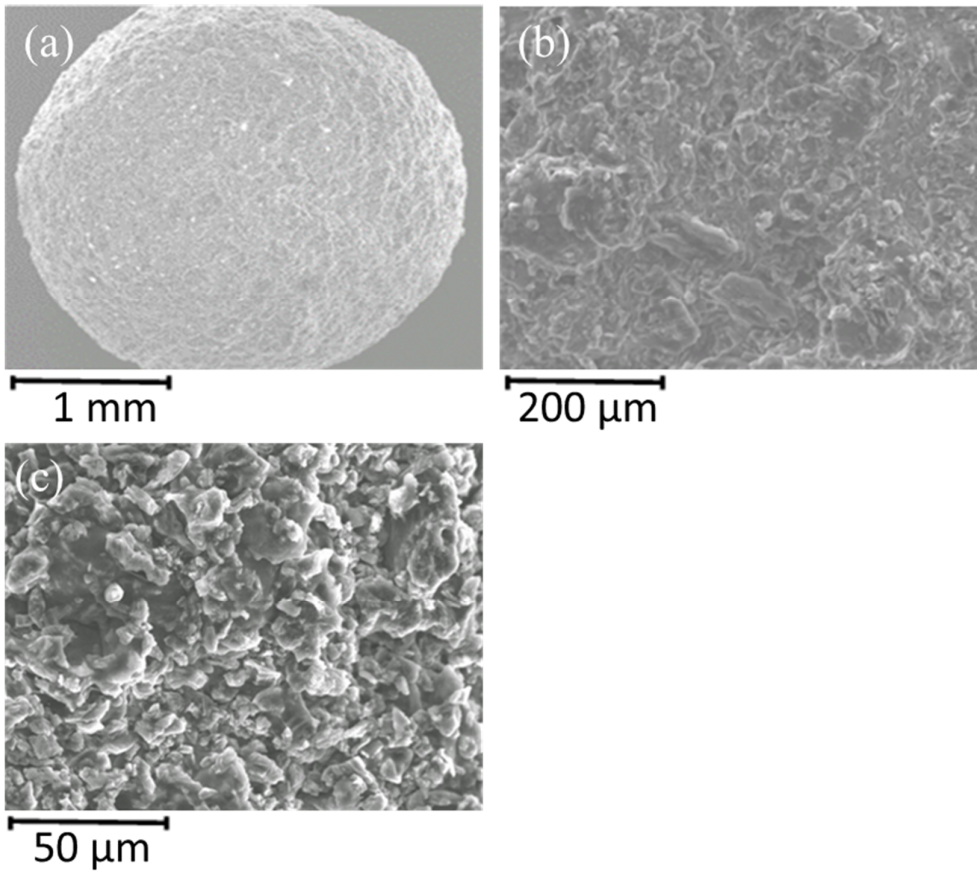

Figure 3.6: SEM micrographs of calcium alginate beads loaded with charcoal at different magnifications.

3.2.1.1.3 Bentonite-loaded Calcium Alginate Beads

SEM micrographs were recorded of the bentonite-loaded calcium alginate beads to examine the morphology and surface structure of the beads at the required magnification at room temperature. The bentonite-loaded calcium alginate beads were not spherical in shape (Figure 3.7(a)) and they exhibited a rough surface morphology which was substantially more heterogeneous compared to the charcoal-loaded calcium alginate beads (Figure 3.6(a)) and the calcium alginate beads (Figure 3.2(a)). There were a lot of imperfections present on the surface of the beads at the lower magnification, which were also present at the higher magnifications (Figure 3.7(b) and Figure 3.7(c)). These observations are consistent with those reported by Singh and co-workers who noted that their starch-alginate beads had a spherical shape, whereas their bentonite-starch-alginate beads had an oval shape.[24] They proposed that the loss of the spherical shape occurred due to the increase of the viscosity of the starch-alginate solution upon the addition of the clay particles. Moreover, Kevadiya and co-workers reported an increase in the surface roughness of their alginate beads upon addition of clay particles of montmorillonite (which is closely related to bentonite).[25]

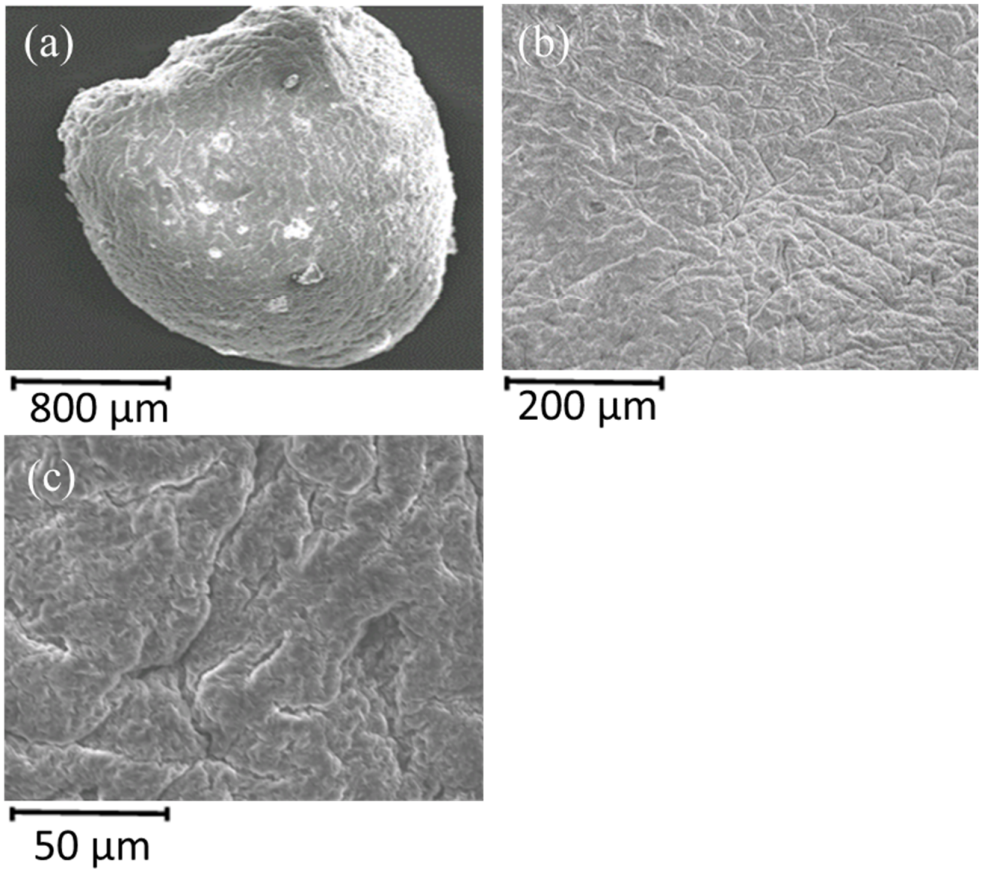

Figure 3.7: SEM micrographs of calcium alginate beads loaded with bentonite at different magnifications.

In order to confirm that the bentonite, which is a hydrated aluminium silicate ($Al_2O_34SiO_22H_2O$), was present within the beads, EDX spectra were recorded. Although EDX allows for the identification of the elements present in the sample, it is generally not suitable as a quantitative measurement.[26] A typical EDX spectrum is given in Figure 3.8. The spectrum showed lines which were assigned as arising from aluminium and silicon which were indicative of the presence of the bentonite. Lines were also assigned to elements not present in the simple calcium alginate beads such as iron, magnesium, sulphur and phosphorus, however, bentonite is a natural clay and these are all common impurities found within it.[27] An EDX spectrum of bentonite powder given in Figure 3.9, shows that iron and magnesium were present in the powder.

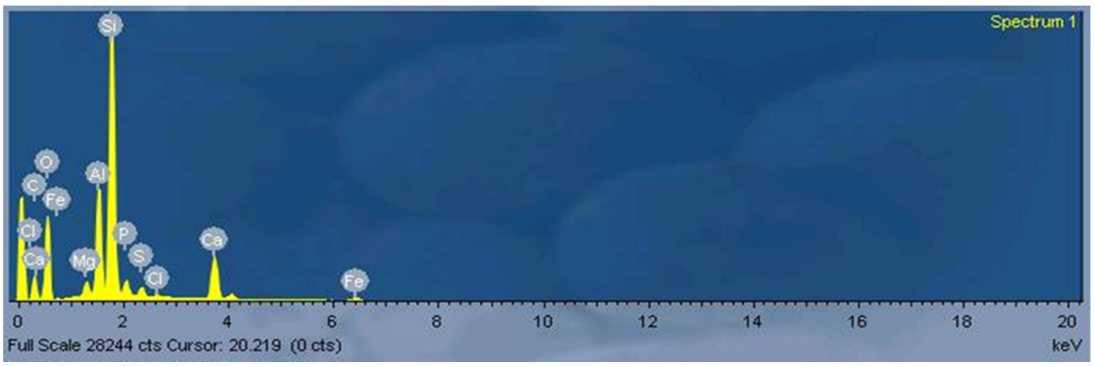

Figure 3.8: EDX spectrum of a bentonite-loaded calcium alginate bead.

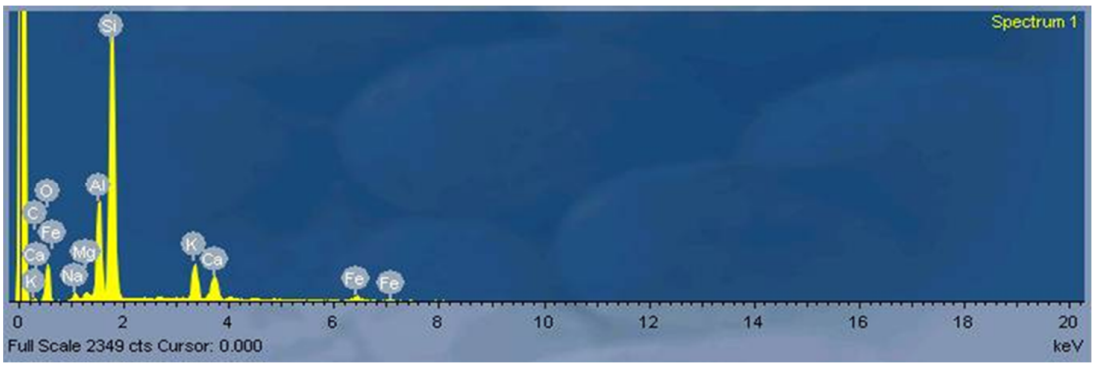

Figure 3.9: EDX spectrum of a bentonite powder.

3.2.1.1.4 Polypyrrole-coated Calcium Alginate Beads

Polypyrrole belongs to the class of polymers known as conducting polymers. The chemical structure of polypyrrole is given in Figure 3.10. There has been extensive interest in making polypyrrole-hydrogel composite materials mainly for biomedical applications such as drug-delivery and biosensors.[28,29] Polypyrrole has known hydrophobic properties[30] and it previously has been used as a means to reduce the porosity of alginate films.[29] Therefore, the polypyrrole-alginate composite beads might show an improvement in controlled release over the calcium alginate beads.

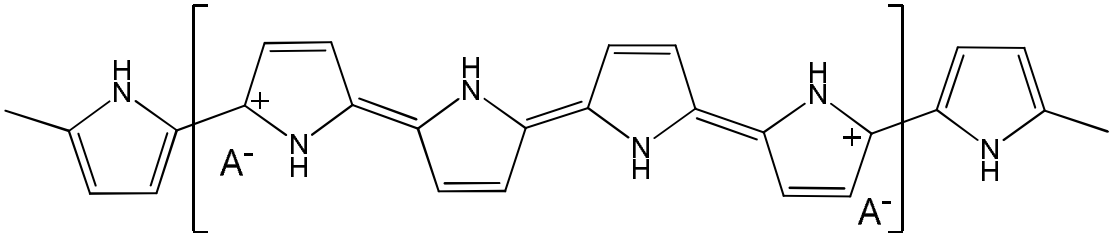

Figure 3.10: Structure of polypyrrole in its oxidised form. A- represents an anion which is required to balance the charge on the polymer backbone.

The first stage of forming the polypyrrole-coated calcium alginate beads was to immerse the calcium alginate beads in a solution of the oxidising agent $FeCl_3$ (0.05 M). The details of the experiment are given in Chapter 2, Section 2.3.3. SEM micrographs were recorded after immersion and are shown in Figure 3.11. The xerogel beads coated with $FeCl_3$ exhibited a substantially different surface morphology compared to the parent calcium alginate beads (Figure 3.2). The surface of the $FeCl_3$ coated beads was covered with rough troughs and folds, which were needle-like in shape; these were evenly distributed on the surface of the bead as can be clearly seen in the micrograph recorded at higher magnifications (Figure 3.11(b) and (c)). This suggests that the addition of the $FeCl_3$ to the beads was uniform throughout the surface. Unlike the calcium alginate beads there were no cracks visible on the immediate surface of the $FeCl_3$ coated beads.

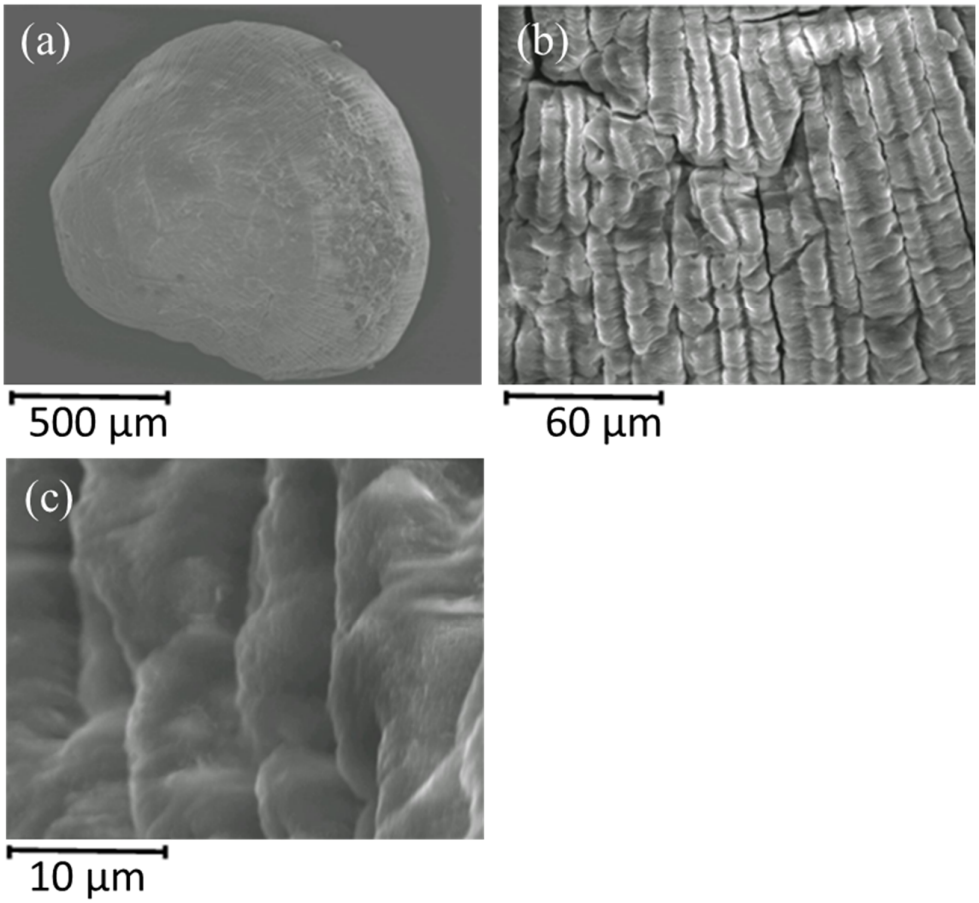

Figure 3.11: SEM micrographs of sodium alginate beads coated with $FeCl_3$ at different magnifications before polypyrrole added.

EDX analysis was used to confirm that the beads were coated in a layer of $FeCl_3$. An EDX spectrum of a typical bead is shown in Figure 3.12. Bands were clearly present at 7.18, 6.40 and 7.05 keV, which were assigned to the Lβ, Kα and Lα lines of iron, respectively.[21]

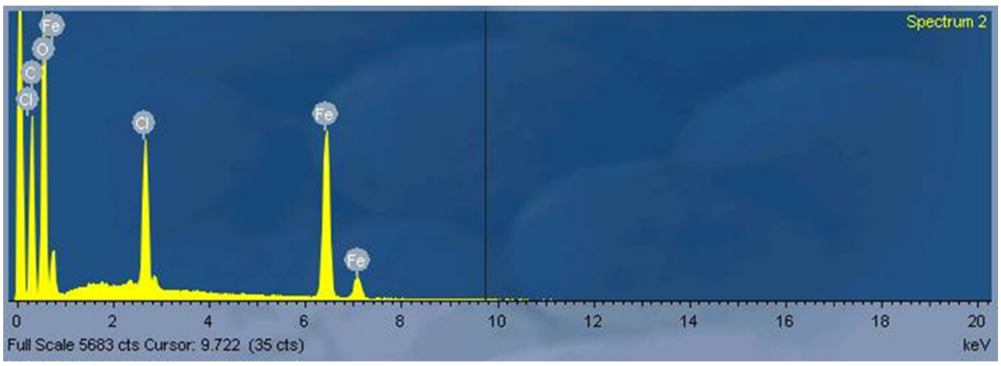

Figure 3.12: EDX spectrum of calcium alginate beads coated with $FeCl_3$.

The calcium alginate beads coated in $FeCl_3$ were then immersed in pyrrole and polymerisation was observed to occur on the bead since the bead changed colour from brown/orange to a very deep black colour. SEM micrographs were then recorded of the beads in their xerogel and freeze-dried forms.

(a) Xerogel Polypyrrole-Coated Alginate Beads

SEM micrographs of the xerogel beads at three different magnifications are given in Figure 3.13. It was apparent that the addition of the pyrrole to the surface of the beads had a significant impact on the surface morphology of the beads in comparison to the beads coated with $FeCl_3$. The surface morphology of these beads no longer displayed the same organised array of 'needle-like' folds and troughs which were distributed evenly on the surface of the $FeCl_3$ coated beads (Figure 3.11). The surface of the polypyrrole coated beads can be characterised by uneven wrinkled surface folds which were clearly visible on the surface on the beads at the three different magnifications.

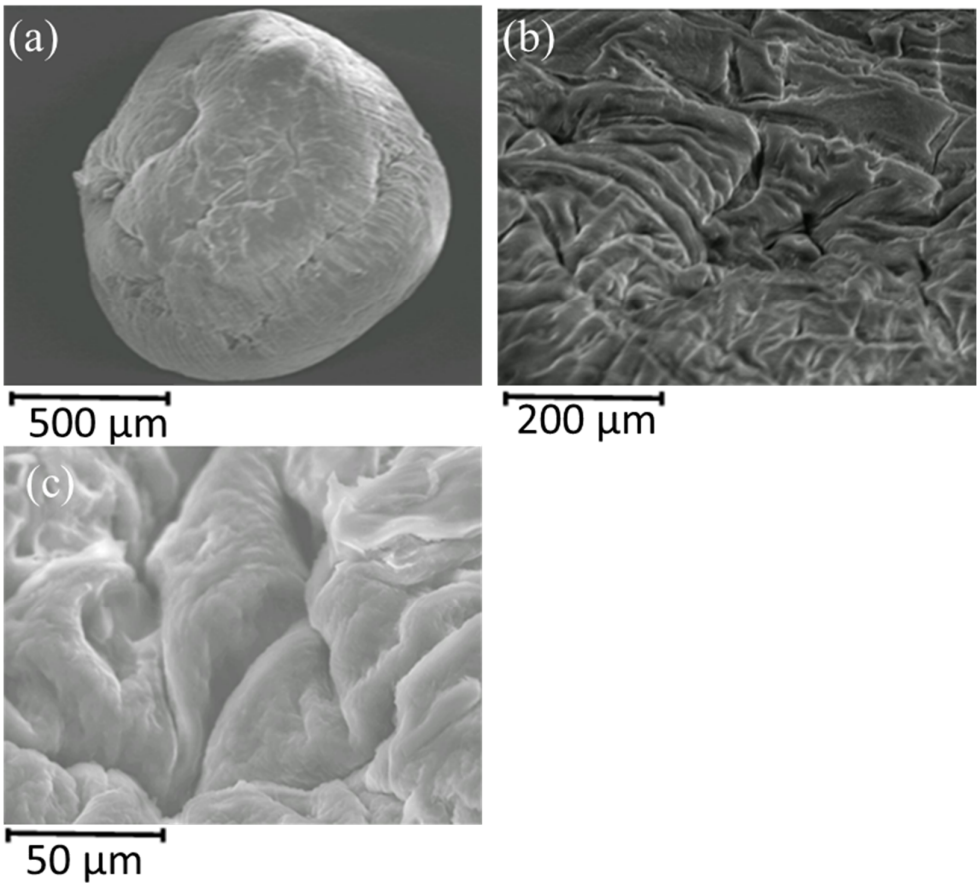

Figure 3.13: SEM micrographs of air-dried polypyrrole-coated calcium alginate beads.

EDX analysis was used to confirm that the beads coated with a layer of polypyrrole still had FeCl present. An EDX spectrum of a typical bead coated with a layer of polypyrrole is shown in Figure 3.14. Bands were clearly present at 7.18, 6.40 and 7.05 keV, which were assigned to the Lβ, Kα and Lα lines of iron, respectively.[21]

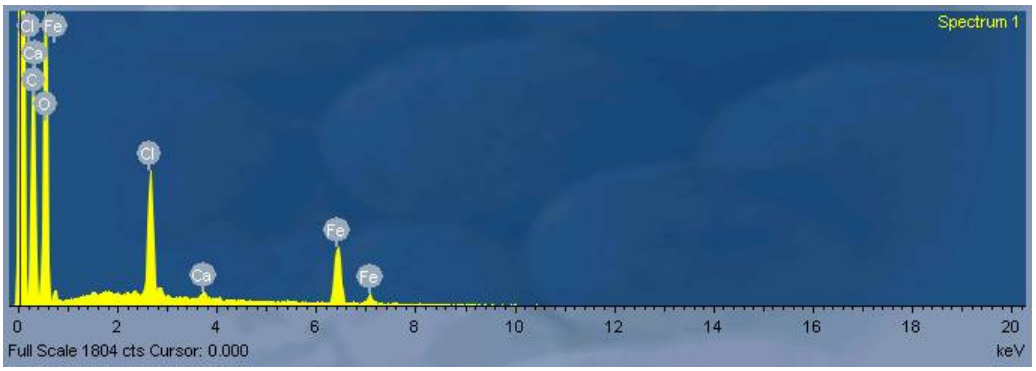

Figure 3.14: EDX spectrum of air-dried polypyrrole-coated calcium alginate beads.

(b) Freeze-Dried Polypyrrole Coated Beads

After freeze-drying, the beads were analysed using SEM and the results are shown in Figure 3.15. Freeze-drying preserves the micro-structure of the beads while keeping the bead in its swollen state. This allows the main features of the swollen bead structure to be examined. The micrographs of the freeze-dried polypyrrole coated calcium alginate bead in Figure 3.15(a) showed that the beads were much larger than the analogous air-dried beads shown in Figure 3.13(a). This suggests that the freeze-drying process had kept the beads in their swollen state. In contrast to the surface of the freeze-dried calcium alginate beads, which displayed a collapsed morphology (Figure 3.5), the morphology of the beads shown here displayed a swollen morphology. SEM micrographs of freeze-dried polypyrrole beads, (Figure 3.15 (a) and (b)), show that there are two distinct layers present. An outer rough coating of polypyrrole, which is no longer covering the whole surface of the beads as it is unevenly distributed on the surface of the beads. The inner layer is the smooth surface of the calcium alginate bead.. The detachment and possible shrinkage of this outer layer from the inner smooth surface could be due to the freeze-drying process. There are pores visible in Figure 3.15(a) and 3.15(b), which was not seen in the freeze-dried micrographs of the calcium alginate beads (Figure 3.5). At a higher magnification the morphology of the polypyrrole layer was rough but arranged in a regular array of almost cube like structures. (Figure 3.15(c)).

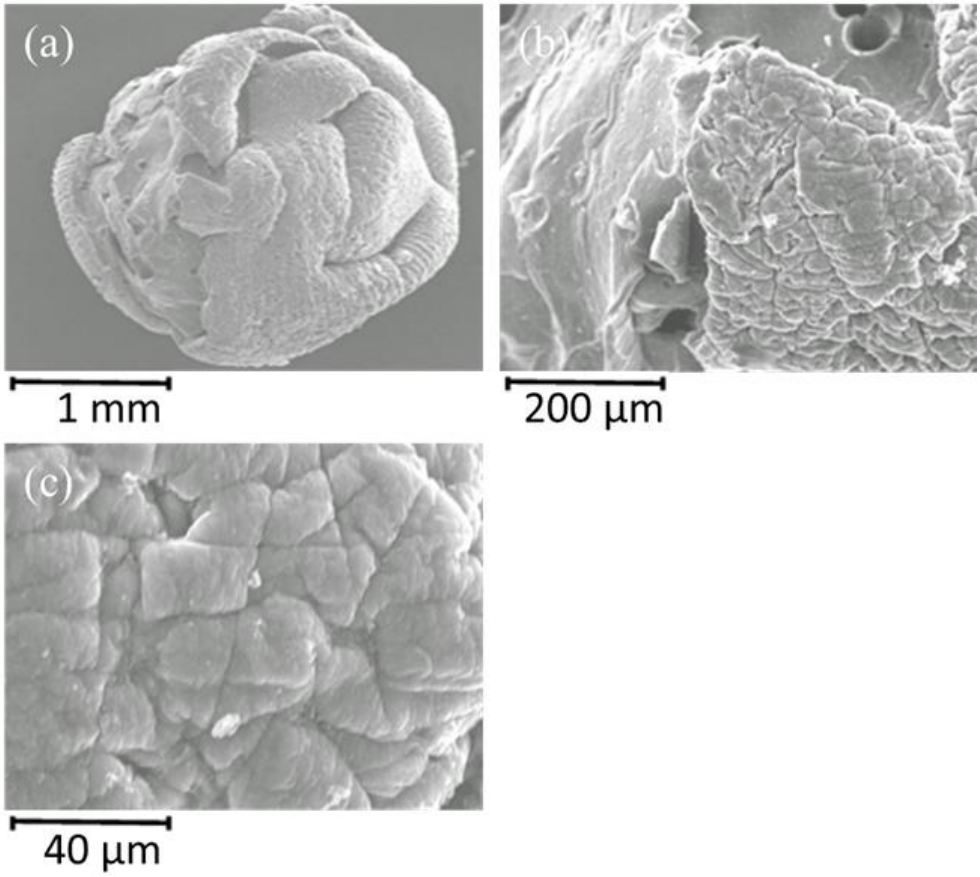

Figure 3.15: SEM micrographs of freeze-dried polypyrrole-coated calcium alginate beads at different magnifications.

3.2.1.2 Size of the Beads

In order to determine the size of the beads and to ensure that the beads were formed with a reasonably narrow size distribution the diameters of samples of each bead type were measured. The Gilosonic autosiever allowed a measurement of the size distribution of beads, while an average diameter was determined by measuring the diameter of a sample of beads using the Olympus BX5IM Microscope or SEM where appropriate. For each batch of beads, the beads were filtered out of the crosslinking solutions and rinsed three times with deionised water. Each batch was allowed to dry at room temperature until a constant weight was recorded.[31]

3.2.1.2.1 Calcium Alginate Beads

The diameters of the dried bead (n = 20) were measured under the microscope and an average diameter of 570 μm was determined. Then the beads ((n = 200) × 3) were passed through the sieves of the autosiever. The number of beads which passed through the three sieves (<500 μm, 600 – 500 μm, and 600 – 710 μm) for each sample are plotted in Figure 3.16. It was determined that 97% of the beads had diameters between 500 - 600 μm.

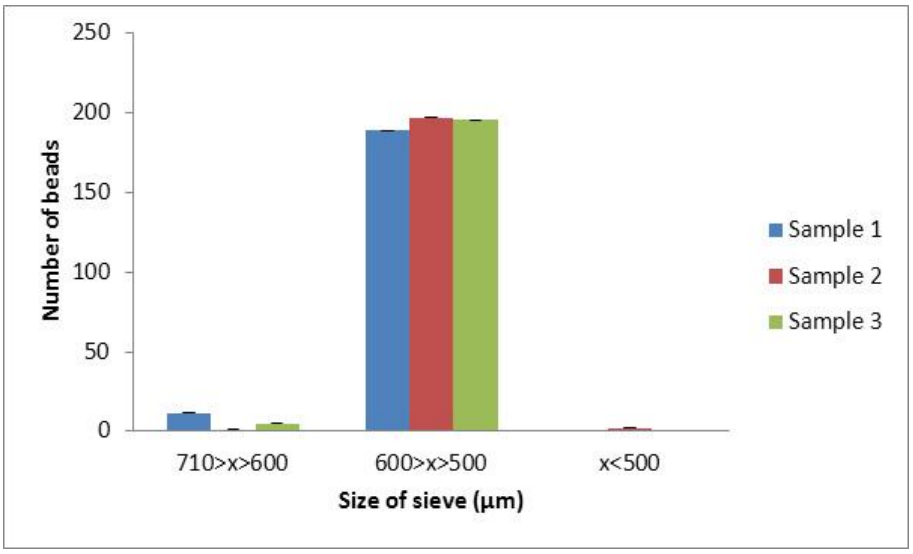

Figure 3.16: Size distribution of calcium alginate beads ((n = 200) × 3) determined using an autosieve.

A study was carried out to examine the effect that different concentrations of $CaCl_2$ (0.125 M, 0.25 M, 0.5 M, 1.0 M) in the crosslinking solution had on the diameters of the beads. After drying to a constant weight, the diameters of twenty beads from each batch were measured using the microscope. The average diameters for each batch of beads are given in Table 3.1. It was found that the diameters of the beads increased upon increasing the concentration of $CaCl_2$ in the crosslinking solution. When the alginate solution drops in to the higher concentration of $CaCl_2$, there are a lot of calcium ions present in the solution, therefore the beads are crosslinked quicker thus allowing less time for the alginate solution to dissipate. Whereas, with the lower concentrations, which contain less calcium ions, the

alginate solution has more time to dissipate into solution, causing the diameters of the beads to be smaller with decreasing concentration of crosslinking solution.

Table 3.1: The Effect of Varying the Concentration of $CaCl_2$ Solution on the Diameter of the Calcium Alginate Beads

$CaCl_2$ Concentration (M)	**Average Diameter (μm)**
0.125	563 ± 13
0.25	570 ± 17
0.50	664 ± 17
1.00	798 ± 22

3.2.1.2.2 Charcoal-loaded Calcium Alginate Beads

For the charcoal-loaded calcium beads the beads were all larger than the maximum sieve size of the autosiever which was 1400 μm. An average diameter of 2141 μm was determined for the beads (n = 20) using the SEM. The largest bead in this sample was found to have a diameter of 2390 μm and the smallest was found to have a diameter of 1860 μm. Therefore, the addition of charcoal to the calcium alginate beads (average diameter 570 μm) resulted in a substantial increase in bead size.

3.2.1.2.3 Bentonite-loaded Calcium Alginate Beads

The diameters of a sample (n = 20) of beads were measured using the SEM. An average diameter of 989 μm was observed. The largest diameter recorded was 1050 μm and the smallest diameter of the beads recorded was 909 μm. Samples ((n = 200) × 3) were placed in the autosiever in order to determine their range of diameters. The beads were trapped by either the 1180 – 1000 μm or the 1000 – 850 μm sieve and the results are plotted in Figure 3.17. The increase in bead size for both the charcoal-loaded and bentonite-loaded alginate beads compared to the analogous calcium alginate beads was consistent with the findings of other researchers. For example, Singh *et al.* produced starch-alginate beads using 12% w/v starch, 1% w/v sodium alginate and 0.1 M $CaCl_2$ with a mean diameter of 1.07 ±

0.08 mm, while this increased to 1.14 ± 0.08 mm when 4% w/v bentonite was added to the starch-alginate solution.[24]

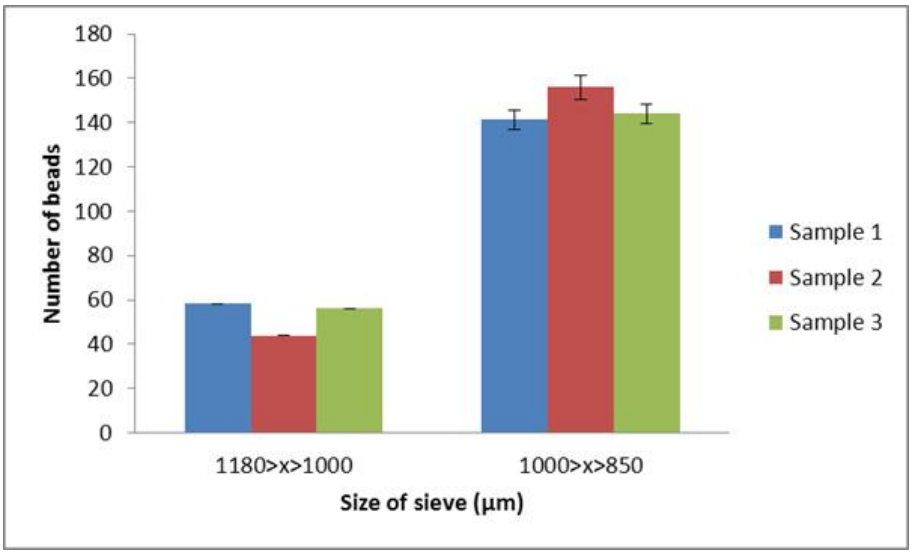

Figure 3.17: Size distribution the bentonite-loaded calcium alginate beads ((n = 200) × 3) determined using the autosiever.

3.2.1.2.4 Polypyrrole-coated Calcium Alginate Beads

The diameters of a sample (n = 20) of beads were measured using the SEM. An average diameter of 611 µm was observed. The largest diameter recorded was 653 µm and the smallest beads diameter was 558 µm. Then samples ((n = 200) × 3) were placed in the autosiever to determine their range of diameters. The beads were trapped by either the 710 – 600 µm or the 600 – 500 µm sieve and the results are plotted in Figure 3.18.

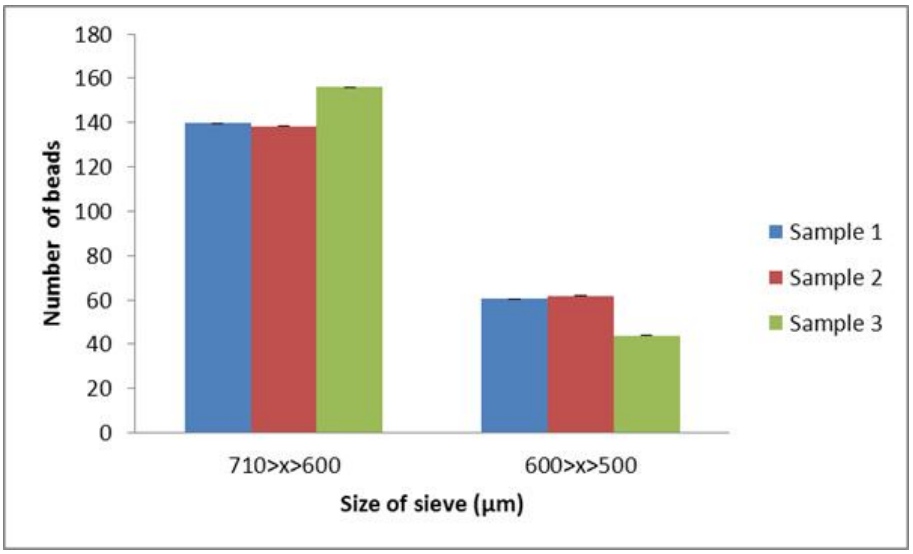

Figure 3.18: Size distribution the polypyrrole-coated calcium alginate beads (n = 200 × 3) determined using the autosiever.

In conclusion, the control calcium alginate hydrogel beads had the smallest diameters and the charcoal-loaded calcium alginate beads had the largest diameters. An overall summary of the size distribution of the four different types of beads studied is given in Table 3.2.

Table 3.2: Summary of the Size Distribution of the Four Beads Types.

Size Range of Sieves	% Calcium Alginate Beads in each sieve	% Charcoal-loaded Calcium Alginate Beads in each sieve	% Bentonite-loaded Calcium Alginate Beads in each sieve	% Polypyrrole-coated Calcium Alginate Beads in each sieve
x< 500	0.34	0	0	0
600 > x > 500	96.83	0	0	27.66
710 > x > 600	2.83	0	0	72.34
850 > x > 710	0	0	0	0
1000 > x > 850	0	0	73.61	0
1180 > x > 1000	0	0	26.39	0
1140 > x > 1180	0	0	0	0
x > 1400	0	100	0	0

3.2.1.3 Swelling of Beads

3.2.1.3.1 Calcium Alginate Beads

The swelling characteristics of the calcium alginate xerogel beads were determined by immersing dried test samples in deionised water, NaCl, NaOH and HCl solutions. (1% w/v sodium chloride solution, NaOH solution (pH 9), and HCl solution (pH 4)) as shown in Figure 3.19. In each case the solutions (20 ml) were held at 20 ± 1°C. For each measurement twenty dried beads were weighed and then placed in the solution. At specific times the beads were removed from the hydration medium. The excess surface-adhered liquid drops were removed by blotting the beads on filter paper.[32,33] The beads were then weighed on a four-figure electronic

balance. The swelling ratio was calculated as (W*s*-W*d*)/W*d*, where W*s* is the weight of swollen beads after filtration and W*d* is the dry weight of the hydrogel beads.[34]

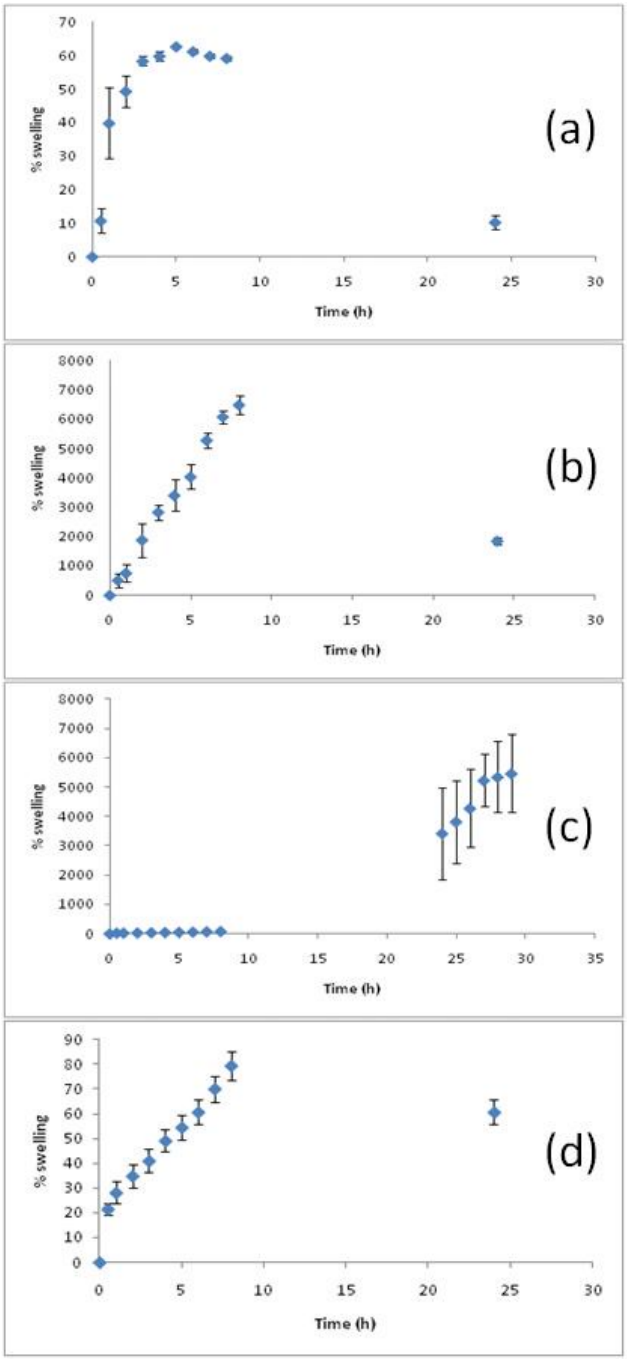

Figure 3.19: Swelling ratios (%) as a function of time of calcium alginate beads in (a) deionised water (b) 1% w/v NaCl solution (c) NaOH solution at pH 9 and (d) HCl solution at pH 4. Solutions were held at 20 ± 1°C.

The alginate beads increased quickly in weight in deionised water and reached their maximum swelling ratio after 5 h. The overall weight remained constant for the next 5 h. When the beads were weighed after 24 h of immersion a decrease in weight was recorded, indicating that the beads were disintegrating. Vlachou *et al.* observed similar overall trends when they immersed calcium alginate polymers capsules in distilled water.[35] The swelling of the calcium alginate beads studied here was significantly higher in the NaCl solution than in any of the other solutions. The beads took in approximately 60 times their original weight of water in the NaCl solution. The swelling observed in the NaCl solution is due to the ion exchange mechanism available with NaCl solution (Ca^{2+} exchanged for Na^{+}).[36] The calcium ions that were responsible for crosslinking the alginate chains were replaced with the sodium ions from the solution. Since there is only one positive charge on the sodium ion, the crosslinking was weakened dramatically. The beads increased in weight over 10 h, but, at the 24 h time point a dramatic decrease in weight was observed, indicating that the beads have undergone disintegration. Disintegration occurred as the replacement of the calcium ions for sodium ions had reached such a significant level that the sodium alginate chains were dissolving in the solution.

Over the first 8 h of measurement the swelling of the beads in the NaOH solution was similar to that observed in deionised water. However, after 24 h of immersion the beads increased dramatically in weight, reaching a %EDS value of approximate 3500% at 25 h. This slower swelling than observed in the NaCl solution may be due to the Na^{+}/Ca^{2+} ion exchange process. The concentration of Na^{+} ions in the NaCl solution was 0.17 M compared to 0.01mM in the NaOH solution. In addition, at the solution pH value of 9 it is likely that most of the carboxylate groups along the polymer backbone were deprotonated leading to increased electrostatic repulsion between the alginate chains. The beads immersed in the acidic solution swell gradually over 10 h reaching a similar %EDS to that recorded at the same time point for the beads immersed in water. Vlachou *et al.* and Sriamornsak *et al.* examined the swelling of their alginate capsules in a 0.1 M HCl solution (pH 1).[35,37] Both authors concluded that when sodium alginate is immersed in acidic solution it is transformed into alginic acid. Alginic acid has the ability to swell slightly on hydration but is virtually insoluble and is known to precipitate from solution at a pH of about 3.5. Therefore, although the beads swell initially to the

same extent as they do in water, as the polymer chains are held together by simple entanglement and not the calcium ion, the beads do not undergo disintegration through the ion exchange of calcium ions for hydrogen ions and their weight remains constant. At the pH of 4 used in the present study it is likely that a percentage of the uronic groups were deprotonated. The pK_a of mannuronic acid is 3.38 and and that of guluronic acid is 3.65,[37,38] therefore the calcium ion crosslinks are likely to still have played some part in holding the polymer chains of the bead together, and this probably explains the small decrease in mass recorded for these beads at the 24 h time period.

3.2.1.3.2 Charcoal-loaded Calcium Alginate Beads

The %EDS values as a function of time for the charcoal-loaded calcium alginate beads immersed in a range of solutions held at 20 ± 1°C are given in Figure 3.20.

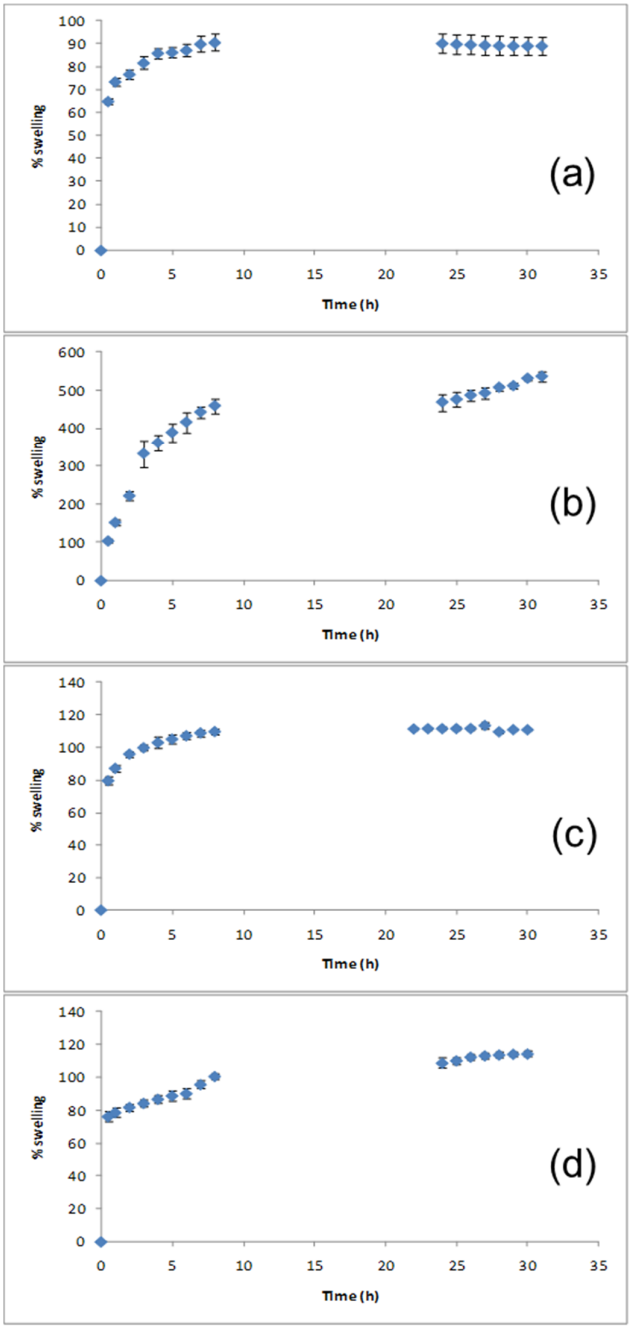

Figure 3.20: Swelling ratios (%) as a function of time of charcoal-loaded calcium alginate beads in (a) deionised water (b) 1% w/v NaCl solution, (c) NaOH solution at pH 9 and (d) HCl solution at pH 4. Solutions were held at 20 ± 1°C.

Overall the results on the swelling behaviour of the charcoal-loaded calcium alginate beads indicated that these beads were more stable than the calcium alginate beads. In deionised water the beads reached their maximum swelling of 80% in 10 h, after this time the weight of the beads stayed constant and no disintegration was observed after 32 h of immersion. In the sodium chloride solution the beads increased slowly in weight for the first 10 h, reaching a %EDS value of approximately 500%. This was significantly smaller than the value recorded at this time period in the analogous experiment carried out on the calcium alginate beads (7000%). Moreover, strikingly in comparison to the experiment on the calcium alginate beads no decrease in bead weight was observed over 30 h of immersion. This indicates that either the calcium/sodium ion exchange process was significantly disfavoured in these beads or that the presence of the charcoal was preventing the beads from disintegrating even after ion exchange has taken place. The %EDS values recorded for the beads immersed in NaOH or HCl solutions were similar to those recorded for the beads in deionised water. In both cases swelling was quite low and after the beads had reached their maximum weight no decrease in weight was then recorded over the time period of the experiment.

3.2.1.3.3 Bentonite-loaded Calcium Alginate Beads

The results for each of the swelling studies carried out on the calcium alginate beads loaded with bentonite are given in Figure 3.21.

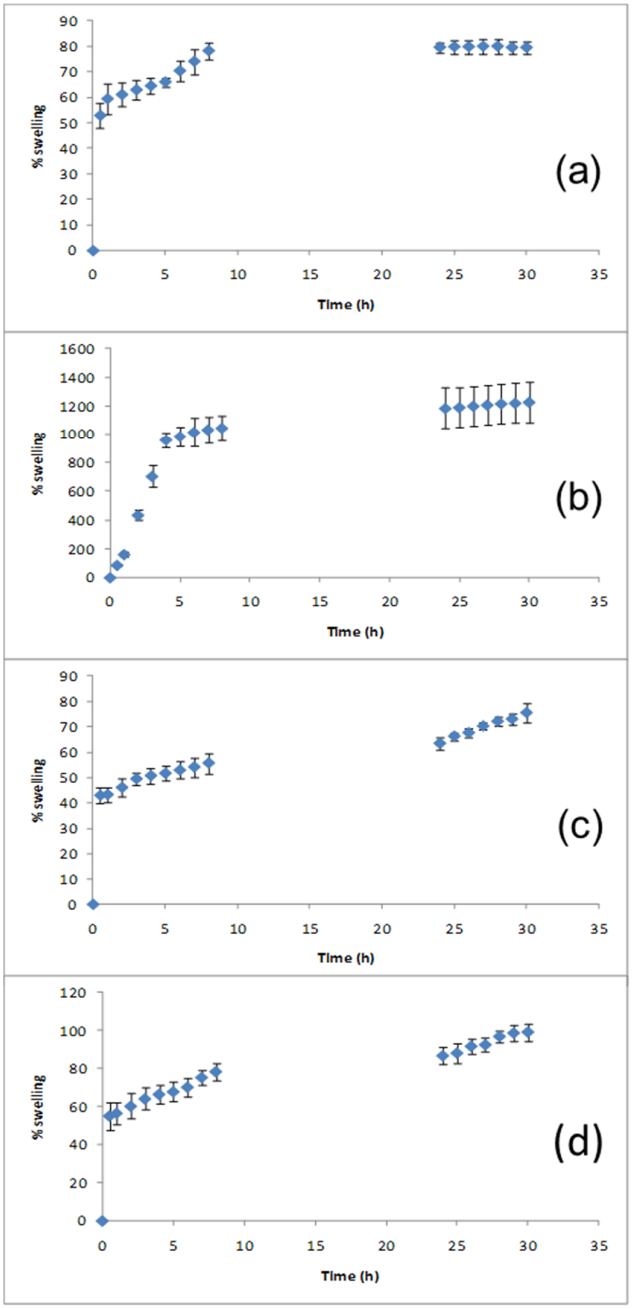

Figure 3.21: Swelling ratios (%) as a function of time of bentonite-loaded calcium alginate beads in (a) deionised water (b) 1% w/v NaCl solution, (c) NaOH solution at pH 9 and (d) HCl solution at pH 4. Solutions were held at 20 ± 1°C.

In general the results for the swelling behaviour of the beads loaded with bentonite were very similar to those obtained for the beads loaded with charcoal. The results for the swelling in deionised water were similar to those observed by other researchers on related systems. For example, Singh *et al.* have previously investigated the swelling behaviour in water of starch-alginate and bentonite-starch-alginate beads and found that the addition of bentonite only resulted in a small decrease in the water uptake of the beads in comparison to the control beads.[24] As for the calcium alginate and charcoal-loaded calcium alginate beads the maximum swelling was observed in the NaCl solution indicating that the ion exchange process was still taking place for these beads. However, the %EDS values recorded were significantly lower than those determined for the calcium alginate beads immersed under similar conditions. The overall trends observed indicate that the presence of the inorganic filler in the beads reduced their propensity to disintegrate when immersed in the four different solutions and reduced the degree to which the beads swell when immersed in a NaCl solution.

3.2.1.3.4 Polypyrrole-coated Calcium Alginate Beads

A study was carried out on the swelling properties of polypyrrole-coated calcium alginate beads in four different solutions and the results are presented in Figure 3.22.

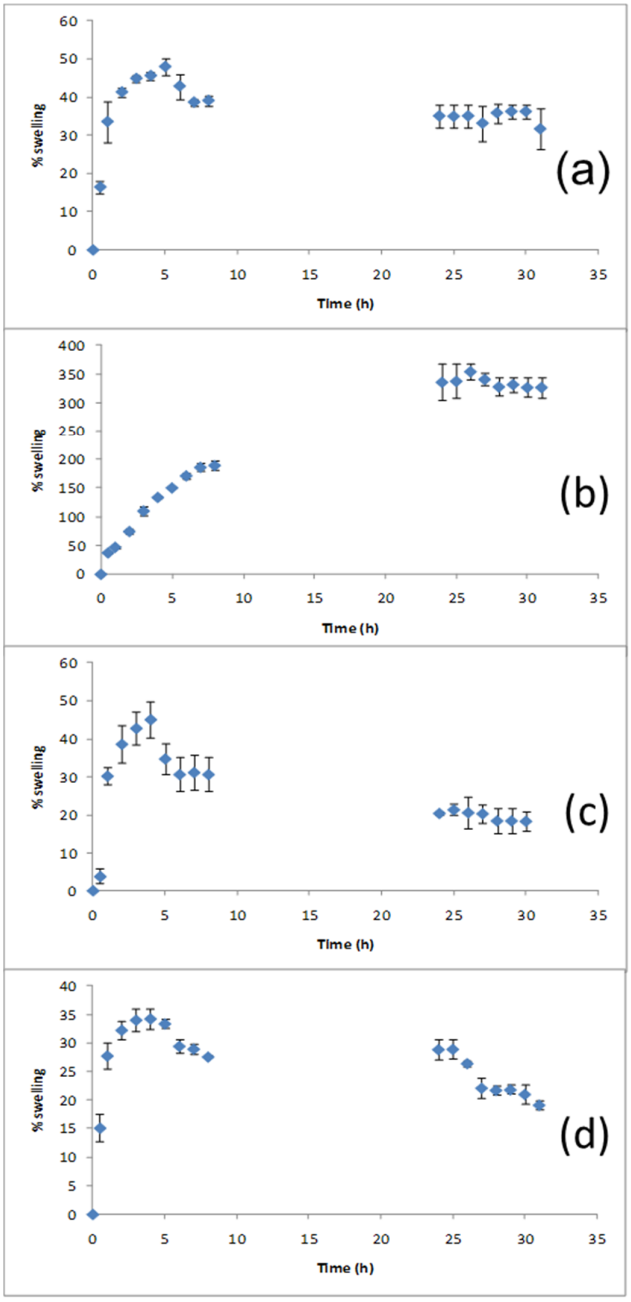

Figure 3.22: Swelling ratios (%) as a function of time of polypyrrole-coated calcium alginate beads in (a) deionised water (b) 1% w/v NaCl solution (c) NaOH solution at pH 9 and (d) HCl solution at pH 4. Solutions were held at 20 ± 1°C.

The swelling ratios of the polypyrrole-coated alginate beads immersed in deionised water were very similar to those recorded for the calcium alginate beads. The beads increased in weight gradually over 8 h and at this stage they had reached the maximum swelling, after this time there was a decrease in weight of the beads, indicating that the beads were undergoing a small amount of decomposition. However, the swelling ratio increase of 30% remains constant from 24 h to 30 h of immersion. The same quick total disintegration that was observed with the calcium alginate beads was not observed here, indicating that the polypyrrole was keeping the beads stable and preventing further disintegration in deionised water. In the sodium chloride solution there was a gradual swelling over the first 10 h and then there was a further increase in weight when the beads were weighed at 24 h which remained constant up to 30 h. The swelling of these beads never reached a swelling ratio as high as the calcium alginate beads. This would indicate that the polypyrrole coating was keeping the beads intact and preventing them from swelling to a stage where they became unstable. In the NaOH solution there is a slight increase in swelling ratio over the first 5 h of immersion which was very similar to that observed with the deionised water. After this time the polypyrrole coating started to disintegrate from around the beads, and the swelling media became discoloured. There are a number of known reactions that can take place between NaOH and polypyrrole. The first is that the Cl^- dopant ion can be replaced by OH^-, secondly the polymer backbone can be hydroxylated, and thirdly some of the pyrrole units can be deprotonated.[39] The swelling ratio decreased to 20% and remained constant after this time, indicating that the polypyrrole that was left on the beads was keeping them stable and preventing any further disintegration. In the HCl solution the beads underwent the least amount of swelling only reaching a swelling ratio of 35% in total. This was a very similar trend to that observed for the behaviour of the calcium alginate beads in the acidic solution.

3.2.1.3.5 Summary of Swelling Results for Beads

A summary of the results for the swelling experiments on the different bead types is given in Table 3.3. The % swelling for each of the four types of beads in deionised water was quite similar when recorded at the 8 h time period. However, a significant difference was observed at the 25 h reading, while the calcium alginate

beads had undergone substantial amounts of decomposition the modified calcium alginate beads were still intact. When the beads were immersed in the acid solution all the beads showed an intake of water over the first 8 h and this intake was maintained when the values were determined at the 25 h time period. This indicates that all the bead types were remaining intact over the course of the experiment. The most striking difference in the swelling behaviour between the calcium alginate beads and the modified calcium alginate beads was observed when the beads were immersed in solutions containing the Na^+ ion. A much more substantial intake of water was observed for the calcium alginate beads at 8 h in NaCl solution and at 25 h in the NaOH solution compared to the other beads. Moreover, the calcium alginate beads had completely decomposed after immersion in the NaCl solution for 25 h, while the other bead types remained intact. This indicates that the inorganic fillers and polypyrrole coating were disfavouring the Ca^{2+}/Na^+ ion exchange or that even after this exchange has taken place, the filler or polymer is holding the beads together. Of the three types of modified calcium alginate beads studied, the polypyrrole-coated calcium alginate beads consistently showed the lowest % swelling in the four media studied.

Table 3.3: Summary of Swelling Ratios (%) of Alginate Beads in Deionised Water, 1% w/v NaCl solution, NaOH solution (pH = 9), and HCl solution (pH = 4).

		Calcium Alginate Beads	**Charcoal-loaded Calcium Alginate Beads**	**Bentonite-loaded Calcium Alginate Beads**	**Polypyrrole-coated Calcium Alginate Beads**
% Swelling at 8 h*	Deionised Water	59	90	79	39
	NaCl (0.17 M)	6481	485	1045	189
	NaOH (1×10^{-5} M)	82	100	56	31
	HCl (1×10^{-4} M)	79	109	78	28
% Swelling at 25 h*	Deionised Water	10	90	80	34
	NaCl (0.17 M)	0	468	1183	336
	NaOH (1×10^{-5} M)	3421	108	66	21
	HCl (1×10^{-4} M)	61	111	87	29

* Solutions were held at 20 ± 1 °C

3.2.2 Study on the Stability of NBPT using NMR Spectroscopy

As stated in the Introduction to this Chapter studies have shown that the stability of NBPT is pH dependent. Therefore it was important to determine if the NBPT was stable within the four types of bead matrices used in this study. Before commencing this study the decomposition products of NBPT in D_2O under acidic and basic conditions were analysed using ^{1}H and ^{31}P NMR spectroscopy. In this study, H^+ or OH^- were added to D_2O, therefore neither the pH or pD scales strictly apply. Therefore, the acidic/basicity level of the solution was simply indicated by

the pH level recorded. The pH values recorded for the solutions used for this study were 1, 4, 7 and 14. The D_2O was brought to the required pH values using HCl, buffer solutions, or NaOH respectively. ^{1}H and ^{31}P NMR spectra were taken of the D_2O solutions at the same recorded pH values before the NBPT solution was added. Each of the samples was run over a period of three weeks to monitor the stability of the NBPT.

It is known from the literature that *n*-butylamine is a decomposition product of NBPT;[9] therefore ^{1}H NMR spectra were recorded of *n*-butylamine in D_2O and in D_2O with added acid or base. The spectra are shown in Figure 3.23(a-c). Figure 3.23(b) shows a ^{1}H NMR spectrum recorded of *n*-butylamine in D_2O and the four signals for the butyl group are clearly visible. Upon addition of base the spectrum recorded (Figure 3.23(a)) showed very little changes, indicating that no chemical reaction has taken place. However, upon addition of the acid (Figure 3.23(c)) the signals changed their position and the signal for the CH_2 group directly attached to the nitrogen broadened. These changes occurred as the *n*-butylamine was converted to *n*-butylammonium chloride upon reaction with the HCl.

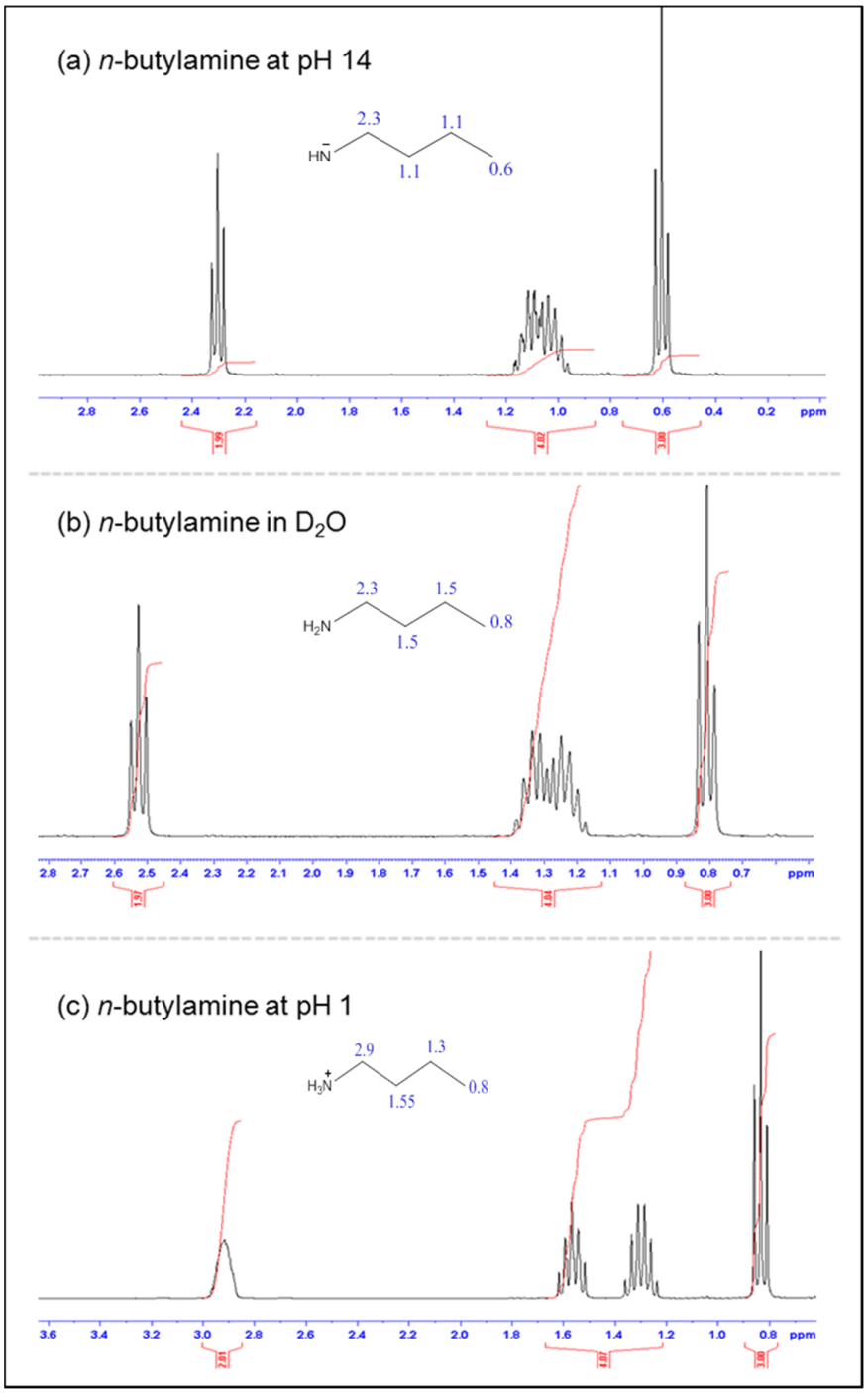

Figure 3.23: ^{1}H NMR spectrum recorded of n-butylamine in (a) D_2O with added NaOH (b) D_2O (c) D_2O with added HCl.

The ^{1}H and ^{31}P NMR spectra recorded of NBPT in D_2O are given in Figure 3.24(a) and (b) respectively. As for the ^{1}H NMR spectrum recorded of the *n*-

butylamine the signals for the butyl group were clearly visible. The signal for the CH_2 group attached directly to the N was a multiplet, whereas for *n*-butylamine this signal was a triplet. This difference arose due to the extra coupling to the phosphorus atom in the NBPT. This coupling was also observed in the ^{31}P NMR spectrum of NBPT as the signal for the phosphorus was split into a triplet.

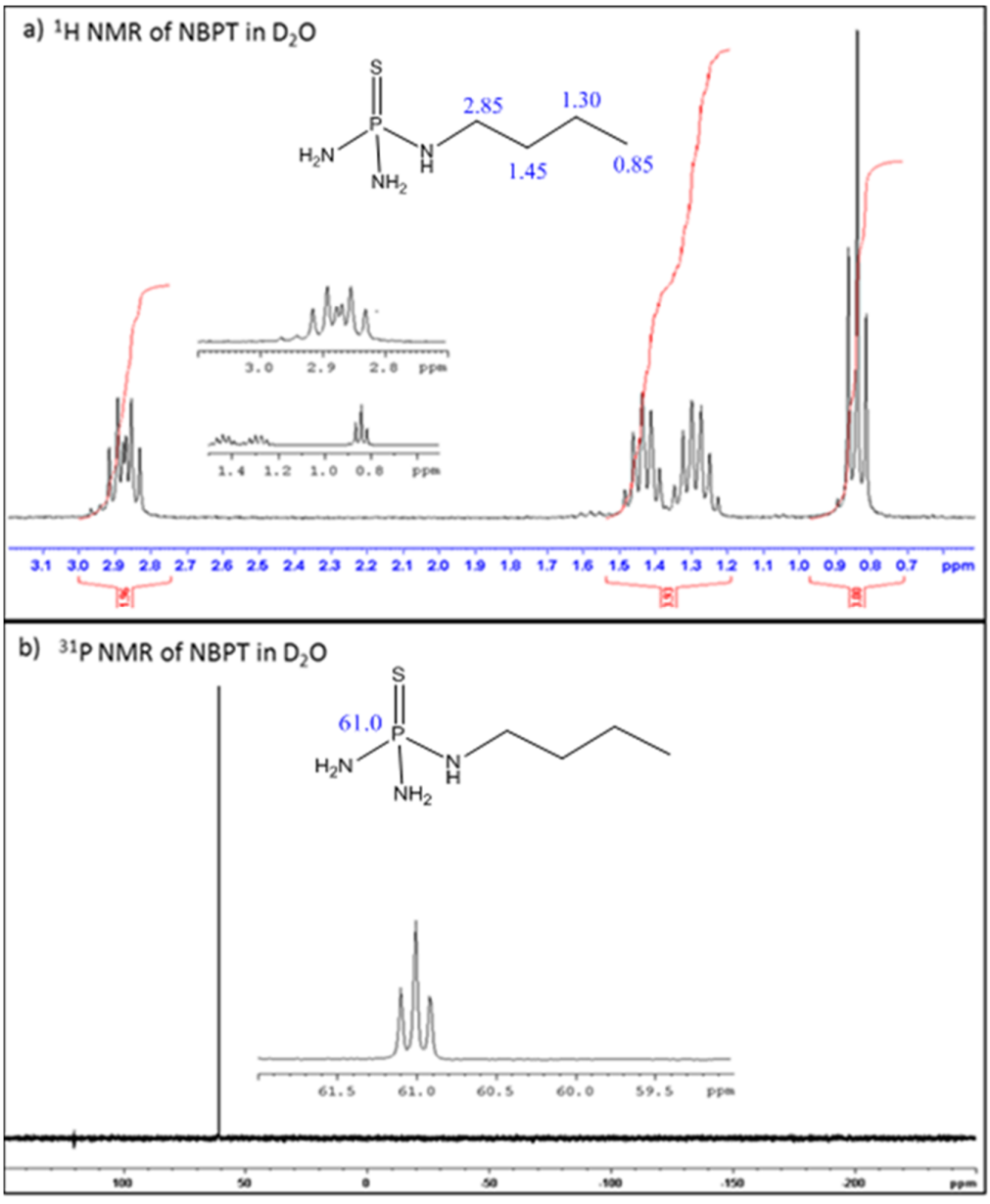

Figure 3.24: (a) ^{1}H NMR and (b) ^{31}P NMR spectra of NBPT in D_2O

The ^{1}H and ^{31}P NMR spectra of NBPT in D_2O with HCl added so that the pH meter recorded a pH value of 1 are given in Figure 3.25. As can be observed from the initial ^{1}H NMR spectrum, the NBPT immediately reacted with the acid and formed *n*-butylammonium chloride. The signal for the CH_2 group directly attached to the N of the *n*-butyl group had lost the coupling to phosphorus and the signals for the *n*-butyl group were identical to those for *n*-butylammonium chloride (Figure 3.18(b)). This finding is similar to the result found by Douglas *et al,* [9] who assigned the initial step of NBPT under acid conditions to the reaction given in Scheme 3.1. The initial ^{31}P NMR spectrum shows that a number of new phosphorus containing products were formed. It can be observed that the *n*-butylammonium chloride remained in solution over the three weeks of measurement and no new organic decomposition products were formed. Whereas, the initial phosphorus decomposition products underwent further reaction as is clearly observed by the changes in ^{31}P NMR spectra recorded over that time period.

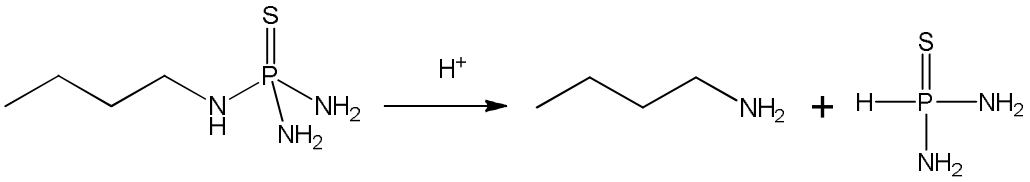

Scheme 3.1: Proposed reaction of NBPT with acid

The experiment outlined above was then repeated whilst added HCl to the D_2O until the pH meter recorded a pH value of 4. The ^{1}H and ^{31}P NMR spectra of NBPT in this solution are shown in Figure 3.26. It can be observed from both sets of spectra that the NBPT was still present in the solution over the three weeks. However, even in the initial ^{1}H NMR spectrum (t = 30 min) there were peaks observed which could be assigned as arising from *n*-butylammonium chloride and these peaks increased in relative intensity compared to those of NBPT over the course of the experiment, indicating that the NBPT was slowly decomposing. Similarly in the initial ^{31}P NMR spectrum along with the triplet signal assigned as a rising from the NBPT a singlet peak at 53.5 ppm was observed, which increased in intensity compared to the phosphorus signal for NBPT over the period of 3 weeks.

When NBPT was added to D_2O, which was kept at a pH value of 7, using the appropriate buffer, the ^1H NMR spectra recorded over the three week time period (Figure 3.27) indicated that essentially no decomposition of the NBPT was occurring. This finding was supported from the data obtained from the ^{31}P experiments which showed only a small increase in relative intensity of the peak at 53.5 ppm which is assigned to the primary phosphorus containing decomposition product.

The ^1H and ^{31}P NMR spectra recorded for NBPT in a highly basic solution of D_2O (NaOH solution was added to the D_2O until a pH value of 14 was recorded) are given in Figure 3.28. Both set of spectra indicate the NBPT immediately reacted with the base and no further reaction took place over the course of the experiment. The main set of signals in the ^1H NMR spectrum can be assigned as arising from *n*-butylamine by comparison with spectrum recorded of *n*-butylamine recorded under analogous conditions given in Figure 3.23. However, a further two signals at 2.60(m) and 1.25(m) ppm were observed which most likely were due to minor decomposition products. Two phosphorus containing decomposition products were observed in the ^{31}P NMR spectra recorded with a small signal occurring at 54.9(t) ppm and a major signal at 53.5(s) ppm.

From the $^{\mathbf{1}}H$ and ^{31}P NMR spectroscopic study it was concluded that the NBPT was relatively stable at neutral pH values and the main features of the NMR spectra of the decomposition products were identified. Using this information a study was carried out using NMR spectroscopy to determine the stability of NBPT within the four types of bead matrices (Figure 3.29). The NBPT was loaded into samples of the calcium alginate beads, charcoal-loaded calcium alginate beads, bentonite-loaded calcium alginate and polypyrrole-coated calcium alginate beads. The air-dried beads (n = 50) were immersed in D_2O (2 ml) and the NBPT was allowed to release into solution over 24 h. The D_2O solutions were then monitored using $^{\mathbf{1}}H$ and ^{31}P NMR spectroscopy (Figure 3.29), to test the stability of the NBPT in the different beads. For each case both the ^1H and ^{31}P NMR spectra matched that of NBPT and no decompostion products were observed. Therefore it was concluded that these beads could be used to encapsulate and release the urease inhibitor NBPT.

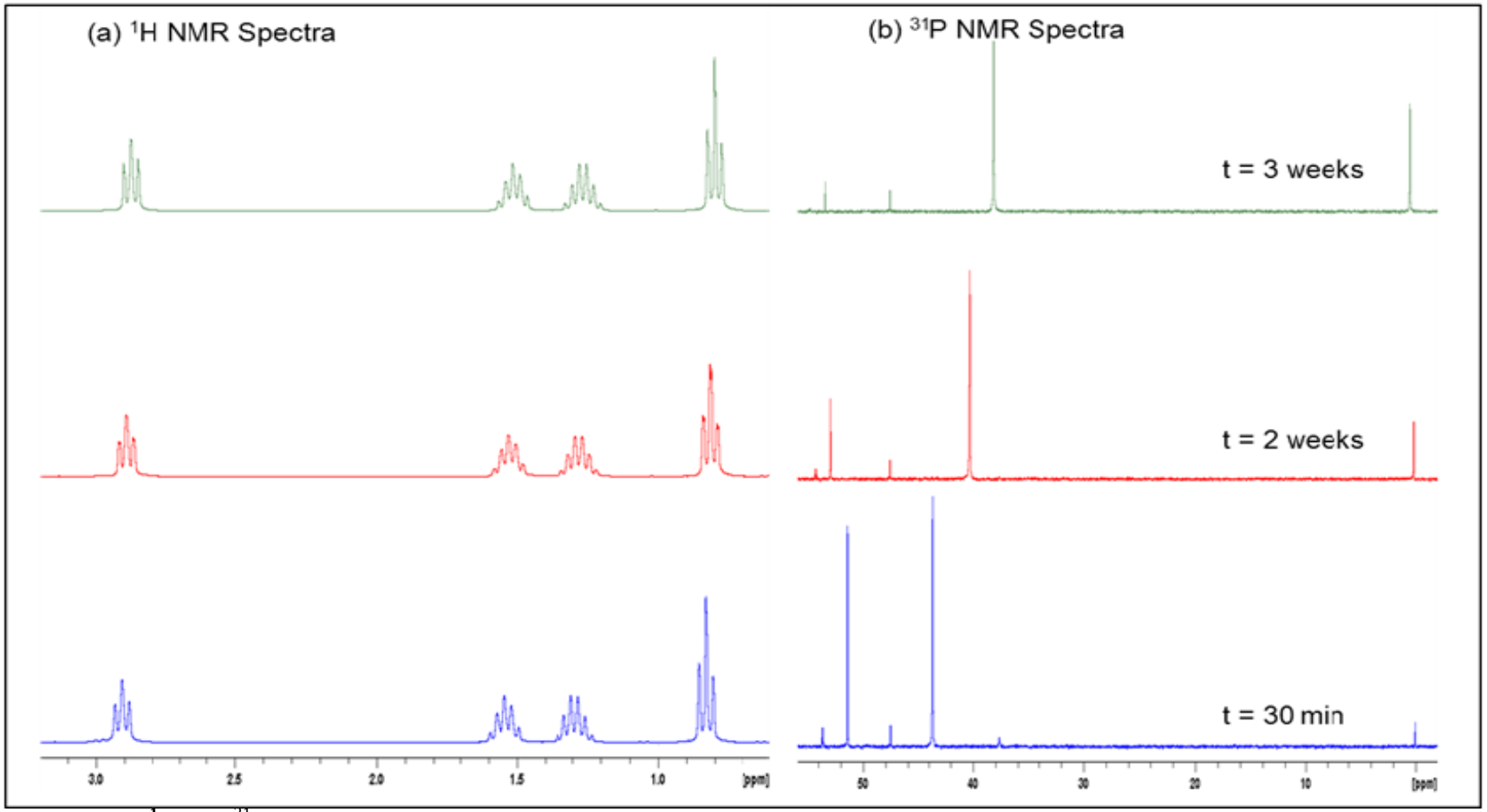

Figure 3.25: ^{1}H and ^{31}P NMR spectra recorded as a function of time of NBPT in D_2O upon addition of HCl so that a pH value of 1 was indicated.

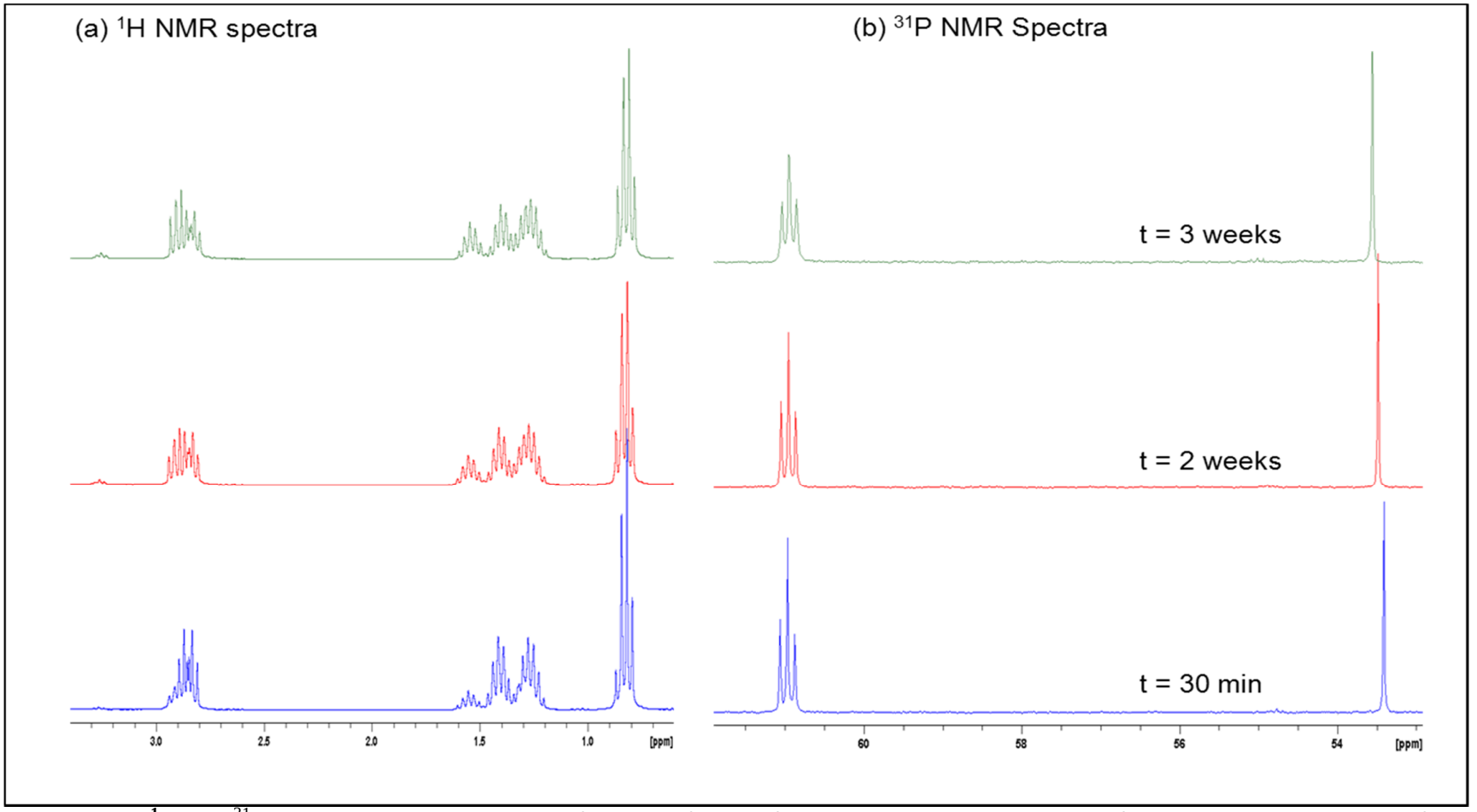

Figure 3.26: ^{1}H and ^{31}P NMR spectra recorded as a function of time of NBPT in D_2O upon addition of HCl so that a pH value of 4 was indicated.

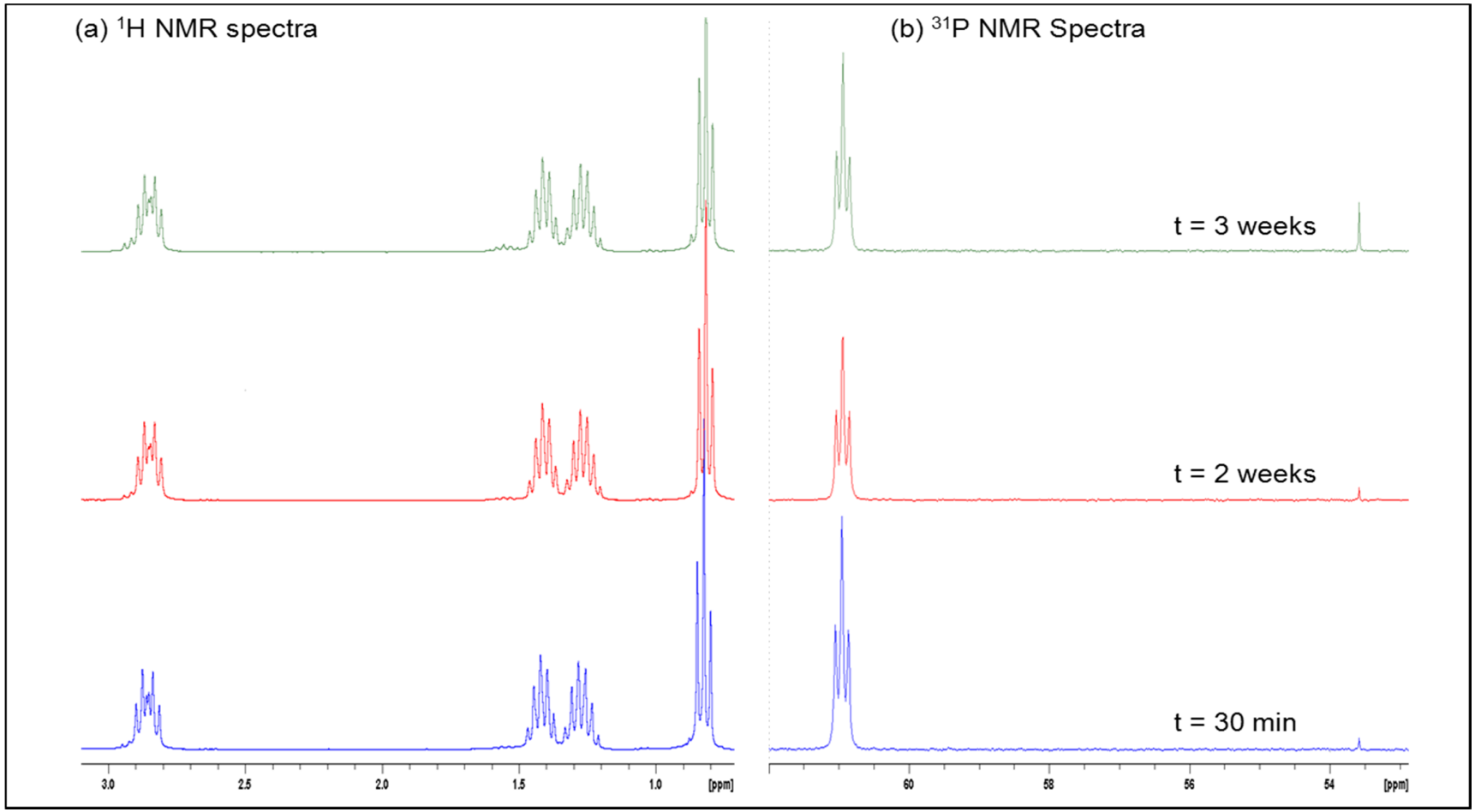

Figure 3.27: ^{1}H and ^{31}P NMR spectra recorded as a funtion of time.of NBPT in D_2O with added buffer so that the pH value of 7 was indicated.

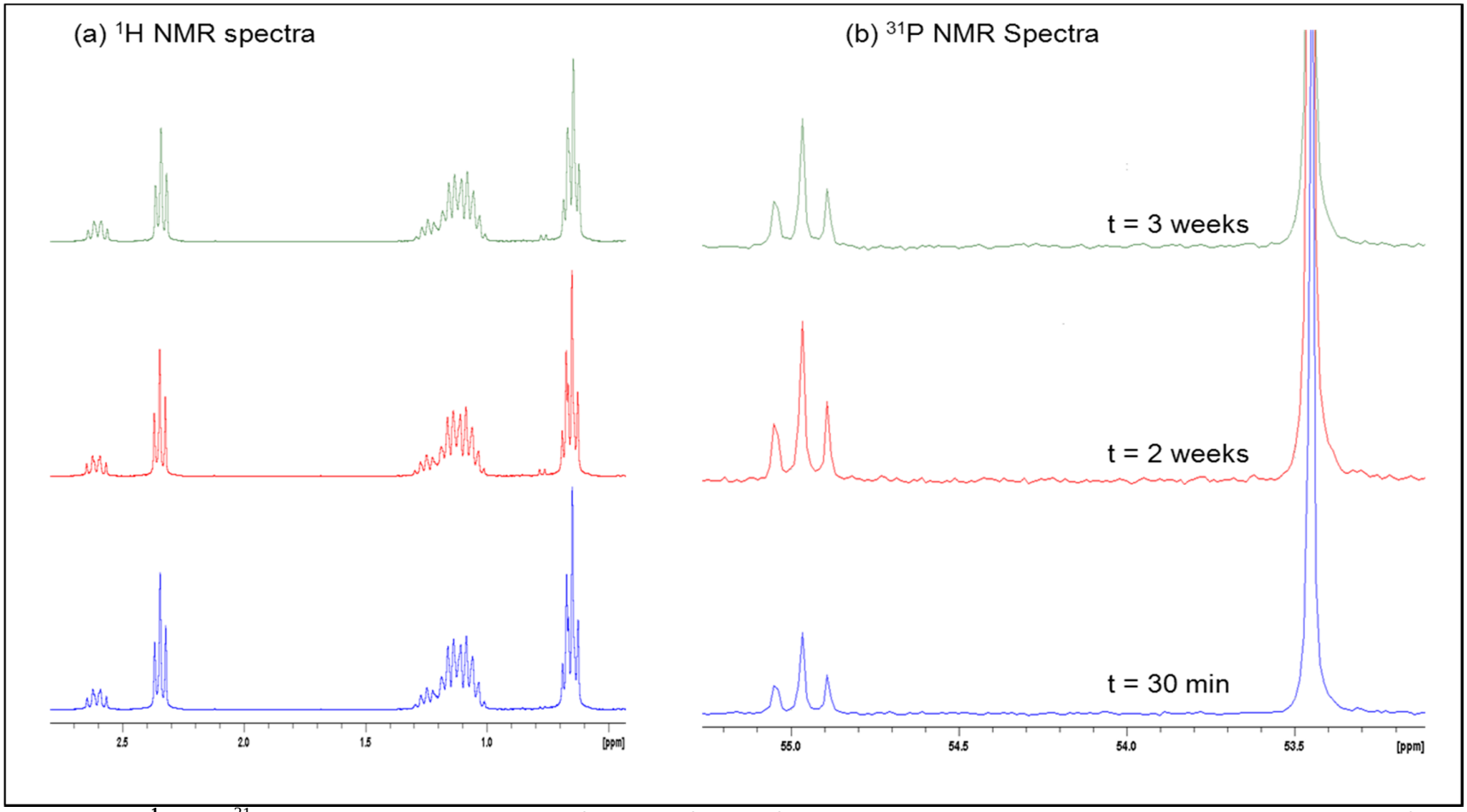

Figure 3.28: ^{1}H and ^{31}P NMR spectra recorded as a function of time of NBPT in D_2O with added NaOH, so that the pH value of 14 was indicated.

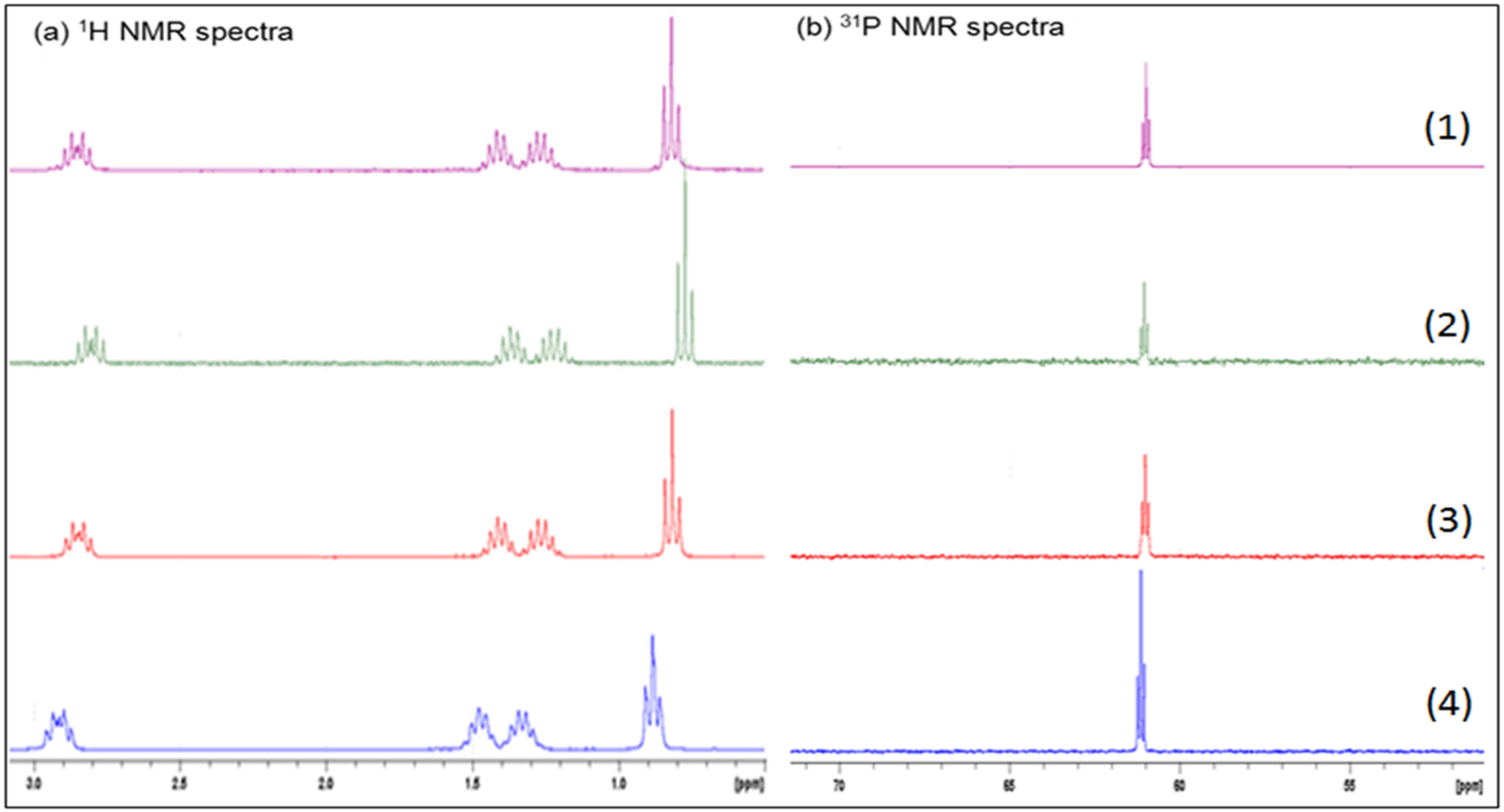

Figure 3.29: ^{1}H and ^{31}P NMR spectra of NBPT released from (1) alginate beads, (2) bentonite beads, (3) charcoal beads and (4) polypyrrole beads (n = 50). Spectra recorded after beads were immersd in D_2O for 24 h.

3.2.3 NBPT Release Studies from the Alginate Beads

3.2.3.1 UV/Vis Spectrum of NBPT in Water

The technique that was chosen to monitor the release of NBPT from the beads was UV/Vis spectrscopy. Before the release studies commenced UV/Vis spectra of NBPT at different concentrations were recorded. Figure 3.30 shows a typical absorbance spectrum of NBPT in water at a concentration of 1.25×10^{-4} M. The spectrum shows that NBPT has an absorbance band with a λ_{max} value at 212 nm in water.

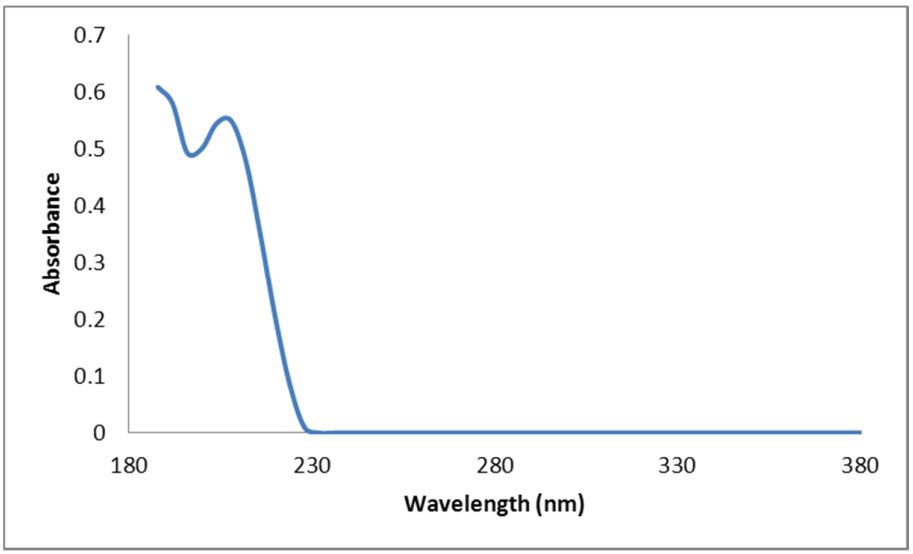

Figure 3.30: UV/Vis spectrum of NBPT (1.25×10^{-4} M) in deionised water.

3.2.3.2 Release of NBPT from Calcium Alginate Beads

Figure 3.31 shows the release of compound(s) from NBPT loaded calcium alginate beads crosslinked with different amounts of calcium ions. Batches of the different bead types were soaked in an aqueous solution of NBPT (0.05 M) for 24 h. The beads were rinsed and dried at room temperature before the release studies were carried out. As can be observed from the spectra all the beads released NBPT and an additional material into the deionised water that absorbed in the same region as NBPT. However, complementary ^{1}H NMR experiments using D_2O had shown that NBPT release was taking place (Figure 3.29). For each type of bead the release of the NBPT and the additional material was very fast and all release was achieved after

30 min of immersion. Moreover, there was no decrease in the rate of release upon increasing the amount of calcium crosslinks in the beads. The experiment was then repeated without stirring the beads to investigate what effect agitation had on the rate of release of compounds from the beads and the results are presented in Figure 3.32.

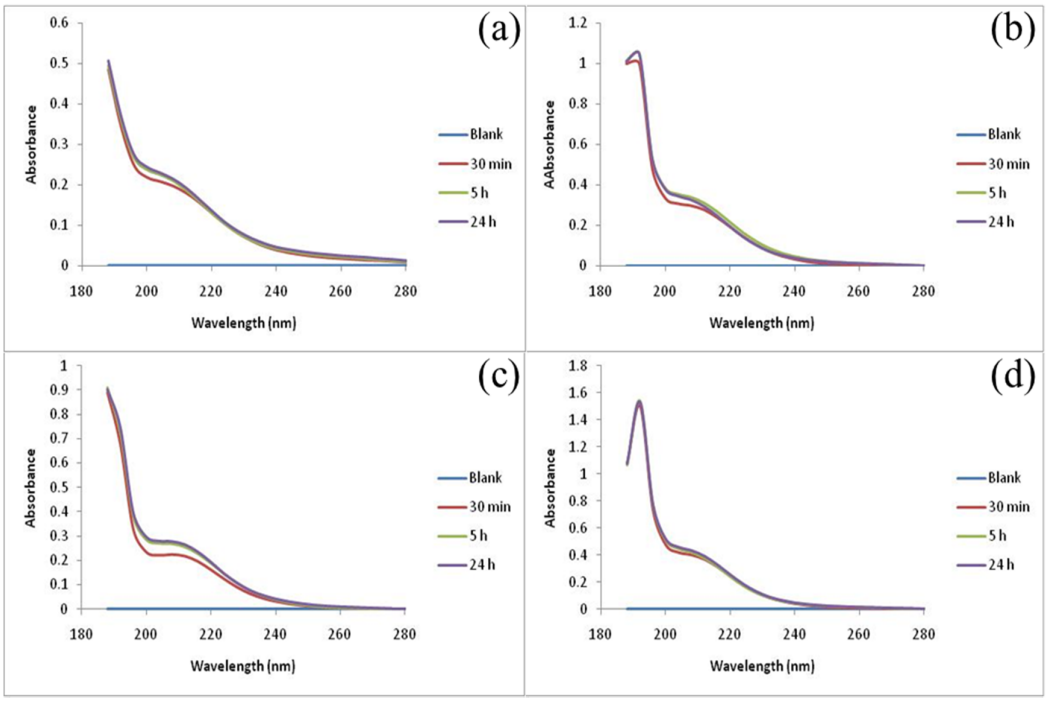

Figure 3.31: UV/Vis spectra of material released into deionised water (20 ml) as a function of time from NBPT loaded calcium alginate beads (n = 100) crosslinked in a solution containing (a) 0.125 M, (b) 0.25 M, (c) 0.50 M and (d) 1.0 M calcium chloride. Solutions were held at 20 ± 1°C with stirring.

The data presented in Figure 3.32 indicates that as for the unstirred experiment the degree of crosslinking did not appear to have much effect on slowing the rate of release of the NBPT from the beads. Upon comparison of the spectra given in Figure 3.31 to those presented in Figure 3.32 it is clear that the release of compounds from the analogus beads was signifcantly slower when the beads were not stirred. For example in Figure 3.32(b) the absorbance at 212 nm after 30 min immersion is only 0.041 absorbance units, whereas in Figure 3.31(b) it is 0.277 absorbance units. Moreover, in Figure 3.31(b) there is no difference between that absorbance at 212

nm after 30 min or 5 h immersion, while in Figure 3.32(b) the absorbance at 212 nm after 5 h immersion has increased to 0.234 absorbance units. This indicates that in the first experiment all the NBPT was released in the first 30 min of immersion but this was not the case in the unstirred experiment. However, release of NBPT was still too fast for the beads to be considered as a controlled release system for NBPT.

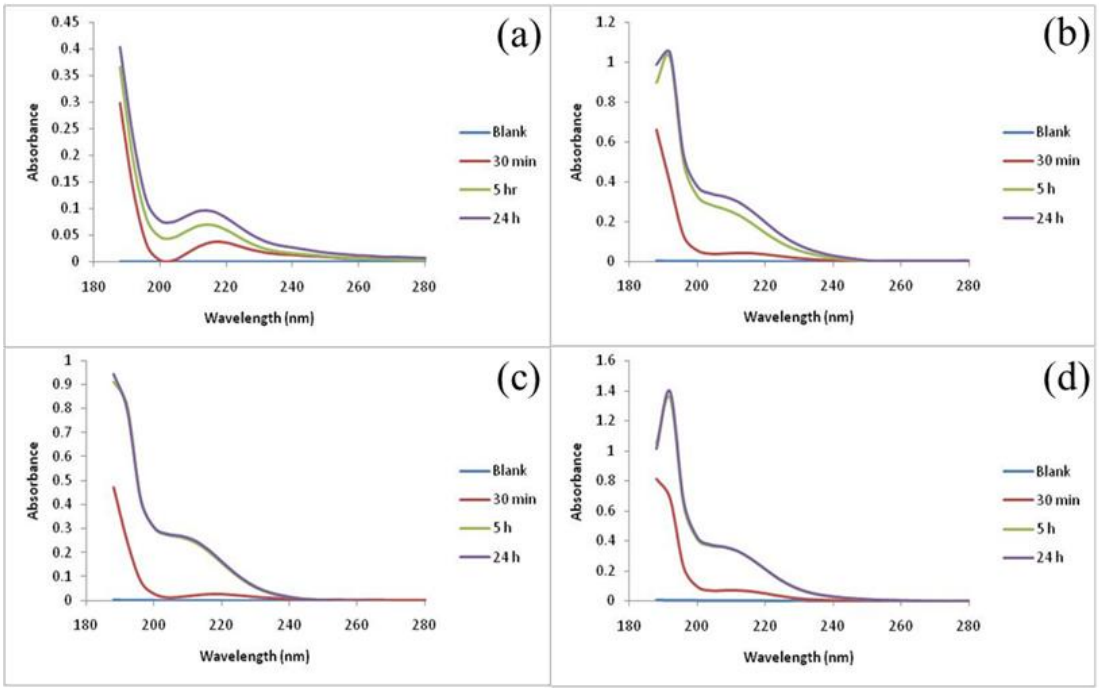

Figure 3.32: UV/Vis spectra of material released into deionised water (20 ml) as a function of time from calcium alginate beads (n = 100) loaded with NBPT crosslinked in a solution containing (a) 0.125 M, (b) 0.25 M, (c) 0.50 M and (d) 1.0 M calcium chloride. Solutions were held at 20 ± 1°C with no stirring.

3.2.3.3 Release of NBPT from Charcoal-loaded Calcium Alginate Beads

In order to first determine the UV/Vis spectrum of chemicals released from the bead matrix, the charcoal-loaded alginate beads were placed into deionised water and the absorbance spectrum of the surrounding medium was monitored over time. Examples of the UV/Vis spectra recorded are given in Figure 3.33. Separate experiments were carried out in which the beads were agitated (Figure 3.33(a)) or not agitated (Figure 3.33(b)) during the course of the experiment. Material was released from these beads which gave an absorbance in the UV region of the

spectrum. If the beads were not agitated all the material was released from the beads after 5 h of immersion and there was very little difference between the spectrum recorded of the release medium at the 5 h and 24 h time periods. If the beads were agitated all the material was released within 30 min.

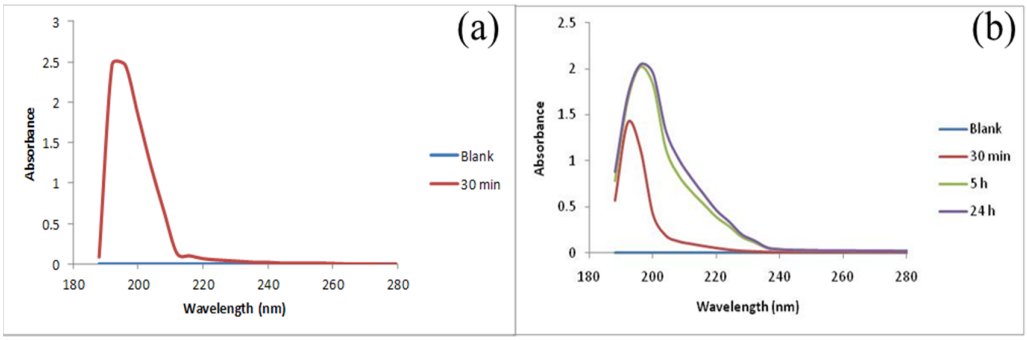

Figure 3.33: UV/Vis spectra of material released into deionised water (20 ml) as a function of time from charcoal-loaded calcium alginate beads (n = 100). Solutions were held at 20 ± 1°C (a) with stirring and (b) without stirring.

The urease inhibitor NBPT was loaded into the charcoal-loaded alginate beads by immersing the beads into a solution of the inhibitor (0.05 M). The beads were then dried before the release studies were carried out. A ^{1}H NMR study using D_2O confirmed that NBPT was released from the beads (Figure 3.29). Figure 3.34(a) shows the UV/Vis spectra recorded to investigate the release of NBPT from the alginate beads loaded with charcoal while the beads were stirred. A very broad intense band was observed in the UV region of the spectrum of the release solution recorded after 30 min immersion. This band increased slightly in intensity in the spectrum recorded after 5 h immersion and then remained unchanged at the 24 h time period. This indicates that all the material (including NBPT) was released from the beads within 5 h. Figure 3.34(b) shows UV/Vis spectra recorded for the release of NBPT into deionised water from charcoal-loaded calcium alginate beads which were not agitated. As can be observed in Figure 3.32(b) the band in the 200 – 240 nm region increased in intensty between the spectra recorded after 5 h and 24 h immersion. This indicates that the rate of release of chemicals from the beads was significantly reduced in the absence of agitation. The spectra recorded of the material released from the 'blank' charcoal-loaded calcium alginate beads without

stirring, after 5 h immersion looked essentially identical to the spectra recorded at 24 h of immersion (Figure 3.33(b)). Whereas, the absorbance bands in the spectrum recorded of the material released from the NBPT loaded beads at 24 h had increased in intensity compared to those in the spectrum recorded at 5 h. This indicates that a species was being released from the NBPT loaded beads in additional to the material released from the blank beads and it is reasonable to assume that this species is NBPT. This would indicate that the NBPT was being released more slowly from the charcoal-loaded calcium alginate beads compared to the calcium alginate beads and by comparison with the data presented in Figure 3.34(b), it would appear that even after 24 h of immersion not all of the NBPT had been released from the beads. However, the release was still too fast for the beads to be used as an urease inhibitor delivery system and the release was completely uncontrolled if the beads were agitated.

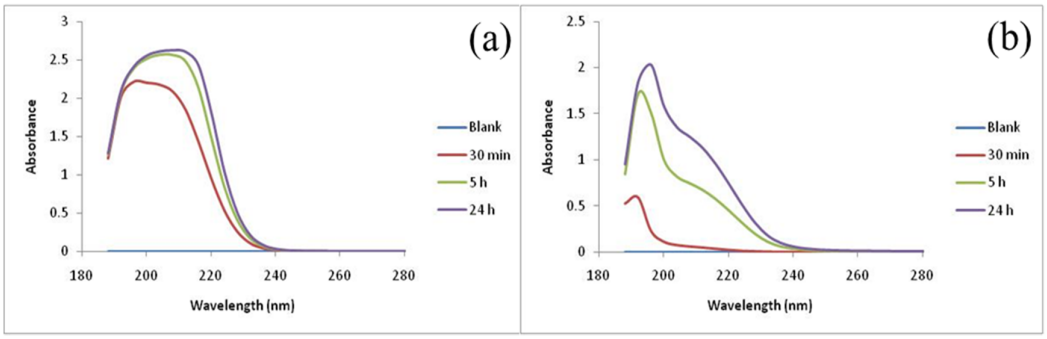

Figure 3.34: UV/Vis spectra of material released into deionised water (20 ml) as a function of time from charcoal-loaded calcium alginate beads (n = 100) loaded with NBPT. Solutions were held at 20 ± 1°C (a) with stirring and (b).without stirring.

3.2.3.4 Release of NBPT from Bentonite-loaded Calcium Alginate Beads

Preliminary experiments were carried out to determine the UV/Vis spectrum of chemicals released from the bead matrices. Two sets of the bentonite-loaded calcium alginate beads were immersed in deionised water either with or without stirring. The water was sampled as a function of time and a UV/Vis spectrum was recorded. The sample was then returned to the release medium in order to minimise differences in release medium volume between samples. Sample of the spectra recorded are given in Figure 3.35(a) and (b).

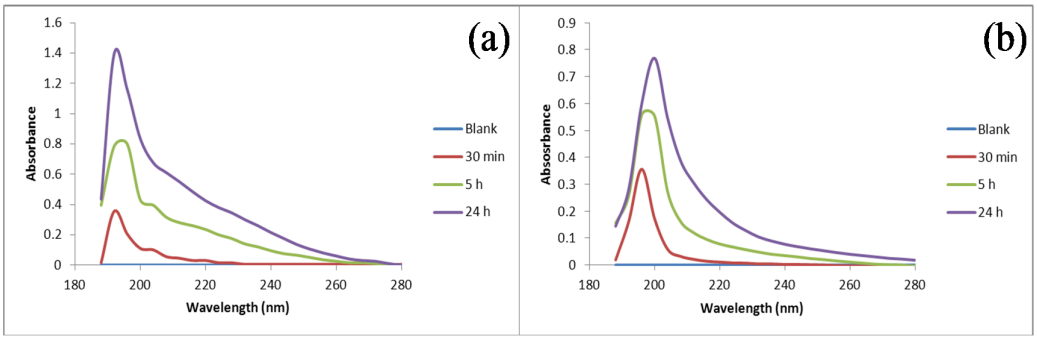

Figure 3.35: UV/Vis spectra of material released into deionised water (20 ml) as a function of time from bentonite-loaded calcium alginate beads (n = 100). Solutions were held at 20 ± 1°C (a) with stirring and (b) without stirring.

The release experiment was then repeated with the bentonite-loaded alginate beads which contained NBPT. Preliminary studies uing ^{1}H NMR spectroscopy confirmed that NBPT was released from these beads (Figure 3.29). The release data obtained using UV/Vis spectroscopy are presented in Figure 3.36. As can clearly be seen in the spectra given in Figure 3.36(a) an additional band is present compared to the spectra given in Figure 3.35(a). This additional band was assigned as arising from NBPT. When the beads were stirred (Figure 3.36(a)) this band was seen to increase in intensity between the 30 min and 5 h time period. A similar result was observed for the experiment carried out with no stirring, although the actual intensity of the additional band was lower, suggesting that in this case a significant component of the NBPT was still trapped within the beads.

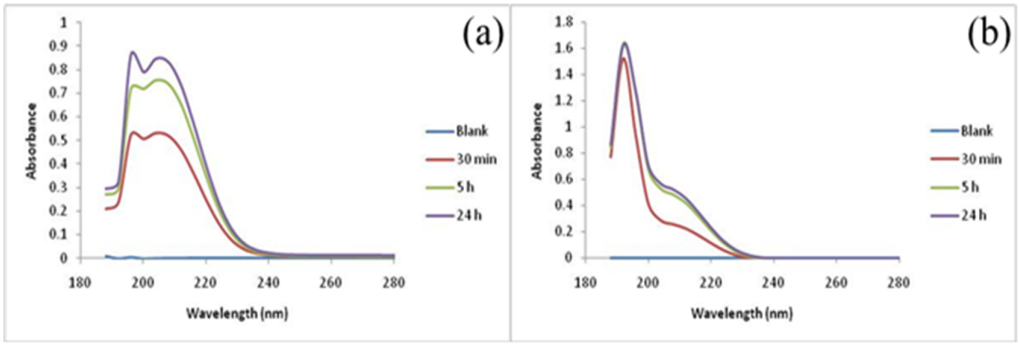

Figure 3.36: UV/Vis spectra of alginate beads loaded with bentonite and crosslinked with 0.25 M calcium chloride containing NBPT. Solutions were held at 20 ± 1°C (a) with stirring and (b) without stirring.

3.2.3.5 Release of NBPT from Polypyrrole-coated Calcium Alginate Beads

In order to first determine the UV/Vis spectrum of chemicals released from the bead matrix the polypyrrole coated alginate beads were placed in deionised water. Examples of the UV/Vis spectra recorded of the surrounding water are given in Figure 3.37. Chemicals were released from the bead matrix which exhibited an absorbance in the region of 200-240 nm which would interfere with our ability to monitor the release of NBPT from these beads.

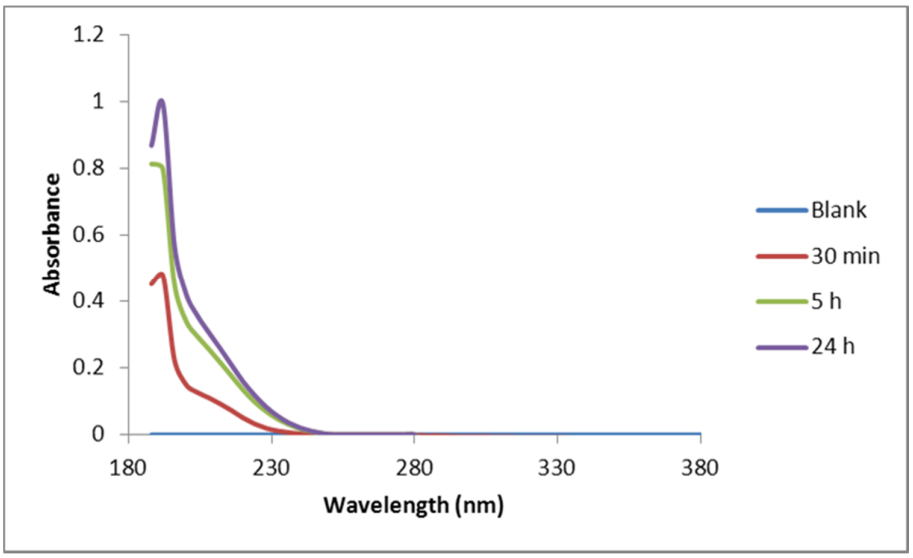

Figure 3.37: UV/Vis spectra of material released in to deionised water (20 ml) as a function of time from polypyrrole-coated calcium alginate beads (n = 100). Solutions were held at 20 ± 1°C and were not stirred.

NBPT was loaded into the polypyrrole-coated calcium alginate beads and release experiments into deionised water were carried out. Studies using ^{1}H NMR spectroscopy confirmed that NBPT was released from these beads (Figure 3.29). When the beads were stirred the UV/Vis spectrum recorded at 30 min of the surrounding solution showed an intense band with a λ_{max} at 212 nm. There was only a small increase in the intensity of this band when the solution was sampled at 5 h and no further increase was recorded after 24 h of immersion (Figure 3.38(a)). This indicates that essentially all the chemicals including NBPT were released within 30 min of immersion. When the experiment was repeated without stirring, the UV/Vis spectra recorded of the surrounding solution (Figure 3.38(b)) indicated that

chemicals were being released from the beads at a much slower rate. Moreover the band which appears as a shoulder between 208 nm to 220 nm was more pronounced than in the analogous spectra recorded for the experiment on the 'blank' beads (Figure 3.37). This shoulder band was assigned as NBPT. This band clearly increased in intensity in the spectrum recorded after 24 h immersion compared to that recorded after 5 h immersion (Figure 3.38(b)). This indicates that NBPT was being released fairly slowly from these beads. As previously observed for the charcoal and bentonite-loaded beads the difference in the spectra recorded for the stirred compared to the unstirred beads would suggest that for the latter case a certain amount of the NBPT remained trapped within the bead matrix even after 24 h of immersion.

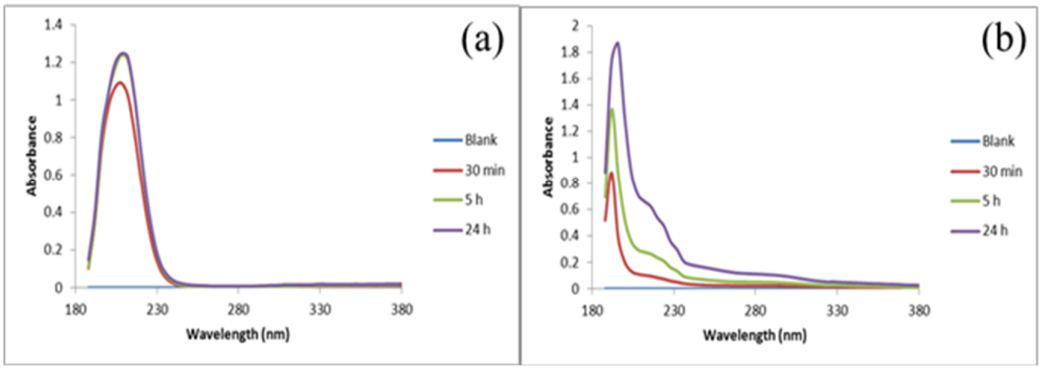

Figure 3.38: UV/Vis spectra of alginate beads coated with polypyrrole and crosslinked with 0.25M calcium chloride. Solutions were held at 20 ± 1°C (a) with stirring and (b) without stirring.

3.3 Conclusions

1. Four types of calcium alginate beads were fabricated for this study. To the best of our knowledge the polypyrrole-coated calcium alginate beads are novel.
2. The bead morphology and bead size distribution were determined and in general the findings are consistent with those of literature reports.
3. An in-depth study into the swelling behaviour of the beads was carried out. Novel results concerning the swelling of bentonite-loaded, charcoal-loaded and polypyrrole-coated calcium alginate beads showed that these beads are more resistant to swelling under basic conditions and to the presence of NaCl in the solution than their calcium alginate analogues. For the bead types studied the polypyrrole-coated calcium alginate showed the lowest amount of swelling in all the media studied. It would be very interesting to extend studies to further characterise this composite bead.
4. The decomposition products of NBPT, and its stability within the four beads types, were investigated using NMR spectrscopy. This indicates that NBPT decomposes at an acidic pH value of 4 and at higly basic pH values.
5. The release studies on the four bead types indicated that release of NBPT was very uncontrolled if the beads were agitated. Release was slowed down significantly if the beads were not agitated. The most promising results for developing a controlled release system for NBPT were obtained from the betonite-loaded and polypyrrole-coated calcium alginate beads as it would appear for the unagitated beads that a siginificant proportion of the NBPT remained within the bead matrix even after 24 h of immersion in deionised water. However, further studies would need to be carried out to reduce the pore size in these beads, for example by increasing the thickness of the polypyrrole coating, in order to prevent the rapid release which occurs upon agitation.

3.4. References

(1) Zaman, M.; Saggar, S.; Blennerhassett, J. D.; Singh, J. *Soil Biology & Biochemistry* **2009**, *41*, 1270-1280.
(2) Francisco, S. S.; Urrutia, O.; Martin, V.; Peristeropoulos, A.; Garcia-Mina, J. M. *Journal of the Science of Food and Agriculture* **2009**, *91*, 1569-1575.
(3) Gill, J. S.; Bijay, S.; Khind, C. S.; Yadvinder, S. *Nutrient Cycling in Agroecosystems* **1999**, *53*, 203-207.
(4) Ansari, F. L.; Wadood, A.; Ullah, A.; Iftikhar, F.; Ul-Haq, Z. *Journal of Enzyme Inhibition and Medicinal Chemistry* **2009**, *24*, 151-156.
(5) Font, M.; Dominguez, M. J.; Sanmartin, C.; Palop, J. A.; San-Francisco, S.; Urrutia, O.; Houdusse, F.; Garcia-Mina, J. M. *Journal of Agricultural and Food Chemistry* **2008**, *56*, 8451-8460.
(6) Manunza, B.; Deiana, S.; Pintore, M.; Gessa, C. *Soil Biology & Biochemistry* **1999**, *31*, 789-796.
(7) Dominguez, M. J.; Sanmartin, C.; Font, M.; Palop, J. A.; Francisco, S. S.; Urrutia, O.; Houdusse, F.; Garcia-Mina, J. M. *Journal of Agricultural and Food Chemistry* **2008**, *56*, 3721-3731.
(8) Varel, V. H.; Nienaber, J. A.; Freetly, H. C. *Journal of Animal Science* **1999**, *77*, 1162-1168.
(9) Douglass, E. A.; Hendrickson, L. L. *Journal of Agricultural and Food Chemistry* **1991**, *39*, 2318-2321.
(10) Hendrickson, L. L.; Douglass, E. A. *Soil Biology & Biochemistry* **1993**, *25*, 1613-1618.
(11) Murray, H. H. *Acta Geodynamica et Geomaterialia* **2005**, *2*, 127-134.
(12) Paul, P.; Gon, D. P.; Banerjee, D. *Chemical Fibers International* **2011**, *61*, 208-209.
(13) Fernández-Pérez, M.; González-Pradas, E.; Villafranca-Sánchez, M.; Flores-Céspedes, F. *Chemosphere* **2001**, *43*, 347-353.
(14) Garrido-Herrera, F. J.; Gonzalez-Pradas, E.; Fernandez-Perez, M. *Journal of Agricultural and Food Chemistry* **2006**, *54*, 10053-10060.
(15) Singh, B.; Sharma, D. K.; Kumar, R.; Gupta, A. *Applied Clay Science* **2010**, *47*, 384-391.
(16) Tayyebi, A.; Khanchi, A.; Ghofrani, M. B.; Outokesh, M. *Separation Science and Technology* **2010**, *45*, 288-298.
(17) Aminabhavi, T. M.; Patil, M. B.; Bhat, S. D.; Halgeri, A. B.; Vijayalakshmi, R. P.; Kumar, P. *Journal of Applied Polymer Science* **2009**, *113*, 966-975.
(18) Andreeva, D. V.; Gorin, D. A.; Shchukin, D. G.; Sukhorukov, G. B. *Macromolecular Rapid Communications* **2006**, *27*, 931-936.
(19) Solak, E. K.; Asman, G.; Camurlu, P.; Sanli, O. *Vacuum* **2008**, *82*, 579-587.
(20) Hurteaux, R.; Edwards-Levy, F.; Laurent-Maquin, D.; Levy, M. C. *European Journal of Pharmaceutical Sciences* **2005**, *24*, 187-197.
(21) http://xdb.lbl.gov/Section1/Table_1-3.pdf.
(22) Tavakol, M.; Vasheghani-Farahani, E.; Dolatabadi-Farahani, T.; Hashemi-Najafabadi, S. *Carbohydrate Polymers* **2009**, *77*, 326-330.
(23) Santagapita, P. R.; Mazzobre, M. F.; Buera, M. d. P. *Food Research International* **2012**, *47*, 321-330.
(24) Singh, B.; Sharma, D. K.; Kumar, R.; Gupta, A. *Applied Clay Science* **2009**, *45*, 76-82.

(25) Kevadiya, B. D.; Joshi, G. V.; Patel, H. A.; Ingole, P. G.; Mody, H. M.; Bajaj, H. C. *Journal of Biomaterials Applications* **2010**, *25*, 161-177.
(26) Goldstein, J. I.; Newbury, D.; Joy, D.; Lyman, C.; Echlin, P.; Lifshin, E.; Sawyer, L.; Micheal, J. *Scanning Electron Microscopy and X-Ray Microanalysis, p 570*; 3rd ed.; Springer, **2007**.
(27) Lange, K.; Rowe, R. K.; Jamieson, H.; Flemming, R. L.; Lanzirotti, A. *Applied Geochemistry* **2010**, *25*, 1056-1069.
(28) Hwang, H. R.; Roh, J. G.; Lee, D. D.; Lim, J. O.; Huh, J. S. *Metals and Materials International* **2003**, *9*, 287-291.
(29) Chen, S.; Chen, W.; Xue, G. *Macromolecular Bioscience* **2008**, *8*, 478-483.
(30) Hermelin, E.; Petitjean, J.; Lacroix, J.-C.; Chane-Ching, K. I.; Tanguy, J.; Lacaze, P.-C. *Chemistry of Materials* **2008**, *20*, 4447-4456.
(31) Araújo, M. M.; Teixeira, J. A. *International Biodeterioration and Biodegradation* **1997**, *40*, 63-74.
(32) Abd, E.-G. M. A.; Hashem, M. S.; El-Awady, M. K.; Rabie, A. M. *Carbohydrate Polymers* **2012**, *89*, 667-675.
(33) Chen, S.-C.; Wu, Y.-C.; Mi, F.-L.; Lin, Y.-H.; Yu, L.-C.; Sung, H.-W. *Journal of Controlled Release* **2004**, *96*, 285-300.
(34) Isiklan, N. *Journal of Applied Polymer Science* **2007**, *105*, 718-725.
(35) Vlachou, M.; Naseef, H.; Efentakis, M.; Tarantili, P. A.; Andreopoulos, A. G. *Journal of Biomaterials Applications* **2001**, *16*, 125-138.
(36) Sriamornsak, P.; Kennedy, R. A. *International Journal of Pharmaceutics* **2008**, *358*, 205-213.
(37) Sriamornsak, P.; Thirawong, N.; Korkerd, K. *European Journal of Pharmaceutics and Biopharmaceutics* **2007**, *66*, Pages 435-450.
(38) De Kerchove, A. J.; Elimelech, M. *Macromolecules* **2006**, *39*, 6558-6564.
(39) Van Dyke, L. S.; Kuwabata, S.; Martin, C. R. *Journal of the Electrochemical Society* **1993**, *140*, 2754-2759.

Chapter 4:

Anti–Fungal Activity of Silver Impregnated Alginate Beads

4.1 Introduction

The objective of this Chapter was to make polymer supports with antimicrobial properties. These supports could have potential applications in wound dressings or in water disinfection systems. Silver(I) and silver(0) were incorporated into three different polymeric bead supports. All polymer beads were then assessed for their ability to slowly release the silver(I) and silver(0) and over time. The amount of silver incorporated into the different polymeric networks varied with both the concentration of silver nitrate solution in which the beads were immersed in and the nature of the polymer. The stability and robustness of the different polymeric beads were examined. The beads were assessed for their ability to inhibit the growth and/or kill one species of fungus - *Candida albicans* (ATCC 10231). The three different polymeric bead supports used in this study were (a) sodium alginate beads, which were crosslinked with calcium ions, (b) propylene glycol alginate (PGA)/alginate composite beads which were ionically crosslinked with calcium ions and additionally covalently crosslinked with human serum albumin (HSA) (c) quaternary ammonium alginate/alginate composite beads, which were ionically crosslinked with calcium ions.

Silver has been used since ancient times to control infections, and also for the treatment of burns and wounds.[1-4] Research into the antimicrobial properties of silver has continued to grow over the last number of years and due to the development of strains of microbes which are resistant to antibiotic therapies.[5,6] There are now many different silver complexes exhibiting a broad spectrum of antimicrobial action.[2] Metallic silver(0) which is relatively inert,[3] is oxidized in the body by wound fluid and bodily fluids to silver(I).[3] It is this silver(I) ion that is biologically active and that is responsible for the attributed antimicrobial properties of silver complexes in the body.[1,2,5] The potent antifungal activity of silver(I) ions is well established[7] although the exact mode of action is still poorly understood. It is thought that the silver(I) ion inhibits the enzyme phosphomonnose isomerase of *C.albicans* by binding to thiol groups on cytosine residues. This enzyme is essential in the synthesis of the cell wall, and any interruption to this enzyme leads to the breakdown of the cell wall and eventually to the release of vital nutrients, such as phosphates and glutamine.[8]

Fungi are an important cause of human infection and the yeast species of the genus *Candida* are the most pathogenic fungi. While a large number of *Candida* species are found in the environment, only approximately a dozen or so are associated with colonization and infection of humans.[9] One of the most common fungal species to affect humans is the yeast *C. albicans* (Figure 4.1). *C. albicans* is an opportunistic pathogen which is widely recognised as being the most common species, inducing a wide range of superficial and systemic infections in patients with compromised immune system.[9-11]

Figure 4.1: Image of *C.albicans* infections in (a) the mouth[12] and (b) the toes.[13]

C. albicans is a dimorphic fungus,[11] which is normally present in mouth (Figure 4.1(a)), vagina, and rectum; it can take two forms, single yeast cells or the hyphal form.[9,14] Most of the time it exists as oval, single yeast cells (Figure 4.2(a)), which reproduce by budding. Under normal conditions (body temperature, pH, and the presence of serum) it may develop into a hyphal form (Figure 4.2(b)). The ability to switch rapidly from yeast to filamentous growth or vice versa in response to certain environmental conditions is considered to be a critical virulence factor for *C. albicans.*[14] The yeast form is important for dissemination through the blood stream and it adheres to endothelial surfaces. The filamentous forms are more adapted for invasion through the host epithelial tissue and have higher resistance to phagocytosis due to their morphology. Experimental studies support the proposal that the morphological transition is an essential virulence factor for C. albicans[15,16] and it is for this reason it is known as a pathogenic yeast species.[9]

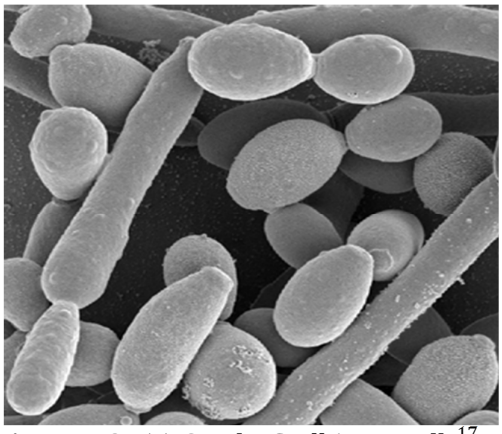
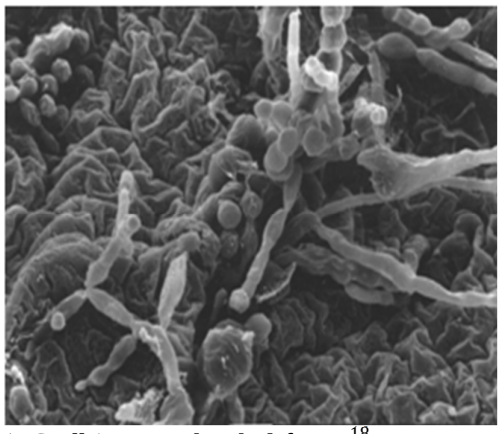

Figure 4.2: (a) Single *C.albicans* cells[17] and (b) *C.albicans* in hyphal form.[18]

There have been a number of studies looking at the activity of silver containing biopolymers in relation to the inhibition of the growth of micro-organisms.[1,2,4,19-21] In the present study we are investigating if the polymers with and without silver can inhibit the growth of the fungi *C. albicans*. The growth curve (Figure 4.3), provides a useful tool to gain insight into the growth characteristic of fungi, and it is important to understand this curve fully when trying to inhibit the growth of the micro-organism.

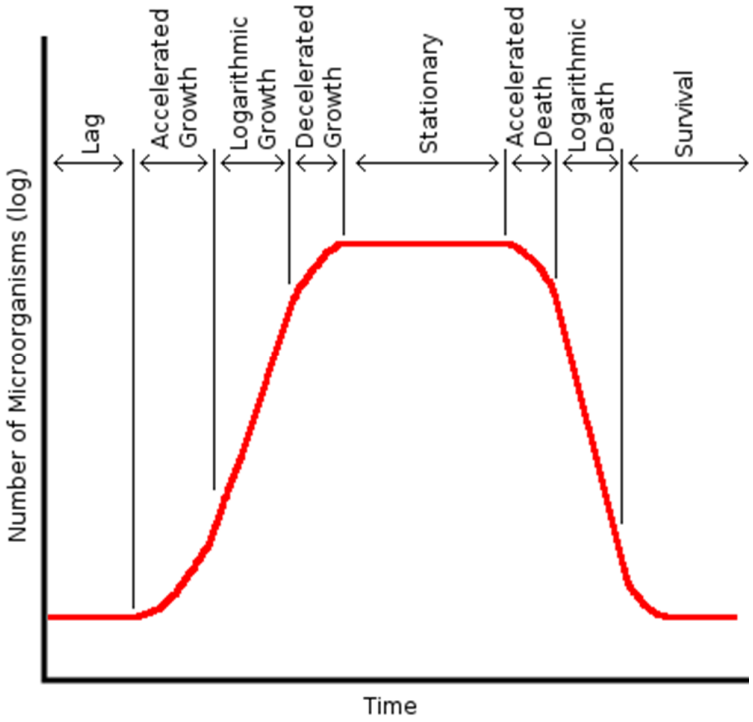

Figure 4.3: Growth curve of microorganisms.[22]

The growth curve of the yeast *C. albicans* can be divided into four main phases. The lag phase is where the cells are acclimatising to the new environmental conditions to which they have been introduced. At this stage there is no significant increase in cell numbers with time. The exponential or logarithmic growth phase in which the cells are now accustomed to their new surroundings and maximum population growth occurs as the cells double in number every twenty minutes. The stationary phase is where the rapid growth ceases due to limited supply of food nutrients and space. There is no further increase or decrease in population size (population growth is static) as the available nutrients become limited. Finally, the last phase of the growth curve is the death phase, where the cell population rapidly diminishes as the nutrients are completely exhausted. Toxic waste products build up, nutrient supplies are depleted and cells begin to die.

4.2 Results and Discussion

Hydrogels are three dimensional crosslinked polymeric structures that are water insoluble, are highly adsorbent and have the ability to swell in an aqueous environment.[23] Hydrogels possess a degree of flexibility very similar to natural tissue due to their significant water content. For the plate assay, the well assay, the colony count assay and the silver leachate measurement the beads were kept in their swollen state, i.e., in their hydrogel form. A xerogel is a solid formed from the hydrogel by evaporating the pore liquid at relatively low temperature and at ordinary pressure. Xerogels usually retain high porosity and enormous surface area along with small pore size.[24] The beads were dried to their xerogel state for the swelling studies, to record SEM micrographs and to measure the silver content of the beads using AA spectroscopy.

4.2.1 Alginate Hydrogel Beads Crosslinked with Calcium Ions

The formation of the hydrogel beads from alginate (Figure 1.6), takes place due to an ionotropic gelation of spherical drops in the presence of calcium ions.[25] The beads were synthesised as outlined in Chapter 2 (Experimental) Section 2.3. The beads in this section will be identified according to the codes used in Table 4.1 below.

Table 4.1: Codes for Calcium Alginate Beads

Bead code	Description of beads
Alg 1	Crosslinked in 0.25 M $CaCl_2$ solution.
Alg 2	Crosslinked in 0.25 M $CaCl_2$, immersed in 0.01 M $AgNO_3$ solution for 24 h.
Alg 3	Crosslinked in 0.25 M $CaCl_2$, immersed in 0.10 M $AgNO_3$ solution for 24 h.
Alg 4	Crosslinked in 0.25 M $CaCl_2$, immersed in 0.01 M $AgNO_3$ for 24 h, reacted with a 0.10 M $NaBH_4$ solution for 3 h.
Alg 5	Crosslinked in 0.25 M $CaCl_2$, immersed in 0.10 M $AgNO_3$ for 24 h, reacted with a 0.10 M $NaBH_4$ solution for 3 h.
Alg 6	Crosslinked in 0.25 M $CaCl_2$, immersed in 0.001 M $AgNO_3$ for 24 h, reacted with a 0.10 M $NaBH_4$ solution for 3 h.

4.2.1.1 Characterisation of Calcium Alginate Beads

4.2.1.1.1 Surface Morphology of Calcium Alginate Beads

SEM micrographs were recorded of the control beads, Alg 1, which do not contain any silver, as well as beads containing silver(I) and silver(0) to examine the morphology and surface structure of the beads at the required magnification at room temperature. Alg 1 beads were spherical to begin with and had a smooth surface. (Figure 4.4(a)). This corresponds with research carried out by Hurteaux *et al.* and by

Kondolot Solak *et al*. both of whom also reported sodium alginate beads crosslinked with calcium chloride to have a smooth spherical appearance.[26,27] At the lower magnifications (Figure 4.4(a) and (c)) the surface morphology of the Alg 1 beads and the Alg 3 beads was very similar showing no major cracks or indentations on the immediate surface. However, at the higher magnifications ((Figure 4.4(b) and (d)) the Alg 3 beads appeared to have a slightly rougher morphology in comparison to the Alg 1 beads.

Upon comparison of the micrographs recorded of the Alg 1 and Alg 5 beads it was clear that the reaction of the beads with sodium borohydride (which was used to reduce the silver(I) to silver(0)) was having a major effect on the bead structure. The Alg 5 beads were not spherical in shape (Figure 4.4(e)) and they exhibited a substantially different surface morphology compared to the Alg 3 beads (Figure 4.4(f)). On the addition of the beads to the sodium borhydride solution a chemical reaction took place and hydrogen gas was given off according to Equation 4.1.

$$2AgNO_3 + 2NaBH_4 + 6H_2O \longrightarrow 2Ag + 7H_2 + 2NaNO_3 + 2B(OH)_3 \qquad \text{(eq. 4.1)}$$

The release of the hydrogen gas caused the surface of the Alg 5 beads to become very uneven and a great number of indentations and protuberances were present. In addition to distorting the shape and morphology of the beads the reaction caused the beads to become more brittle. It is likely that the rapid release of gas weakened the ionic crosslinking within the beads, which in turn could be the cause of the beads swelling and disintegrating during the colony count assay described later in Section 4.2.1.2.3.

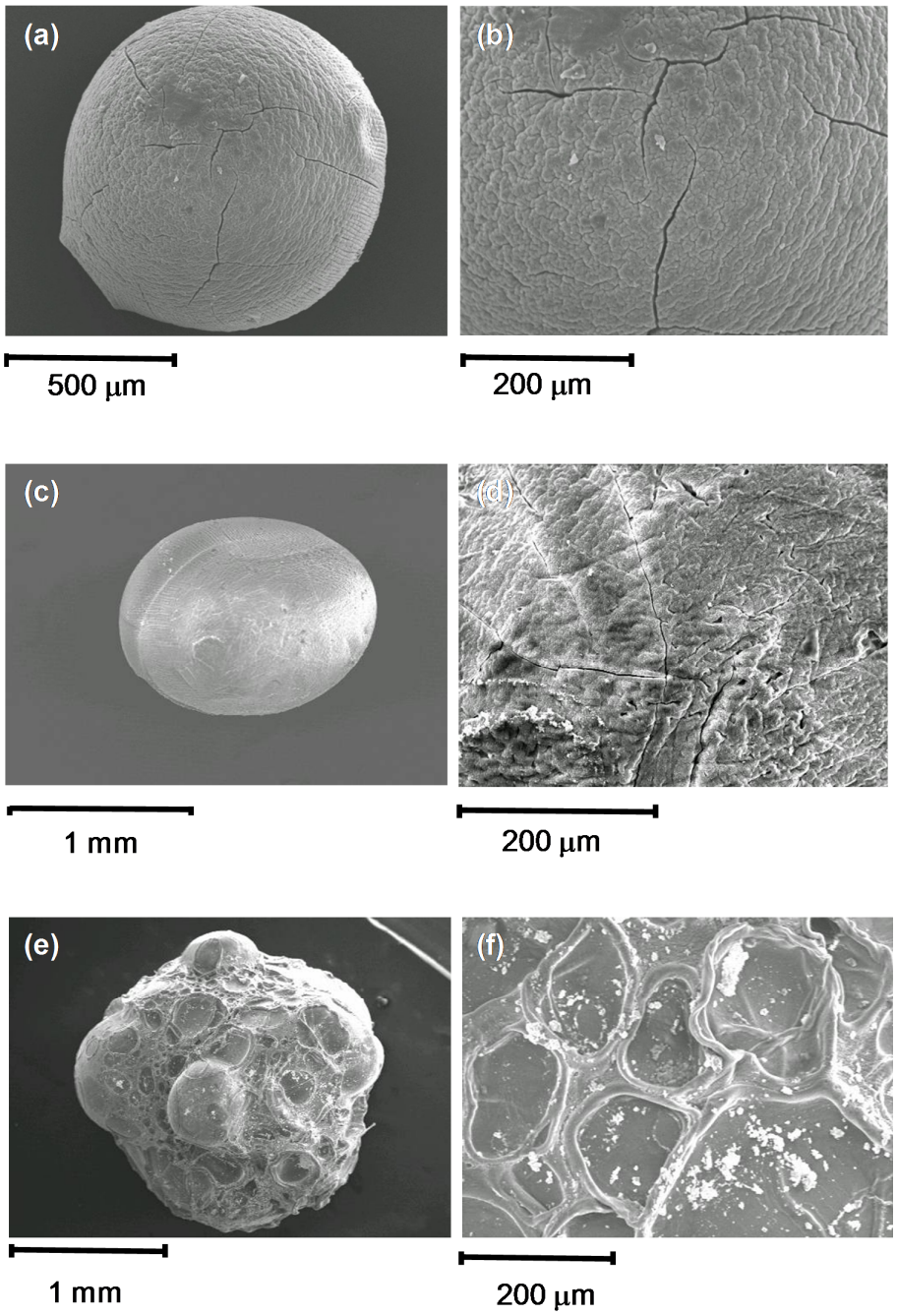

Figure 4.4: SEM micrographs of Alg 1 beads at different magnifications (a) and (b), of Alg 3 beads at different magnifications (c) and (d), and Alg 5 beads at different magnifications (e) and (f). All beads were dried at room temperature.

4.2.1.1.2 Swelling of Alg 1 Beads in Water and Sodium Chloride Solution

The swelling behaviour of the Alg 1 beads was studied by the measurement of the equilibrium swelling degree (ESD). The ESD was calculated from *(Ws-Wd)/Wd,* where W*s* is the weight of swollen beads after filtration and W*d* is the dry weight of the xerogel beads. ESD values for individual formulations of the beads were determined by measuring the extent of swelling of the beads in the different swelling medium at 20 ± 1°C as described in Chapter 2 Section 2.7. The results for the swelling behavior of the Alg 1 beads in both deionised water and NaCl solution have already been presented in Chapter 3 Section 3.2.1.3. In summary, swelling of the Alg 1 beads occurred over about 10 h, and when the mass of the beads was taken after a 24 h time period for both solutions, the mass of the beads had decreased indicating that the beads were undergoing disintegration in the swelling media.[28] Swelling was significantly higher for beads immersed in a NaCl (1% w/v) solution than in deionised water. The beads take in approximately 60 times their original weight of water in the NaCl solution at the maximum swelling point, compared to only a 1.6 times increase in weight in deionised water. Similar swelling behavior of calcium ion crosslinked alginate beads in water and sodium chloride solutions was reported by Sriamornsak and co-workers.[29] The swelling observed in the NaCl solution is due to the ion exchange mechanism available with NaCl solution (Ca^{2+} exchanged for Na^{+}).[25,30,31]

4.2.1.1.3 Identification of Silver within the Calcium Alginate Beads

A typical EDX spectrum of a bead without silver (Alg 1 bead) is shown in Figure 4.5(a) and a typical EDX spectrum of a bead containing silver (Alg 3 bead) is shown in Figure 4.5(b). From analysis of the EDX spectra silver was detected in each of the sets of beads Alg 2, Alg 3, Alg 4, Alg 5 and Alg 6. The presence of silver was indicated by the occurrence of 3 bands at 2.98, 3.15 and 3.35 keV (Figure 4.5(b)), which are assigned to the Lα1, Lβ1 and Lβ2 lines of Ag respectively.[32] A typical EDX spectrum of an Alg 5 bead is shown in Figure 4.5(c) and a SEM micrograph of the surface of beads in the region from which the EDX was recorded is given in Figure 4.5(d). A microcluster of silver can be clearly observed in Figure

4.5(d) indicating that at least some of the silver(0) trapped in the Alg 5 beads was outside of the nano-domain.

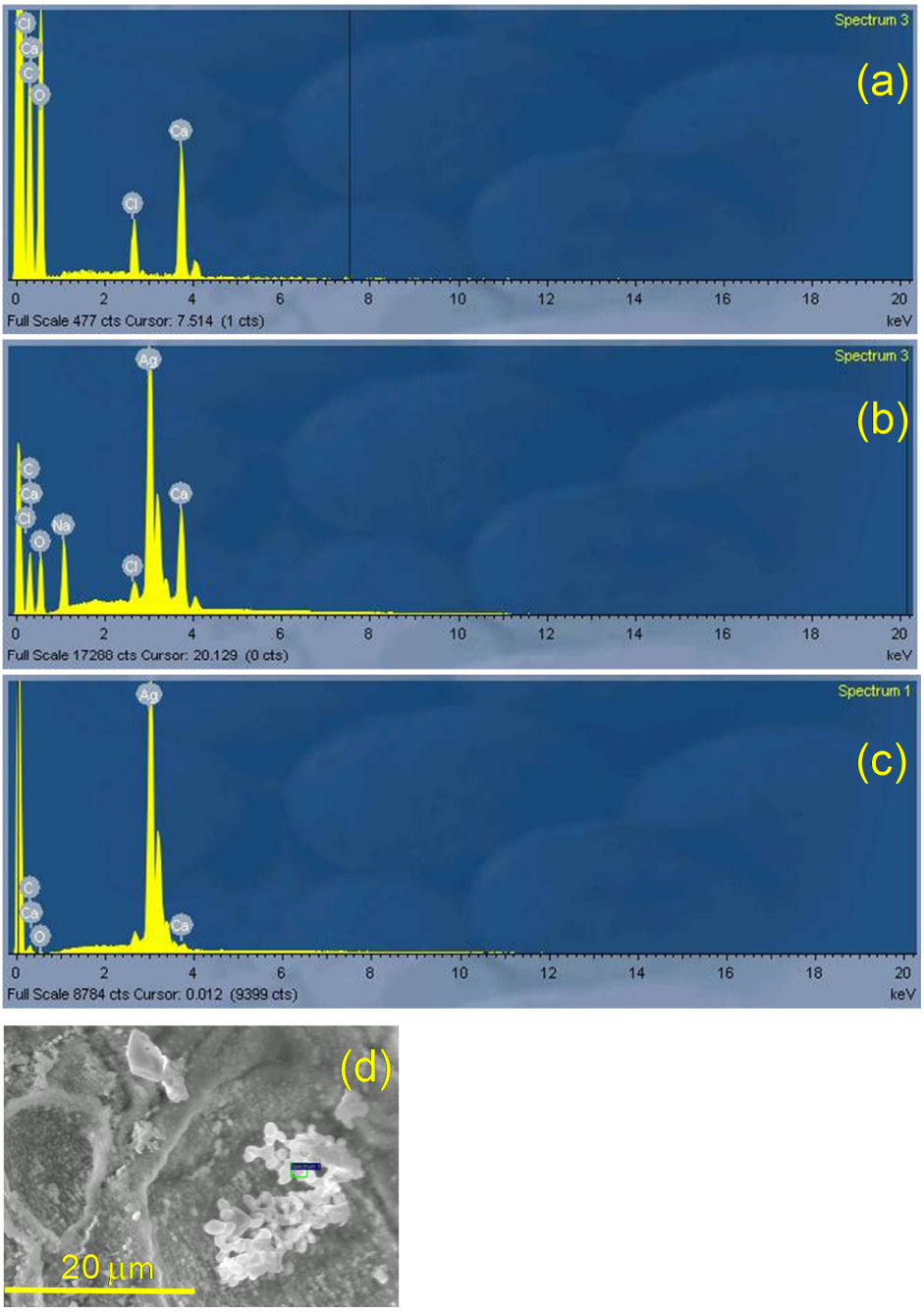

Figure 4.5: EDX analysis of (a) Alg 1 beads, (b) Alg 3 beads (c) Alg 5 beads showing the presence of silver in the Alg 3 and Alg 5. (d) SEM micrograph of the surface of an Alg 5 bead showing the region at which the EDX (c) was recorded.

EDX is not generally used as a quantitative technique, so in order to quantify the amount of silver within the bead further analysis was carried out using AA spectroscopy.

4.2.1.1.4 Quantifying the amount of Silver present in the Calcium Alginate Beads

AA spectroscopy was used to quantify the amount of silver present in the different polymer networks containing the different amounts of silver in the silver(I) and silver(0) states. Atomic absorption standard solutions were prepared by using a silver nitrate sample of high purity (99.999%) and calibration plots at the appropriate concentrations were recorded. Three independent measurements were averaged for each sample. In order to quantify the amount of silver present in the beads, the beads were destroyed using acid digestion and the amount of the silver in the beads was determined as outlined in Chapter 2, Section 2.9.8. The readings were recorded in absorbance and using the calibration curve this was converted to concentration. From this the mass of silver in thirty beads for each of the bead type was calculated and is plotted in Figure 4.6.

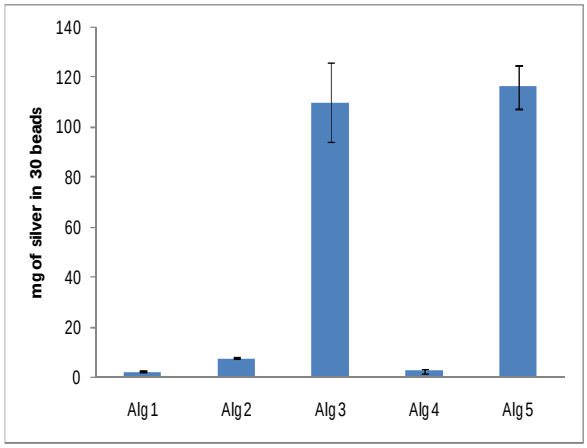

Figure 4.6: The mass of silver (mg) present in thirty calcium alginate beads as determined using AA spectroscopy. Each bead type studied is defined in the figure.

Surprisingly there was a positive result obtained for the presence of silver for the control alginate beads, Alg 1, as shown in Figure 4.6, which had been shown using EDX analysis in Section 4.2.1.1.3 to contain no silver. This shows that there was a systematic error in the measurement of the amount of silver present in the beads using the AA technique. In order to get a true representation of the amount of silver contained within the polymeric supports the value obtained for the Alg 1 beads was subtracted from each of the values obtained for the other beads. When this correction was applied the result for the Alg 2 beads shows that 1.5 mg of the total weight of the 30 beads was silver. As expected the silver content is a lot higher for the Alg 3 beads. The Alg 3 beads contained approximately 70 times more silver than the Alg 2 beads. The reading for silver in the Alg 4 beads was the same, within the experimental error, as that obtained for the control Alg 1 beads. EDX (Section 4.2.1.1.3) confirmed the presence of silver in these beads, but the amount of silver in these beads could not be quantified using AA. There was a little less silver in these beads than the Alg 2 beads from which they are formed, and a reason for the decrease could be due to the fact that some of the silver was lost when the beads were reacted with the sodium borohydride solution. The Alg 5 beads contained a similar amount of silver to the Alg 3 beads from which they were formed.

4.2.1.1.5 Quantifying the amount of Silver in the Leachate from the Calcium Alginate Beads

One of the aims of the project was to develop polymeric beads which potentially could be used in a water disinfection system. Therefore we set out to determine the relative amounts of silver released from the different types of beads into water. AA spectroscopy was used to quantify the amount of silver released from the beads into deionised water over a period of 24 h. Hydrogel beads (n = 30) were taken and placed into a set volume of deionised water (10 ml). The beads were left in this solution for 24 h at a constant temperature of 30 ± 1°C. The beads were filtered and the filtrate was made up to 100 ml. The readings were recorded in absorbance and using the calibration curve (Chapter 2, Section 2.9.8), this was converted to concentration. From this the mass of silver leached from thirty beads, for each of the bead type was calculated the results are shown in Figure 4.7.

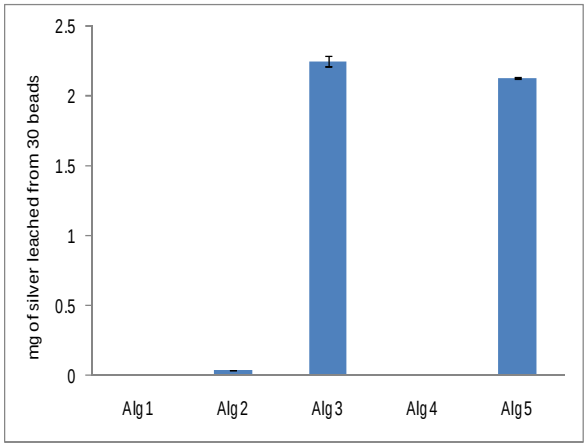

Figure 4.7: The amount of silver leached from 30 calcium alginate beads into deionised water (10 ml) held at 30 ± 1°C over a period of 24 h. Each bead type studied is defined in the figure.

There was a zero reading obtained for the Alg 1 beads which was expected as these beads did not contain any silver. The Alg 2 beads released forty times less silver than the Alg 3 beads. The Alg 4 beads released very little silver, releasing comparable amounts to the Alg 2 beads from which they were formed. Similarly, the Alg 5 beads released approximately the equivalent amount of silver as the Alg 3 beads. However we are uncertain of the oxidation state of the silver released from the Alg 4 and Alg 5 beads in this experiment. One limitation with the use of AA spectroscopy to determine the concentration of ionic silver or silver(0) released from the beads is that AA spectroscopy will measure all silver regardless of its oxidation state.[1] Silver(0) can be dispersed in water if the silver is in the nanoparticulate form and aqueous colloidal solutions of nano-silver have been used as the source of nano-silver particles for products like (a) medical products for example plasters and wound dressing,[33,34] (b) disinfectants[35] and (c) water disinfectants.[36]

4.2.1.2 Biological Testing

Three different assays were used to study the different effects of the polymer beads on the growth of the *C. albicans*. The plate assay was used to measure the inhibitory effect of the polymer on the growth of the *C. albicans* on agar. When a

sample was placed onto a plate and it inhibits the growth of the fungi, it is known as a fungistatic agent. The well assay was used to measure the inhibitory effect of the leachate on the growth of the *C. albicans* on solid support of agar. The third assay was the colony count assay in which the polymers were incubated with the fungi and the number of living cells was counted as a function of time in order to measure the fungicidal or killing ability of the polymers. For this assay to work the fungi must be growing at their most active state i.e. exponential, as at the other stages of growth there would be other factors hindering the growth of the fungi.

The experimental details of the biological testing experiments are given in Chapter 2, section 2.9.11. Briefly they are as follows. *C. albicans* cells were plated out on yeast extract peptone dextrose (YEPD) agar plates at a concentration of 1×10^6 cells per ml. The plates were incubated for 1 h at 37 ± 1°C. For the plate assay, the polymer samples were placed on the plates, which were then incubated for 24 h at 37 ± 1°C and the zones of inhibition around the samples were then measured. For the well assay, 30 polymer beads were placed into tubes containing deionised water (10 ml) at 30 ± 1°C. After the plates were incubated for 1 h at 37 ± 1°C, wells were excavated using a sterilized cork with a diameter of 3 mm. The test solution (30 µl) was added to the wells and the plates were incubated for 24 h at 37 ± 1°C and the zones of inhibition around the wells were measured. For each the colony count test 10 ml of the medium containing 1×10^6 cells were placed in a sterilized flask containing 10 polymer beads and the flask was held at 30 ± 1°C while continually shaken at 200 rpm on a rotary shaker. The solution was sampled, the number of colonies formed on the agar plates was counted and the total number of surviving organisms was then calculated. Photographs of each plate at each time interval were also taken. Each experiment was performed in triplicate and the results are reported as the mean ± the standard error.

4.2.1.2.1 Plate Assay using Calcium Alginate Beads

The activity of the silver containing beads was compared to that of a control which consisted of the Alg 1 beads which did not contain silver. For each plate Alg 1 beads were put on the plates along with the test samples, so that result could be easily compared within a plate. Ten beads of each sample were placed onto the

plates. A photograph of a typical plate assay experiment is shown in Figure 4.8. All tests were done in triplicate.

Figure 4.8: Photograph of a typical plate assay containing ten Alg 3 beads on the left hand side of the plate, and ten Alg 1 beads on the right hand side of the plate.

To measure zones of inhibition (ZOI),[37] the vertical and horizontal diameters, of the sample, in this case the beads were measured in mm. The vertical and horizontal diameters of the sample and the zone itself were then measured. Then using the formula for the area of a circle, $A = \pi r^2$ the area covered by the beads and the total area of inhibition were calculated. The area under the beads was subtracted from the total area of inhibition to give the area of the zone of inhibition. Results for the plate assay are shown in Table 4.2 below:

Table 4.2: Results for the Plate Assay for Calcium Alginate Beads

Bead Code	Total area* (mm^2)	Zone of Inhibition* (mm^2)	Description
Alg 1	102 ± 5	-	No zone of inhibition
Alg 2	104 ± 5	-	Direct inhibition
Alg 3	179 ± 25	83 ± 27	Zone of inhibition
Alg 4	298 ± 30	184 ± 30	Zone of inhibition
Alg 5	364 ± 24	237 ± 24	Zone of inhibition

* ZOIs were recorded after 24 h using ten beads on each plate and plates were held at 37 ± 1°C.

The Alg 3 beads caused direct inhibition beneath the beads and gave very clear zones of inhibition around the beads, which can be seen in the photograph of the plate shown in Figure 4.8. These zones of inhibition were measured, and on average the Alg 3 beads gave zones of inhibition of 83 mm^2. The Alg 2 beads showed that there was only direct inhibition beneath the beads. For the Alg 4 and Alg 5 beads, which contained the reduced silver, there was zones of inhibition on average of 184 mm^2 and 237 mm^2 measured around the beads respectively. Both these zones of inhibition were very similar in area given that there was an enormous increase in the concentration of silver in the Alg 5 beads compared to the Alg 4 beads. The zones of inhibition were so big around the Alg 4 and Alg 5 beads that it was concluded that it could not just be the silver alone that was having this effect on the growth of the *C. albicans* and that there must be another component within the silver(0) containing beads having a major effect on inhibiting the growth of the *C. albicans*. Results from this section will be discussed further in Section 4.2.1.2.4.

4.2.1.2.2 Well Assay using Calcium Alginate Beads

The beads (n = 30) were immersed in deionised water (10 ml) for 24 h held at 30 ± 1°C and then the amount of silver in the leachate was found using AA

spectroscopy. In addition to this, samples of the leachate were collected and used in the well assay so that we could directly correlate any effect of the leachate on the *C. albicans* with the concentration of silver present in the leachate. Results from the well assay showed that the leachate from the beads containing the reduced silver, Alg 4 and Alg 5 had no inhibitory effect on *C. albicans*, as can be seen from Table 4.3 below. The leachate from the Alg 3 beads was the only leachate that had an effect in this assay.

Table 4.3: Results for the Well Assay for Calcium Alginate Beads

Bead Code	**Zone of Inhibition*** **(mm^2)**	**Description**
Alg 1	-	No zone of inhibition
Alg 2	-	No zone of inhibition
Alg 3	39 ± 10	Zone of inhibition
Alg 4	-	No zone of inhibition
Alg 5	-	No zone of inhibition

* The leachate was extracted from 30 beads into 10 ml of deionised water held at 30 ± 1°C for 24 h. ZOIs were recorded after 24 h and plates were held at 37 ± 1°C.

The results for the Alg 2 and Alg 4 beads were as expected, as a very low concentration of silver had leached from these beads and their leachate should have little ability to inhibit the growth of *C. albicans*. However, the results for the Alg 5 beads were unexpected. In Section 4.2.1.1.5 it was shown that there was approximately the same amount of silver leached from the Alg 3 and Alg 5 beads over a 24 h period. Therefore one would expect that the sizes of the zones of inhibition caused by the leachate from the Alg 3 beads would be the same as the sizes of the zones caused by the leachate from the Alg 5 beads. However, this was not the case as can be seen from the photograph of a typical result given in Figure 4.9. There are small zones present around the leachate from the Alg 3 beads on the

left hand side of the plate but there is clearly no zones present around the leachate from the Alg 5 beads on the right hand side of the plate. In order to explain this result we would suggest that the silver released from the Alg 5 beads is nanoparticulate and in the zero oxidation state. A number of studies have shown that silver nanoparticles aggregate in solution with a consequent decrease in their antimicrobial properties.[38,39]

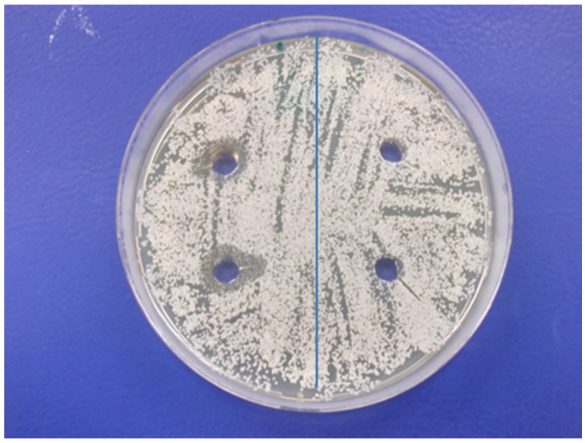

Figure 4.9: Photograph of a typical well assay experiment. Wells on the left hand side of the plate contain leachate from Alg 3 beads and wells on the right hand side of the plate contain leachate from Alg 5 beads.

4.2.1.2.3 Colony Count Assay using Calcium Alginate Beads

The results for the colony count assay for *C. albicans* when placed in contact with the Alg 1, Alg 3 and Alg 5 beads are given in Figure 4.10. Upon determining the number of viable cells at time periods over the first 6 h (Figure 4.10(a)) it can be observed that the Alg 1 and Alg 5 beads were having no fungicidal effect on the *C. albicans* and exponential growth continued over the 24 h time period (Figure 4.10(b)). A photograph (Figure 4.11(a)) showing the number of cells grown on the agar plate for a solution of *C. albicans* which was in contact with the Alg 1 beads for 24 h clearly shows that the fungus was still in its exponential phase of growth. Therefore the calcium alginate bead support did not have any effect on the growth of the colonies. We would propose that the absence of a fungicidal effect for the Alg 5

beads which contained silver in the zero oxidation state was due to the large size of the silver particles trapped in the alginate bead. The beads were a dark brown colour which is indicative of large silver nanoparticles[40] and the SEM micrographs recorded of the beads indicated that at least some of the silver(0) was present as microclusters (Figure 4.5(d)). Studies have shown that there is an inverse relationship between the size of silver nanoparticles and their antimicrobial activity.[39,41] The Alg 3 beads had a significant fungicidal effect on the *C. albicans* with no viable cells being observed in the medium at 24 h (Figure 4.10(b)). A photograph of a typical agar plate used to culture the viable cells after a 24 h time period is shown in Figure 4.11(b) and clearly no viable cells are observed. Interestingly there was a lag time to the activity of the Alg 3 beads. The beads behaved similarly to the control beads up to the 1 h time period. This was probably directly related to the time it took for the beads to swell in the medium. Studies in Chapter 3 Section 3.2.1.3 showed that the beads swell over a number of h at 20 ± 1°C in water and NaCl solutions. As the pores of the beads open silver ions will be delivered from the support more readily. In addition there will be an increased amount of contact kill as the solution of *C. albicans* cells permeates through the pores of the beads more readily. The Alg 3 performed efficiently in bringing down the fungi count to almost zero, showing that Alg 3 could, in principle, have the potential to be used as an effective material for water disinfection as they are highly active. However, all the alginate beads used in this study underwent such significant swelling that they had disintegrated over the 24 h time period. Moreover, the swelling studies carried out on the calcium ion crossed linked alginate beads and reported in Chapter 3 Section 3.2.1.3 have shown that even in deionised water at a temperature of 20 ± 1°C the beads had begun to disintegrate after approximately 10 h. Therefore, alginate beads could only be used in water disinfection applications if their properties could be tailored to reduce the amount of disintegration.

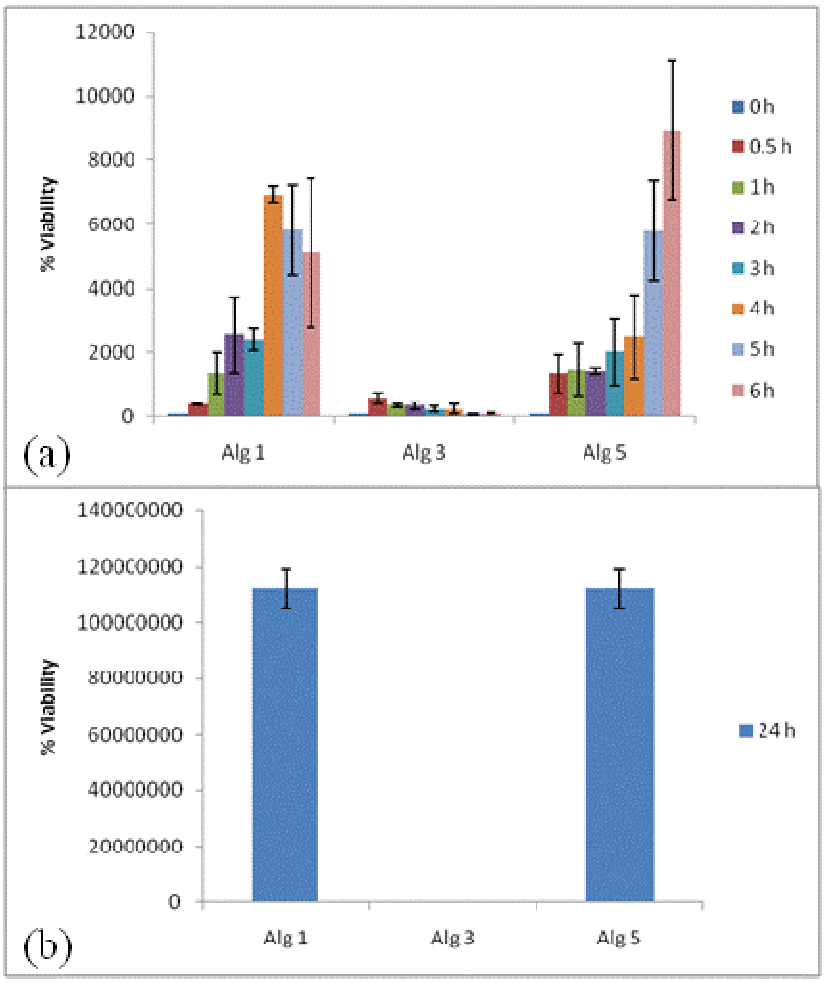

Figure 4.10: The number of viable *C. albicans* cells present in YEPD medium upon shaking with the Alg 1, Alg 3 and Alg 5 beads. Medium was held at 30 ± 1°C. (a) Results over first 6 h and (b) results after 24 h. Alg 1 V's Alg 3 = ***, P<0.0001. Alg 1 V's Alg 5 = ns.

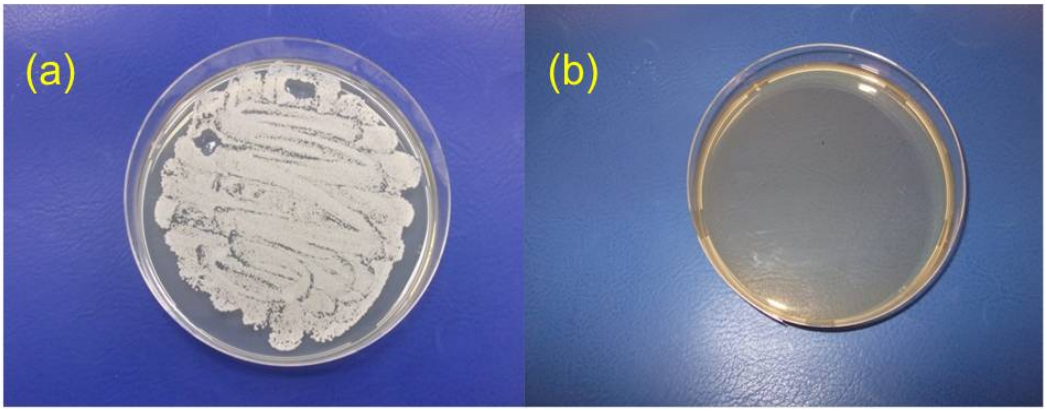

Figure 4.11: Photograph of a typical agar plate used to calculate the number of viable *C. albicans* cells growing in the medium after the colonies have been in 24 h contact with (a) Alg 1 beads and (b) Alg 3 beads.

4.2.1.2.4 Anti *C. albicans* Activity Associated with Plate Assays using Alg 4, Alg 5 and Alg 6 Beads

The results of the plate assay experiments using Alg 4 and Alg 5 (Section 4.2.1.2.1) showed that these beads gave very similar zones of inhibition towards the growth of *C. albicans* (Table 4.2), even though they contained different masses of silver. Studies carried out using AA spectroscopy (Section 4.2.1.1.4) determined that the Alg 4 beads contained significantly less silver than the Alg 5 beads and the amount present in the Alg 6 beads should be even lower. Table 4.4 shows the size of zones of inhibition towards the growth of *C.albicans* for the Alg 4, Alg 5 and Alg 6 beads. Therefore it was clear that there was no direct correlation between size of the zone of inhibition and amount of silver present in the bead. Therefore, it was deduced that another compound present in the bead must be active towards *C. albicans* and it was this reagent which was responsible for the observed zones of inhibition. The Alg 4, Alg 5, and Alg 6 beads contained silver in the zero oxidation state which was produced by reacting silver(I) encapsulated in the beads with a solution of sodium borohydride (0.10 M). The reaction to reduce Ag(I) to Ag(0) is given in Equation 4.1 below.

$$2AgNO_3 + 2NaBH_4 + 6H_2O \longrightarrow 2Ag + 7H_2 + 2NaNO_3 + 2B(OH)_3 \qquad \text{(eq. 4.1)}$$

Either the unreacted sodium borohydride and/or the boric acid could have caused the observed large zones of inhibition.

Table 4.4: Results for the Plate Assay for Calcium Alginate Beads Containing Silver(0)

Bead Code	Total Area* (mm^2)	Zone of Inhibition* (mm^2)	Description
Alg 4	298 ± 30	184 ± 30	Zone of inhibition
Alg 5	365 ± 24	237 ± 24	Zone of inhibition
Alg 6	244 ± 31	123 ± 31	Zone of inhibition

* ZOIs were recorded after 24 h using 10 beads on each plate and plates were held at 37 ± 1°C.

To further investigate if the sodium borohydride was having an effect on the inhibition of growth of the *C. albicans*, the Alg 1 beads which did not contain silver(I) were immersed in a sodium borohydride (0.10 M) solution. The sodium borohydride underwent an immediate reaction with the Alg 1 beads resulting in the evolution of a gas. This was an unexpected result, sodium borohydride is not sufficiently basic to react with hydroxyl moieties, and previously Kristiansen *et al.* have shown that sodium borohydride will selectively reduce only the aldehyde groups of the mannuronate or guluronate residues of partially oxidized alginates.[42] Therefore the sodium borohydride must have been reacting with carboxylic acid groups on the sugar units. It was expected at the pH of the solution (6.0) that the alginate would be fully deprotonated as the pK_a of mannuronic and guluronic acid are 3.38 and 3.65 respectively.[43] However, obviously this is not the case within the hydrogel beads in which there is a high concentration of carboxylate groups and the possibility of H-bonding interactions with the hydroxyl and carboxylate groups on surrounding residues. Sodium borohydride is known to react with ethanoic acid

according to Equation 4.2,[44] and a similar reaction must be taking place with the carboxylic acid groups in the alginate hydrogel beads.

$$NaBH_4 + 3CH_3COOH \longrightarrow NaBH(CH_3COO)_3 + 3H_2 \qquad \text{(eq. 4.2)}$$

However, the products of the reaction are actually more complicated as in addition to the above reaction it is known that sodium borohydride and salts like $NaBH(CH_3COO)_3$ will hydrolyse in aqueous solution. Retnamma *et al*. have shown that sodium borohydride will undergo hydrolysis in aqueous solution at room temperature[45] according to an idealized reaction given in Equation 4.3.

$$NaBH_4 + 4H_2O \longrightarrow NaB(OH)_4 + 4H_2 \qquad \text{(eq. 4.3)}$$

There have been extensive studies carried out on the hydrolysis products of sodium borohydride and it is known that as well as the $B(OH)_4^-$, that other species may be present in the solution including $B(OH)_3$ and $B_4O_7^{2-}$ depending on conditions such as temperature and pH.[45,46] Boric acid and borate salts are well known to have antimicrobial activity,[47-49] and a number of researchers have reported impregnating hydrogels with boric acid in order to make polymeric materials which might be used in biomedical applications.[50,51] When solid samples of sodium borohydride and boric acid were employed in the plate assay experiment all the growth of *C. albicans* was inhibited on the plate.

The Alg 1 beads were reacted with sodium borohydride and tested towards the inhibition of growth of *C. albicans* using the plate assay. Similar zones of inhibition were recorded to those observed for the Alg 4, Alg 5 and Alg 6 beads (Table 4.4). This finding strongly indicated that either unreacted sodium borohydride or the boron containing product of reaction of the sodium borohydride with the beads or water was having the major effect on the inhibition of the growth of *C. albicans* on the plates. Following reaction with the sodium borohydride the alginate beads were subjected to extensive washing to try and remove the chemical that was causing the

zones of inhibition. When the plate assay was carried out using these beads, the zones of inhibition for *C. albicans* growth decreased but there was still direct inhibition visible under the beads together with smaller zones around the beads. This proved that there was still some very active material present in small amounts.

In contrast to the plate assay experiments when the leachate from Alg 4 and Alg 5 were tested towards the growth of *C. albicans* there was no significant inhibition of growth (Table 4.3). In addition, when the fungicidal abilities of the Alg 5 beads were tested towards *C. albicans* in the colony count assay there was no significant difference in their properties compared to the control beads over a 24 h period (Figure 4.10). From this it was assumed that it must be the unreacted sodium borohydride which was having the large influence towards inhibiting the growth of *C. albicans* in the plate assays. Studies involving the leachate or the colony count assays were carried out under conditions which would promote the hydrolysis of sodium borohydride. It would appear that the hydrolysis products of sodium borohydride (boric acid, and borates) are less active toward *C. albicans* than sodium borohydride itself.

The above finding is interesting as sodium borohydride is used regularly in the literature as a reducing agent[20,52-55] to form silver nanoparticles which are then tested for their antimicrobial capabilities. It has not been generally reported that the sodium borohydride or the products of its reaction with silver(I) could be active against the growth of microbes.

4.2.2 Propylene Glycol Alginate (PGA)/Alginate Composite Hydrogel Beads Crosslinked with Calcium Ions and also Covalently Crosslinked with Human Serum Albumin (HSA)

Propylene glycol alginate (Figure 4.12) is a partially esterified derivative formed from the reaction between propylene oxide and alginic acid[56] (Scheme 4.1), in which approximately 70% of the carboxylic groups are esterified with propylene glycol.[57,58] Callewaert *et al*. have previously formed microspheres using a mixture of both PGA and alginate.[59] The beads were initially gelled in a solution containing calcium ions and subsequently HSA was covalently linked to the PGA through amide bonds forming a membrane over the beads. These researchers found that PGA/alginate microspheres so formed offered better resistance towards freezing, lyophilization, sterilisation and also showed increased mechanical strength compared to ionically crosslinked alginate beads.[56,59,60] In addition, studies showed that this polymer composite material is bio-compatible.[26,59]

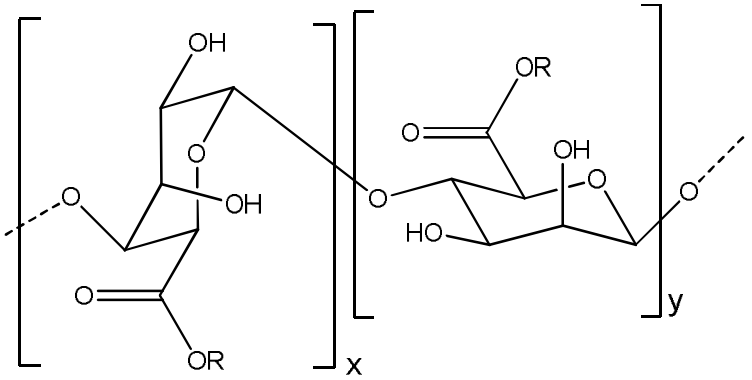

Figure 4.12: Structure of propylene glycol alginate (PGA) chain, R can represent hydrogen or C_3H_7O as the alginic acid is only partially esterified.

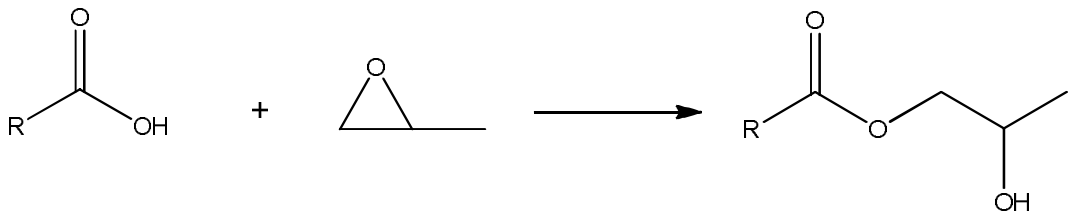

Scheme 4.1: Reaction between alginic acid and propylene oxide to form propylene glycol alginate where R represents the rest of the alginic acid chain.

The propylene glycol alginate/alginate composite beads are held together by both ionic bonds and covalent crosslinkages as opposed to the calcium alginate beads which contain only ionic bonds. Due to the additional covalent component in their bonding it was expected that these beads would form a more stable support for the silver. To date, this type of bead has not been studied as a support for silver(I) or silver(0) and no investigation on how the beads so formed prevent the growth of *C. albicans* has been previously carried out. The synthesis of the beads was outlined in detail in Chapter 2 (Experimental) Section 2.3.4. The beads in this section will be identified according to the codes given in Table 4.5 below.

Table 4.5: Codes for the PGA/Alginate Composite Beads

Bead code	**Description of different beads**
PGA 1	1% w/v sodium alginate, 2% w/v PGA, crosslinked in 10% w/v $CaCl_2$, and then in 5% w/v HSA, 0.025 M NaOH solution.
PGA 2	1% w/v sodium alginate, 2% w/v PGA, crosslinked in 10% w/v $CaCl_2$, and then in 5% w/v HSA, 0.025 M NaOH solution, immersed in 0.01 M $AgNO_3$ solution for 24 h.
PGA 3	1% w/v sodium alginate, 2% w/v PGA, crosslinked in 10% w/v $CaCl_2$, and then in 5% w/v HSA, 0.025 M NaOH solution, immersed in 0.10 M $AgNO_3$ solution for 24 h.
PGA 4	1% w/v sodium alginate, 2% w/v PGA, crosslinked in 10% w/v $CaCl_2$, and then in 5% w/v HSA, 0.025 M NaOH solution, immersed in 0.01 M $AgNO_3$ for 24 h, reacted with a 0.10 M $NaBH_4$ solution for 3 h.
PGA 5	1% w/v sodium alginate, 2% w/v PGA, crosslinked in 10% w/v $CaCl_2$, and then in 5% w/v HSA, 0.025 M NaOH solution, immersed in 0.10 M $AgNO_3$ for 24 h, reacted with a 0.10 M $NaBH_4$ solution for 3 h.

4.2.2.1 Characterisation of PGA/Alginate Composite Beads

4.2.2.1.1 Surface Morphology of PGA/Alginate Composite Beads

SEM micrographs of PGA 1, PGA 3 and PGA 5 were recorded at set magnifications for direct comparison at room temperature (Figure 4.13). The three types of PGA beads were not as spherical as their calcium alginate analogues (Figure 4.4). This difference arose due to the PGA/alginate mixture being more viscous before the beads were made. The drops of PGA solution suspended from the syringe tip for longer causing the beads to become more elongated and which resulted in oval shaped beads. For the PGA 1 beads at the lower magnification (Figure 4.13(a)) the surface morphology appeared slightly rough and this rough morphology was clearly visible at the high magnifications (Figure 4.13(b)). In comparison to the PGA 1 beads the PGA 3 beads look smoother at both magnifications (Figure 4.13(c) and (d)). The beads have no cracks or indentations on the immediate surface, even though there are folds on the surface of the PGA 3 beads at the higher magnification, the overall surface appears smoother in comparison to the control (PGA 1) at the same magnification. The PGA 5 beads were very similar in their morphology to the Alg 5 beads in that they appear swollen, due to the reaction that took place when the beads were placed in the sodium borohydride solution. The surface of these beads appeared to have a large number of indentations and overall a very uneven surface at both magnifications (Figure 4.13(e) and (f)).

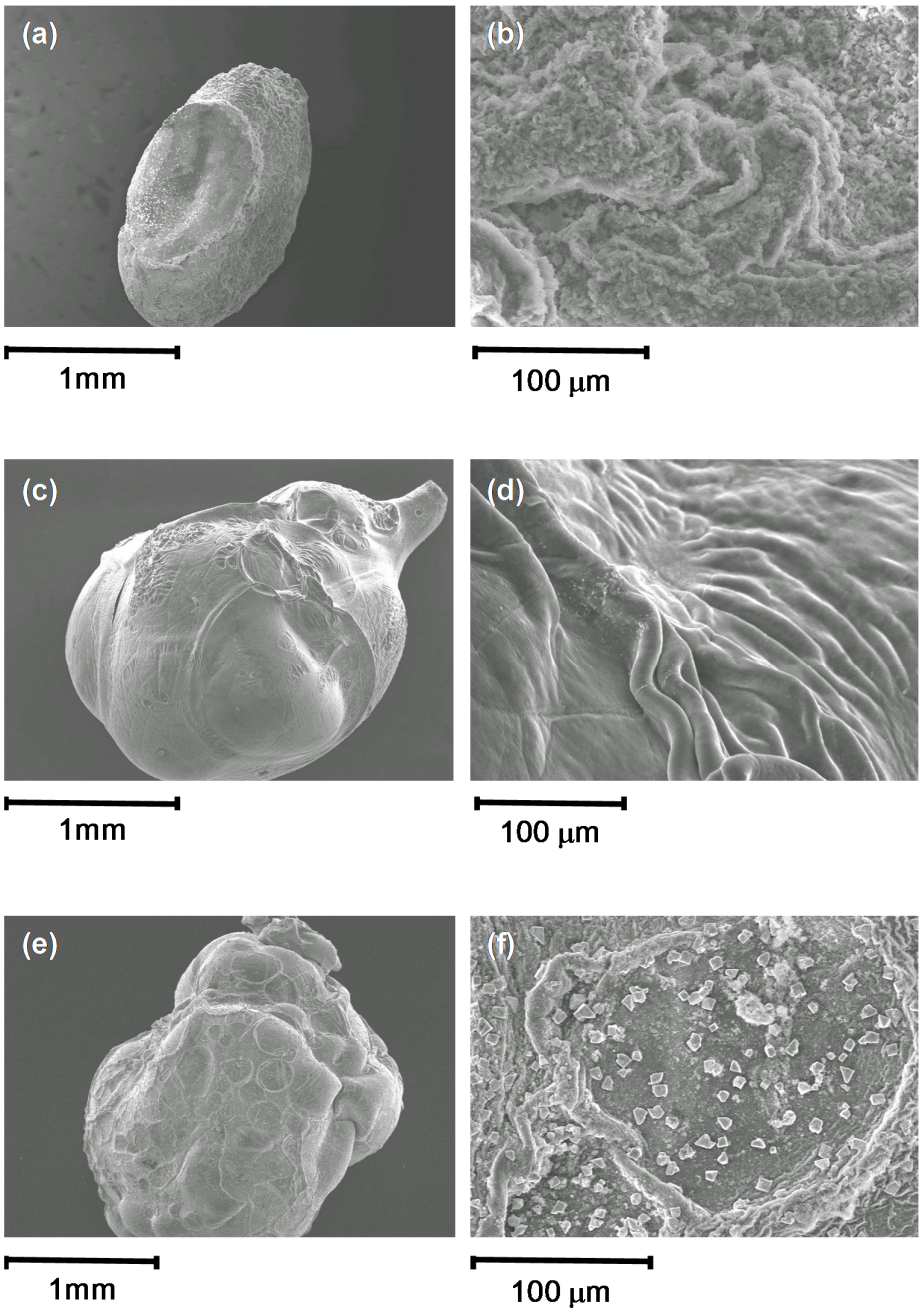

Figure 4.13: SEM micrographs of PGA 1 beads at different magnifications (a) and (b), of PGA 3 beads at different magnifications (c) and (d) and PGA 5 beads at different magnifications (e) and (f). All beads were dried at room temperature.

4.2.2.1.2 Swelling of PGA 1 Beads in Water and Sodium Chloride Solution

Swelling studies were performed on the PGA 1 beads and the ESD was calculated as described in Chapter 2 Section 2.7.1. The ESD values which were determined after 8 h of immersion in the medium are given in Table 4.6. It can be clearly seen that there was approximately a tenfold increase in the intake of water in the NaCl solution compared to in deionised water, indicating that the ion exchange mechanism of swelling is still significant for these beads. However, it is reduced compared to the Alg 1 beads studied previously (Section 4.2.1.1.2) which had an ESD value of 6481% after the same immersion time in the same concentration of NaCl solution. This suggests that the amide linkages were reducing the degree of swelling of the PGA 1 beads. The plots for the swelling ratio of the beads as a function of time in water and in the saline solution are shown in Figure 4.14(a) and (b), respectively.

Table 4.6: Summary of Swelling Ratios (%) of PGA 1 Beads in Deionised Water and in 1% w/v NaCl Solution at 20 ± 1°C

Medium	% Swelling after 8 h
H_2O	82
1% w/v NaCl	666

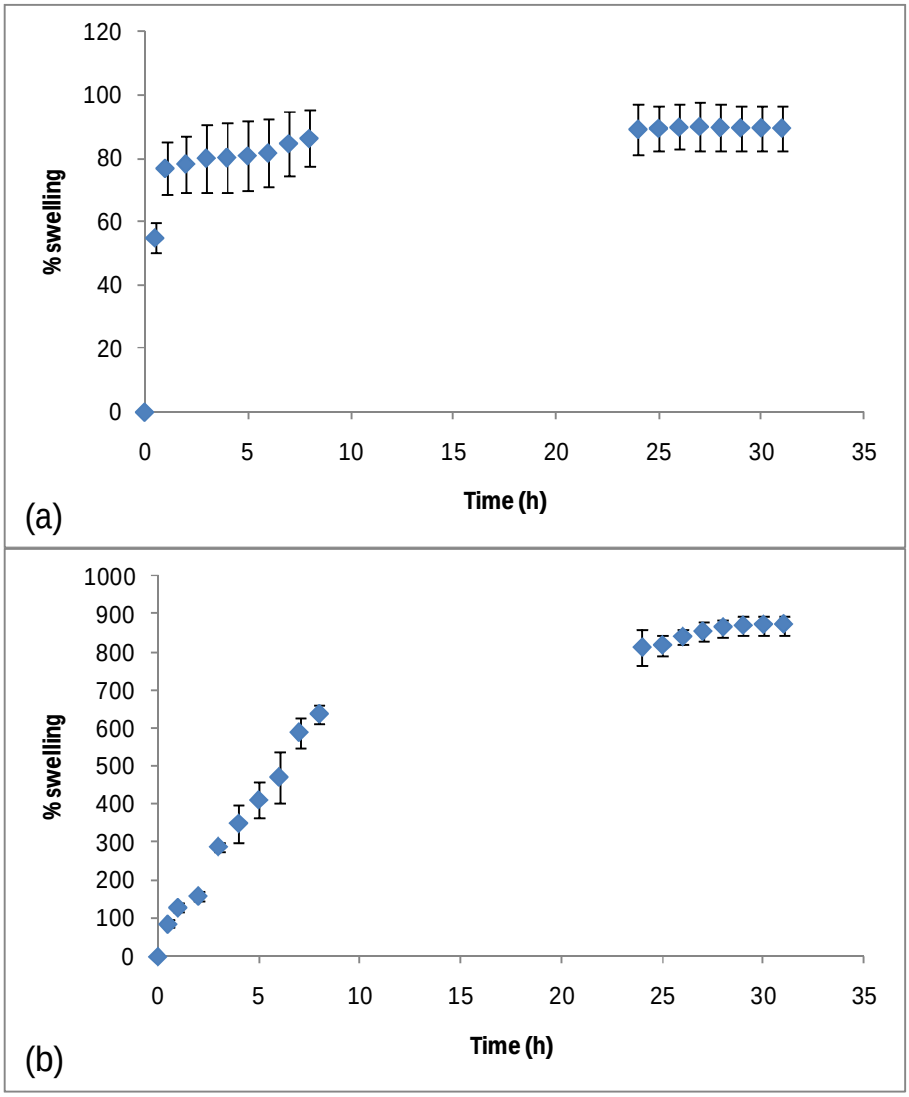

Figure 4.14: ESD ratios (%) as a function of time of PGA 1 beads (n = 20) in (a) deionised water and (b) in 1% w/v NaCl solution at 20 ± 1°C.

The PGA 1 beads increased quickly in weight in deionised water and reached an overall swelling ratio of approximately 80%. Most of the swelling was done in the first hour, and then the beads increased in weight slowly up to the 10 h time period. From this point onwards the beads stayed at the same swollen state and did not decrease or increase in weight even after 24 h. In contrast to the alginate (Alg 1) beads (Section 4.2.1.1.2) there was no evidence that beads disintegrated in the water over 24 h of immersion.

In the saline medium the PGA 1 beads took in water gradually to reach a swelling ratio of 700% after 10 h (Figure 4.14(b)). The beads continued to increase in weight and at the 30 h time point the weight began to level off at a swelling ratio of 900%, after this no major increase or decrease in weight was observed. The beads did not become delicate or fragile in the sodium chloride solution, in comparison to the alginate beads. This proved that the covalent crosslink between the PGA and HSA maintained the integrity of the beads and thus prevented them from disintegrating when they were in their swollen state.

4.2.2.1.3 Identification of Silver within the PGA/Alginate Composite Beads

EDX analysis carried out on PGA 1, PGA 3 and PGA 5 beads showed the three characteristic silver L_{α}, L_{β} and $L_{\beta 2}$ lines between 2.98 and 3.35 keV confirming the presence of silver in these beads.[32] An EDX spectrum of a PGA 1 bead is given in Figure 4.15(a), while EDX spectrum of a PGA 2 bead is given in Figure 4.15(b). An EDX spectrum of a PGA 5 bead is given in Figure 4.15(c) with a SEM micrograph recorded from the same region of the bead shown in Figure 4.15(d). The silver in the PGA 5 beads had undergone reduction using sodium borohydride and the beads were dark brown in colour. The SEM micrographs show microcrystals over the surface of the bead which we would suggest predominantly consist of silver in the zero oxidation state. Similar microcrystals for silver have been observed in the literature.[61] This indicates that at least some of the silver(0) species present in the PGA 5 beads lay outside the nano-domain.

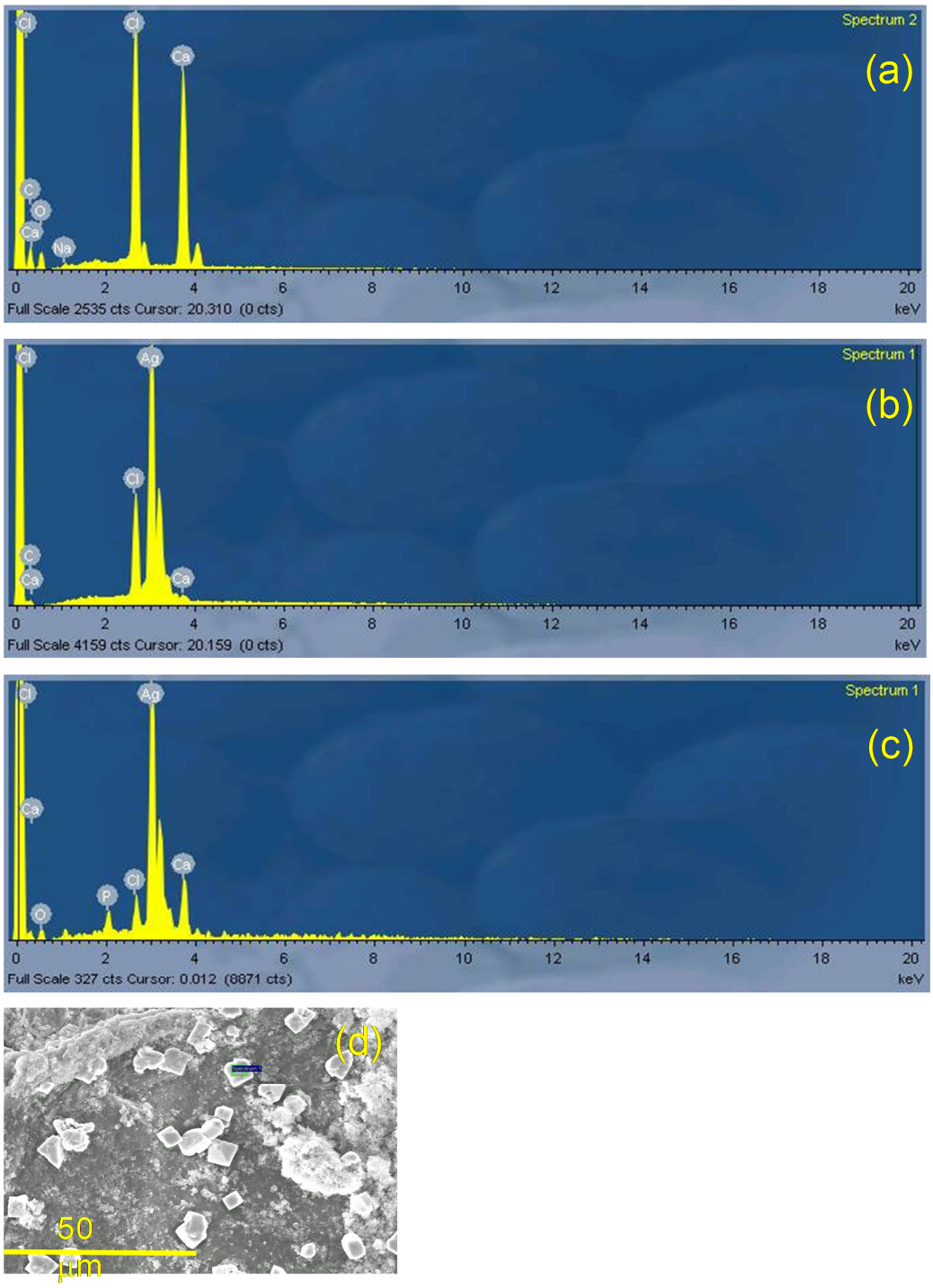

Figure 4.15: EDX analysis of (a) PGA 1 beads and (b) PGA 3 beads and (c) PGA 5 beads showing the presence of silver in the PGA 3 and PGA 5, (d) SEM micrograph of the surface of a PGA 5 bead showing the region at which the EDX (c) was recorded.

4.2.2.1.4 Quantifying the amount of Silver present in the PGA/Alginate Composite Beads

AA spectroscopy was used to quantify the amount of silver present in the different PGA beads containing the different concentrations of silver in the silver(I) and silver(0) states. The mass (mg) of silver in thirty beads was calculated and is plotted in Figure 4.16.

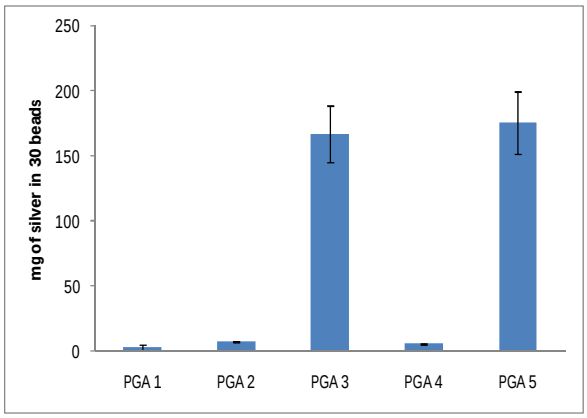

Figure 4.16: The mass (mg) of silver present in thirty PGA beads as determined using AA spectroscopy. Each bead type studied is defined in the figure.

Similarly to the alginate beads, a positive result was obtained for the PGA 1 beads as shown in Figure 4.16. This shows that there was a systematic error in the measurement of silver using this method. This value was subtracted to get the true value of silver contained within the beads. The PGA 2 contained approximately 60 times less silver than the PGA 3 beads, showing that there was a correlation between the concentration of AgNO3 that the beads were immersed in and the amount retained within the beads. Within the experimental error of this experiment the reading for silver in the PGA 4 beads was no different to that of the control PGA 1 beads, so therefore we cannot quantify the amount of silver in these beads. The PGA 5 beads contained approximately the same amount of silver as the PGA 3 beads from which they were formed. The amount of silver contained within the PGA beads was quite similar to that determined for the analogous alginate bead which was simply crosslinked in calcium chloride solution as determined in Section 4.2.1.1.4. For

example 30 beads of Alg 3 were found to contain 105 ± 15 mg of silver while 30 beads of PGA 3 were found to contain 160 ± 20 mg of silver. This indicates that under our experimental conditions the amount of silver that was incorporated into the bead was mainly dependent on the concentration of silver nitrate solution that the beads were immersed in and had little dependence on the nature of the polymer support.

4.2.2.1.5. Quantifying the amount of Silver in the Leachate from the PGA/Alginate Composite Beads

AA spectroscopy was used to quantify the amount of silver that was released from the PGA beads into deionised water over a period of 24 h. The average of the three readings was determined and the results are shown in Figure 4.17.

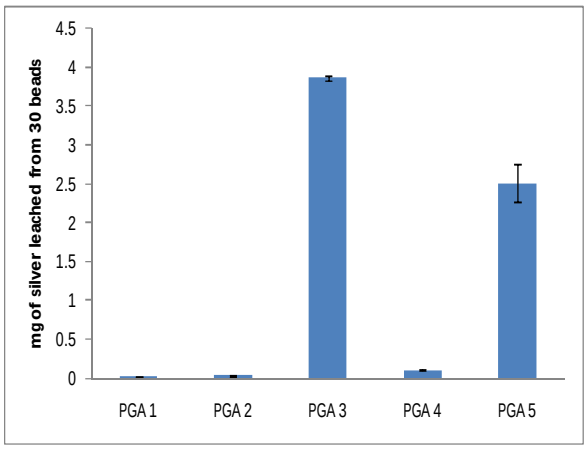

Figure 4.17: The amount of silver leached from 30 PGA beads into deionised water (10 ml) held at 30 ± 1°C over a period of 24 h. Each bead type studied is defined in the figure.

There was a small reading obtained for the PGA 1 bead which, as these beads did not contain any silver, indicated that there was a systematic error in our experimental method and this reading had to be subtracted from the readings recorded for the other beads. The PGA 4 beads released a very small quantity of silver, while the value determined for the PGA 2 beads was within the experimental

error of the value determined for the control beads so it cannot be concluded that silver was released from the PGA 2 beads using this experimental data. The leaching results indicated that there was approximately 1.5 times more silver leached from the PGA 3 beads than the PGA 5 beads. The amount of silver leached from the PGA beads was similar to that released from the simple alginate beads investigated in Section 4.2.1.1.5. Using identical conditions to those outlined here, the analogue beads of PGA 3, the Alg 3 beads, released approximately 2 mg of silver compared to the 3.7 mg of silver released by the PGA 3 beads.

4.2.2.2 Biological Testing

The *in vitro* anti-fungal activity of the silver in the PGA beads was evaluated against the fungi *C. albicans*, using the three different assays described in Section 4.2.1.2. (Plate assay, well assay and colony count assay).

4.2.2.2.1 Plate Assay using the PGA/Alginate Composite Beads

Results for the plate assay, which demonstrated the fungistatic ability of the PGA beads, are shown in Table 4.7 below. The PGA 3 beads caused direct inhibition beneath the beads and gave very clear zones of inhibition around the beads, which can be seen in the photograph of a typical plate shown in Figure 4.18. These zones of inhibition were measured, and on average the PGA 3 beads resulted in zones of inhibition of 143 mm^2. The PGA 2 beads showed that there was only direct inhibition beneath the beads. The lack of zones of inhibition around the PGA 2 beads can be explained by the low concentration of silver absorbed and released from the beads. For the PGA 4 and PGA 5 beads which contained the reduced silver there was zones of inhibition on average of 276 mm^2 and 294 mm^2 measured around the beads, respectively. Both zones of inhibition were very similar in area given that there was a substantial increase in the concentration of silver in the PGA 5 beads compared to the PGA 4 beads (Figure 4.16). The zones of inhibition were so large around the PGA 4 and PGA 5 beads that it was concluded that it was sodium borohydride or one of its products of reaction with the beads or with water that was caused the effect, as was previously discussed for the alginate beads in Section 4.2.1.2.4.

Table 4.7: Results for the Plate Assay for PGA/Alginate Composite Beads

Bead Code	Total Area* (mm^2)	Zone of Inhibition* (mm^2)	Description
PGA 1	365 ± 15	-	No zone of inhibition
PGA 2	364 ± 20	-	Direct inhibition
PGA 3	377 ± 27	143 ± 24	Zone of inhibition
PGA 4	477 ± 29	276 ± 38	Zone of inhibition
PGA 5	477 ± 28	294 ± 21	Zone of inhibition

*ZOIs were recorded after 24 h using ten beads on each plate and plates were held at 37 ± 1°C.

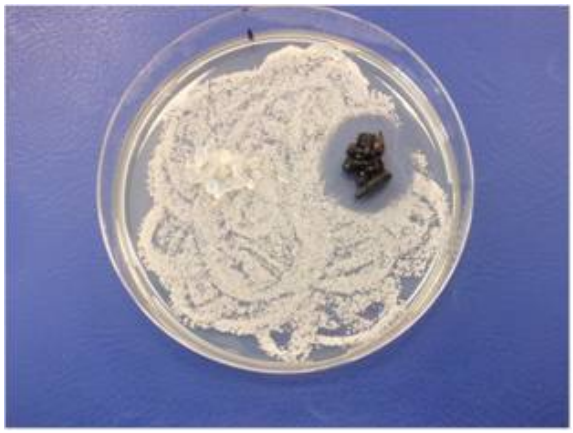

Figure 4.18: Photograph of a typical plate assay experiment for the PGA beads. The ten beads on the left hand side of the plate are PGA 1 beads and it can be clearly seen that there is no inhibition of *C. albicans* occurring around these beads. The ten beads on the right hand side of the plate are the PGA 5 beads.

4.2.2.2.2 Well Assay using the PGA/Alginate Composite Beads

Results from the well assay showed that only the leachate from the PGA 3 beads had an effect on the growth of the *C. albicans*. A summary of results for this assay is shown in Table 4.8.

Table 4.8: Results for the Well assay for PGA/Alginate Composite Beads

Bead Code	Zone of Inhibition* (mm^2)	Description
PGA 1	-	No zone of inhibition
PGA 2	-	No zone of inhibition
PGA 3	37 ± 7	Zone of inhibition
PGA 4	-	No zone of inhibition
PGA 5	-	No zone of inhibition

*The leachate was extracted from 30 beads into 10 ml of deionised water held at 30 $\pm$ 1°C for 24 h. ZOI were recorded after 24 h and plates were held at 37 $\pm$ 1°C.

The results for this assay were unexpected as the PGA 5 beads did not show any zones of inhibition. The results obtained using AA spectroscopy (Section 4.2.2.1.5) clearly showed that there was silver leached from the PGA 5 beads, approximately 30% less than that which was released from the PGA 3 beads. So we would have expected the leachate from the PGA 5 beads to have had some inhibitory effect on the growth of *C. albicans.* However, a similar result occurred for the leachate studies for the simple alginate beads (Section 4.2.1.2.2) and it is proposed that the lack of activity of the leachate from the PGA 5 beads arose because the silver was released as nanoparticles which are known to aggregate in solution with a loss in antimicrobial activity. The zones obtained for the leachate from the PGA beads were similar to those obtained on the well assay studies on the simple alginate beads analogues (Section 4.2.1.2.2). This reflects the comparable amounts of silver which were released from both sets of beads. A photograph of a typical well assay experiment for the PGA beads is shown in Figure 4.19.

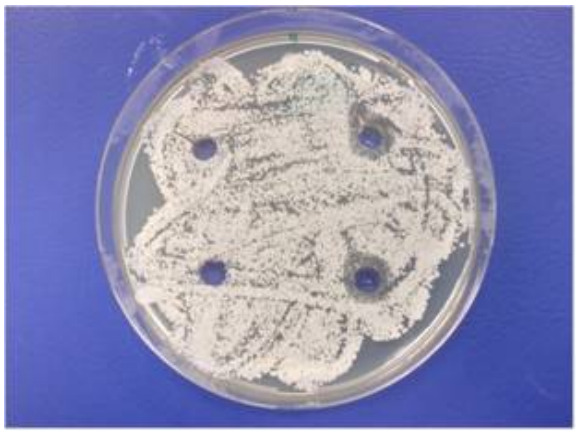

Figure 4.19: A photograph of a typical well assay experiment using PGA beads. The wells on the left hand side of the plate contain the leachate from the PGA 1 beads and it can be clearly seen that there is no inhibition of the growth of *C. albicans* occurring around these beads. The wells on the right hand side of the plate contain the leachate from the PGA 3 beads.

4.2.2.2.3 Colony Count Assay using the PGA/Alginate Composite Beads

The results obtained from the colony count assay are summarised in Figure 4.20. This study was not carried out on the PGA 4 beads as we had deduced that these beads would have little activity towards *C. albicans*. When the assay was carried out using the PGA 1 beads the number of colonies increased gradually over time and after 24 h there were an exponential number of cells growing on the plates which can be clearly seen from the images in Figure 4.21(b). This clearly indicated that the propylene glycol alginate/alginate support was having no effect on the growth of the colonies. The results obtained using the PGA 2 and PGA 5 beads were very similar to those recorded for the control PGA 1 beads. This indicates that even though these beads did contain silver, that they were not having a fungicidal effect on the *C. albicans* cells. This probably occurred for the PGA 2 beads as the amount of silver(I) contained within the beads was too low to produce an effect. For the PGA 5 beads which did contain a large amount of silver it is proposed that the lack of ability of these beads to kill the *C. albicans* arose because the size of silver particles was too large. Similar results were obtained for the simple alginate beads (Section 4.2.1.2.3). The colony assay showed clearly that the PGA 3 beads had the greatest effect on killing the cells in the medium. The effect of the presence of silver

within the bead was not seen until after the two hour mark. Before two hours had elapsed this growth of cells within the medium, containing each of the different types of beads was very similar (Figure 4.20(a)). This lag time probably arose as it took time for the PGA 3 beads to swell. When this occurred silver was then released more efficiently from the beads and a significant amount of the cells could come into direct contact with the silver supported on the polymer by diffusing through the pores in the beads. After 2 h the PGA 3 beads started to kill the *C. albicans* colonies. The silver continued to destroy the colonies overtime and after 24 h there are very few cells growing on the plate as can be seen in Figure 4.21(b) which shows a photograph of a typical colony count experiment taken after 24 h of contact of PGA 3 beads with the cell culture. Whereas Figure 4.21(a) shows a photograph of a plate for a cell culture which had been in contact with the control beads for 24 h. However, when the medium surrounding the PGA 3 beads was sampled at time periods of greater than 24 h it was clear that there was renewed growth of the *C. albicans*. Therefore it would appear under the conditions of this experiment that the PGA 3 beads could not completely eradicate the *C. albicans.* However, as they had better structural integrity than the simple alginate beads, which were ionically crosslinked with calcium ions, and they did not disintegrate in the YEPD medium, these beads hold promise as support for silver in water disinfection applications.

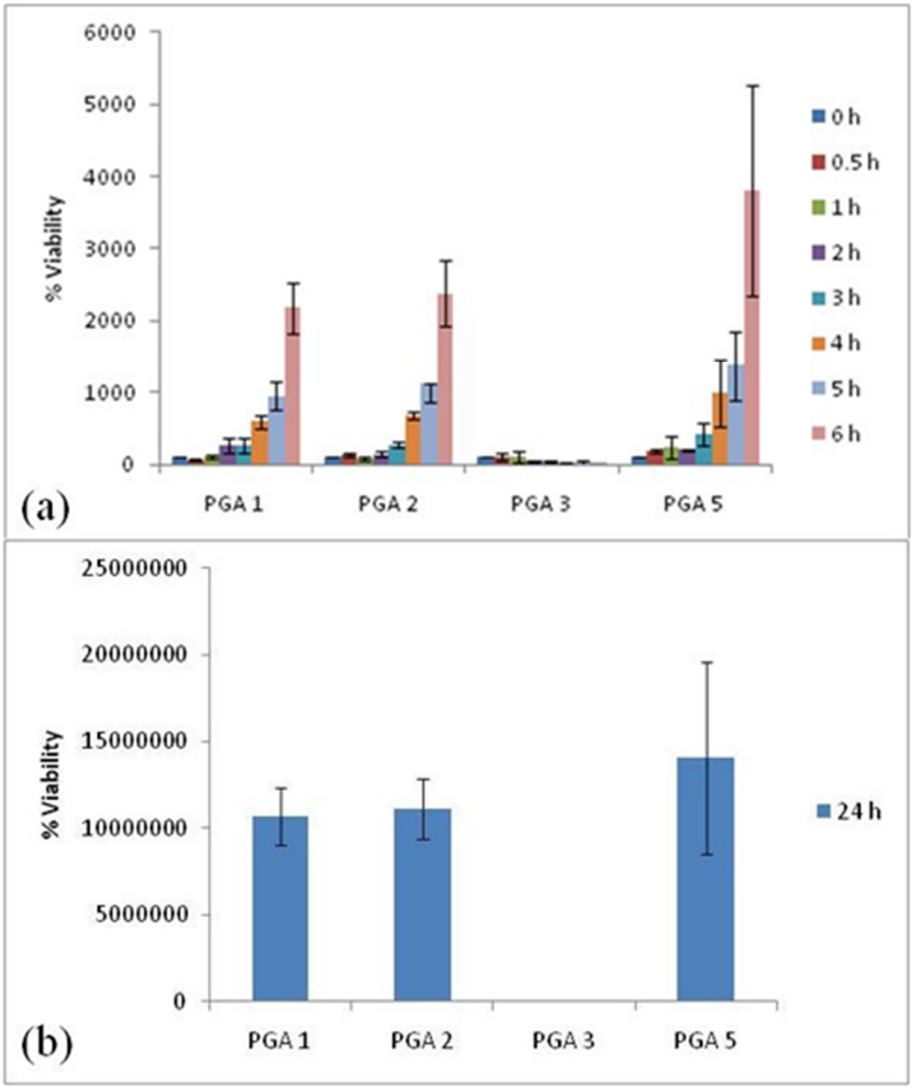

Figure 4.20: The number of viable *C. albicans* cells present in YEPD medium upon shaking with the PGA 1, 2, 3 and 5 beads. Medium was held at 30 ± 1°C, (a) results over first 6 h (b) results after 24 h. PGA 1 V's PGA 2 = ns, PGA 1 V's PGA 3 = *** P<0.0001, PGA 1 V's PGA 5 = ns.

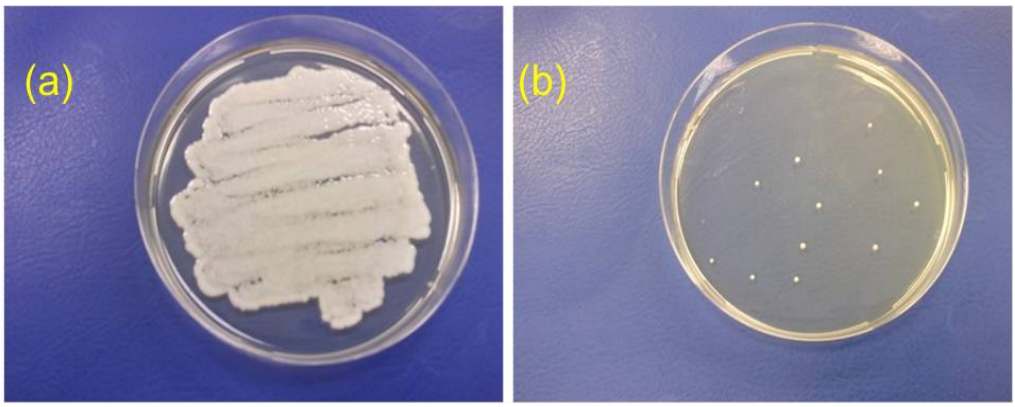

Figure 4.21: Photograph of a typical agar plate used to culture the number of viable *C. albicans* cells growing in the medium after the colonies have been in 24 h contact with (a) PGA 1 and (b) PGA 3 beads.

4.2.3 Quaternary Ammonium Alginate/Alginate Composite Beads Crosslinked with Calcium Ions

A previous study had shown that when alginate was functionalised with a quaternary ammonium group and beads were then formed through calcium ion crosslinkage that the beads have good activity against the growth of a range of microbes including *E. coli*, *S. aureus* and *C. albicans*.[62] The alginate was derivatised by reaction with 3-(trimethoxysilyl)-propyloctadecyldimethylammonium (TSA) chloride (Scheme 4.2) in acid solution. This reaction anchors the TSA group to the polymer backbone by a covalent non-hydrolysable bond. The antimicrobial activity of the polymer was deduced to arise due to the TSA group, as the unfunctionalised alginate control beads showed no activity and it is well documented that quaternary ammonium groups have antimicrobial activity.[62-64] The study carried out in this section set out to investigate if incorporating silver into this type of bead could have an additional effect on their known antimicrobial activity. The beads were synthesised as outlined in Chapter 2 Section 2.3.5. Before silver ions could be incorporated the chloride ions associated with the TSA group were exchanged for nitrate ions to reduce the formation of silver chloride and enable silver ions to be incorporated into the beads. When the reaction with sodium borohydride to reduce the silver within the beads was attempted an exothermic process took place and a substantial amount of hydrogen gas was released which cause the beads to disintegrate. Therefore no studies were carried out on the TSA functionalised beads containing silver in the zero oxidation state. The different beads used in this section are identified by the codes given in Table 4.9.

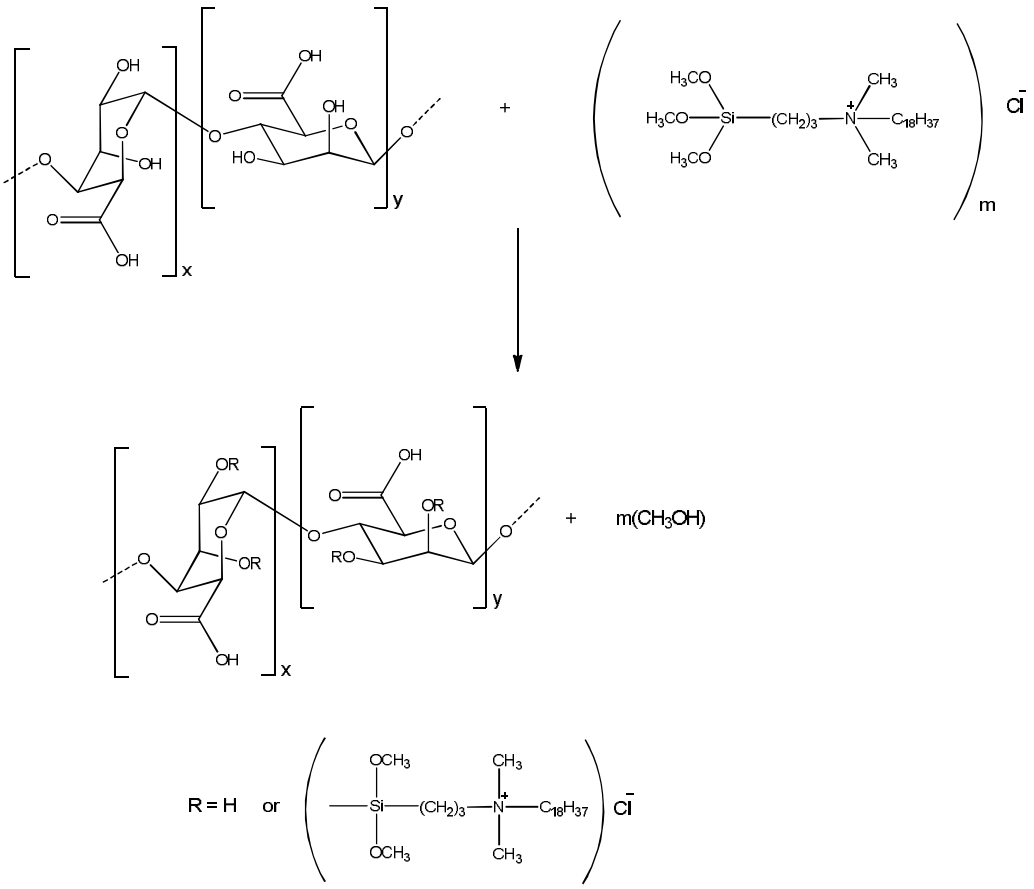

Scheme 4.2: The reaction between sodium alginate and 3-(trimethoxysilyl)-propyloctadecyldimethylammonium chloride to form TSA.

Table 4.9: Codes for the TSA and Control Beads

Bead code	Description of different beads
Alg 7	4% w/v sodium alginate, crosslinked in 5% w/v $CaCl_2$.
TSA 1	4% w/v sodium alginate, 0.02 M TSA, pH was adjusted to 4.0 with acetic acid at room temperature, crosslinked in 5% w/v $CaCl_2$.
TSA 2	4% w/v sodium alginate, 0.02 M TSA, pH was adjusted to 4.0 with acetic acid at room temperature, crosslinked in 5% w/v $CaCl_2$. Ion exchange was performed on the beads with 0.05 M Nitric acid to remove the Cl^- ions. Immersed in 0.01 M $AgNO_3$ for 24 h.
TSA 3	4% w/v sodium alginate, 0.02 M TSA, pH was adjusted to 4.0 with acetic acid at room temperature, crosslinked in 5% w/v $CaCl_2$. Ion exchange was performed on the beads with 0.05 M Nitric acid to remove the Cl^- ions. Immersed in 0.10 M $AgNO_3$ for 24 h.

4.2.3.1 Characterisation of the TSA/Alginate Composite Beads

4.2.3.1.1 Surface Morphology of the TSA/Alginate Composite Beads

SEM micrographs recorded of TSA 3 beads, TSA 1 beads before they were washed with nitric acid and after they were washed with nitric acid (0.05 M) in order to exchange the chloride for nitrate ions are shown in Figure 4.22. The TSA 1 beads (Figure 4.5(a)) were of a similar spherical shape to the Alg 1 beads, this was due to the lower viscosity of the TSA/alginate solution which allowed the droplets of solution to fall from the syringe immediately with little distortion in shape. The SEM micrograph recorded of the TSA 1 beads at the higher magnification (Figure 4.22(b)) shows a surface which appears rough and slightly wrinkled. A similarly folded surface morphology was previously observed for beads formed from chitosan functionalised with long hydrophobic groups.[65]

After the TSA 1 beads were washed in nitric acid (0.05 M) they appeared less symmetrical in shape (Figure 4.22(c)), but they still exhibited the 'wrinkled' surface morphology (Figure 4.22(d)). The SEM recorded of the TSA 3 beads showed that

they appeared less symmetrical in shape compared to the TSA 1 beads at the lower magnification (Figure 4.22(d)). In addition the TSA 3 beads have a much rougher morphology than the TSA 1 beads and, a lot of cracks and major indentations were observed in the SEM recorded at a higher magnification (Figure 4.22(f)).

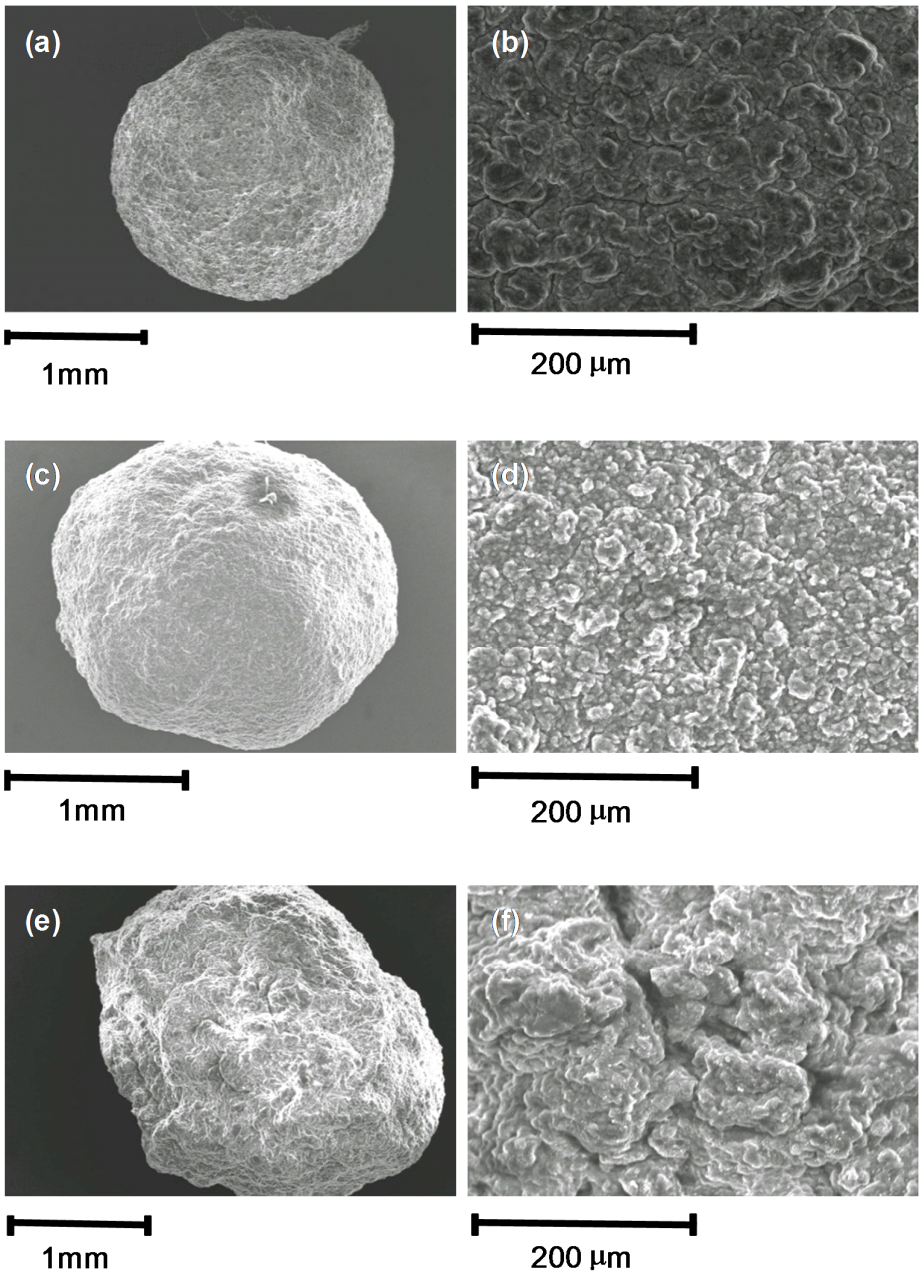

Figure 4.22: SEM micrographs of TSA 1 beads at different magnifications (a) and (b), of TSA 1 beads after they were washed with nitric acid to exchange the chloride ions at different magnifications (c) and (d) and TSA 3 beads at different magnifications (e) and (f). All beads were dried at room temperature.

4.2.3.1.2 Swelling of TSA 1 Beads in Water and Sodium Chloride Solution

The swelling studies were performed on the TSA 1 beads and the EDS values were determined as described in Chapter 2, Section 2.7.1. The % swelling of the TSA 1 beads in the two media after 8 h are shown in Table 4.10. Surprisingly, the % swelling of the TSA 1 beads in deionised water is quite similar to that in the NaCl solution. This was in marked contrast to the results observed for the Alg 1 and PGA 1 beads which exhibited increased swelling in the NaCl solution. The TSA 1 beads showed the least swelling in NaCl solution of the three sets of beads studied, even though in contrast to the PGA the alginate chains were only held together by electrostatic interactions. Previous studies on a related polysaccharide polymer, *N*-acylated chitosan, have shown when the alkyl chain is long that, in addition to the H-bonding interactions holding the unfunctionalised chitosan polymer chains together, the chains are also held together by hydrophobic interactions.[66] These interactions increase both the mechanical strength of the polymer matrix and its resistance to swelling in water. In addition, the positive charge on the ammonium group on the surface of the TSA beads may have caused the sodium ion to be repelled from the bead. In support of this proposal it was observed that it took longer for the TSA beads to become impregnated with silver ions compared to the calcium alginate or PGA beads. Figure 4.23 shows the percentage swelling of the TSA 1 beads as a function of time. As can be seen from the Figure, the beads absorbed water rapidly over a period of about 10 h after which time they exhibited no substantial increase in weight. Moreover, there was no evidence in this study that the beads were beginning to lose weight and disintegrate, even after immersion in either of the media for 32 h. This indicates that these beads are more structurally stable in solution than the simple calcium alginate beads.

Table 4.10: Summary of swelling ratios (%) of TSA 1 beads in deionised water and in 1% w/v NaCl solution at 20 ± 1°C

Medium	% swelling after 8 h
H_2O	82
1% w/v NaCl	120

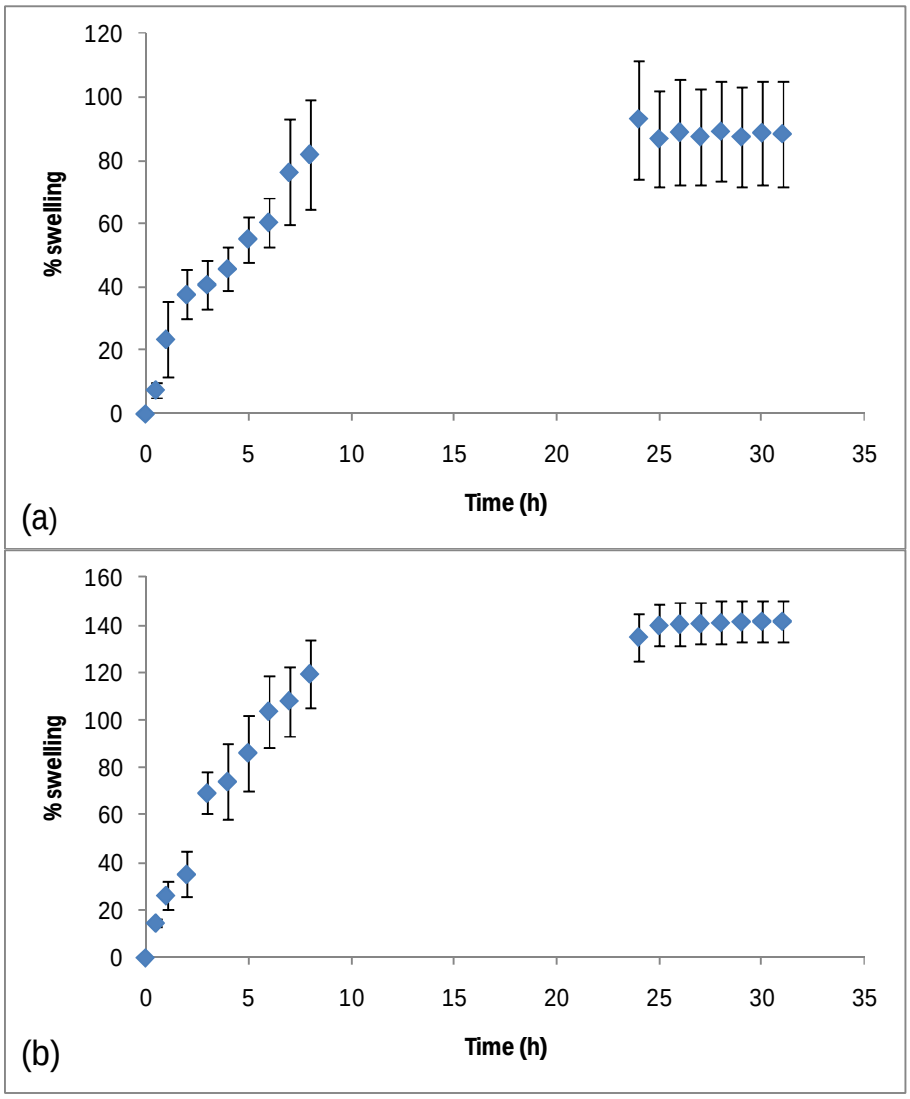

Figure 4.23: Swelling ratios (%) as a function of time of TSA 1 beads in (a) deionised water and (b) 1% w/v NaCl solution at 20 ± 1°C.

4.2.3.1.3 Identification of Silver within the TSA/Alginate Composite Beads

EDX analysis were carried out on all the TSA and control Alg 7 beads. The results for the three sets of TSA beads all showed a line at 1.74 keV which is assigned as the $L_{\alpha 1}$ line of silicon[32] and arises from the TSA group attached to the alginate polymer chain (Figure 4.24(a)) . The EDX spectrum of the TSA 2 and TSA 3 beads showed the three lines for silver between 2.98 and 3.15 keV.[32] An EDX spectrum recorded for a TSA 1 bead is shown in Figure 4.24(a) and that for a TSA 3 bead is given in Figure 4.24(b). A SEM micrograph recorded of the surface of the TSA 3 bead (Figure 4.24(c)), at the point on the surface at which the EDX spectrum shown in Figure 4.24(b) was recorded, showed clusters of cubic structures with side lengths in the sub-micron region. It is likely that these structures are crystals of AgCl, which are known to grow in cubic form[67] and they arose because even after the ion exchange took place some chloride ions were still present on the bead.

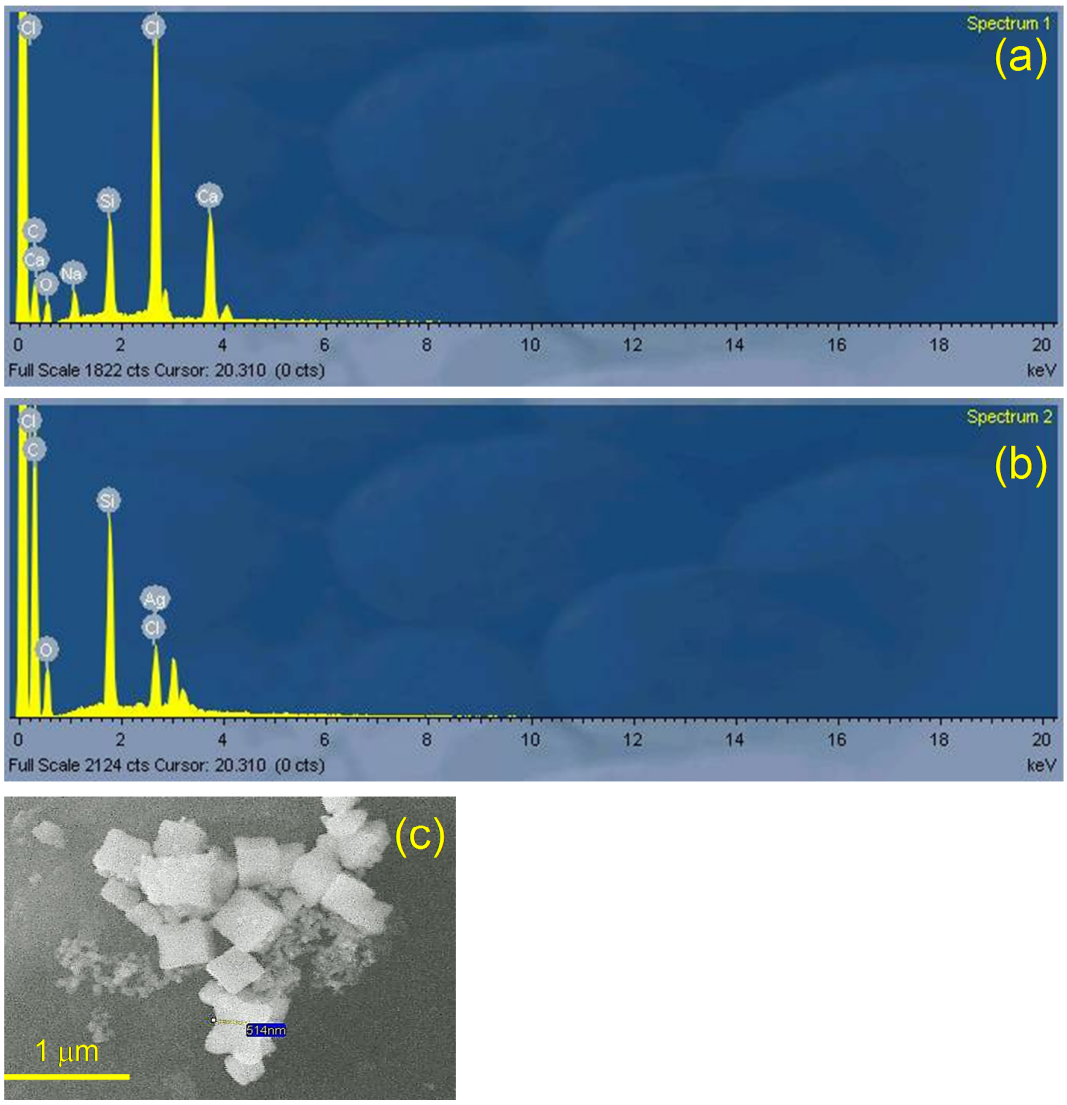

Figure 4.24: EDX spectra of (a) TSA 1 beads and (b) TSA 3 beads showing the absence and presence of silver in the beads respectively. (c) SEM micrograph of the surface of a TSA 3 bead showing the region at which the EDX (b) was recorded.

4.2.3.1.4 Quantifying the amount of Silver in the TSA/Alginate Composite Beads

AA spectroscopy was used to quantify the amount of silver present in the different TSA beads prepared with the different concentrations of silver(I) ions. The amount of silver in thirty beads was calculated and a summary of the results is given in Figure 4.25.

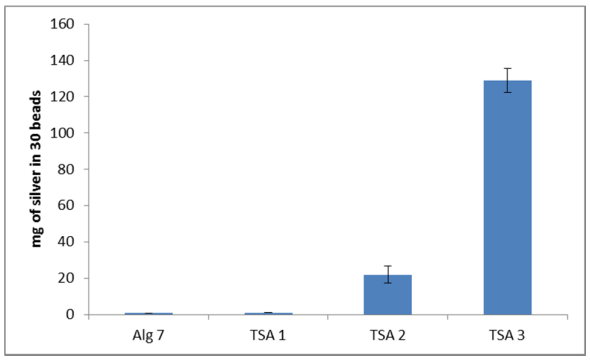

Figure 4.25: The mass (mg) of silver present in thirty TSA beads as determined using AA spectroscopy. Each bead type studied is defined in the figure.

As observed previously for the calcium alginate and PGA beads there was a positive result obtained for the control, Alg 7, beads as shown in Figure 4.25. A positive result was also obtained for the TSA 1 beads which also contained no silver. The value obtained for the TSA 1 beads was subtracted from the values for the TSA 2 and TSA 3 beads to get the true value of silver contained within these beads. The TSA 2 beads had a small quantity of silver present in them, while the TSA 3 beads had approximately six times more, which was expected as they were immersed in a solution containing a higher concentration of silver nitrate.

4.2.3.1.5 Quantifying the Amount of Silver in the Leachate from the TSA/Alginate Composite beads

AA Spectroscopy was used to quantify the amount of silver released from the TSA beads into deionised water over a period of 24 h. The average of the three readings was determined and the results are shown in Figure 4.26.

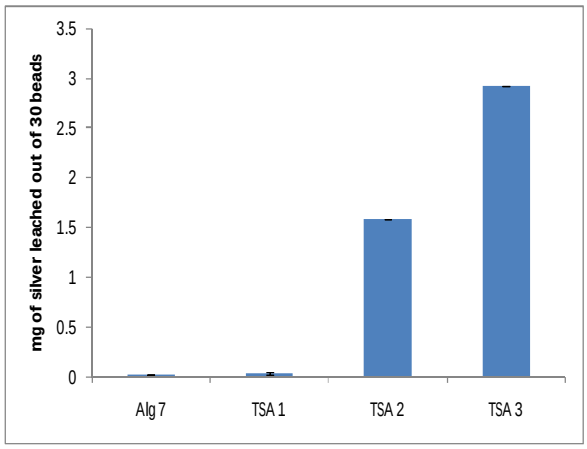

Figure 4.26: The amount of silver leached from 30 TSA beads and control beads into deionised water (10 ml) held at 30 ± 1°C over a period of 24 h. Each bead type studied is defined in the figure.

There was an almost zero reading obtained for the Alg 7 and the TSA 1 beads which was expected as the beads did not contain any silver. The TSA 2 and the TSA 3 beads did release silver into the water. The TSA 3 beads released a similar amount of approximately 3 mg of silver compared to when this experiment was carried out on the analogous Alg 3 and PGA 3 beads. Interestingly the TSA 2 beads released substantially more silver (approximately 1.5 mg) compared to the Alg 2 and PGA 2 analogues (approximately 0.1 mg). This may correspond to the SEM micrograph recorded of the TSA 2 beads which showed that there were silver salt clusters deposited on the bead surface.

4.2.3.2 Biological Testing

The *in vitro* anti-fungal activity of the TSA beads was evaluated against the fungi *C. albicans*, using the three different assays described in Section 4.2.1.2. (Plate assay, well assay and colony count assay),

4.2.3.2.1 Plate Assay using the TSA/Alginate Composite and Control Alginate Beads

Results for the plate assay, which demonstrated the fungistatic ability of the TSA beads, are shown in Table 4.11. As can be seen from Table 4.11 the presence of the TSA group on the bead was resulting in the alginate having an inhibitory effect towards the growth of *C. albicans* as the TSA functionalised beads which did not contain any silver resulted in a ZOI of 24 mm^2. This is in contrast to the analogous unfunctionalised alginate bead, Alg 7, which produced no zones of inhibition. Surprisingly, within experimental error there was no difference in the activity of the TSA 1 and TSA 2 beads. However, the TSA 2 beads were still more active than the analogous calcium alginate and PGA beads, Alg 2 and PGA 2, which only resulted in direct inhibition when used in the same assay. When the TSA 3 beads which contained the higher amount of silver(I) ions were used in this assay a very large ZOI was recorded on the plate for the growth of *C. albicans.* This zone covered an area of 307 mm^2 compared to the ZOIs of 83 mm^2 and 143 mm^2 recorded when the experiment was carried out using the Alg 3 and PGA 3, which contained approximately the same amount of silver.

Table 4.11: Results for the Plate Assay for TSA/Alginate Composite and Control Alginate Beads

Bead Code	Total Area* (mm^2)	Zone of Inhibition* (mm^2)	Description
Alg 7	98 ± 9	-	No zone of inhibition
TSA 1	102 ± 11	24 ± 11	Zone of inhibition
TSA 2	92 ± 3	14 ± 3	Zone of inhibition
TSA 3	413 ± 20	306 ± 20	Zone of inhibition

* ZOIs were recorded after 24 h using ten beads on each plate and plates were held at 37 ± 1°C.

4.2.3.2.2 Well Assay using the TSA/Alginate Composite and Control Alginate Beads

Results from the well assay showed that only the leachate from the TSA 3 beads was having a significant inhibitory effect on the growth of the *C. albicans*. A summary of results for this assay is shown in Table 4.12. The leachate from the control Alg 7 beads did not show any inhibition around the wells which was expected as these beads contained no silver or TSA. The TSA 1 beads showed very small zones of inhibition around the wells, indicating that a proportion of the quaternary ammonium groups were not covalently attached to the alginate and had come out of the beads into solution. The leachate from the TSA 2 beads did not result in a zone of inhibition. These beads had been placed in a column and washed in nitric acid to exchange the chloride for a nitrate ion, so it is likely that any TSA which were simply adsorbed on the bead were also removed in this step. The TSA 2 beads contained similar amounts of silver compared to Alg 2 and PGA 2 which also showed no activity towards inhibiting the growth of *C. albicans* in this assay. The AA spectroscopic studies on the leachate from these beads had indicated that these beads released a larger amount of silver than the Alg 2 or PGA 2 beads but even at this concentration the presence of silver in solution did not inhibit the growth of *C. albicans*. The leachate from TSA 3 beads which released a similar amount of silver to the Alg 3 and PGA 3 beads as determined using AA spectroscopy resulted in a very similar sized zone of inhibition to these beads of 40 mm^2. The leachate from the TSA 3 beads that was placed into the well gave clear defined zones of inhibition as can be seen from a photograph of a typical plate given in Figure 4.27.

Table 4.12: Summary of Results for the Well Assay for TSA/Alginate Composite and Control Calcium Alginate beads

Bead Code	Zone of Inhibition* (mm^2)	Description
Alg 7	-	No zone of inhibition
TSA 1	2 ± 1	Zone of inhibition
TSA 2	-	No Zone of inhibition
TSA 3	40 ± 7	Zone of inhibition

The leachate was extracted from 30 beads into 10 ml of deionised water held at 30 ± 1°C for 24 h. ZOI were recorded after 24 h and plates were held at 37 ± 1°C.

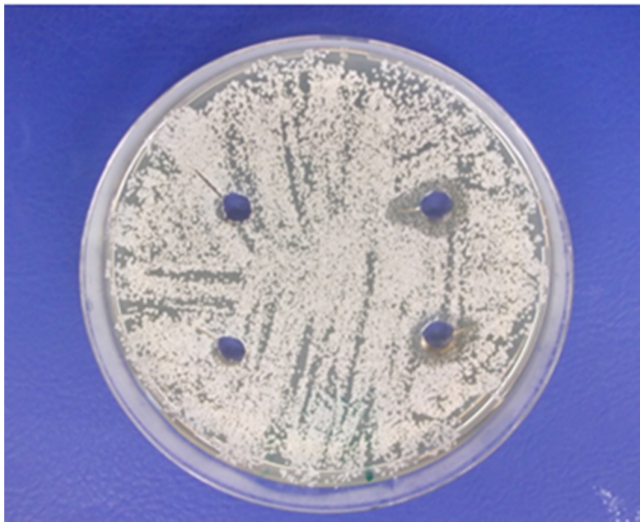

Figure 4.27: A photograph of a typical well assay experiment. The wells on the left hand side of the plate containing the leachate from thirty TSA 2 beads and it can be clearly seen that there are no zones of inhibition occurring around these beads. The wells on the right hand side of the plate contain the leachate from the TSA 3 beads.

4.2.3.2.3 Colony Count Assay using the TSA/Alginate Composite and Control Calcium Alginate Beads

For the initial measurement (0 h) of the colony count assay each of the cell suspensions contained the same number of cells (Figure 4.28). Thirty beads were then added to each of the cultures and the suspensions were shaken. For the cell culture which was shaken with the control Alg 7 beads there was a steady increase in the number of cells present in the medium over the 6 h of measurement and by 24 h the *C. albicans* had reached its exponential phase of growth. For the assay carried out using the TSA functionalised alginate beads, TSA 1, there was also an increase in the number of cells growing in the medium as a function of time. Although the number of viable cells recorded in the medium was lower than that for the control, (Alg 7 beads at the 5 h sample), when the measurement was taken after 6 h there was an identical number of *C. albicans* cells in this medium compared to the control. When the measurement was carried out at 24 h the *C. albicans* was in its exponential phase of growth. A photograph of a typical plate sampled at 24 h for the experiment using the TSA 1 beads clearly shows the presence of a significant number of viable *C. albicans* present (Figure 4.29(a)). This indicated that the TSA group only had a mild fungicidal effect on *C. albicans*. More promising results were recorded for the TSA 2 and TSA 3 beads. Clearly from the results obtained at the 6 h and 24 h time periods the TSA 2 beads were killing the *C. albicans.* This is in contrast to the results obtained in Section 4.2.2.2.3 from the colony count assay on the PGA 2 beads, which contained a similar quantity of silver to the TSA 2 beads, in which the growth of the *C. albicans* was not inhibited at all and matched that of the control experiment. For the study carried out using the TSA 3 beads there were no viable *C. albicans* cells cultured on the plate at the 6 h time period and only a very small amount of regrowth of the cell in the sample taken after 24 h. Figure 4.29 shows a photograph of a plate used to grow a sample of cell the culture at this time period and only a few cultures can be observed. Superficially these results appear similar to those acquired from the colony count assay on the analogous calcium alginate-silver containing beads (Alg 3) which are given in Section 4.2.1.2.3. However, whereas the Alg 3 beads had swollen and disintegrated in the cell culture medium releasing all their silver contents, after 6 h the TSA 3 beads had swollen to a much lower

extent and had remained intact. Therefore the TSA 3 polymeric material is a very promising material to use in water disinfection systems or surgical dressings.

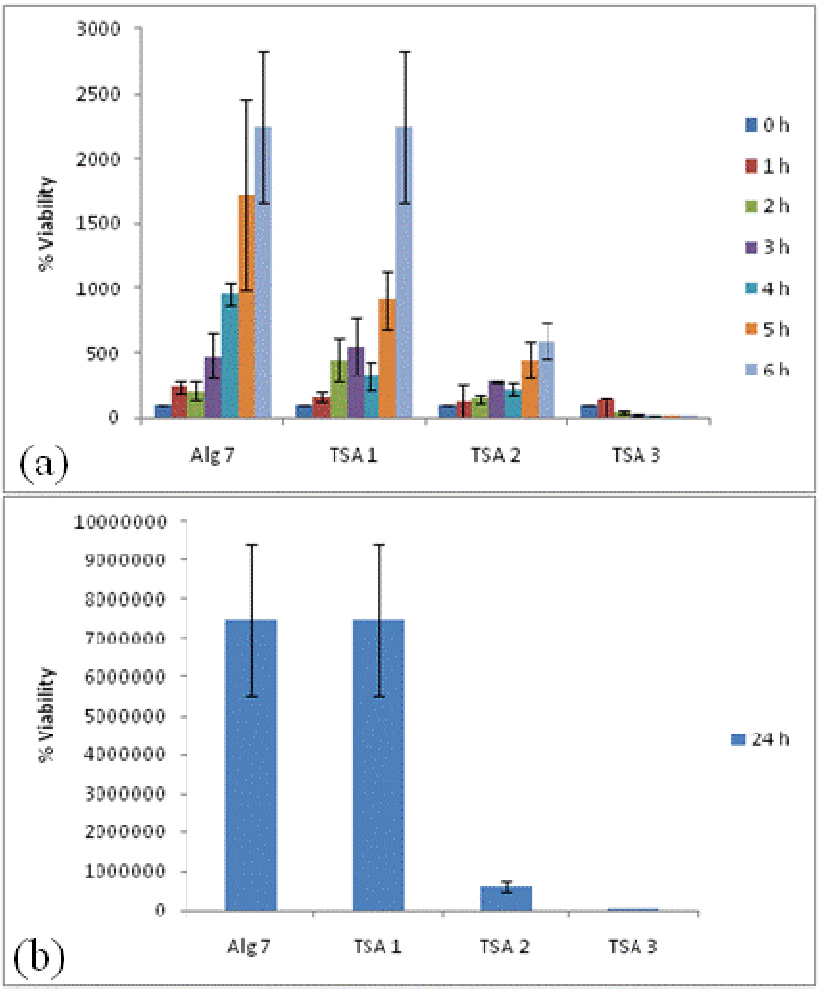

Figure 4.28: The number of viable *C. albicans* cells present in YEPD medium upon shaking with the Alg 7, TSA 1, TSA 3 and TSA 5 beads. Medium was held at 30 ± 1°C, (a) results over first 6 h (b) results after 24 h. Alg 7 V's TSA 1 = ns. Alg 7 V's TSA 2 = **, P = 0.0013, Alg 7 V's TSA 3 = ***, P = 0.0005.

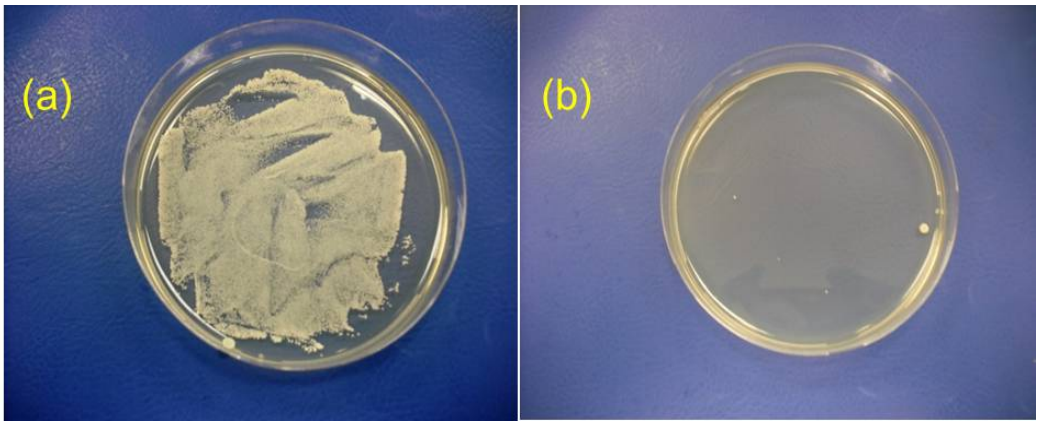

Figure: 4.29: Photograph of a typical agar plate used to culture the number of viable C. albicans cells growing in the medium after the colonies have been in 24 h contact with (a) TSA 1 beads and (b) TSA 3 beads.

4.3 Conclusions

1. The Alg 1, PGA 1 and TSA 1 beads were studied with respect to their swelling behavior in deionised water and in sodium chloride solution. The three beads increased in weight by a quite similar % ratio in the deionised water after 8 h of immersion. However, the TSA 1 beads only increased in mass by 120% compared to 666% for the PGA 1 beads and 6481% for the Alg 1 beads when the beads were immersed in sodium chloride solution for 8 h. This indicates that the TSA 1 beads are resistant to swelling associated with the cation exchange mechanism. Moreover, only the Alg 1 beads showed signs that they were disintegrating in the two solutions after 24 h of immersion. A summary of the swelling behavior of the three types of beads studied is given in Table 4.13.

Table 4.13: Summary of Swelling Behavior of Three Bead Types

	Medium held at 20 ± 1°C	**Alg 1**	**PGA 1**	**TSA 1**
% swelling after 8 h Immersion	H_2O	60%	86%	82%
	1% w/v NaCl	6481%	636%	120%
Stability of Bead after 24 h Immersion	H_2O	Decrease in weight	Weight stayed constant	Weight stayed constant
	1% w/v NaCl	Decrease in weight	Weight stayed constant	Weight stayed constant

2. For the three types of polymer supports only the TSA support showed some activity against the growth of *C. albicans* and this effect was quite mild as indicated by the colony count assay.

3. Both sodium borohydride, which was used to reduce the silver in the beads, and boric acid were shown to have a good activity against the growth of *C. albican*s. We propose that it was a boron based compound, and not silver which was responsible for the large activity of the Alg 4, Alg 5, Alg 6, PGA 4 and PGA 5 beads in the plate assay experiment.

4. The leachate from the Alg 5 and PGA 5 beads showed no activity in the well assay experiment even though they contained similar concentrations of silver to the leachate from the Alg 3 and PGA 3 beads which showed a small effect. It is likely that this arose because the silver released from the Alg 5 and PGA 5 beads is in the zero oxidation state and the antimicrobial activity of silver(0) particles is known to be related to particle size.

5. Under the experimental conditions used the calcium alginate and PGA/alginate composite beads immersed in a solution of 0.1 M $AgNO_3$ showed greater activity against the growth of C. *albicans* than their silver(0) impregnated analogues. This may be because the silver(0) particles were mainly not formed in the nano-domain. Silver(0) species were not formed for the TSA support as the beads disintegrated upon reaction with sodium borohydride.

6. Of all the beads studied the TSA 3 beads showed the highest activity against the growth of *C. albicans* in the plate assay experiment. Moreover, they showed better fungicidal ability towards *C. albicans* in the colony count assay than the PGA 3 beads and the beads remained intact, whereas, the Alg 3 beads disintegrated in this study. Therefore, of the three polymer supports studied, it would appear the TSA support shows the greatest potential to be used in materials for water disinfection or in wound dressings. A summary of the results for the Alg 3, PGA 3, and TSA 3 in relation to the biological assays is given in Table 4.14.

Table 4.14: Summary of Biological Activity of Alg 3, PGA 3 and TSA 3 Beads Correlated with their Silver Content and Ability to Leach Silver.

		Alg 3	**PGA 3**	**TSA 3**
Plate Assay ZOI	10 beads	83 ± 27 mm^2	143 ± 24mm^2	306 ± 20 mm^2
Well Assay ZOI	leachate from 30 beads	39 ± 10 mm^2	37 ± 7 mm^2	40 ± 7 mm^2
Colony Count Assay % Viability	6 h	27	10	5
	24 h	4	57	2
Mass of silver in 30 beads		105 ± 15 mg	160 ± 20 mg	128 ± 10 mg
Mass of silver leached out of 30 beads		2.2 ± 0.1 mg	3.8 ± 0.1mg	2.9 ± 0.1 mg

4.4 References

(1) Lalueza, P.; Monzón, M.; Arruebo, M.; Santamaría, J. *Materials Research Bulletin* **2011**, *46*, 2070-2076.
(2) Brandt, O.; Mildner, M.; Egger, A. E.; Groessl, M.; Rix, U.; Posch, M.; Keppler, B. K.; Strupp, C.; Mueller, B.; Stingl, G. *Nanomedicine: Nanotechnology, Biology and Medicine* **2012**, *8*, 478-488.
(3) Rai, M.; Yadav, A.; Gade, A. *Biotechnology Advances* **2008**, *27*, 76-83.
(4) Travan, A.; Pelillo, C.; Donati, I.; Marsich, E.; Benincasa, M.; Scarpa, T.; Semeraro, S.; Turco, G.; Gennaro, R.; Paoletti, S. *Biomacromolecules* **2009**, *10*, 1429-1435.
(5) Wu, J.; Hou, S.; Ren, D.; Mather, P. T. *Biomacromolecules* **2009**, *10*, 2686-2693.
(6) Dutta, S.; Shome, A.; Kar, T.; Das, P. K. *Langmuir* **2011**, *27*, 5000-5008.
(7) Rowan, R.; McCann, M.; Kavanagh, K. *Medical Mycology* **2010**, *48*, 498-505.
(8) Bhandari, A.; Jones, D. G.; Schullek, J. R.; Kham, V.; Schunk, C. A.; Tamanaha, L. L.; Chen, D.; Yuan, Z.; Needels, M. C.; Gallop, M. A. *Bioorganic and Medicinal Chemistry Letters* **1998**, *8*, 2303-2308.
(9) Moran, G. P.; Coleman, D. C.; Sullivan, D. J. *International journal of microbiology* **2012**, *2012*, 1-7.
(10) Rowan, R.; Moran, C.; McCann, M.; Kavanagh, K. *Biometals* **2009**, *22*, 461-467.
(11) McCullough, M. J.; Ross, B. C.; Reade, P. C. *International Journal of Oral and Maxillofacial Surgery* **1996**, *25*, 136-144.
(12) http://www.stdsandyou.com/yeastinfection/yeast-infection-candida-thrush-oral-mouth.html.
(13) http://botit.botany.wisc.edu/toms_fungi/jan99.html.
(14) Han, T. L.; Cannon, R. D.; Villas-Boas, S. G. *Fungal Genetics and Biology* **2011**, *48*, 747-763.
(15) Lo, H. J.; Kohler, J. R.; DiDomenico, B.; Loebenberg, D.; Cacciapuoti, A.; Fink, G. R. *Cell* **1997**, *90*, 939-949.
(16) Gale, C. A.; Bendel, C. M.; McClellan, M.; Hauser, M.; Becker, J. M.; Berman, J.; Hostetter, M. K. *Science* **1998**, *279*, 1355-1358.
(17) http://medicineworld.org/cancer/lead/10-2007/how-candida-albicans-transforms.html.
(18) http://www.sbs.utexas.edu/mycology/sza_images_sem.htm.
(19) Bozanic, D. K.; Dimitrijevic-Brankovic, S.; Bibic, N.; Luyt, A. S.; Djokovic, V. *Carbohydrate Polymers* **2011**, *83*, 883-890.
(20) Babu, V. R.; Kim, C.; Kim, S.; Ahn, C.; Lee, Y. I. *Carbohydrate Polymers* **2010**, *81*, 196-202.
(21) Kampf, G.; Dietze, B.; Grosse-Siestrup, C.; Wendt, C.; Martiny, H. *Antimicrobial Agents and Chemotherapy* **1998**, *42*, 2440-2442.
(22) http://water.me.vccs.edu/courses/env108/Lesson5_print.htm.
(23) Panic, V.; Adnadjevic, B.; Velickovic, S.; Jovanovic, J. *Chemical Engineering Journal* **2010**, *156*, 206-214.
(24) Andrade-Espinosa, G.; Escobar-Barrios, V.; Rangel-Mendez, R. *Colloid and Polymer Science* **2010**, *288*, 1697-1704.

(25) Bajpai, S. K.; Sharma, S. *Reactive and Functional Polymers* **2004**, *59*, 129-140.
(26) Hurteaux, R.; Edwards-Levy, F.; Laurent-Maquin, D.; Levy, M. C. *European Journal of Pharmaceutical Sciences* **2005**, *24*, 187-197.
(27) Solak, E. K.; Asman, G.; Camurlu, P.; Sanli, O. *Vacuum* **2008**, *82*, 579-587.
(28) Vlachou, M.; Naseef, H.; Efentakis, M.; Tarantili, P. A.; Andreopoulos, A. G. *Journal of Biomaterials Applications* **2001**, *16*, 125-138.
(29) Sriamornsak, P.; Kennedy, R. A. *International Journal of Pharmaceutics* **2008**, *358*, 205-213.
(30) Bajpai, S. K.; Tankhiwale, R. *Reactive and Functional Polymers* **2006**, *66*, 1565-1574.
(31) Huang, X.; Xiao, Y.; Lang, M. *Carbohydrate Polymers* **2012**, *87*, 790-798.
(32) http://xdb.lbl.gov/Section1/Table_1-3.pdf.
(33) Maneerung, T.; Tokura, S.; Rujiravanit, R. *Carbohydrate Polymers* **2008**, *72*, 43-51.
(34) Chaudhry, Z.; Sammet, S.; Coffey, R.; Crockett, A.; Yuh, W. T. C.; Miller, S. *Burns* **2009**, *35*, 1080-1085.
(35) Singh, G.; Patankar, R. B.; Gupta, V. K. *Polymer-Plastics Technology and Engineering* **2010**, *49*, 1329-1333.
(36) MacCuspie, R. I. *Journal of Nanoparticle Research* **2011**, *13*, 2893-2908.
(37) Percival, S. L.; Slone, W.; Linton, S.; Okel, T.; Corum, L.; Thomas, J. G. *International Wound Journal* **2011**, *8*, 237-243.
(38) Sondi, I.; Salopek-Sondi, B. *Journal of Colloid and Interface Science* **2004**, *275*, 177-182.
(39) Lok, C. N.; Ho, C. M.; Chen, R.; He, Q. Y.; Yu, W. Y.; Sun, H.; Tam, P. K. H.; Chiu, J. F.; Che, C. M. *Journal of Biological Inorganic Chemistry* **2007**, *12*, 527-534.
(40) Mock, J. J.; Barbic, M.; Smith, D. R.; Schultz, D. A.; Schultz, S. *Journal of Chemical Physics* **2002**, *116*, 6755-6759.
(41) Zhang, H.; Chen, G. *Environmental Science & Technology* **2009**, *43*, 2905-2910.
(42) Kristiansen, K. A.; Schirmer, B. C.; Aachmann, F. L.; Skjak-Braek, G.; Draget, K. I.; Christensen, B. E. *Carbohydrate Polymers* **2009**, *77*, 725-735.
(43) De Kerchove, A. J.; Elimelech, M. *Macromolecules* **2006**, *39*, 6558-6564.
(44) Panfilov, A. V.; Markovich, Y. D.; Zhirov, A. A.; Ivashev, I. P.; Kirsanov, A. T.; Kondrat'ev, V. B. *PHARMACEUTICAL CHEMISTRY JOURNAL* **2000**, *34*, 34-35.
(45) Retnamma, R.; Novais, A. Q.; Rangel, C. M. *International Journal of Hydrogen Energy* **2011**, *36*, 9772-9790.
(46) Kojima, Y.; Suzuki, K.; Fukumoto, K.; Sasaki, M.; Yamamoto, T.; Kawai, Y.; Hayashi, H. *International Journal of Hydrogen Energy* **2002**, *27*, 1029-1034.
(47) Schmidt, M.; Schaumberg, J. Z.; Steen, C. M.; Boyer, M. P. *International journal of microbiology* **2010**, 930410-930465.
(48) De Seta, F.; Schmidt, M.; Vu, B.; Essmann, M.; Larsen, B. *Journal of Antimicrobial Chemotherapy* **2009**, *63*, 325-336.
(49) Houlsby, R. D.; Ghajar, M.; Chavez, G. O. *Antimicrobial Agents and Chemotherapy* **1986**, *29*, 803-806.

(50) Saha, N.; Saarai, A.; Roy, N.; Kitano, T.; Saha, P. *Journal of Biomaterials and Nanobiotechnology*, **2011**, *2*, 85-90.
(51) Bursali, E. A.; Coskun, S.; Kizil, M.; Yurdakoc, M. *Carbohydrate Polymers* **2011**, *83*, 1377-1383.
(52) Grace, M.; Chand, N.; Bajpai, S. K. *Journal of Engineered Fibers and Fabrics* **2009**, *4*, 24-35.
(53) Gangadharan, D.; Harshvardan, K.; Gnanasekar, G.; Dixit, D.; Popat, K. M.; Anand, P. S. *Water Research* **2010**, *44*, 5481-5487.
(54) Jiang, X. C.; Chen, C. Y.; Chen, W. M.; Yu, A. B. *Langmuir* **2010**, *26*, 4400-4408.
(55) Yeh, C. H.; Zhao, Q. L.; Lee, S. J.; Lin, Y. C. *Sensors and Actuators a-Physical* **2009**, *151*, 231-236.
(56) Sarker, D. K.; Wilde, P. J. *Colloids and Surfaces B-Biointerfaces* **1999**, *15*, 203-213.
(57) Gray, C. J.; Griffiths, A. J.; Stevenson, D. L.; Kennedy, J. F. *Carbohydrate Polymers* **1990**, *12*, 419-430.
(58) Sinquin, A.; Hubert, P.; Marchal, P.; Choplin, L.; Dellacherie, E. *Colloids and Surfaces a-Physicochemical and Engineering Aspects* **1996**, *112*, 193-200.
(59) Callewaert, M.; Laurent-Maquin, D.; Edwards-Levy, F. *International Journal of Pharmaceutics* **2007**, *344*, 161-164.
(60) Edwards-Levy, F.; Levy, M. C. *Biomaterials* **1999**, *20*, 2069-2084.
(61) Li, C. R.; Lu, N. P.; Mei, J.; Dong, W. J.; Zheng, Y. Y.; Gao, L.; Tsukamoto, K.; Cao, Z. X. *Journal of Crystal Growth* **2011**, *314*, 324-330.
(62) Kim, Y. S.; Kim, H. W.; Lee, S. H.; Shin, K. S.; Hur, H. W.; Rhee, Y. H. *International Journal of Biological Macromolecules* **2007**, *41*, 36-41.
(63) Kim, H. W.; Kim, B. R.; Rhee, Y. H. *Carbohydrate Polymers* **2010**, *79*, 1057-1062.
(64) Krysinski, J.; Placzek, J.; Skrzypczak, A.; Blaszczak, J.; Predki, B. *Qsar & Combinatorial Science* **2009**, *28*, 995-1002.
(65) O'Carroll, C. Ph.D, National University of Ireland Maynooth, **2012**.
(66) Le Tien, C.; Lacroix, M.; Ispas-Szabo, P.; Mateescu, M. A. *Journal of Controlled Release* **2003**, *93*, 1-13.
(67) Han, L.; Wang, P.; Zhu, C.; Zhai, Y.; Dong, S. *Nanoscale* **2011**, *3*, 2931-2935.

Chapter 5:

Anti–Bacterial Activity of Silver Impregnated Alginate Beads

5.1 Introduction

Bacteria are simple unicellular organisms which lack a membrane-bound nucleus and because of this, bacteria are termed as prokaryotes.[1] The major component of the bacterial genome is a double stranded circular DNA molecule. All prokaryotes possess a cell wall which maintains the shape of the cell,[2] and prevents the cell from bursting if it comes in contact with a hypotonic medium. Bacteria can come in a variety of shapes. The three most common being round (cocci), rod shaped (bacilli) or spiral (spirilla).[1] Despite their simplicity, bacteria have an enormous range of metabolic capacities, and can be found in some of the most extreme environments on earth.

Bacteria can be divided into two main classes which are based on differences in the structure of their cell wall. These are Gram-positive bacteria which have a cell wall which contains a thick layer of peptidoglycan and Gram-negative bacteria which have a cell wall which contains a thin layer of peptidoglycan. Peptidoglycan is a biopolymer made up of a carbohydrate backbone which is crosslinked with oligopeptides.[2] Its presence gives significant structural strength to the bacteria cell wall.[2,3] Figure 5.1 shows in detail the difference in the cell wall of both Gram-positive and Gram-negative bacteria. Both Gram-positive and Gram-negative bacteria are encased in a cell membrane which can contain membrane proteins. Outside of this membrane lies the periplasm space which contains enzymes and outside of this is the cell wall. For Gram-positive bacteria the cell wall can contain up to forty layers of peptidoglycan making these bacteria structurally very strong. These layers are highly hydrophobic and thus prevent hydrophilic compounds from entering the cell, whereas, lipophilic compounds can diffuse through this layer quite readily. The cell wall of Gram-positive bacteria also contains other polymeric compounds such as teichoic and teichuronic acids.[4] It is these polymers which can act as antigens when the bacteria infect another organism. For Gram-negative bacteria the cell wall only contains one or two layers of peptidoglycan making these cells structurally much weaker than Gram-positive cells. Outside of the peptidoglycan layers of the Gram-negative cell wall lies an outer membrane. This membrane contains channels (porins) and membrane proteins which allow hydrophilic species to pass through the cell wall. The outside of this membrane is

coated with lipopolysaccharides; these hydrophilic groups prevent lipophilic compounds from entering the cell wall. In addition they can act as antigens and endotoxins, which are toxins which are released upon destruction of the cell wall. It is this outer membrane, which generally makes Gram-negative bacteria more toxic and more resistant to the immune system and treatment than Gram-positive species. Many antibiotics are lypophilic and therefore will pass across the cell wall of Gram-positive bacteria more easily than that of Gram-negative bacteria. In addition, a large number of antibiotics act on bacteria by inhibiting the synthesis of the crosslinks in peptidoglycan preventing the formation of a fully functionally bacterial cell wall and thus are more effective against Gram-positive bacteria.

The emergence of multi-drug resistant bacterial strains which can impact severely on public health is causing great concern. Therefore the focus of current research is based on developing new cost effective antimicrobial agents, which are effective against a broad range of these multi-drug resistant bacteria. One area of this research is to develop antimicrobial polymers as they have shown promise as a means to enhance the chemical stability and efficacy of some existing antimicrobial agents.[5] In addition, if the agent is covalently linked to the solid support the risk of the antimicrobial agent being released into the water system is reduced. Of the metal based compounds, silver-based materials have proved the most promising as they exhibit a broad-spectrum activity and have been shown to be less likely to induce microbial resistance than antibiotics.[6,7] Moreover, silver impregnated polymer supports, like the biopolymer-metal combinations studied here, are attracting much attention because of their long-term biocidal activity, chemical stability, and their relative low cost.

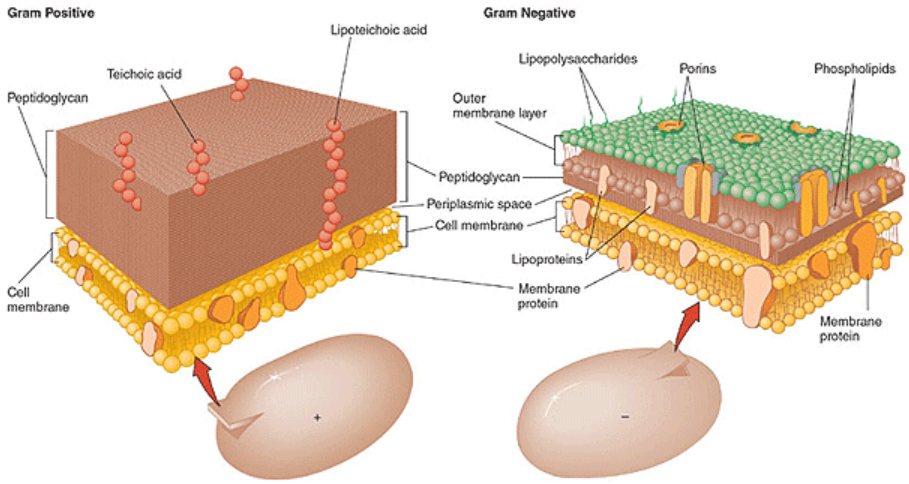

Figure 5.1: Outline of cell wall of a Gram-positive and Gram-negative Bacterium.[8]

The antibacterial effects of silver salts[7,9,10] and silver metal[11,12] are well known and silver is currently used to control bacterial growth in a variety of applications, including membrane bio fouling,[13-15] water purification,[3] dental work,[16] catheters,[10,17] and burn wounds[18,19]. One of the huge advantages of silver is that while it possesses anti-bacterial efficacy, which is comparable to or better than other heavy metals, silver has almost no reported known toxic effects on mammals,[20] including humans. Studies have shown that only the silver ions exhibit activity against bacteria, so that the biocidal effect of silver metal on bacteria must be based on its oxidation.[21,22] Silver ions work against bacteria in a number of ways. Firstly, silver ions can bind readily to the thiol group of membrane bound proteins causing them to become inactive. This interaction results in the leakage of intracellular substances. Secondly, one of the enzymes that silver ions interact with is important for bacterial respiration.[13,22] The interaction inhibits the action of these respiratory enzymes leading to the formation of reactive oxygen species, which are toxic to the bacteria cells. Either of these interactions of silver ions with bacterial enzymes or proteins will eventually result in cell death.[10] As well as having a microbiocidal effect silver(I) can also exert a bacteriostatic effect.[23] Silver ions can bind to bacterial RNA and DNA preventing them from replicating and inhibiting bacterial cell

growth.[24,25] When silver ions enter the bacteria cells they have the ability to bind to DNA molecules resulting in the DNA being forced into a structure which prevents replication.

Gram-negative bacteria are more sensitive to silver ions than Gram-positive bacteria.[26] Silver ions are hydrophilic, and therefore they have the ability to enter the periplasmic space through the outer membrane porins. Gram-positive bacteria lack these pores and have a thick peptidoglycan layer to prevent the entry of any hydrophilic molecules.

In this study we set out to investigate the potential of silver impregnated alginate beads as polymer systems which could be used in water disinfection systems. The anti-bacterial performances of three types of alginate beads, (a) sodium alginate beads, which were crosslinked with calcium ions, (b) composite propylene glycol alginate beads, (PGA-alginate), which were crosslinked with calcium ions and additionally covalently crosslinked with human serum albumin (HSA) and (c) composite alginate beads which were functionalised using 3-(trimethoxysilyl)-propyloctadecyldimethylammonium chloride and were crosslinked with calcium ions. All three materials were evaluated against five different strains of bacteria. The bacteria were as follows: (a) Gram-positive bacteria, *Staphyloccoccus aureus*, and methicillin resistant *Staphyloccoccus aureus* (MRSA), (b) Gram-negative bacteria, *Pseudonomas aeruginosa* (27853), *Pseudonomas aeruginosa* (10145) and *Escherichia coli* (*E.coli)*. Three types of biological assays were carried out on the bacteria, a plate assay using the beads, a well assay using the leachate from the beads, and a colony count assay using the beads. Ionic silver was first encapsulated into the different types of alginate beads, and then the silver ions were reduced to metallic silver.

5.2 Results and Discussion

The beads used in this Chapter are identical to those studied in Chapter 4 and are given identical codes which are outlined in Table 5.1. The physical properties of these beads such as silver content, swelling characteristics and surface morphology have previously been described in the appropriate Sections in Chapter 4. The experimental details of the biological assays are given in Chapter 2, Section 2.9.12.

Table 5.1: Summary of Bead Codes

Bead code	Description of Different Beads
Alg 1	2% w/v sodium alginate, crosslinked in 0.25 M $CaCl_2$ solution.
Alg 2	2% w/v sodium alginate, crosslinked in 0.25 M $CaCl_2$, immersed in 0.01 M $AgNO_3$ solution for 24 h.
Alg 3	2% w/v sodium alginate, crosslinked in 0.25 M $CaCl_2$, immersed in 0.10 M $AgNO_3$ solution for 24 h.
Alg 4	2% w/v sodium alginate, crosslinked in 0.25 M $CaCl_2$, immersed in 0.01 M $AgNO_3$ for 24 h, reacted with a 0.10 M $NaBH_4$ solution for 3 h.
Alg 5	2% w/v sodium alginate, crosslinked in 0.25 M $CaCl_2$, immersed in 0.10 M $AgNO_3$ for 24 h, reacted with a 0.10 M $NaBH_4$ solution for 3 h.
Alg 6	2% w/v sodium alginate, crosslinked in 0.25 M $CaCl_2$, immersed in 0.001 M $AgNO_3$ for 24 h, reacted with a 0.10 M $NaBH_4$ solution for 3 h.
PGA 1	1% w/v sodium alginate, 2% w/v PGA, 5% w/v HSA, crosslinked in 10% w/v $CaCl_2$, 0.025 M NaOH solution.
PGA 2	1% w/v sodium alginate, 2% w/v PGA, 5% w/v HSA, crosslinked in 10% w/v $CaCl_2$, 0.025 M NaOH solution, immersed in 0.01 M $AgNO_3$ solution for 24 h.
PGA 3	1% w/v sodium alginate, 2% w/v PGA, 5% w/v HSA, crosslinked in 10% w/v $CaCl_2$, 0.025 M NaOH solution, immersed in 0.1 M $AgNO_3$ solution for 24 h.

Bead code	Description of Different Beads
PGA 4	1% w/v sodium alginate, 2% w/v PGA, 5% w/v HSA, crosslinked in 10% w/v $CaCl_2$, 0.025 M NaOH solution, immersed in 0.01 M $AgNO_3$ for 24 h, reacted with a 0.10 M $NaBH_4$ solution for 3 h.
PGA 5	1% w/v sodium alginate, 2% w/v PGA, 5% w/v HSA, crosslinked in 10% w/v $CaCl_2$, 0.025 M NaOH solution, immersed in 0.1 M $AgNO_3$ for 24 h, reacted with a 0.10 M $NaBH_4$ solution for 3 h.
Alg 7	4% w/v sodium alginate, crosslinked in 5% w/v $CaCl_2$.
TSA 1	4% w/v sodium alginate, 0.02 M TSA, pH was adjusted to 4.0 with acetic acid at room temperature, crosslinked in 5% w/v $CaCl_2$.
TSA 2	4% w/v sodium alginate, 0.02 M TSA, pH was adjusted to 4.0 with acetic acid at room temperature, crosslinked in 5% w/v $CaCl_2$. Ion exchange was performed on the beads with 0.05 M nitric acid to remove the Cl^- ions. Immersed in 0.01 M $AgNO_3$ for 24 h.
TSA 3	4% w/v sodium alginate, 0.02 M TSA, pH was adjusted to 4.0 with acetic acid at room temperature, crosslinked in 5% w/v $CaCl_2$. Ion exchange was performed on the beads with 0.05 M nitric acid to remove the Cl^- ions. Immersed in 0.10 M $AgNO_3$ for 24 h.

5.2.2 Studies on *Staphylococcus aureus*

5.2.2.1 Introduction to *Staphylococcus aureus*

The name *Staphylococcus* is derived from the Greek word *staphyle* which means “a bunch of grapes”. This name arises from the fact that the colonies of this bacteria[27] grow in a clusters of yellow–white spheres which resemble a bunch of grapes (Figure 5.2). This Gram-positive species is non-motile and non-spore forming. It is a facultative anaerobic bacterium which means that it can undergo respiration in the presence of air and change to fermentation in its absence.

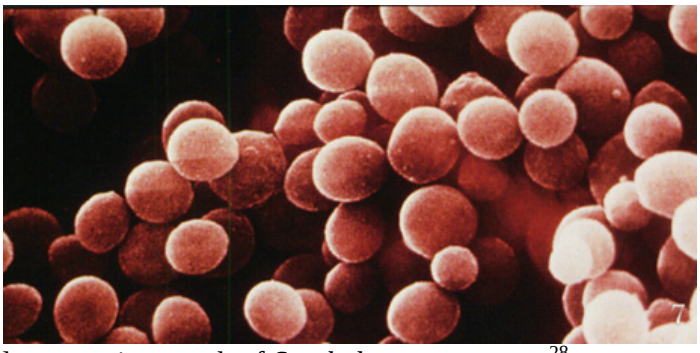

Figure 5.2: Electron micrograph of *Staphylococcus aureus*[28]

Many different strains of *Staphylococci* bacteria can infect humans, and in the region of 20% of healthy adults would be expected to be persistent carriers of this bacterium, most commonly in the nose or on the skin.[29] *Staphylococci* are spread by contact with a surface which is carrying the bacteria. Most of the time *Staphylococci* infection will not result in disease, but if the skin is damaged the bacteria can break through the protective mechanisms of the body, resulting in infection. *Staphylococcus aureus (S. aureus)* is the most common strain of *Staphylococci* bacteria. *S. aureus* can infect a wide range of tissues and can cause diseases in humans ranging from insignificant skin infections to serious infections. Examples of serious diseases which are caused by *S. aureus* infections are bacteremia, endocarditis and pneumonia[30,31] and it is a significant cause of blood infections in people requiring haemodialysis.[32] As *S. aureus* has a number of mechanisms to resist attack by the immune system these infections can be difficult to overcome.[33] *S. aureus* is currently the most common cause of infection in patients in hospital.[34] Another common illness associated with *S. aureus* infection is food poisoning, which occurs by ingesting food which has been contaminated with toxins produced by *S. aureus.*[35] Not only can *S. aureus* infections be serious in terms of the public health they also can have a negative economic impact. One study in the US (over the years 1996-2001) determined that the average cost of treatment of each haemodialysis-dependent patient admitted to hospital with a *S. aureus* blood stream infection was approximately $24,000.[32]

5.2.2.2 Plate Assay on *S. aureus*

For each plate assay experiment, 10 beads were placed on the agar plate as outlined in detail in Chapter 2, Section 2.9.12. The results for the different beads are summarised in Figure 5.3 and Table 5.2. The control Alg 1 and PGA 1 beads showed no sign of inhibition against *S. aureus*. In both cases the bacteria grew under and around the beads with no visible sign of inhibition. All the calcium alginate and PGA beads which contained the silver(I) ion showed similar zones of inhibition in the range of 19-30 mm^2. This finding is consistent with previous studies in which an increase in the size of the zone of inhibition towards the growth of *S. aureus* was observed upon addition of silver ions to an organic or inorganic polymer.[36,37] However, it is surprising that there was not a larger difference in the sizes of the zones of inhibition of the Alg 2 and PGA 2 beads compared to their Alg 3 and PGA 3 analogues, as was outlined in Chapter 4, the latter contained a substantially higher amount of silver(I) ions. One study on a chitosan-nylon membrane recorded a similar finding, in that the zone of inhibition of growth of *S. aureus* increased from 11 to 15 mm in diameter upon immersing the membrane in 0.2 and 0.5 mM solutions of $AgNO_3$.[36] However, upon repeating the experiment with increased concentrations of $AgNO_3$ up to 1.5 mM no further increase in the size of the zone of inhibition was observed. It may be that in order to observe the influence of the amount of silver(I) ions in the beads on the plate assay that we would need to study beads which contained an even lower amount of silver than the amount contained in the beads used in the present study. For the beads that contained silver in the zero oxidation state (Alg 4, Alg 5, PGA 4 and PGA 5) there was only direct inhibition of the growth of *S. aureus* under the beads. This indicates that the silver in the zero oxidation state was not having as much effect as silver in the +1 oxidation state on inhibiting the growth of *S. aureus* in this assay. Previous studies have shown that when silver nanoparticles are trapped in biopolymer matrices that clear zones of inhibition towards the growth of *S. aureus* were formed around the polymer.[38,39] However, the average nanoparticle size in the first of these studies was determined to be about 6 nm and to be 100 nm in the second, suggesting that little of the silver(0) particles trapped in the beads studied here had diameters of less than 100 nm. The presence of a zone of inhibition around the TSA 1 beads shows that this polymer support did have the ability to inhibit the growth of *S. aureus.* However, when the TSA beads

were impregnated with silver(I) ions the zone of inhibition increased in size, giving the biggest zone of inhibition determined in this assay. Again the zone of inhibition for the TSA 3 beads was not significantly different to that of the TSA 2 beads even though they contained substantially more silver.

Table 5.2: Results for the Plate Assay on *S. aureus* using a Range of Bead Types

Bead Code	**Silver Content in 30 Beads (mg)**	**Total Area (mm^2)**	**Zone of Inhibition* (mm^2)**	**Description**
Alg 1	0	-	0	No zone of inhibition
Alg 2	8 ± 0.5	97 ± 4	19 ± 7	Zone of inhibition
Alg 3	110 ± 8.7	104 ± 8	21 ± 8	Zone of inhibition
Alg 4	3 ± 0.5	-	0	Direct inhibition
Alg 5	116 ± 15.9	-	0	Direct inhibition
PGA 1	0	-	0	No zone of inhibition
PGA 2	7.3 ± 0.3	104 ± 6	19 ± 6	Zone of inhibition
PGA 3	167 ± 22.0	111 ± 4	28 ± 6	Zone of inhibition
PGA 4	6 ± 0.3	-	0	Direct inhibition
PGA 5	176 ± 23.9	-	0	Direct inhibition
Alg 7	0	-	0	No zone of inhibition
TSA 1	1 ± 0.05	87 ± 5	18 ± 5	Zone of inhibition
TSA 2	28 ± 4.45	112 ± 17	59 ± 20	Zone of inhibition
TSA 3	129 ± 6.5	138 ± 8	76 ± 10	Zone of inhibition

*ZOIs were recorded after 24 h using ten beads on each plate and plates were held at 37 ± 1°C

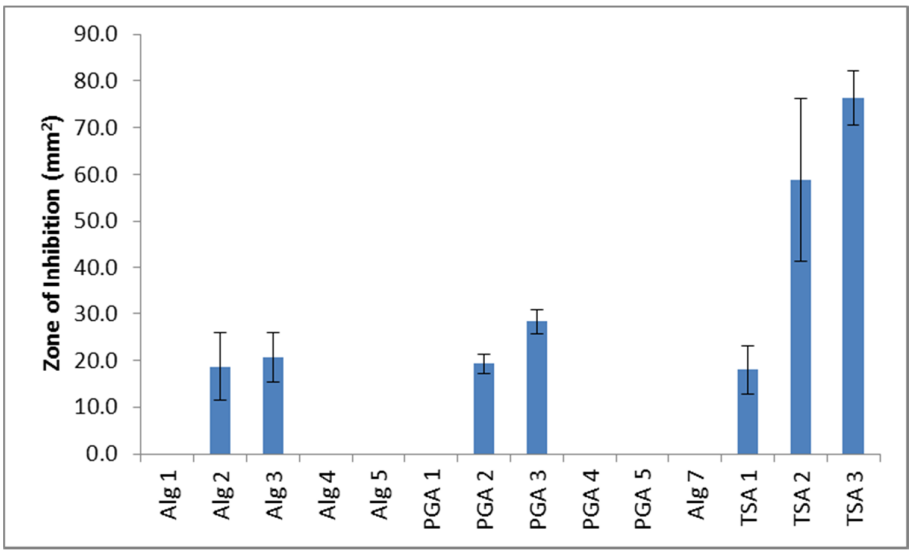

Figure 5.3: Zones of inhibition for the growth of *S. aureus* measured using a plate assay. ZOIs were recorded after 24 h using 10 beads on each plate and plates were held at 37 ± 1°C. Each bead type used is defined in the figure.

5.2.2.3 Well Assay on *S. aureus*

For each set of beads, silver was leached from 30 beads into 10 ml of deionised water held at 30 ± 1°C over a period of 24 h. In each case a sample of the solution was then poured into a well, with a diameter of 3 mm, which was bored into the agar plates. The culture of *S. aureus* was spread on the plates which were held at 37 ± 1°C for 24 h, at which time the zone of inhibition was measured. A summary of the results of the well assay experiment for the three types of beads are given in Table 5.3 and Figure 5.4. As can been seen from Table 5.3 the leachate from all of the control beads resulted in no zone of inhibition in this assay, indicating that the polymer supports themselves did not leach any species which was active against the growth of *S. aureus.* All the beads which contained silver in the zero oxidation state (Alg 4, Alg 5, PGA 4, and PGA 5) did not produce a zone of inhibition in this assay. These beads do release a certain amount of silver, which was determined by AA, and is shown in the Table 5.3. We would propose that this lack of activity occurs because the sizes of the silver particles upon release, or due to aggregation in solution, are too big to have effective antimicrobial activity against the growth of *S. aureus.*[22,24,40] This would be consistent with the plate assay carried out on *S. aureus*,

(Section 5.2.2.2) in which the silver(0) containing beads only showed direct inhibition. The leachate for the beads containing the silver(I) (Alg 2, Alg 3, PGA 2, PGA 3, TSA 2, and TSA 3) all showed activity against the growth of *S. aureus*.

Table 5.3: Results for the Well Assay on *S. aureus* using a Range of Bead Types

Bead Code	**Mass of Silver Leached from 30 Beads[a] (mg)**	**Zone of Inhibition (mm^2)[b]**	**Description**
Alg 1	0	0	No zone of inhibition
Alg 2	0.04 ± 0.001	29 ± 5	Zone of inhibition
Alg 3	2.24 ± 0.002	59 ± 4	Zone of inhibition
Alg 4	0.01 ± 0.004	0	No zone of inhibition
Alg 5	2.12 ± 0.03	0	No zone of inhibition
PGA 1	0	0	No zone of inhibition
PGA 2	0.03 ± 0.005	12 ± 3	Zone of inhibition
PGA 3	3.86 ± 0.024	15 ± 3	Zone of inhibition
PGA 4	0.10 ± 0.011	0	No zone of inhibition
PGA 5	2.50 ± 0.024	0	No zone of inhibition
Alg 7	0	0	No zone of inhibition
TSA 1	0.03 ± 0.009	0	No zone of inhibition
TSA 2	1.58 ± 0.005	6 ± 1	Zone of inhibition
TSA 3	2.91± 0.002	22 ± 1	Zone of inhibition

[a]The leachate was extracted from 30 beads into 10 ml of deionised water held at 30 ± 1°C for 24 h.

[b]ZOIs were recorded after 24 h and plates were held at 37 ± 1°C.

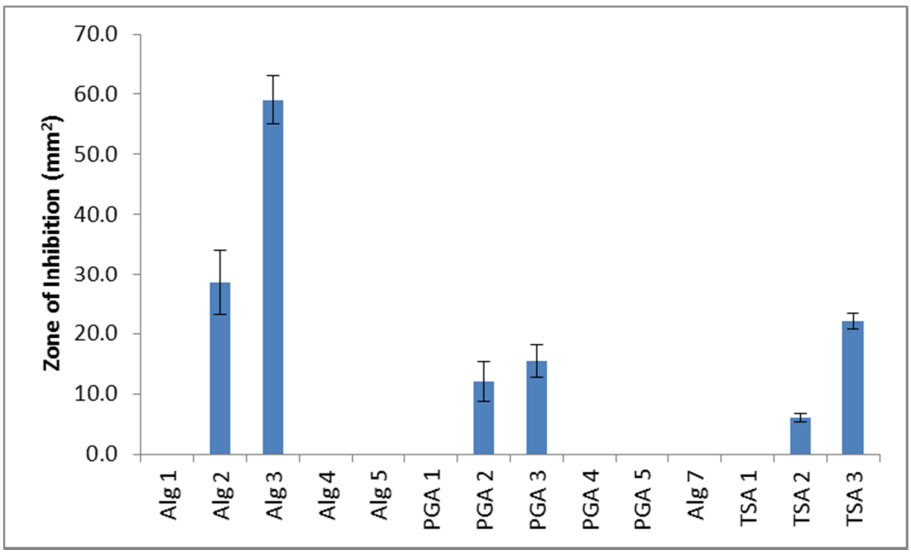

Figure 5.4: Zones of inhibition for the growth of *S. aureus* from well assays using leachate from 30 beads held in 10 ml of deionised water at 30 ± 1°C for 24 h. ZOI were recorded after 24 h and plates were held at 37 ± 1°C. Each bead type used is defined in the figure.

5.2.2.4 Colony Count Assay on *S. aureus*

For each colony count experiment, 100 beads were shaken with 10 ml of a culture containing *S. aureus* for 24 h held at 37 ± 1°C. At different periods of time the cells were then sampled and cultured on agar plates held at 37 ± 1°C. The colony count on the plate was carried out after 24 h. This study was carried out on the following beads Alg 1, Alg 3, Alg 5, PGA 1, PGA 3, PGA 5, Alg 7, TSA 1, TSA 2 and TSA 3. These bead types were selected as it was thought that they would give a good representation of the overall trends displayed by the beads. There were two possible types of action of bactericidal activity in this assay: (i) contact-kill, as these beads are hydrogels there was a constant flow of media throughout the beads, and bacteria which were passing through the pores would be killed by the presence of silver within the beads and (ii) the diffusion of silver out of the beads into the cell culture could kill the bacteria in the bulk solution.[41]

Figure 5.5(a) shows the results for the colony count assay using the calcium alginate beads. The first trend that can be clearly observed is that there was an initial reduction in the growth of the bacteria once the beads were added to the cell culture

solutions. All three samples had the same number of colonies of bacteria growing at 0 h, once the beads were added there was a reduction in the number of colonies for each of the three samples. However, there was a greater reduction in the number of colonies in the media in contact with either the Alg 3 or the Alg 5 beads compared to that in contact with the control Alg 1 beads. In addition at the 4 h time period the number of *S. aureus* colonies which were in contact with the Alg 1 beads had started to increase and continued to grow till the last time measurement was taken at 24 h. This was not the case for the cultures in contact with the Alg 3 and Alg 5 beads. This would indicate that the silver in the Alg 3 and Alg 5 beads was having a biocidal effect on *S. aureus.* For the Alg 3 beads, after 4 h the number of colonies continued to decrease until the 6 h time point was reached. When the numbers of colonies were counted at 24 h a dramatic increase in the cell growth was observed, showing that the silver present in the beads had inhibited the growth but did not completely kill the bacteria present in the media. A similar trend was observed for the Alg 5 beads, after 4 h there was a gradual decrease in the number of colonies growing. These beads did not result in a substantial decrease in the number of colonies as the Alg 3 beads. Similarly to the study using the Alg 3 beads at the 24 h time point the number of colonies had started to increase. The Alg 3 and Alg 5 beads have the ability to reduce the number of viable *S. aureus* cells growing in the media for 6 h and after this time the bacteria started to grow successfully again. This shows that the silver in the beads was not completely eradicating the bacteria. Moreover, the calcium alginate beads were not stable in the medium used for the colony count assay and the beads increased in size substantially during the assay and had completely disintegrated at 6 h.

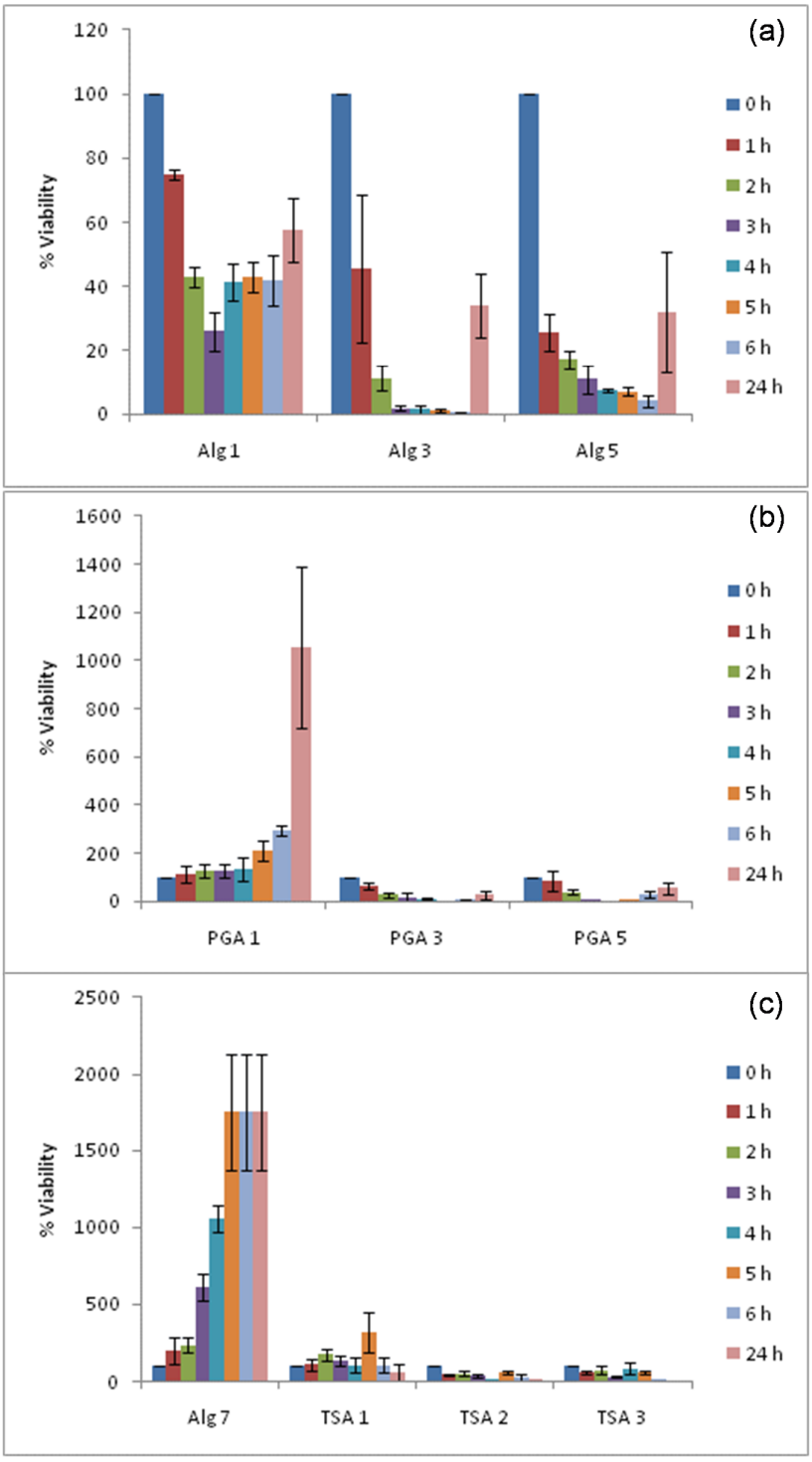

Figure 5.5: The % viability of *S. aureus* cells present in nutrient broth media upon shaking with (a) calcium alginate beads (b) PGA beads and (c) TSA beads as a function of time. The tests were done using 100 beads in 10 ml of nutrient broth

held at a constant temperature of 37 ± 1°C. Each bead type used is defined in the figure.

The colony count assay on *S. aureus* was then performed using the PGA beads (PGA 1, PGA 3 and PGA 5), which are analogues to the calcium alginate beads discussed above. The results are plotted in Figure 5.5(b). Initially (t = 0 h) the number of colonies for the three sets of beads were the same within experimental error and were still similar when they were counted after 1 h of contact with each of the three types of beads. The colonies in contact with the PGA 1 beads started to increase slightly from 0 h to 1 h, whereas the numbers of colonies in the media in contact with the PGA 3 and PGA 5 beads had started to decrease slightly after 1 h. After 2 h the numbers of colonies in the cell culture in contact with the PGA 1 beads were still increasing slowly, while those in contact with the PGA 3 or PGA 5 beads were decreasing slowly. The number of colonies for the culture surrounding the PGA 1 beads increased more rapidly during the 6 h to 24 h time. During this time period the bacteria had reached their exponential growth phase. For the medium in contact with the PGA 3 or PGA 5 beads the number of colonies continued to decrease over the 3 h to 5 h time period. At the 6 h time period the number of colonies started to grow slowly again for both sets of beads. After 24 h the number of colonies was increasing slowly, but in comparison to the results obtained using the control PGA 1 beads, the PGA 3 and PGA 5 beads were exhibiting a significant bactericidal effect on *S. aureus*. Moreover, although the PGA beads became swollen in the cell culture medium during the 24 h time period, they remained intact.

The colony count assay was then carried out on *S. aureus* using the TSA and control alginate beads (TSA 1, TSA 2, TSA 3 and Alg 7) and the results are given in Figure 5.5(c). At the initial reading (t = 0 h) the number of viable cells growing in the medium in contact with the four types of beads was similar within experimental error. However, in the time period from 1 h to 5 h the number of viable cells in contact with the Alg 7 beads increased dramatically. This was in sharp contrast to the findings for the cell culture in contact with the TSA 1 beads, which did not contain silver. For these samples, the number of viable cells in the media remained low only increasing very slightly by the 5 h time period. This indicates that in

contrast to the other two polymer supports the TSA polymer did exhibit antibacterial activity against *S. aureus.* This finding is consistent with the results obtained for the plate assay on *S. aureus* (Section 5.2.2.2) in which a clear zone of inhibition was observed around the TSA 1 beads. The TSA 2 and TSA 3 beads performed slightly better than the TSA 1 beads over this time period. As the TSA 1 bead support was quite active against the growth of *S. aureus*, this would indicate that the silver was only having a small contributing effect. In the time period, from 5 h to 24 h the number of viable cells in the media in contact with the Alg 7 beads remained constant, indicating that the cell growth had passed through its exponential stage and that growth was limited by the amount of nutrients present in the media and not the beads.

In summary the results show that for all the beads which were active against the growth of *S. aureus* in this study only the bactericidal effect of the TSA 3 beads was sufficient to completely kill all the cells after 24 h. However, statistical analysis of the difference in the activity of all the silver containing beads compared to the control beads (Table 5.4) show that the silver containing beads did have a bactericidal effect on *S. aureus.*

Table 5.4: p-values for the Difference in the Bactericidal Activity against *S. aureus* of the Beads Studied compared to that of the Appropriate Control Beads

Control bead vs. Bead	**p-value**	**p-value summary**	**Bactericidal activity of bead is statistically significantly different compared to that of appropriate control bead**
Alg 1 vs. Alg 3	p < 0.0001	***	Yes
Alg 1 vs. Alg 5	p < 0.0001	***	Yes
PGA 1 vs. PGA 3	p < 0.0001	***	Yes
PGA 1 vs. PGA 5	p < 0.0001	***	Yes
Alg 7 vs. TSA 1	p < 0 .0001	***	Yes
Alg 7 vs. TSA 2	p < 0.0001	***	Yes
Alg 7 vs. TSA 3	p < 0.0001	***	Yes

Interestingly, the TSA 1 beads which contained no silver were nearly as active as the TSA 2 and TSA 3 beads. This would indicate that the contact kill mechanism was a substantial contributor to the bactericidal activity of the beads as the quaternary ammonium group is covalently attached to the alginate and so would remain attached to the bead during this assay. Moreover, at the 24 h time period the TSA 2 and TSA 3 beads were more active against the *S. aureus* than the Alg 3 which had completely disintegrated during the course of the assay releasing all their silver. The similar bactericidal effect of the Alg 3 compared to Alg 5 and PGA 3 compared to PGA 5 indicates that the oxidation state of the silver was not a significant factor in the activity of these beads against *S. aureus.*

5.2.3 Studies on methicillin resistant *Staphylococcus aureus* (MRSA)

5.2.3.1 Introduction to methicillin resistant *Staphyloccoccus aureus* (MRSA)

MRSA, like *S. aureus,* is a facultative anaerobic Gram-positive coccal bacterium that grows in a pattern resembling a cluster of grapes (Figure.5.6(a)). MRSA is any strain of *S. aureus* that has developed resistance to β-lactam antibiotics.[42,43] β-lactam antibiotics act by causing the transpeptidases enzymes which are important in bacteria cell-wall formation to become inactive. MRSA contains a gene, mecA,[44,45] which stops β-lactam antibiotics deactivating these enzymes.[46] The development of this resistance means that an MRSA infection is more difficult to treat with standard types of antibiotics than normal strains of *S. aureus.*

MRSA is especially dangerous when it occurs in hospitals or nursing homes, where people may have open wounds, be undergoing invasive treatments, and/or have weakened immune systems.[47] *S. aureus* infections, including MRSA, generally start as a red rash (Figure 5.6(b)) which can turn into abscesses that require surgical treatment. In addition to causing skin infection the bacteria can infect other parts of the body including bones, bloodstream and lungs.[48] Moreover, studies have shown that both the incidence of hospital associated and community associated MRSA is on the increase and it is now a global health concern.[49]

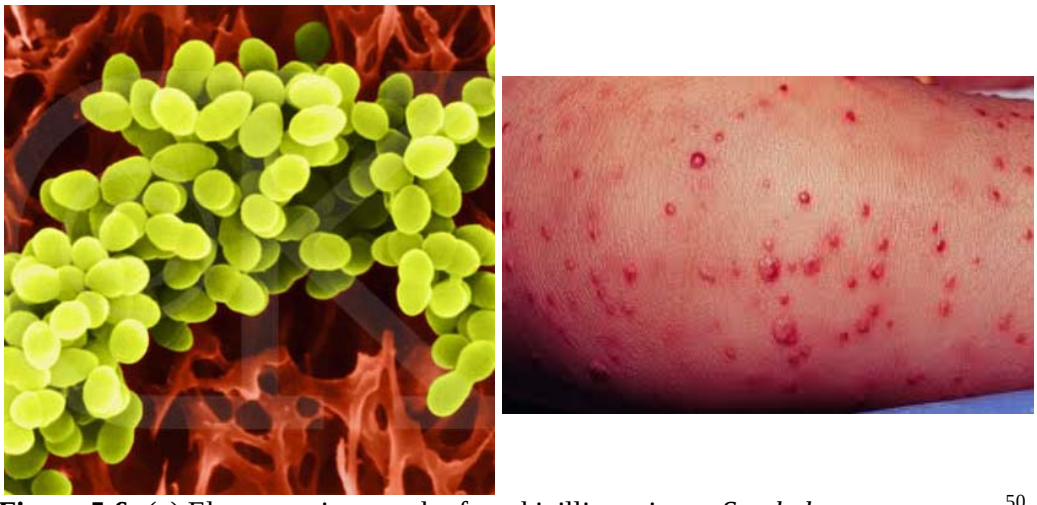

Figure 5.6: (a) Electron micrograph of methicillin resistant *Staphylococcus aureus.*[50] (b) Photograph of methicillin resistant *Staphylococcus aureus* infection.[51]

5.2.3.2 Plate Assay on MRSA

A summary of the observed zones of inhibition for the growth of MRSA using the calcium alginate based beads is given in Table 5.5 and is plotted in Figure 5.7. The control beads, Alg 1, PGA 1 and Alg 7, showed no activity in this assay showing that these polymer supports had no activity against the growth of MRSA. The results for the TSA 1 beads showed direct inhibition, indicating that when this polymer support was in direct contact with the bacteria no growth could occur. The results in the plate assay for the other strain of *S. aureus* (Table 5.2) showed a zone of inhibition for the growth of the bacteria. This finding would support literature reports that certain strains of MRSA are more resistant to the biocidal effect of quaternary ammonium compounds than normal strains of *S. aureus.*[52] Direct inhibition of the growth of MRSA was observed for each of the beads which contained silver in the zero oxidation state (Alg 4, Alg 5, PGA 4 and PGA 5). This effect is similar to that observed with these beads in the plate assay using the other strain of *Staphylococcus* (Table 5.2). Previous studies on the effect of silver alginate dressing against MRSA and a normal strain of *S. aureus* found that the normal strain was slightly more resistant to the silver in the dressing than the MRSA.[53] Zones of inhibition were only observed for the beads containing silver in the +1 oxidation state. In contrast to the plate assay carried out on the other strain of *Staphylococcus* (Table 5.2), the size of the zone of inhibition was dependent on the amount of

silver(I) contained within the beads. A larger zone of inhibition was observed for the bead type containing the higher amount of silver(I).

Table 5.5: Results for the Plate Assay on MRSA using a Range of Bead Types

Bead Code	**Silver Content in 30 Beads (mg)**	**Total area* (mm^2)**	**Zone of Inhibition* (mm^2)**	**Description**
Alg 1	0	-	0	No zone of inhibition
Alg 2	8 ± 0.5	73 ± 14	23 ± 14	Zone of inhibition
Alg 3	110 ± 8.7	188 ± 20	99 ± 20	Zone of inhibition
Alg 4	3 ± 0.5	-	0	Direct inhibition
Alg 5	116 ± 15.9	-	0	Direct inhibition
PGA 1	0	-	0	No zone of inhibition
PGA 2	7.3 ± 0.3	95 ± 1	16 ± 1	Zone of inhibition
PGA 3	167 ± 22.0	113 ± 4	31 ± 4	Zone of inhibition
PGA 4	6 ± 0.3	-	0	Direct inhibition
PGA 5	176 ± 23.9	-	0	Direct inhibition
Alg 7	0	-	0	No zone of inhibition
TSA 1	1 ± 0.05	-	0	Direct inhibition
TSA 2	28 ± 4.45	74 ± 4	13 ± 3	Zone of inhibition
TSA 3	129 ± 6.5	107 ± 14	46 ± 14	Zone of inhibition

*ZOIs were recorded after 24 h using ten beads on each plate and plates were held at 37 ± 1°C.

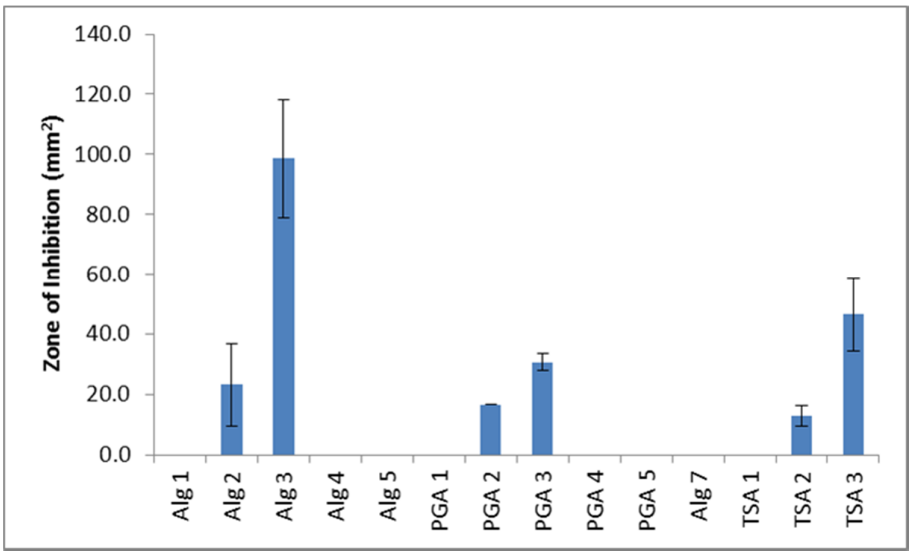

Figure 5.7: Zones of inhibition for the growth of MRSA measured using a plate assay. ZOIs were recorded after 24 h using 10 beads on each plate and plates were held at 37 ± 1°C. Bead type used is defined in the figure.

5.2.3.3 Well Assay on MRSA

Results for the well assay on MRSA are presented in Table 5.6 and Figure 5.8. The results for the leachates from the control beads (Alg 1, PGA 1, Alg 7 and TSA 1) against MRSA showed no inhibition. In addition, the leachate from the beads (Alg 4, Alg 5, PGA 4 and PGA 5) which contained silver in the zero oxidation state also showed no inhibitory effect on the growth of MRSA. Zones of inhibition were also not observed from the leachate for two of the sets of beads (PGA 2 and TSA 2 beads) containing the lower amount of silver(I) ions. Zones of inhibition were observed for the three sets of beads containing the higher amount of silver(I) ions (Alg 3, PGA 3 and TSA 3). The leachate from the Alg 2 beads also produced a zone of inhibition. It was observed for each of the three bead types, increasing the amount of silver(I) present in the bead resulted in an increased effect of their leachate. For example, the leachate from the Alg 2 beads gave zones of inhibition of 26 mm^2 around the wells, while that from the Alg 3 beads gave on average a zone of inhibition of 60 mm^2 (Figure 5.8). The higher the concentration of silver(I) ions leached from the beads the more effective they were at inhibiting the growth of the MRSA. From the well assay it can be concluded that the silver in the +1 oxidation

state is the most effective at inhibiting the growth of MRSA when it is leached out of the beads. In general, for the leachate which did result in a zone of inhibition, the sizes of the zones were similar to those observed for the analogous experiment carried out using the other strain of *Staphylococcus* (Table 5.3). This indicates that in solution the activity of silver ions against MRSA and the methicillin-sensitive strain of *S. aureus* were similar.

Table 5.6: Results for the Well Assay on MRSA using a Range of Bead Types

Bead Code	**Mass of Silver Leached from 30 Beads[a] (mg)**	**Zone of Inhibition[b] (mm^2)**	**Description**
Alg 1	0	0	No zone of inhibition
Alg 2	0.04 ± 0.001	26 ± 5	Zone of inhibition
Alg 3	2.24 ± 0.002	60 ± 3	Zone of inhibition
Alg 4	0.01 ± 0.004	0	No zone of inhibition
Alg 5	2.12 ± 0.03	0	No zone of inhibition
PGA 1	0	0	No zone of inhibition
PGA 2	0.03 ± 0.005	0	No zone of inhibition
PGA 3	3.86 ± 0.024	11 ± 1	Zone of inhibition
PGA 4	0.10 ± 0.011	0	No zone of inhibition
PGA 5	2.50 ± 0.024	0	No zone of inhibition
Alg 7	0	0	No zone of inhibition
TSA 1	0.03 ± 0.009	0	No zone of inhibition
TSA 2	1.58 ± 0.005	0	No zone of inhibition
TSA 3	2.91± 0.002	15 ± 1	Zone of inhibition

[a]The leachate was extracted from 30 beads into 10 ml of deionised water held at 30 ± 1°C for 24 h.

[b]ZOIs were recorded after 24 h and plates were held at 37 ± 1°C.

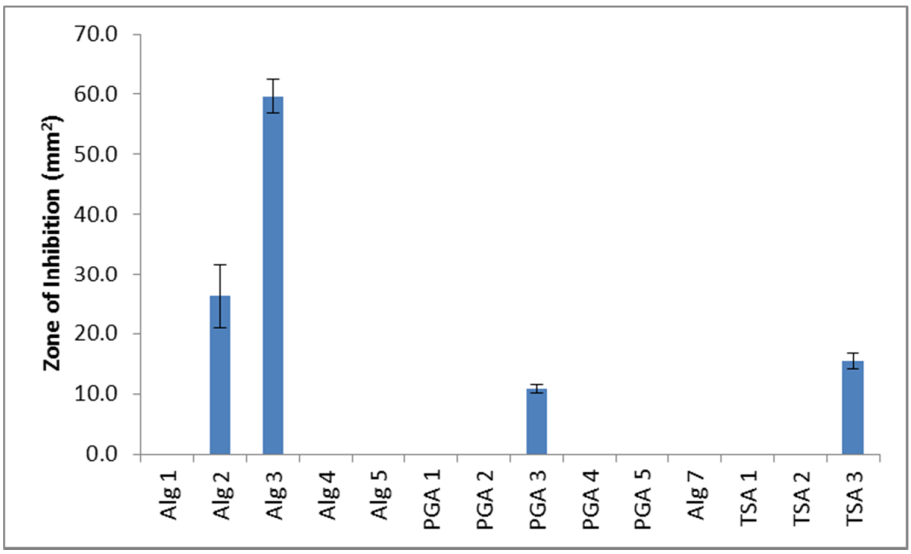

Figure 5.8: Zones of inhibition for the growth of MRSA from well assays using leachate from 30 beads held in 10 ml of deionised water at 30 ± 1°C for 24 h. ZOIs were recorded after 24 h and plates were held at 37 ± 1°C. Each bead type used is defined in the figure.

5.2.3.4 Colony Count Assay on MRSA

The results for the calcium alginate beads (Alg 1, Alg 3 and Alg 5) which were tested using this assay are given in Figure 5.9(a). The alginate beads were added after the colonies were counted (0 h, Figure 5.9(a)). For each of the cultures in contact with the three types of beads the number of colonies had decreased when a sample was taken after 1 h and again at 2 h. However, there was a greater reduction in the number of colonies observed for the culture in contact with the Alg 3 and Alg 5 beads than for the control Alg 1 beads. This proved that the silver in the Alg 3 and Alg 5 beads are having a bactericidal effect on the colonies in the solution. For the assay involving the Alg 1 beads the colony count stayed approximately constant between 2 h and 6 h, whereas for both the Alg 3 and Alg 5 bead assays a further reduction in the number of colonies was observed at this time period. After 24 h the number of cells in contact with the control Alg 1 beads had increased substantially. While, after 24 h the number of colonies of MRSA in the media in contact with both the Alg 3 and Alg 5 beads had also started to increase (Figure 5.9(a)). In both cases the number of colonies was not as high as for the control experiment but this shows that the bactericidal effect of the silver in the beads was starting to decrease. The

bactericidal effect of the Alg 1, Alg 2 and Alg 3 beads was very similar to that previously observed when carrying out the colony count assay on the other stain of *Staphyloccocus* (Figure 5.5(a)). However, it should be noted that these beads had disintegrated in the cell culture medium after 6 h.

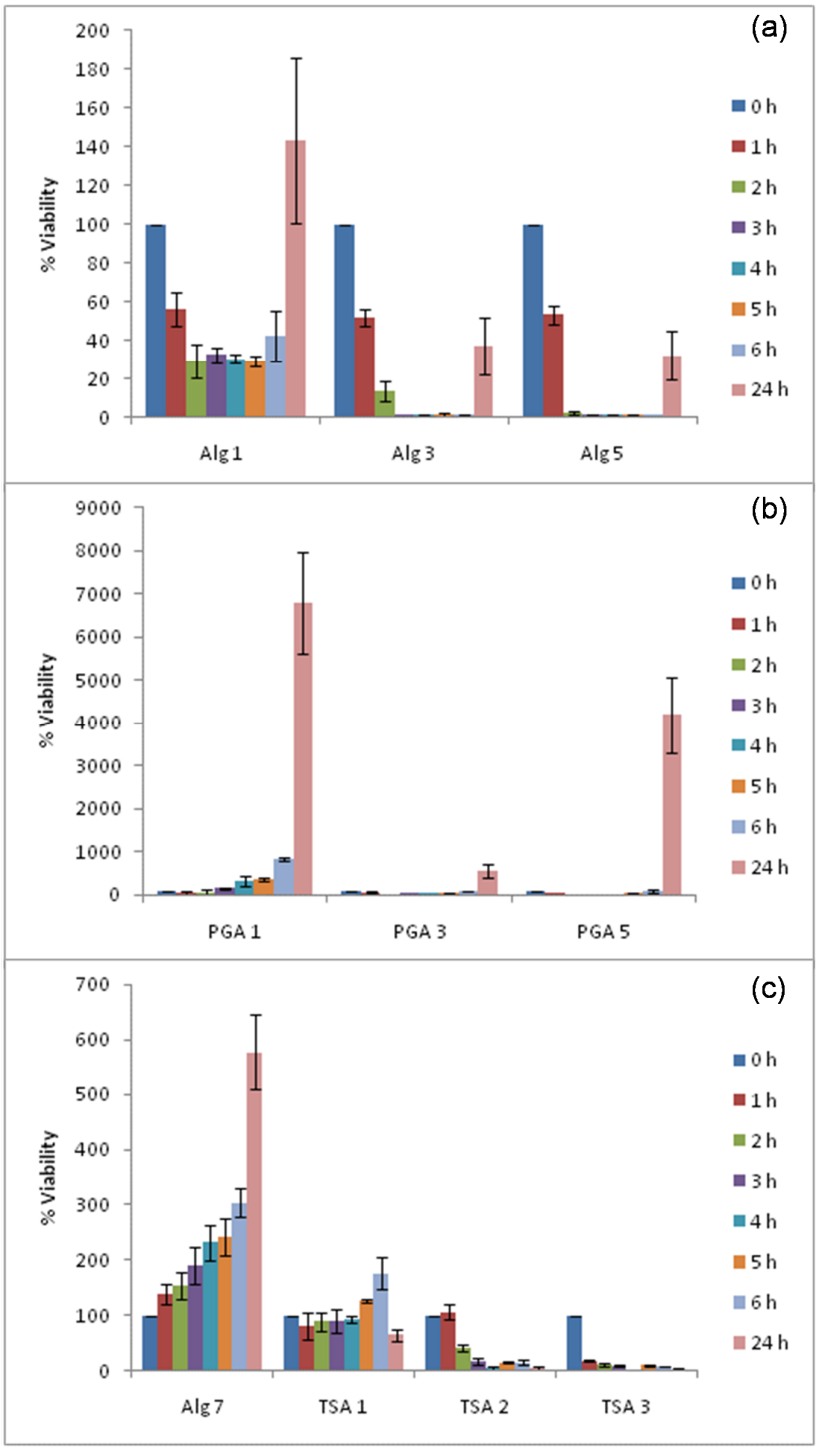

Figure 5.9: The % viability of MRSA cells present in nutrient broth media upon shaking with (a) calcium alginate beads (b) PGA beads and (c) TSA beads as a function of time. The tests were done using 100 beads in 10 ml of nutrient broth held at a constant temperature of 37 ± 1°C. Each bead type used is defined in the figure.

The study was then repeated using three types of PGA beads and the results are shown in Figure 5.9(b). Initially the numbers of colonies were the same for the three different sets of beads, PGA 1, PGA 3, and PGA 5, while in each case the number of colonies had decreased when samples were taken after 1 h. For the assays recorded after 2 h there was no cell growth observed for the media in contact with the PGA 3 and PGA 5 beads. Whereas, a colony count which was similar to that recorded at 1 h was determined for the media in contact with the control PGA 1 beads. After 3 h an increase in the colony count was recorded for the MRSA cells in contact with the PGA 1 beads and this increase continued over the 24 h of the experiment. The results show that the PGA 3 and the PGA 5 beads were having a bactericidal effect after 3 h. However, over an extended time period the number of colonies of MRSA which were in contact with either the PGA 3 or PGA 5 beads began to increase. The PGA 3 beads were still exhibiting a bactericidal effect on the MRSA cells after 24 h, as the number of colonies were less than that which was observed for the control assay. However, at 24 h the PGA 5 beads were having no effect on the growth of MRSA as the number of colonies recorded at this time period was the same within experimental error of that recorded for the control experiment. This is in stark contrast to the colony count assay performed on the other strain of *Staphylococcus* (Figure 5.5(b)) in which the PGA 5 beads were observed to have a reasonable bactericidal effect at the 24 h time period.

The most promising set of results were recorded for the colony count assay carried out using the TSA beads. The results for this assay are given in Figure 5.9(c). Two control beads were used in this assay the Alg 7 and TSA 1 beads both of which contained no silver. As can be observed from the plot given in Figure 5.9(c) the quaternary ammonium group present on the TSA 1 beads did appear to have some inhibitory effect on the growth of the MRSA. The number of colonies of MRSA which were in contact with the Alg 7 beads steadily increased over the 24 h time period. Whereas, for the experiment using the TSA 1 beads the number of colonies remained fairly constant over the first 4 h, and then there was a small increase during the 5 h to 6 h time period, followed by a drop at the 24 h time period. When these beads were tested against the other strain of *S. aureus* a more significant bactericidal effect was observed which is consistent with the literature reports that MRSA strains can be more resistant to the action of quaternary ammonium

compounds than normal *S. aureus* strains.[52] When the experiment was repeated for the TSA beads which contained silver(I) ions, (TSA 2 and TSA 3), it would appear that the silver(I) was having an additional effect. A very low colony count reading was recorded after 24 h for MRSA which was in contact with the both TSA 3 and TSA 2 beads. The latter contained the lower amount of silver.

A summary of the p-values for the activity of the different beads compared to control beads is given in Table 5.7. It can be seen that all the silver-containing beads and the TSA 1 have a significant increase in their bactericidal effect compared to the control beads. However, by considering all the data presented in Figure 5.9 it would appear that the best sets of beads with respect to killing MRSA in the colony count assay were the TSA 2 and TSA 3 beads. In fact, the TSA 2 beads were more active than the Alg 3 and PGA 3 beads which contained a substantially higher amount of silver. This indicates that in this assay both the silver and the quaternary ammonium groups in the TSA 2 and TSA 3 beads were exhibiting a bactericidal effect towards MRSA. In addition it is likely that the contact kill was having the more significant bactericidal effect on the MRSA, as the TSA beads which remained intact throughout the course of the assay were having a larger effect than the Alg 3 and Alg 5 beads which disintegrated releasing all the silver.

Table 5.7: p-values for the Difference in the Bactericidal Activity against MRSA of the Beads Studied compared to that of the Appropriate Control Beads

Control bead vs Bead	**p-value**	**p-value summary**	**Bactericidal activity of bead is statistically significantly different compared to that of appropriate control bead**
Alg 1 vs. Alg 3	$p < 0.0001$	***	Yes
Alg 1 vs. Alg 5	$p < 0.0001$	***	Yes
PGA 1 vs. PGA 3	$P < 0.0001$	***	Yes
PGA 1 vs. PGA 5	$p = 0.0035$	**	Yes
Alg 7 vs. TSA 1	$p < 0$ .0001	***	Yes
Alg 7 vs. TSA 2	$p < 0.0001$	***	Yes
Alg 7 vs. TSA 3	$p < 0.0001$	***	Yes

5.2.4 Studies on *Escherichia coli*

5.2.4.1 Introduction to *Escherichia coli*

Escherichia coli are a Gram-negative,[54] facultative anaerobic,[55] rod-shaped bacteria (Figure 5.10) that exist either singly or in pairs.[56,57] The cells are typically about 2.0 μm long and 0.5 μm in diameter. Depending on the environmental conditions *E. coli* can form thin hair-like structures, called flagella,[58] which allow the bacteria to move and to attach to human cells.

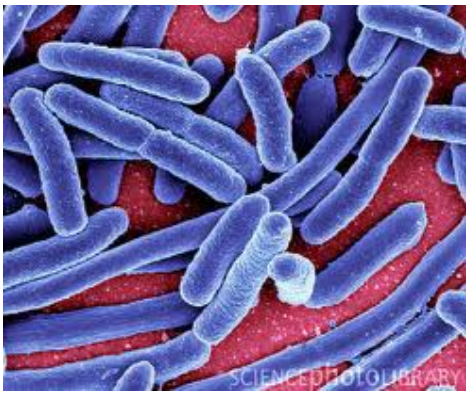

Figure 5.10: Electron micrograph of *Escherichia coli*.[59]

There are many strains of *E. coli* which are commonly found in the lower intestine of warm-blooded organisms.[7,55] Most *E. coli* strains are harmless,[60,61] and these strains are part of the normal flora of the lower intestine. Their presence can benefit the hosts by producing vitamin K2 and by preventing pathogenic bacteria from growing within the intestine. However, these non-pathogenic *E. coli* can result in disease if they move outside of the intestine,[7] for example, if they move into the urinary tract, they can result in bladder or kidney infections.[62] *E. coli* is a frequent cause of many common bacterial infections, such as cholecystitis,[63] bacteremia,[64] neonatal meningitis[65] and pneumonia.[66,67] Pathogenic *E. coli* strains (enterovirulent *E. coli* strains) which can be found in the intestine as a result of eating contaminated food can produce toxins,[61] which can result in symptoms such as diarrhea, [54,60] and intestinal inflammation.[60]

5.2.4.2 Plate Assay on *E. coli*

It was expected that the *E. coli* would be less tolerant of the presence of silver than the strains of *S. aureus* as studies have shown that Gram-negative bacteria are generally more susceptible to the effect of silver than Gram-positive bacteria.[26] However, as the results for the plate assays carried out on *E. coli* summarised in Table 5.8 and Figure 5.11 show, in general that the results are very similar to those recorded for the previously mentioned *Staphylococcus* bacteria. The control beads, Alg 1, PGA 1 and Alg 7, had no inhibitory effect on the growth of *E. coli*, while the TSA 1 control beads did show direct inhibition. It would be expected that the TSA 1 beads would be less active against *E. coli* than against *S. aureus* (Table 5.2), as it is known that generally Gram-negative bacteria are more resistant to quaternary ammonium groups.[68] The beads that contained silver in the zero oxidation state, (Alg 4, Alg 5, PGA 4 and PGA 5) all showed direct inhibition. Zones of inhibition against the growth of *E. coli* were only recorded for beads which contained silver in the +1 oxidation state. The largest zone of inhibition was recorded for the TSA 3 beads of 84 ± 13 mm^2. This indicates that there was a clear additive effect on the inhibition of the growth of *E. coli* upon the addition of silver(I) to the TSA beads. Overall the presence of silver in the polymer beads had a similar inhibitory effect on the growth of both *S. aureus* (Table 5.2) and *E. coli*. This is consistent with the study carried out by Ma *et al.* who found no difference in the bacteriostatic effect of silver(I) impregnated chitosan–nylon-6 blended membranes against these two bacteria.[36]

Table 5.8: Results for the Plate Assay on *E. coli* using a Range of Bead Types

Bead Code	**Silver Content in 30 Beads (mg)**	**Total area* (mm^2)**	**Zone of Inhibition* (mm^2)**	**Description**
Alg 1	0	-	0	No zone of inhibition
Alg 2	8 ± 0.5	134 ± 7	31 ± 7	Zone of inhibition
Alg 3	110 ± 8.7	107 ± 5	39 ± 5	Zone of inhibition
Alg 4	3 ± 0.5	-	0	Direct inhibition
Alg 5	116 ± 15.9	-	0	Direct inhibition
PGA 1	0	-	0	No zone of inhibition
PGA 2	7.3 ± 0.3	121 ± 3	21 ± 3	Zone of inhibition
PGA 3	167 ± 22.0	118 ± 6	23 ± 6	Zone of inhibition
PGA 4	6 ± 0.3	-	0	Direct inhibition
PGA 5	176 ± 23.9	-	0	Direct inhibition
Alg 7	0	-	0	No zone of inhibition
TSA 1	1 ± 0.05	64 ± 5	0	Direct inhibition
TSA 2	28 ± 4.45	87 ± 3	23 ± 3	Zone of inhibition
TSA 3	129 ± 6.5	146 ± 13	84 ± 13	Zone of inhibition

*ZOIs were recorded after 24 h using ten beads on each plate and plates were held at $37 \pm 1^{\circ}C$

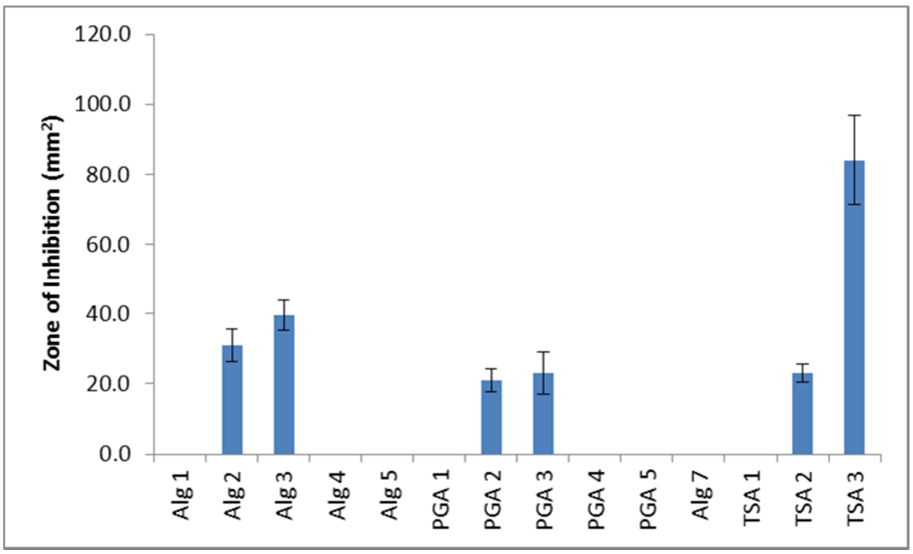

Figure 5.11: Zones of inhibition for the growth of *E. coli* measured using a plate assay. ZOIs were recorded after 24 h using 10 beads on each plate and plates were held at 37 ± 1°C. Bead type used is defined in the figure.

5.2.4.3 Well Assay on *E. coli*

Similar trends were observed in the well assays carried out on *E. coli* to those carried out in the preceding sections on the *Staphyloccoccus* bacteria. The results are summarised in Table 5.9 and Figure 5.12. Zones of inhibition were only observed for the leachate from the beads which contained silver in the +1 oxidation state. This clearly shows that even though the beads which contain the reduced silver did release silver into the leachate, it was not in a form which was active against *E. coli.*

Table 5.9: Results for the Well Assay on *E. coli* using a Range of Bead Types

Bead Code	Silver leached from 30 Beads[a] (mg)	Zone of Inhibition[b] (mm^2)	Description
Alg 1	0	0	No zone of inhibition
Alg 2	0.04 ± 0.001	33 ± 5	Zone of inhibition
Alg 3	2.24 ± 0.002	117 ± 17	Zone of inhibition
Alg 4	0.01 ± 0.004	0	No zone of inhibition
Alg 5	2.12 ± 0.03	0	No zone of inhibition
PGA 1	0	0	No zone of inhibition
PGA 2	0.03 ± 0.005	5 ± 2	Zone of inhibition
PGA 3	3.86 ± 0.024	19 ± 3	Zone of inhibition
PGA 4	0.10 ± 0.011	0	No zone of inhibition
PGA 5	2.50 ± 0.024	0	No zone of inhibition
Alg 7	0	0	No zone of inhibition
TSA 1	0.03 ± 0.009	0	No zone of inhibition
TSA 2	1.58 ± 0.005	9 ± 1	Zone of inhibition
TSA 3	2.91± 0.002	23 ± 3	Zone of inhibition

[a]The leachate was extracted from 30 beads into 10 ml of deionised water held at 30 ± 1°C for 24 h.

[b]ZOIs were recorded after 24 h and plates were held at 37 ± 1°C.

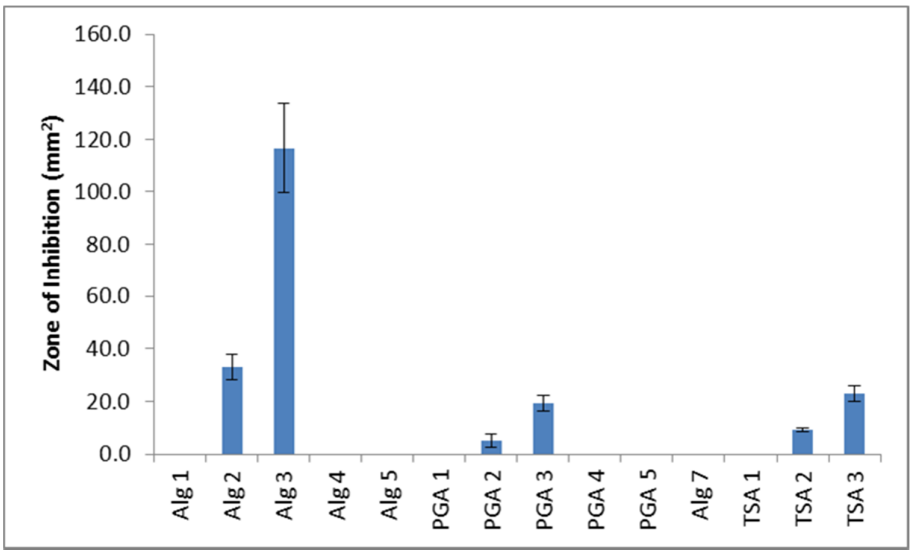

Figure 5.12: Zones of inhibition for the growth of *E. coli* from well assays using leachate from 30 beads held in 10 ml of deionised water at 30 ± 1°C for 24 h. ZOIs were recorded after 24 h and plates were held at 37 ± 1°C. Bead type used is defined in the figure.

5.2.4.4 Colony Count Assay for *E. coli*

A colony count assay on *E. coli* was carried out using the different bead types. The results of this assay using the calcium alginate beads are given in Figure 5.13(a). At the start of the experiment (0 h) the number of colonies in the medium in contact with each of the three types of beads was the same within experimental error. However, by the 3 h time period it was clear that the Alg 1 beads were having no bactericidal effect with a large increase in the number of viable colonies measured. Moreover, the number of *E. coli* colonies in the medium in contact with the Alg 1 beads continued to increase over the 24 h time period measured. Over the 1 h to 5 h time period it would appear that the Alg 3 and Alg 5 beads were having a similar but mild bactericidal effect on the *E. coli*. For both cases the number of viable cells was increasing but at a slower rate than for the control (Alg 1) experiment. However, for both Alg 3 and Alg 5 at the 6 h time mark the number of colonies had decreased significantly and remained low when the cultures were sampled after 24 h. This sharp decrease in the number of viable cells coincided with the time at which the calcium alginate beads burst in the medium releasing all their silver.

The results for the PGA beads given in Figure 5.13(b) correspond well with those previously observed for the colony count assay on the MRSA beads. For the cell culture in contact with the control PGA 1 beads there was a slow increase in the number of viable cells over the first 5 h, and then a faster increase in the 6 h to 24 h time period. In contrast for the PGA 3 and PGA 5 beads the colony count remained low over the first 5 h of the experiment. At the 6 h and 24 h time periods the number of viable cells for the media in contact with both set of beads had increased but a more significant increase was observed for that in contact with the PGA 5 beads. This indicates that the silver(0)-containing beads (PGA 5) had a lower bactericidal effect on *E. coli* than the silver(I)-containing beads (PGA 3).

A summary of the results for the colony count assay on *E. coli* using the TSA and control calcium alginate bead (Alg 7) are given in Figure 5.13(c). Again the results for this assay compare well with those carried out on the Gram-positive bacteria, MRSA, (Figure 5.9(c)). As expected the control Alg 7 beads exhibited no bactericidal effect on the *E. coli* and the number of viable cells increased rapidly and had passed through its exponential phase during the 6 h to 24 h time period. In comparison the TSA 1 beads, which did not contain silver, showed a mild bactericidal effect which is consistent with the known general higher resistance of Gram-negative bacteria towards quaternary ammonium groups.[68] The number of viable cells in the colony stayed low for the first 5 h of the experiment followed by a small increase in the number between the 5 h to 24 h time period. When silver(I) was added to the beads the bactericidal effect was enhanced. For the culture in contact with the TSA 2 beads the number of viable *E. coli* cells remained very low over the 24 h of the experiment. While for the TSA 3 beads the effect was even more pronounced with near complete eradication of *E. coli* when the culture was sampled after 24 h. As previously observed for MRSA the quaternary ammonium groups and the silver(I) ions had a significant additive bactericidal effect with the TSA 2 beads having a greater effect than the PGA 3 beads which contained more silver. This again indicates that the contact kill mechanism must be an important contribution to observed activity of the TSA beads.

The p-values for the statistical significance of the activity of different bead types in the colony count assay on *E. coli* compared to that of the control beads are

given in Table 5.10. The values show that all the silver containing beads and the TSA 1 beads were significantly more active than the control beads.

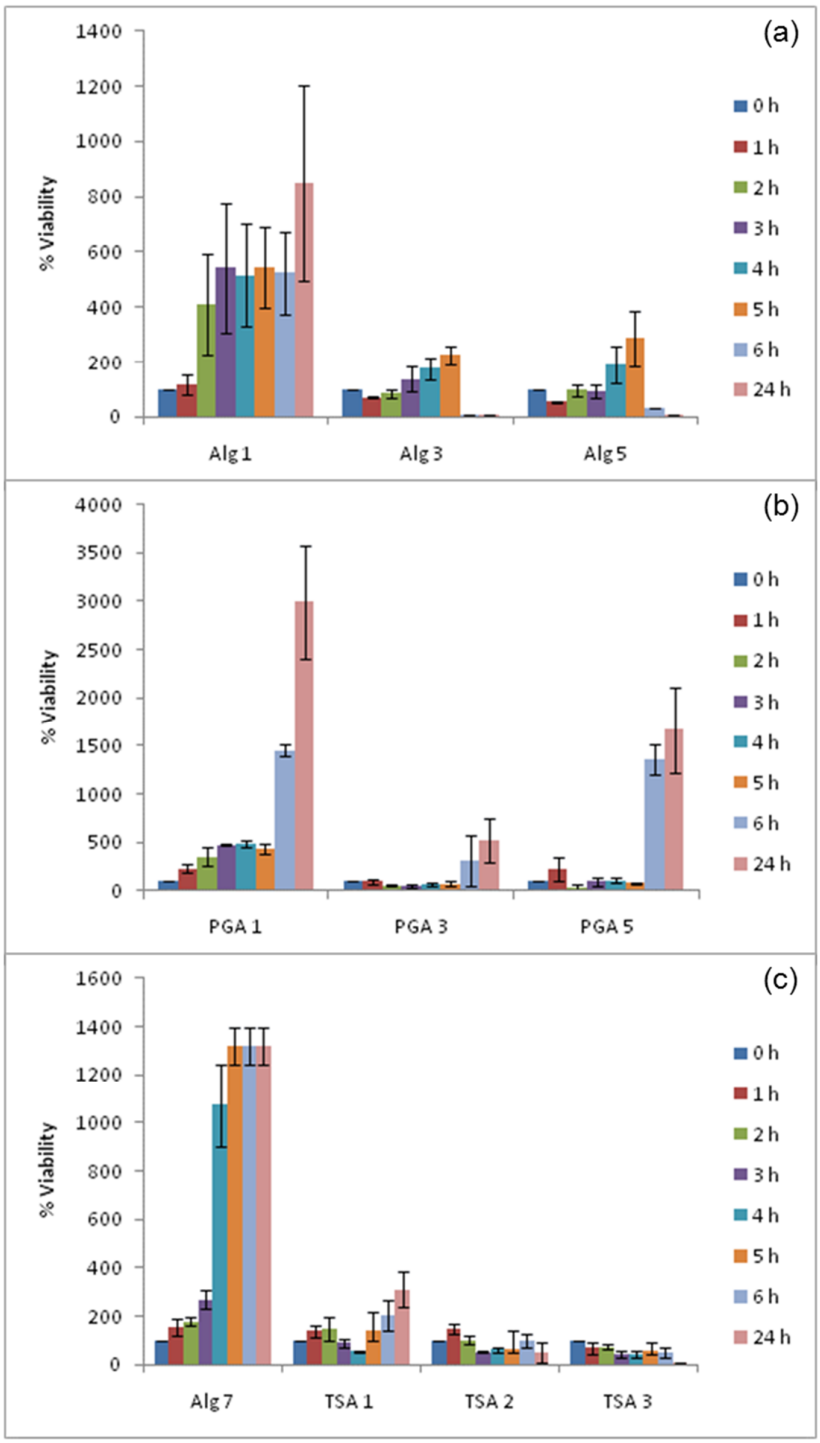

Figure 5.13: The % viability of *E. coli* cells present in nutrient broth media upon shaking with (a) calcium alginate beads (b) PGA beads and (c) TSA beads as a function of time. The tests were done using 100 beads in 10 ml of nutrient broth held at a constant temperature of 37 ± 1°C. Each bead type used is defined in the figure.

Table 5.10: p-values for the Difference in the Bactericidal Activity against *E. coli* of the Beads Studied compared to that of the Appropriate Control Beads

Control bead vs. Bead	p-value	p-value summary	Bactericidal activity of bead is statistically significantly different compared to that of appropriate control bead
Alg 1 vs. Alg 3	$p < 0.0001$	***	Yes
Alg 1 vs. Alg 5	$p < 0.0001$	***	Yes
PGA 1 vs. PGA 3	$p < 0.0001$	***	Yes
PGA 1 vs. PGA 5	$p = 0.0009$	***	Yes
Alg 7 vs. TSA 1	$p < 0$ .0001	***	Yes
Alg 7 vs. TSA 2	$p < 0.0001$	***	Yes
Alg 7 vs. TSA 3	$p < 0.0001$	***	Yes

5.2.5 Studies on *Pseudonomas aeruginosa* (27853 and 10145)

5.2.5.1 Introduction to *Pseudonomas aeruginosa* (27853 and 10145)

Pseudomonas aeruginosa is a Gram-negative,[69-71] rod-shaped bacterium measuring 0.5 to 0.8 µm by 1.5 to 3.0 µm (Figure 5.14), belonging to the family *Pseudomonadaceae.* It is an obligate aerobic microbe meaning that it requires oxygen to survive.[72] However, it can survive in conditions with little or no oxygen.[73] Almost all strains are able to move using a single polar flagellum. The typical *Pseudomonas* bacterium is found in a biofilm attached to a surface,[74,75] alternatively it can take up a planktonic form, in which it is mobile.[2] *P. aeruginosa* is a common microbe in both soil and water.[69] A number of strains of *P. aeruginosa* can grow under quite harsh conditions as they can survive with little nutrition,[41] some are able to grow at temperatures as high as 42°C,[76] while others show resistance to heavy metals and a number of antibiotics.[77]

Figure 5.14: Gram-stained *Pseudomonas aeruginosa* bacteria (pink-red rods)[72]

In common with *S. aureus and E. coli*, *P. aeruginosa* is classified as an opportunistic pathogen[75] in that it rarely causes disease in a healthy persons.[74] However, if the barrier to infection is broken, such as by a wound to the skin, or if the person is suffering from immune deficiency, infection can occur. *P. aeruginosa* typically infects the pulmonary tract,[69] urinary tract,[78] burns,[79, 80] and the blood system.[81] *P. aeruginosa* causes severe and potentially fatal infections in immunocompromised individuals[75] and individuals with cystic fibrosis[69,79] or chronic obstructive pulmonary disease.[82] When *P. aeruginosa* infects the lungs of patients with cystic fibrosis its ability to adapt to microaerobic or anaerobic environments comes into play, as thick layers of lung mucus and alginate formed by the bacterium will surround the bacterial cells limiting the diffusion of oxygen.

5.2.5.2 Plate Assay on *P.aeruginosa* (27853 and 10145)

The results on using *P. aeruginosa* (27853) in the plate assay experiment are summarised in Table 5.11 and Figure 5.15, while those for *P. aeruginosa* (10145) are summarised in Table 5.12 and Figure 5.16. As had previously been observed in the plate assay in the preceding sections on the two strains of *S. aureus* and *E. coli* bacteria the control polymer support beads Alg 1, PGA 1, and Alg 7 showed no inhibitory effect on the either of the two strains of *P. aeruginosa*. For both *P. aeruginosa*, (27853) and (10145), the Alg 4 and Alg 5 beads which contained silver in the zero oxidation state resulted in direct inhibition of the bacteria beneath the beads. Moreover, the zone of inhibition determined for the Alg 2, Alg 3, PGA 2 and

PGA 3 beads, which all contained silver(I), were all in a similar range of approximately 20 to 30 mm^2 for both bacteria. Differences in the activity of the beads against the growth of the two strains of *P. aeruginosa* were shown by the PGA 4 and PGA 5 beads. These beads showed quite large zones of inhibition in the region of 50 to 90 mm^2 against the growth of *P. aeruginosa* (27853), while they only resulted in direct inhibition beneath the beads for *P. aeruginosa* (10145). The former case is the first example we have observed of the silver(0) containing beads resulting in a zone of inhibition against the growth of a bacteria in the plate assays carried out in this project. The TSA beads exhibited further differences in their activity between the two strains of *P. aeruginosa*. Interestingly, the TSA 1 beads showed only direct inhibition against the growth of *P. aeruginosa* (27853), whereas a significant zone of inhibition of 35 ± 12 mm^2 was determined for the growth of *P. aeruginosa* (10145). This indicates that the quaternary ammonium group on the TSA had a significant bacteriostatic effect on the growth of *P. aeruginosa* (10145). This finding was consistent with that recorded for the TSA 2 and TSA 3 beads. The TSA 2 beads exhibited a similar behavior to the TSA 1 beads for both strains of *P. aeruginosa* indicating that the added silver(I), in the amount present in these beads was having little to no added bacteriostatic effect. For the TSA 3 beads which contained a greater amount of silver(I) a zone of inhibition of 20 ± 4 mm^2 was recorded for the *P. aeruginosa* (27853), while one of 106 ± 16 mm^2 was recorded for *P. aeruginosa* (10145). This shows that the silver(I) in these beads was having a combined effect with the TSA support on inhibiting the growth of the two strains of bacteria and that this combined effect was very active against the growth of *P. aeruginosa* (10145).

Table 5.11: Results for the Plate Assay on *P. aeruginosa* (27853) using a Range of Bead Types

Bead code	**Silver Content in 30 Beads (mg)**	**Total area* (mm^2)**	**Zone of Inhibition* (mm^2)**	**Description**
Alg 1	0	-	0	No zone of inhibition
Alg 2	8 ± 0.5	126 ± 4	23 ± 4	Zone of inhibition
Alg 3	110 ± 8.7	121 ± 9	30 ± 9	Zone of inhibition
Alg 4	3 ± 0.5	-	0	Direct inhibition
Alg 5	116 ± 15.9	-	0	Direct inhibition
PGA 1	0	-	0	No zone of inhibition
PGA 2	7.3 ± 0.3	95 ± 1	16 ± 1	Zone of inhibition
PGA 3	167 ± 22.0	100 ± 4	19 ± 4	Zone of inhibition
PGA 4	6 ± 0.3	141 ± 12	63 ± 12	Zone of inhibition
PGA 5	176 ± 23.9	157 ± 24	78 ± 24	Zone of inhibition
Alg 7	0	-	0	No zone of inhibition
TSA 1	1 ± 0.05	-	0	Direct inhibition
TSA 2	28 ± 4.45	-	0	Direct inhibition
TSA 3	129 ± 6.5	82 ± 4	20 ± 4	Zone of inhibition

*ZOIs were recorded after 24 h using ten beads on each plate and plates were held at 37 ± 1°C.

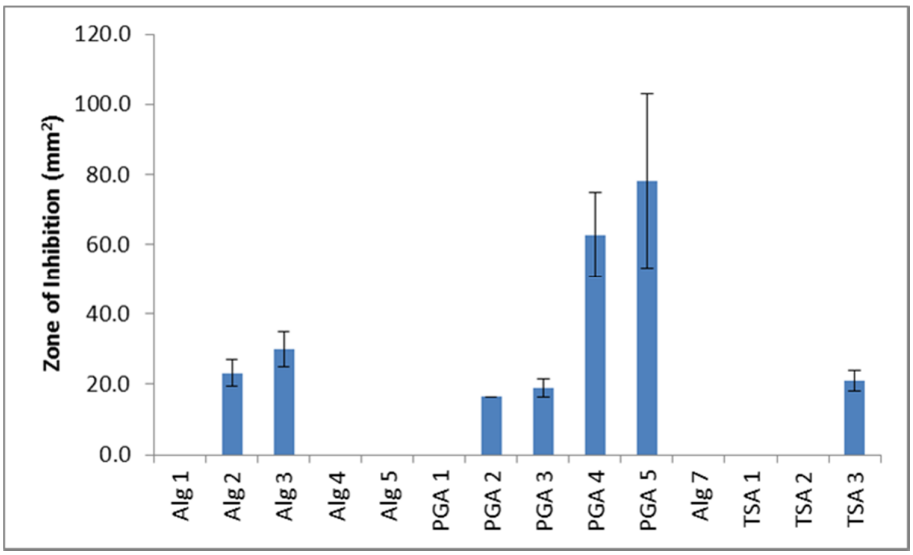

Figure 5.15: Zones of inhibition for the growth of *P. aeruginosa* (27853) measured using a plate assay. ZOIs were recorded after 24 h using 10 beads on each plate and plates were held at 37 ± 1°C. Bead type used is defined in the figure.

Table 5.12: Results for the Plate Assay on P. aeruginosa (10145) using a Range of Bead Types

Bead Code	Silver Content in 30 Beads (mg)	Total area* (mm^2)	Zone of Inhibition * (mm^2)	Description
Alg 1	0	0	0	No zone of inhibition
Alg 2	8 ± 0.5	100 ± 3	17 ± 3	Zone of inhibition
Alg 3	110 ± 8.7	95 ± 3	21 ± 3	Zone of inhibition
Alg 4	3 ± 0.5	-	0	Direct inhibition
Alg 5	116 ± 15.9	-	0	Direct inhibition
PGA 1	0	0	0	No zone of inhibition
PGA 2	7.3 ± 0.3	112 ± 5	24 ± 5	Zone of inhibition
PGA 3	167 ± 22.0	104 ± 5.2	26 ± 5	Zone of inhibition
PGA 4	6 ± 0.3	-	0	Direct inhibition
PGA 5	176 ± 23.9	-	0	Direct inhibition
Alg 7	0	64 ± 9	0	No zone of inhibition
TSA 1	1 ± 0.05	102 ± 12	35 ± 12	Zone of inhibition
TSA 2	28 ± 4.45	120 ± 12	56 ± 12	Zone of inhibition
TSA 3	129 ± 6.5	152 ± 16	106 ± 16	Zone of inhibition

*ZOIs were recorded after 24 h using ten beads on each plate and plates were held at 37 ± 1°C.

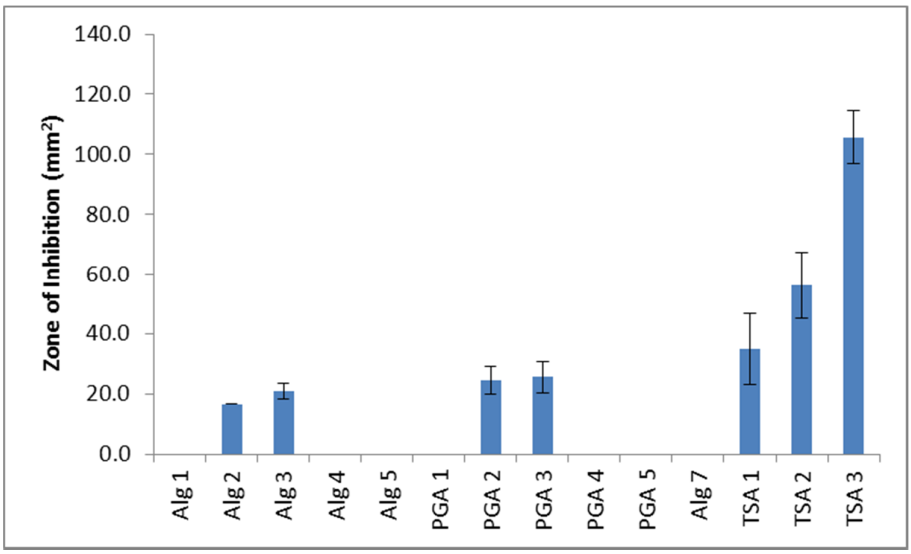

Figure 5.16: Zones of inhibition for the growth of *P. aeruginosa* (10145) measured using a plate assay. ZOIs were recorded after 24 h using 10 beads on each plate and plates were held at 37 ± 1°C. Bead type used is defined in the figure.

5.2.5.3 Well Assay on *P. aeruginosa* (27853 and 10145)

The well assay experiment was then carried out on the two strains of *P. aeruginosa* and the results are given in in Table 5.13 and Figure 5.17 for strain 27853 and in Table 5.14 and Figure 5.18 for strain 10145. Surprisingly, given the significant effect that the PGA beads containing silver(0) (PGA 4 and PGA 5) had against the growth of *P. aeruginosa* (27853) in the plate assay no effect was observed for the well assay using the leachate obtained from these beads. For strain 27853 only leachate from beads containing silver in the +1 oxidation state resulted in a zone of inhibition, and for each type of bead this zone was small for the bead type that contained the lower amount of silver. For example, the zone of inhibition determined for *P. aeruginosa* (27853) was 43 ± 4 mm^2 using the leachate derived from the PGA 3 beads, but only 11 ± 2 mm^2 for the leachate derived from the PGA 2 beads. The results for the well assay using the 10145 strain are also in contrast to the plate assay results outlined above. For the plate assay on the 10145 strain the TSA beads were the most active, whereas the leachate from these beads showed little to no activity against the strain. This suggests that most of their activity in the plate assay experiment derived from the quaternary ammonium groups on the polymer

support as these will not be leached into the water. From the well assay experiments given in Table 5.13 it can be deduced that the leachate from the calcium alginate beads was the most active against the growth of *P. aeruginosa* (10145) and even the leachate from the Alg 4 and Alg 5 beads which contained silver in the zero oxidation state resulted in a zone of inhibition. This is the first example of leachate from beads containing silver(0) having an inhibitory effect on the growth of bacteria in our studies.

Table 5.13: Results for the Well Assay on *P. aeruginosa* (27853) using a Range of Bead Types

Bead Code	**Mass of Silver leached from 30 Beads[a] (mg)**	**Zone of Inhibition (mm^2)**	**Description**
Alg 1	0	0	No zone of inhibition
Alg 2	0.04 ± 0.001	18 ± 4	Zone of inhibition
Alg 3	2.24 ± 0.002	73 ± 5	Zone of inhibition
Alg 4	0.01 ± 0.004	0	No zone of inhibition
Alg 5	2.12 ± 0.03	0	No zone of inhibition
PGA 1	0	0	No zone of inhibition
PGA 2	0.03 ± 0.005	11 ± 2	Zone of inhibition
PGA 3	3.86 ± 0.024	43 ± 4	Zone of inhibition
PGA 4	0.10 ± 0.011	0	No zone of inhibition
PGA 5	2.50 ± 0.024	0	No zone of inhibition
Alg 7	0	0	No zone of inhibition
TSA 1	0.03 ± 0.009	0	No zone of inhibition
TSA 2	1.58 ± 0.005	3 ± 1	Zone of inhibition
TSA 3	2.91± 0.002	28 ± 2	Zone of inhibition

[a] The leachate was extracted from 30 beads into 10 ml of deionised water held at 30 ± 1°C for 24 h.

[b]ZOIs were recorded after 24 h and plates were held at 37 ± 1°C.

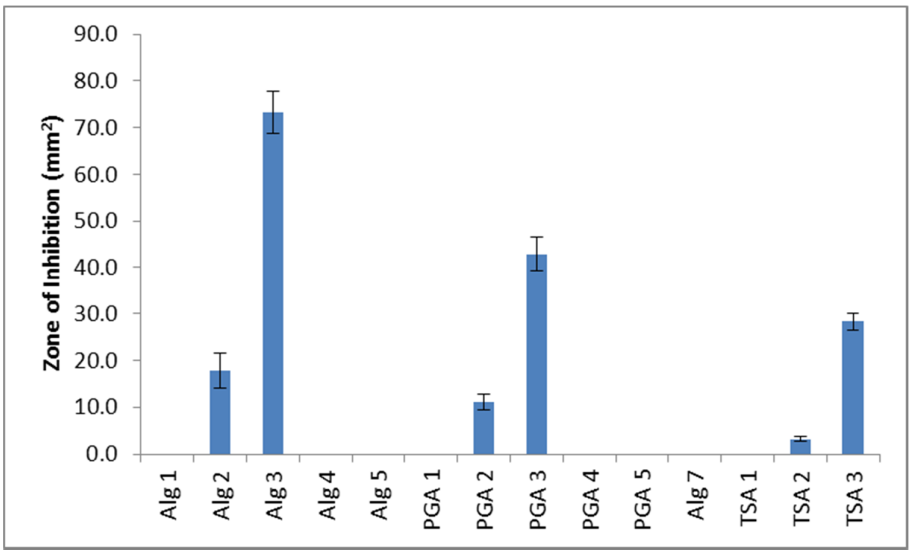

Figure 5.17: Zones of inhibition for the growth of *P. aeruginosa* (27853) from well assays using leachate from 30 beads held in 10 ml of deionised water at 30 ± 1°C for 24 h. ZOIs were recorded after 24 h and plates were held at 37 ± 1°C. Bead types used are defined in the figure.

Table 5.14: Results for the Well Assay on *P. aeruginosa* (10145) using a Range of Bead Types

Bead Code	Mass of Silver leached from 30 Beads[a] (mg)	Zone of Inhibition[b] (mm^2)	Description
Alg 1	0	0	No zone of inhibition
Alg 2	0.04 ± 0.001	32 ± 3	Zone of inhibition
Alg 3	2.24 ± 0.002	50 ± 4	Zone of inhibition
Alg 4	0.01 ± 0.004	21 ± 6	Zone of inhibition
Alg 5	2.12 ± 0.03	25 ± 6	Zone of inhibition
PGA 1	0	0	No zone of inhibition
PGA 2	0.03 ± 0.005	7.6 ± 1	Zone of inhibition
PGA 3	3.86 ± 0.024	65 ± 7	Zone of inhibition
PGA 4	0.10 ± 0.011	0	No zone of inhibition
PGA 5	2.50 ± 0.024	0	No zone of inhibition
Alg 7	0	0	No zone of inhibition
TSA 1	0.03 ± 0.009	0	No zone of inhibition
TSA 2	1.58 ± 0.005	0	No zone of inhibition
TSA 3	2.91± 0.002	15 ± 1	Zone of inhibition

[a] The leachate was extracted from 30 beads into 10 ml of deionised water held at 30 ± 1°C for 24 h.

[b]ZOIs were recorded after 24 h and plates were held at 37 ± 1°C.

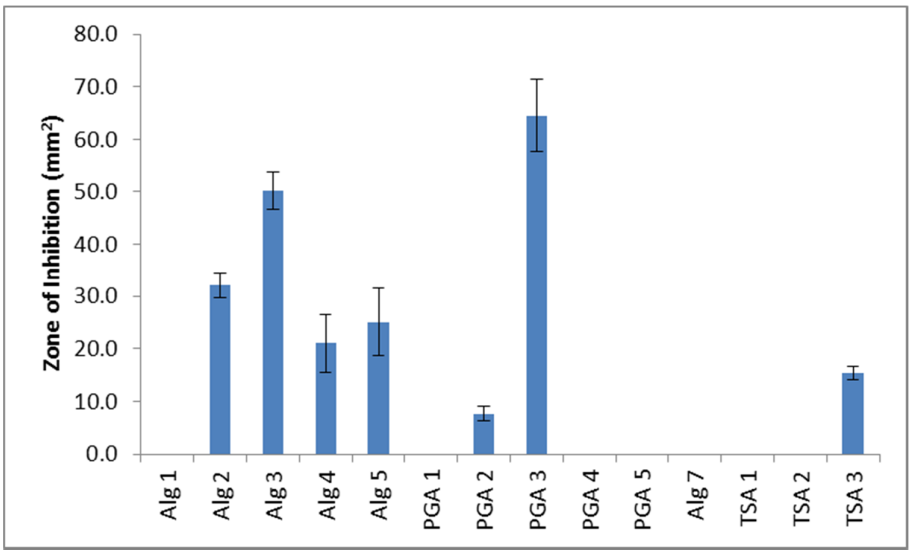

Figure 5.18: Zones of inhibition for the growth of *P. aeruginosa* (10145) from well assays using leachate from 30 beads held in 10 ml of deionised water at 30 ± 1°C for 24 h. ZOIs were recorded after 24 h and plates were held at 37 ± 1°C. Bead types used are defined in the figure.

5.2.5.4 Colony Count Assay on *P. aeruginosa* (27853 and 10145)

Summaries of the results obtained for the colony count assays using *P. aeruginosa* (27853) and (10145) are given in Figure 5.19 and Figure 5.20, respectively. For both strains of bacteria the control beads, Alg 1, PGA 1, and Alg 7, showed no bactericidal activity and the bacteria had surpassed the exponential phase of growth at the 24 h time period. The study on *P. aeruginosa* (27853) using the Alg 3 and Alg 5 beads showed that, as illustrated in Figure 5.19(a), during the early time period (0 h to 2 h) for Alg 3 and (0 h to 1 h) for Alg 5 there was a decrease in the number of viable cells growing in the medium. However, for the time period 3 h to 5 h (Alg 3) and 2 h to 5 h (Alg 5) the number of viable cells increased before significantly decreasing at the 6 h time period and stayed at this number (Alg 3) or decreased further (Alg 5) when the cultures were sampled after 24 h. This sharp decrease in cell number coincided with time at which the beads burst releasing all the silver into the surrounding medium.

In contrast to the results for the calcium alginate beads outlined above the activity of the PGA 3 and PGA 5 beads were quite different against the two strains of *P. aeruginosa*. Both the PGA 3 and PGA 5 beads were able to maintain the number

of viable cells of *P. aeruginosa* (27853) at a very low level at each of the sample times over the 24 h time period (Figure 5.19(b)). Whereas, for *P. aeruginosa* (10145), the number of viable cells for the media in contact with the PGA 3 or PGA 5 beads remained low for the first 5 h. A significant increase in the number of viable cells was then recorded for the assays involving both sets of beads at the 6 h time period and this number increased when the culture was sampled after 24 h. When these findings are compared with the results for the plate assay on these bacteria using the PGA 3 and PGA 5 beads (Table 5.8) it can be seen that the PGA 5 beads also displayed a significant bacteriostatic effect on the growth of *P. aeruginosa* (27853) resulting in a significant ZOI of 78 ± 24 mm^2. In contrast, only direct inhibition beneath the beads was observed for *P. aeruginosa* (10145).

When the colony count assay was carried out on the two strains of *P. aeruginosa* using the TSA beads it was determined that the TSA 1 beads had a very mild bactericidal effect on the *P. aeruginosa* (10145), but essentially no effect on the *P. aeruginosa* (27853) (Figure 5.20(c) and Figure 5.19(c)) respectively. This corresponds with the reported lower activity of quaternary ammonium groups towards Gram-negative bacteria.[68] Of the five types of bacteria studied the quaternary ammonium groups on the TSA beads showed the least bactericidal effect against the two strains of *P. aeruginos*a. However, as observed for the other types of bacteria studied upon adding silver(I) to the TSA beads a significant bactericidal effect occurs. The TSA 2 and TSA 3 beads both showed very good activity towards killing the two strains of *P. aeruginosa*. Moreover, for each strain of *Pseudomonas* even though the TSA 2 beads contained less silver than the TSA 3 beads their activity was about the same.

The results for the statistical analysis of the colony count data on the two strains of *P. aeruginosa* are given in Tables 5.15 and 5.16 As can be seen from the p-values presented all the silver-containing beads are displaying a significantly higher level of bactericidal activity compared to the control beads. In contrast, the beads containing the quaternary ammonium groups did not have a significantly different level of activity against the two strains compared to the control bead.

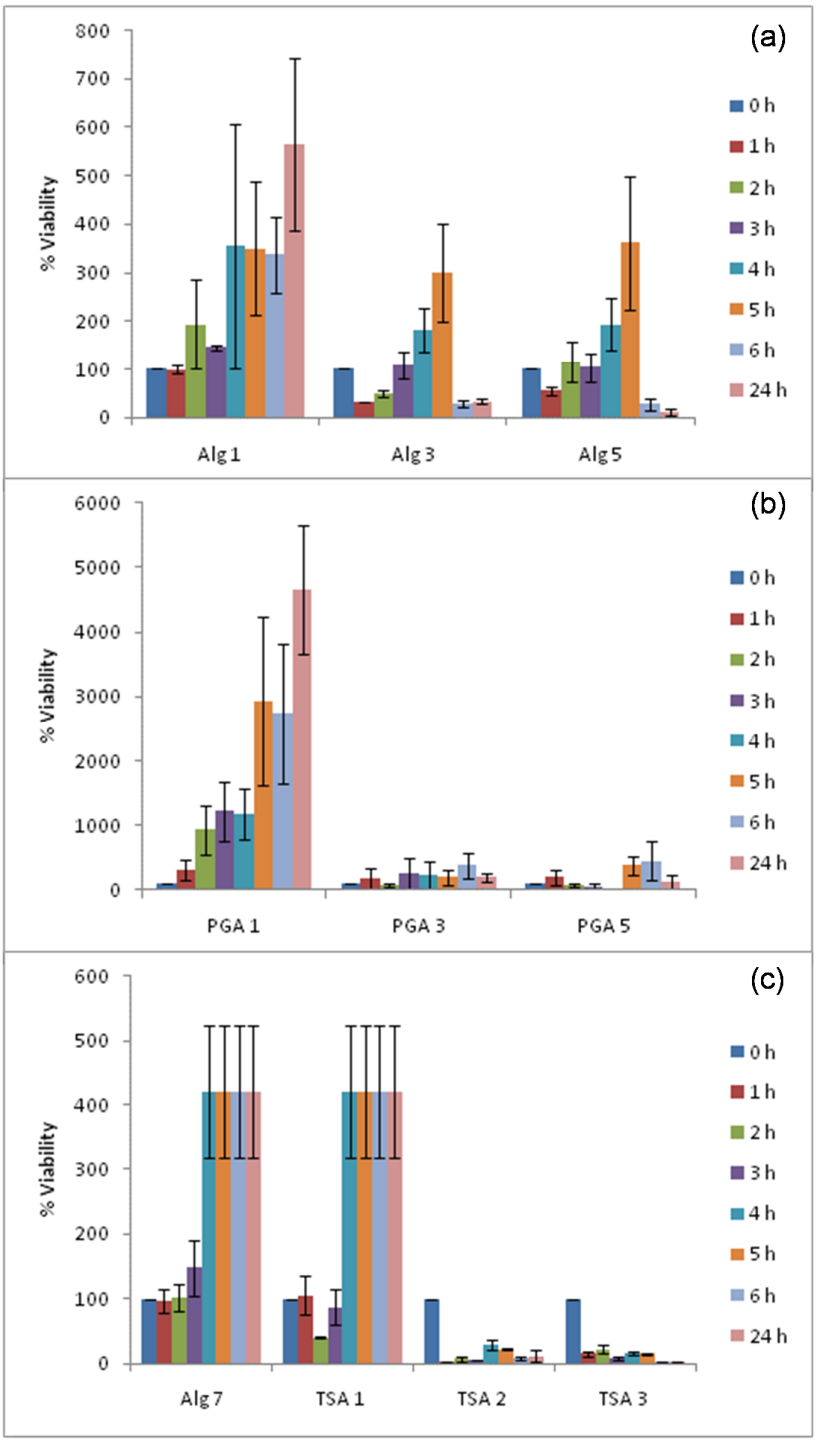

Figure 5.19: The % viability of *P. aeruginosa* (27853) cells present in nutrient broth media upon shaking with (a) calcium alginate beads (b) PGA beads and (c) TSA beads as a function of time. The tests were done using 100 beads in 10 ml of nutrient broth held at a constant temperature of 37 ± 1°C. Each bead type used is defined in the figure.

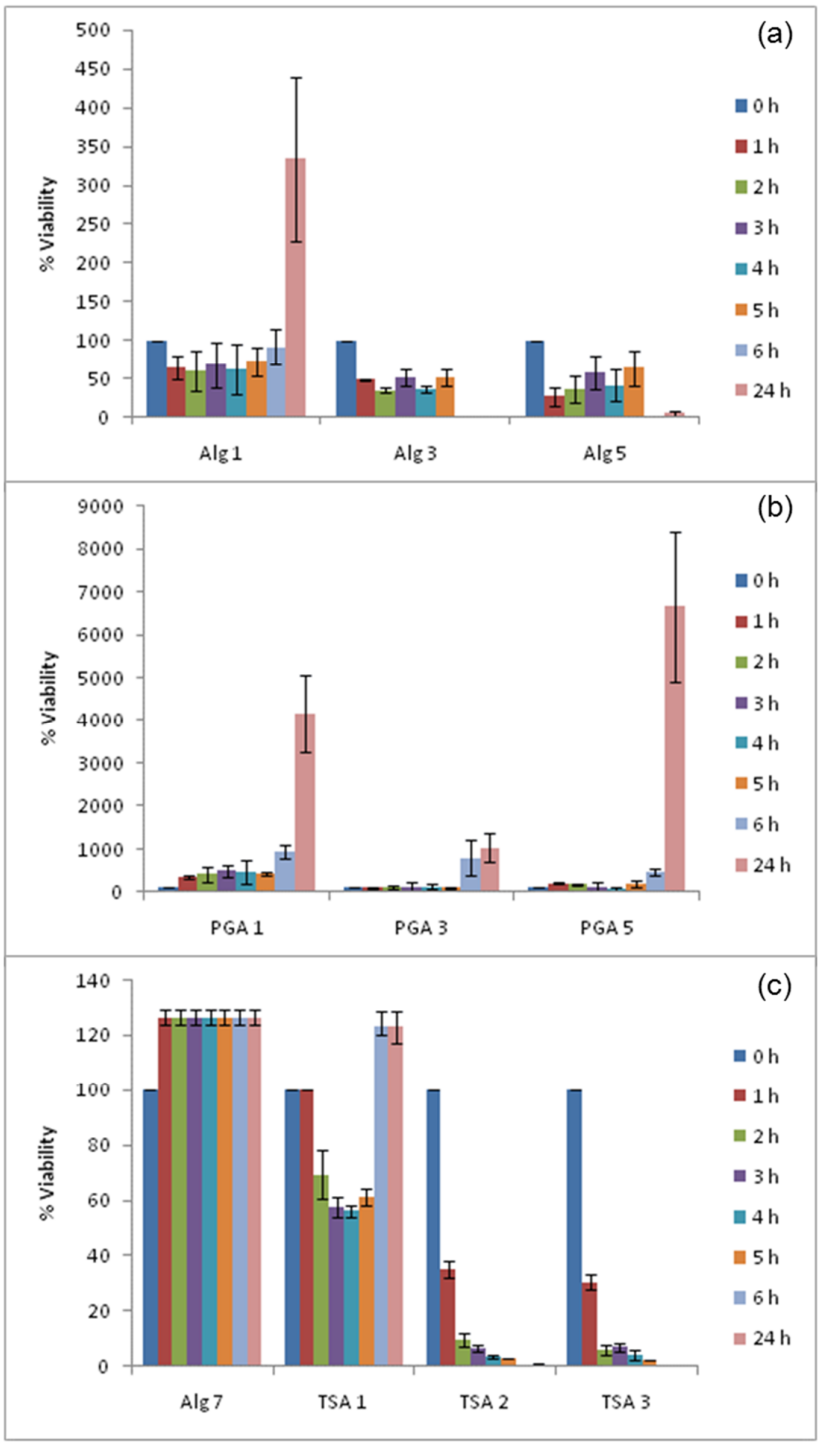

Figure 5.20: The % viability of *P. aeruginosa* (10145) cells present in nutrient broth media upon shaking with (a) calcium alginate beads (b) PGA beads and (c) TSA beads as a function of time. The tests were done using 100 beads in 10 ml of nutrient broth held at a constant temperature of 37 ± 1°C. Each bead type used is defined in the figure.

Table 5.15: p-values for the Difference in the Bactericidal Activity against *P. aeruginosa* (27853) of the Beads Studied compared to that of the Appropriate Control Beads

Control bead vs. Bead	p-value	p-value summary	Bactericidal activity of bead is statistically significantly different compared to that of appropriate control bead
Alg 1 vs. Alg 3	p = 0.0006	***	Yes
Alg 1 vs. Alg 5	p = 0.0053	**	Yes
PGA 1 vs. PGA 3	p = 0.0012	**	Yes
PGA 1 vs. PGA 5	p = 0.0010	***	Yes
Alg 7 vs. TSA 1	p = 0.7052		No
Alg 7 vs. TSA 2	p < 0.0001	***	Yes
Alg 7 vs. TSA 3	p < 0.0001	***	Yes

Table 5.16: p-values for the Difference in the Bactericidal Activity against *P. aeruginosa* (10145) of the Beads Studied compared to that of the Appropriate Control Beads

Control bead vs. Bead	p-value	p-value summary	Bactericidal activity of bead is statistically significantly different compared to that of appropriate control bead
Alg 1 vs. Alg 3	p = 0.0002	***	Yes
Alg 1 vs. Alg 5	p = 0.0003	***	Yes
PGA 1 vs. PGA 3	p < 0.0001	***	Yes
PGA 1 vs. PGA 5	p = 0.7459		No
Alg 7 vs. TSA 1	p = 0.6231		No
Alg 7 vs. TSA 2	p < 0.0001	***	Yes
Alg 7 vs. TSA 3	p < 0.0001	***	Yes

5.3 Conclusions

5.3.1 Comparison of the Plate Assay Data

(a) Gram-positive bacteria (*S. aureus*, MRSA)

For the polymer supports studied only the TSA beads which contained quaternary ammonium groups showed a bacteriostatic effect on the growth of the two bacteria. All the beads which contain silver(0) resulted in direct inhibition of the growth of the bacteria beneath the surface of the beads. Zones of inhibition were observed for both bacteria, for each of the bead types, which contained silver in the +1 oxidation state. A summary of the zones of inhibition observed for the two bacteria using the Alg 3, PGA 3 and TSA 3 beads is given in Table 5.17. As can be observed in Table 5.17, the Alg 3 and the TSA 3 beads showed the higher activity, while the PGA 3 beads were the poorest performing beads against the two bacteria. An interesting observation from the studies on the beads containing silver in the +1 oxidation state was that for *S. aureus*, the calcium alginate and PGA beads often displayed no difference in the size of the zone of inhibition formed for beads containing different amounts of silver. In contrast, a bigger zone of inhibition of MRSA growth was observed for the beads which contained the larger amount of silver. A summary of these finding is given in Table 5.18. This finding was surprising as generally literature reports have shown that there is little difference in resistance of Methicillin-sensitive *S. aureus* and MRSA strains towards silver.[53] In contrast, for the TSA beads there was an increase in size of the zone of inhibition for both bacteria going from the TSA 2 to the TSA 3 beads.

Table 5.17: Summary of the Zones of Inhibition Produced by the Alg 3, PGA 3 and TSA 3 Beads in the Plate Assay on Gram-Positive Bacteria

	Alg 3	PGA 3	TSA 3
S. aureus ZOI	21 ± 8 mm^2	28 ± 6 mm^2	76 ± 10 mm^2
MRSA ZOI	99 ± 20 mm^2	31 ± 4 mm^2	46 ± 14 mm^2

Table 5.18: Comparison of the Size of the Zone of Inhibition Produced by Alg 2, Alg 3, PGA 2 and PGA 3 Beads towards Gram-Positive Bacteria

	Alg 2, Alg 3	PGA 2, PGA 3
S. aureus ZOI	Similar ZOI	Similar ZOI
MRSA ZOI	Bigger for Alg 3	Bigger for PGA 3

(b) Gram-negative bacteria (*E. coli*, *P. aeruginosa* (27853) and (10145))

The polymer support which contained quaternary ammonium groups was the only support which exhibited a bacteriostatic effect on the bacteria. For *E. coli* and the *P. aeruginosa* (10145) strain, the beads which contained silver in the zero oxidation state resulted in direct inhibition of the bacteria growth beneath the beads. In contrast, for the *P. aeruginosa* (27853) strain the PGA beads containing silver(0) resulted in large zones of inhibition, while the analogous Alg beads did not. This was a highly surprising result and was probably related to the silver particle size with that batch of beads. As stated in Chapter 4 the method that was employed to reduce the silver ions to silver(0) was quite uncontrolled and resulted in a wide range of particle sizes, some of which lay outside the nanodomain. Studies have shown that the bactericidal effects of silver(0) nanoparticles are dependent on particle size and shape[83-85] and it is likely that a higher quantity of smaller particles (in the region of 10 -100 nm) were present in the batch of PGA beads. As for the Gram-negative bacteria, in general, the beads containing silver(I) showed the broadest range of antibacterial activity. The results for the Alg 3, PGA 3 and TSA 3 beads are given in Table 5.19. For *E. coli* and *P. aeruginosa* (27853) a larger zone of inhibition was produced by the TSA 3 beads compared to their Alg 3 and PGA 3 analogues. In contrast, the zone of inhibition of *P. aeruginosa* (10145) was broadly similar across the three bead types. This indicates that the quaternary ammonium group was only having a mild bacteriostatic additional effect against strain 10145. As previously observed for *S. aureus* it would appear that the amount of silver(I) present in the Alg and PGA beads does not influence their bacteriostatic effect, but this is not the case for the TSA beads. Table 5.20 gives a summary of these observations.

Table 5.19: Summary of the Zones of Inhibition Produced by the Alg 3, PGA 3 and TSA 3 Beads in the Plate Assay on Gram-Negative Bacteria

	Alg 3	PGA 3	TSA 3
E. coli ZOI	39 ± 5 mm^2	23 ± 6 mm^2	84 ± 13 mm^2
P. aeruginosa (10145) ZOI	21 ± 3 mm^2	26 ± 5 mm^2	106 ± 16 mm^2
P. aeruginosa (27853) ZOI	30 ± 9 mm^2	19 ± 4 mm^2	20 ± 4 mm^2

Table 5.20: Comparison of the Size of the Zone of Inhibition Produced by Alg 2, Alg 3, PGA 2, PGA 3, TSA 2, and TSA 3 Beads towards Gram-Negative Bacteria

	Alg 2, Alg 3	PGA 2, PGA 3	TSA 2, TSA 3
E. coli	Similar ZOI	Similar ZOI	ZOI for TSA 3 is bigger
P. aeruginosa (27853)	Similar ZOI	Similar ZOI	ZOI for TSA 3 is bigger
P. aeruginosa(10145)	Similar ZOI	Similar ZOI	ZOI for TSA 3 is bigger

Taking all the results into consideration the TSA 3 beads would be the best choice for a bead which exhibited a bacteriostatic effect against both Gram-positive and Gram negative bacteria.

5.3.2 Comparison of the Well Assay Data

(a) Gram-positive bacteria (*S. aureus*, MRSA)

For the Gram-positive bacteria only leachate from beads that contained silver in the +1 oxidation state resulted in a zone of inhibition. For the two bacteria studied there is a clear correlation between the amount of silver ions present in the bead and

the size of the zone of inhibition formed by its leachate. MRSA did not form a zone of inhibition around the leachate from silver(I) containing beads, PGA 2 and TSA 2. This correlates well with the plate assay for these bacteria which showed a smaller zone of inhibition when Alg 2 and PGA 2 beads were placed on the plate compared to the Alg 3 and PGA 3 analogues. This indicates that the MRSA was more tolerant to silver(I) ions than the other strain of *S. aureus*. No zone of inhibition was observed for the two bacteria studied when the leachate from beads containing silver(0) was used. Studies reported in Chapter 4 had shown that the beads which contained the reduced silver also released silver into the leachate. However, it is known that the particle size of metallic silver is important in relation to its antimicrobial activity[84] and it would appear that the silver(0) particles released into the leachate were too big to have any bacteriostatic effect on the Gram positive bacteria studied.

(b) Gram-negative bacteria (*E. coli*, *P. aeruginosa* (27853) and (10145))

The leachate from all the silver(I) beads caused a zone of inhibition against the growth of the three bacteria, the only exception being the leachate from TSA 2 when used on *P. aeruginosa* (10145). As for the Gram-positive bacteria the zone was always bigger for the leachate from the beads containing the higher concentration of silver(I). In general, the leachate from the silver(0) containing beads did not result in a zone of inhibition for either of the bacteria. The only exception to this was the leachate from the Alg 4 and Alg 5 beads which did show a zone of inhibition against *P. aeruginosa* (10145). As the activity of silver(0) is known to be particle size dependent[83,85,86] and as there was a distribution of particles sizes within the beads it may be that in this case smaller particles were released.

Overall for the five strains of bacteria studied the silver(0) particles had a lower bacteriostatic effect than the silver ions and that the bacteriostatic effect of the silver(0) is dependent on the particle size of silver(0) released from the beads.

5.3.3 Comparison of the Colony Count Data

(a) Gram-positive bacteria (*S. aureus*, MRSA)

For each of the two types of Gram-positive bacteria the Alg 3 beads exhibited a similar bactericidal effect to their Alg 5 analogues. This indicates that whether the silver was originally in the +1 or 0 oxidation state was not particularly important in this assay. However, the calcium alginate beads were not stable in the cell culture medium, and they increased in size significantly during the assay and finally burst after about 6 h. The PGA beads remained intact during the 24 h of this assay; again it would appear that both the silver(I) and the silver(0) containing beads exhibited a bactericidal effect. However, it would appear that the beads containing silver(I) were generally more active, as they showed increased activity compared to their silver(0) analogues against MRSA after 24 h of contact. While, the activity of the two sets of beads was similar against *S. aureus* over the 24 h of the assay. The polymer support of the TSA beads showed a bactericidal effect against the two bacteria, although this effect was less pronounced for MRSA. For the studies on MRSA this effect was clearly enhanced by the addition of silver(I) to the beads. Moreover, there was no real difference in activity of the TSA 2 or TSA 3 even though they contained different amounts of silver(I) ions. There was only a very small increase in the level of activity against *S. aureus* for the TSA beads which contained silver and those which did not contain silver. However, this may arise as the polymer had such a good bactericidal effect against *S. aureus* that little improvement could be achieved by adding silver(I) to the beads.

(b) Gram negative bacteria (*E. coli*, *P. aeruginosa* (27853) and (10145))

As for the Gram-positive bacteria the Alg 3 and Alg 5 beads exhibited a similar bactericidal effect against all three bacteria. However, the beads had disintegrated after 6 h in the media releasing all their contents. Both the PGA 3 and PGA 5 beads showed a bactericidal effect against *P. aeruginosa* (27853) over the 24 h of the assay. Whereas their effect against *E. coli* and *P. aeruginosa (*10145) only lasted over 5 h and an increase in the number of viable cells was observed in the samples taken at 6 h and 24 h. Moreover, the increase was more substantial for the cell culture in contact with the PGA 5 beads indicating that the silver(0) was having

a lower bactericidal effect. For the TSA beads the polymer support only had a mild bactericidal effect against the two strains of *Pseudomonas,* while it showed a more significant effect against *E. coli.* Both the TSA 2 and TSA 3 beads had a significant bactericidal effect against the two Gram-negative bacteria studied over the 24 h assay. These observations are consistent with a recent study on the action of the well-known quaternary ammonium disinfectant benzalkonium chloride which showed a similar level of activity against *E. coli* and *S. aureus* but a lower level of activity against *P. aeruginosa*.[68]

In summary over the five bacteria studied the TSA 2 or TSA 3 beads showed the best activity in this assay and as the TSA 2 contained the lower amount of silver(I) ions this makes them the most attractive material for using in future bactericidal applications. We would propose that a contact kill mechanism is an important contribution to the observed bactericidal activity of these beads for two reasons, (1). The calcium alginate beads which disintegrated during the course of this assay against some bacteria, showed poorer activity than the TSA 2 and TSA 3 beads which remained intact during the course of this assay. (2) The quaternary ammonium group which was covalently attached to the bead exhibited a bactericidal effect against all the bacteria studied.

5.4 References

(1) Black, J. G. *Microbiology seventh Edition*, **2008**.
(2) Campbell, N.; Reece, J. *Biology sixth Edition*, **2002**; Vol. 6.
(3) Gangadharan, D.; Harshvardan, K.; Gnanasekar, G.; Dixit, D.; Popat, K. M.; Anand, P. S. *Water Research* **2010**, *44*, 5481-5487.
(4) Ward, J. B. *Microbiological Reviews* **1981**, *45*, 211-243.
(5) Sawada, I.; Fachrul, R.; Ito, T.; Ohmukai, Y.; Maruyama, T.; Matsuyama, H. *Journal of Membrane Science* **2012**, *387-388*, 1-6.
(6) Jun, B.-H.; Byun, J.-W.; Kim, J. Y.; Kang, H.; Park, H.-J.; Yoon, J.; Lee, Y.-S. *Journal of Materials Science* **2010**, *45*, 3106-3108.
(7) Rastogi, S. K.; Rutledge, V. J.; Gibson, C.; Newcombe, D. A.; Branen, J. R.; Branen, A. L. *Nanomedicine: Nanotechnology, Biology and Medicine* **2011**, *7*, 305-314.
(8) *http://water.me.vccs.edu/courses/env108/Lesson5_print.htm*.
(9) Brandt, O.; Mildner, M.; Egger, A. E.; Groessl, M.; Rix, U.; Posch, M.; Keppler, B. K.; Strupp, C.; Mueller, B.; Stingl, G. *Nanomedicine: Nanotechnology, Biology and Medicine* **2012**, *8*, 478-488.
(10) Ruparelia, J. P.; Chatteriee, A. K.; Duttagupta, S. P.; Mukherji, S. *Acta Biomaterialia* **2008**, *4*, 707-716.
(11) Monteiro, D. R.; Gorup, L. F.; Takamiya, A. S.; Ruvollo-Filho, A. C.; Camargo, E. R. d.; Barbosa, D. B. *International Journal of Antimicrobial Agents* **2009**, *34*, 103-110.
(12) Wiegand, C.; Heinze, T.; Hipler, U.-C. *Wound Repair and Regeneration* **2009**, *17*, 511-521.
(13) Zhu, X.; Bai, R.; Wee, K.-H.; Liu, C.; Tang, S.-L. *Journal of Membrane Science* **2010**, *363*, 278-286.
(14) Wu, J.; Hou, S.; Ren, D.; Mather, P. T. *Biomacromolecules* **2009**, *10*, 2686-2693.
(15) Ye, S.; Majumdar, P.; Chisholm, B.; Stafslien, S.; Chen, Z. *Langmuir* **2010**, *26*, 16455-16462.
(16) Lalueza, P.; Monzón, M.; Arruebo, M.; Santamaría, J. *Materials Research Bulletin* **2011**, *46*, 2070-2076.
(17) Kampf, G.; Dietze, B.; Grosse-Siestrup, C.; Wendt, C.; Martiny, H. *Antimicrobial Agents and Chemotherapy* **1998**, *42*, 2440-2442.
(18) Rai, M.; Yadav, A.; Gade, A. *Biotechnology Advances* **2008**, *27*, 76-83.
(19) Atiyeh, B. S.; Costagliola, M.; Hayek, S. N.; Dibo, S. A. *Burns* **2007**, *33*, 139-148.
(20) Singh, G.; Patankar, R. B.; Gupta, V. K. *Polymer-Plastics Technology and Engineering* **2010**, *49*, 1329-1333.
(21) Quang, D. V.; Sarawade, P. B.; Hilonga, A.; Kim, J.-K.; Chai, Y. G.; Kim, S. H.; Ryu, J.-Y.; Kim, H. T. *Colloids and Surfaces A: Physicochemical and Engineering Aspects* **2011**, *389*, 118-126.
(22) Maneerung, T.; Tokura, S.; Rujiravanit, R. *Carbohydrate Polymers* **2008**, *72*, 43-51.
(23) Nagy, A.; Harrison, A.; Sabbani, S.; Munson, R. S.; Dutta, P. K.; Waldman, W. J. *International Journal of Nanomedicine* **2011**, *6*, 1833-1852.

(24) Guzman, M.; Dille, J.; Godet, S. *Nanomedicine-Nanotechnology Biology and Medicine* **2012**, *8*, 37-45.
(25) Low, W. L.; Martin, C.; Hill, D. J.; Kenward, M. A. *International Journal of Antimicrobial Agents* **2011**, *37*, 162-165.
(26) Sintubin, L.; De Gusseme, B.; Van der Meeren, P.; Pycke, B. F. G.; Verstraete, W.; Boon, N. *Applied Microbiology and Biotechnology* **2011**, *91*, 153-162.
(27) Ruimy, R.; Armand-Lefevre, L.; Andremont, A. *American Journal of Infection Control* **2005**, *33*, 304-306.
(28) http://textbookofbacteriology.net/staph.html.
(29) Kluytmans, J.; vanBelkum, A.; Verbrugh, H. *Clinical Microbiology Reviews* **1997**, *10*, 505-520.
(30) Van den Berg, S.; Bowden, M. G.; Bosma, T.; Buist, G.; Van Dijl, J. M.; Van Wamel, W. J.; De Vogel, C. P.; Van Belkum, A.; Bakker-Woudenberg, I. A. J. M. *Journal of Immunological Methods* **2011**, *365*, 142-148.
(31) Kanafani, Z. A.; Fowler Jr, V. G. *Enfermedades Infecciosas y Microbiología Clínica* **2006**, *24*, 182-193.
(32) FitzGerald, S. F.; O'Gorman, J.; Morris-Downes, M. M.; Crowley, R. K.; Donlon, S.; Bajwa, R.; Smyth, E. G.; Fitzpatrick, F.; Conlon, P. J.; Humphreys, H. *Journal of Hospital Infection* **2011**, *79*, 218-221.
(33) Burman, J. D.; Leung, E.; Atkins, K. L.; O'Seaghdha, M. N.; Lango, L.; Bernado, P.; Bagby, S.; Svergun, D. I.; Foster, T. J.; Isenman, D. E.; Van den Elsen, J. M. H. *Journal of Biological Chemistry* **2008**, *283*, 17579-17593.
(34) Roghmann, M.; Taylor, K. L.; Gupte, A.; Zhan, M.; Johnson, J. A.; Cross, A.; Edelman, R.; Fattom, A. I. *Journal of Hospital Infection* **2005**, *59*, 27-32.
(35) Hennekinne, J.-A.; Ostyn, A.; Guillier, F.; Herbin, S.; Prufer, A.-L.; Dragacci, S. *Toxins* **2010**, *2*, 2106-2116.
(36) Ma, Y.; Zhou, T.; Zhao, C. *Carbohydrate Research* **2008**, *343*, 230-237.
(37) O'Connor, S. J.; MacKenzie, K. J. D.; Smith, M. E.; Hanna, J. V. *Journal of Materials Chemistry* **2010**, *20*, 10234-10240.
(38) Fan, L.-H.; Pan, X.-R.; Zhou, Y.; Chen, L.-Y.; Xie, W.-G.; Long, Z.-H.; Zheng, H. *Journal of Applied Polymer Science* **2011**, *122*, 2331-2337.
(39) Liu, Y.; Liu, X.; Wang, X.; Yang, J.; Yang, X.-J.; Lu, L. *Journal of Applied Polymer Science* **2010**, *116*, 2617-2625.
(40) Zhang, X.; Niu, H.; Yan, J.; Cai, Y. *Colloids and Surfaces a-Physicochemical and Engineering Aspects* **2011**, *375*, 186-192.
(41) Cui, D.; Szarpak, A.; Pignot-Paintrand, I.; Varrot, A.; Boudou, T.; Detrembleur, C.; Jerome, C.; Picart, C.; Auzely-Velty, R. *Advanced Functional Materials* **2010**, *20*, 3303-3312.
(42) Wilke, M. S.; Lovering, A. L.; Strynadka, N. C. J. *Current Opinion in Microbiology* **2005**, *8*, 525-533.
(43) Kotra, L. P.; Mobashery, S. *Bulletin de l'Institut Pasteur* **1998**, *96*, 139-150.
(44) Rowe, F.; Vargas Superti, S.; Machado Scheibe, R.; Dias, c. G. *Diagnostic Microbiology and Infectious Disease* **2002**, *43*, 45-48.
(45) Ender, M.; McCallum, N.; Berger-Bacchi, B. *International Journal of Medical Microbiology* **2008**, *298*, 607-617.
(46) Berger-Bächi, B. *Médecine et Maladies Infectieuses* **1997**, *27, Supplement 4*, 201-206.

(47) Chiappetta, D. A.; Degrossi, J.; Teves, S.; D'Aquino, M.; Bregni, C.; Sosnik, A. *European Journal of Pharmaceutics and Biopharmaceutics* **2008**, *69*, 535-545.
(48) Moore, C. L.; Hingwe, A.; Donabedian, S. M.; Perri, M. B.; Davis, S. L.; Haque, N. Z.; Reyes, K.; Vager, D.; Zervos, M. J. *International Journal of Antimicrobial Agents* **2009**, *34*, 148-155.
(49) Stefani, S.; Chung, D. R.; Lindsay, J. A.; Friedrich, A. W.; Kearns, A. M.; Westh, H.; MacKenzie, F. M. *International Journal of Antimicrobial Agents* **2012**, *39*, 273-282.
(50) http://www.foogle.biz/mrsa.htm.
(51) http://www.topnews.in/health/scientists-search-superbugs-icus-develop-mrsa-sampling-system-21688.
(52) Akimitsu, N.; Hamamoto, H.; Inoue, R.; Shoji, M.; Akamine, A.; Takemori, K.; Hamasaki, N.; Sekimizu, K. *Antimicrobial Agents and Chemotherapy* **1999**, *43*, 3042-3043.
(53) Percival, S. L.; Thomas, J. G.; Slone, W.; Linton, S.; Corum, L.; Okel, T. *Wound Repair and Regeneration* **2011**, *19*, 767-774.
(54) Nair, R. G.; Roy, J. K.; Samdarshi, S. K.; Mukherjee, A. K. *Colloids and Surfaces B: Biointerfaces* **2011**, *86*, 7-13.
(55) Rensing, C.; Grass, G. *FEMS Microbiology Reviews* **2003**, *27*, 197-213.
(56) Koch, A. L. *Research in Microbiology* **1998**, *149*, 689-701.
(57) Vollmer, W.; Höltje, J.-V. *Current Opinion in Microbiology* **2001**, *4*, 625-633.
(58) Byrd, W.; de Lorimier, A.; Zheng, Z.-R.; Cassels, F. J. *Advanced Drug Delivery Reviews* **2005**, *57*, 1362-1380.
(59) http://melpor.hubpages.com/hub/Understanding-The-E-Coli-Bacteria.
(60) Paton, A. W.; Jennings, M. P.; Morona, R.; Wang, H.; Focareta, A.; Roddam, L. F.; Paton, J. C. *Gastroenterology* **2005**, *128*, 1219-1228.
(61) Kresse, A. U.; Guzmán, C. A.; Ebel, F. *International Journal of Medical Microbiology* **2001**, *291*, 277-285.
(62) Kenneth L, V. *Journal of Infection* **2007**, *55*, 8-18.
(63) Sawada, S.; Harada, K.; Isse, K.; Sato, Y.; Sasaki, M.; Kaizaki, Y.; Nakanuma, Y. *Pathology International* **2007**, *57*, 652-663.
(64) Chung, H.-C.; Lai, C.-H.; Lin, J.-N.; Huang, C.-K.; Liang, S.-H.; Chen, W.-F.; Shih, Y.-C.; Lin, H.-H.; Wang, J.-L. *Antimicrobial Agents and Chemotherapy* **2012**, *56*, 618-622.
(65) Bonacorsi, S. p.; Bingen, E. *International Journal of Medical Microbiology* **2005**, *295*, 373-381.
(66) Okimoto, N.; Hayashi, T.; Ishiga, M.; Nanba, F.; Kishimoto, M.; Yagi, S.; Kurihara, T.; Asaoka, N.; Tamada, S. *Journal of Infection and Chemotherapy* **2010**, *16*, 216-218.
(67) Colling, J.; Allaouchiche, B.; Floccard, B.; Pilleul, F.; Monneuse, O.; Tissot, E. *Journal of Infection* **2005**, *51*, 109-111.
(68) Fazlara, A.; Ekhtelat, M. *Journal of Agricultural and Environmental Science* **2012**, *12*, 23-29.
(69) Høiby, N. *The Netherlands Journal of Medicine* **1995**, *46*, 280-287.
(70) Schultz, M. J.; Speelman, P.; Zaat, S. A. J.; Hack, C. E.; van Deventer, S. J. H.; van der Poll, T. *FEMS Immunology and Medical Microbiology* **2000**, *29*, 227-232.

(71) Vukomanovic, D. V.; Zoutman, D. E.; Marks, G. S.; Brien, J. F.; van Loon, G. W.; Nakatsu, K. *Journal of Pharmacological and Toxicological Methods* **1996**, *36*, 97-102.
(72) http://textbookofbacteriology.net/pseudomonas.html.
(73) Schreiber, K.; Boes, N.; Eschbach, M.; Jaensch, L.; Wehland, J.; Bjarnsholt, T.; Givskov, M.; Hentzer, M.; Schobert, M. *Journal of Bacteriology* **2006**, *188*, 659-668.
(74) Iversen, B. G.; Brantsæter, A. B.; Aavitsland, P. *Journal of Infection* **2008**, *57*, 139-146.
(75) Song, Z.; Kong, K. F.; Wu, H.; Maricic, N.; Ramalingam, B.; Priestap, H.; Schneper, L.; Quirke, J. M. E.; Høiby, N.; Mathee, K. *Phytomedicine* **2010**, *17*, 1040-1046.
(76) Nakazawa, T. *Microbial Drug Resistance* **1979**, *2*, 193-195.
(77) Roy, U.; Nair, D. *Ecotoxicology* **2007**, *16*, 253-261.
(78) Bitsori, M.; Maraki, S.; Koukouraki, S.; Galanakis, E. *Journal of Urology* **2012**, *187*, 260-264.
(79) Kerr, K. G.; Snelling, A. M. *Journal of Hospital Infection* **2009**, *73*, 338-344.
(80) Kobayashi, M.; Tsuda, Y.; Yoshida, T.; Takeuchi, D.; Utsunomiya, T.; Takahashi, H.; Suzuki, F. *Current Drug Targets* **2006**, *7*, 119-134.
(81) Zavascki, A. P.; Barth, A. L.; Goldani, L. Z. *Journal of Antimicrobial Chemotherapy* **2008**, *61*, 1183-1185.
(82) Marin, A.; Monso, E.; Garcia-Nunez, M.; Sauleda, J.; Noguera, A.; Pons, J.; Agusti, A.; Morera, J. *European Respiratory Journal* **2010**, *35*, 295-302.
(83) Kim, H. W.; Kim, B. R.; Rhee, Y. H. *Carbohydrate Polymers* **2010**, *79*, 1057-1062.
(84) Pal, S.; Tak, Y. K.; Song, J. M. *Applied and Environmental Microbiology* **2007**, *73*, 1712-1720.
(85) Guzman, M. G.; Dille, J.; Godet, S. *International Journal of Chemical and Biological Engineering* **2009**, *2*, 104-111.
(86) Lok, C. N.; Ho, C. M.; Chen, R.; He, Q. Y.; Yu, W. Y.; Sun, H.; Tam, P. K. H.; Chiu, J. F.; Che, C. M. *Journal of Biological Inorganic Chemistry* **2007**, *12*, 527-534.

Chapter 6:

Future Work

6.1 Future Work

One of the main areas of the current research which we would like to develop would be the means of impregnating the beads with silver in the zero oxidation state. Generally as outlined in the thesis the beads containing silver in the zero oxidation state were not as active against the micro-organisms as those containing similar amounts of silver in the +1 oxidation state. Evidence from SEM micrographs showed that a significant component of the silver(0) contained within the beads was in the micro-domain. In addition the leachate from the beads in the zero oxidation state did not have the same effect on the micro-organisms as the silver in the +1 oxidation state. It is known that the particle size of silver(0) is important in relation to its antimicrobial activity and that high activity is achieved when the particles are between 9 nm to 62 nm.[1,2] The method employed in the current research to form beads containing silver in the zero oxidation state, was to first impregnate the beads with silver(I) ions and then reduce the silver(I) ions by reacting the beads with sodium borohydride. If the concentration of silver ions was low silver nanoparticles were formed, but there was not sufficient amount of them present to have an effect on the micro-organisms. However, as was the case for the beads studied in Chapter 4 and in Chapter 5, when the concentration of ions was high a lot of the silver(0) was in microstructures. Therefore we need to develop alternative methodologies to impregnate the composite propylene glycol alginate/alginate (PGA) beads and the composite alginate beads functionalised with 3-(trimethoxysilyl)-propyloctadecyldimethylammonium chloride (TSA) with larger amounts of silver nanoparticles which have diameters of approximately 5-20 nm.

The first study we would be interested in carrying out is to incorporate a greater amount of silver nanoparticles into the composite alginate beads, would be based on two different methodologies outlined in two studies in the literature which incorporate silver nanoparticles into an alginate containing film[3] and alginate microbeads.[4] In both cases the silver nanoparticles were characterised by UV/Vis spectroscopy and transmission electron microscopy (TEM) and were shown to have a narrow size distribution between 10-30 nm. Moreover, the film or beads so formed showed anti-bacterial properties. In the first methodology silver nanoparticles were formed by adding silver nitrate solution to an aqueous alginate solution and stirring

for 1 h at 90°C. The alginate acts as both the reducing agent and the capping agent which stabilising the nanoparticles once formed. Films were then formed by mixing the silver nanoparticle-alginate solution with different concentrations of chitosan solution and then casting films from the solutions. It should be possible to substitute the chitosan for the functionalised alginates used in the current research and then form beads by dropping the solution into a solution containing calcium chloride. In the second methodology silver nanoparticles were incorporated into alginate micro beads using an electrochemical approach. In this work the alginate was dissolved in solution containing silver nitrate and potassium nitrate (as the electrolyte). The nanoparticles were formed by electrochemical reduction and beads were then formed using electrostatic extrusion into a calcium chloride gelling solution. Again the alginate acted as a capping agent and prevented the silver nanoparticles from agglomerating. We would intend to repeat this methodology to reduce the silver(I) and then mix the silver nanoparticle-alginate solution with solutions containing either of the functionalised alginates used in the current research. Beads would then be formed using our standing method of dropping the alginate containing solution into a calcium chloride solution.

In the current research polypyrrole/alginate beads were employed as means to deliver NBPT. It would be interesting to investigate if these composite beads could be used to support silver nanoparticles to be applied in anti-microbial applications. In order to do this we would encapsulate silver ions into the alginate beads using similar procedures to those outlined in this thesis. It would be hoped that the silver ions would be able to act as oxidising agents in a similar manner to the $FeCl_3$ used in this project. The silver(I) would oxidise the pyrrole which would form a polymer layer over the beads. At the same time the silver(I) would be reduced to silver(0) which we hope would be trapped as nanoparticles within the polypyrrole matrix. This method has been used previously to form silver nanoparticles with diameters ranging from 2 nm to 50 nm, distributed evenly throughout polypyrrole/poly(styrene-co-methacrylic acid) nanocomposite particles.[5] The beads would then be tested for their anti-fungal and anti-bacterial properties.

A further study that we would be interested in carrying out would be to investigate the anti-microbial properties of silver ion impregnated bentonite-loaded calcium alginate beads. Bentonite is known to have cation exchange properties and

bentonite loaded with silver nitrate has been used as an antibacterial agent. Santos *et al.* have shown that silver ions can be incorporated into bentonite by applying an ion exchange process, and they showed that it was possible to incorporate the active bactericide properties of silver into bentonite.[6] We would try to exchange the mobile cations in bentonite for silver(I) ions and then load the bentonite into the alginate beads using similar methodologies to those used in the current research project. The beads could be then evaluated for their antibacterial properties against the five strains of bacteria and one strain of fungi tested in the current project.

6.2 References

(1) Lok, C. N.; Ho, C. M.; Chen, R.; He, Q. Y.; Yu, W. Y.; Sun, H.; Tam, P. K. H.; Chiu, J. F.; Che, C. M. *Journal of Biological Inorganic Chemistry* **2007**, *12*, 527-534.

(2) Guzman, M. G.; Dille, J.; Godet, S. *International Journal of Chemical and Biological Engineering* **2009**, *2*, 104-111.

(3) Sharma, S.; Sanpui, P.; Chattopadhyay, A.; Ghosh, S. S. *RSC Advances* **2012**, *2*, 5837-5843.

(4) Jovanovic, Z.; Stojkovska, J.; Obradovic, B.; Miskovic-Stankovic, V. *Materials Chemistry and Physics* **2012**, *133*, 182-189.

(5) Zhang, J.; Qiu, T.; Yuan, H.; Shi, W.; Li, X. *Materials Letters* **2011**, *65*, 790-792.

(6) Santos, M. F.; Oliveira, C. M.; Tachinski, C. T.; Fernandes, M. P.; Pich, C. T.; Angioletto, E.; Riella, H. G.; Fiori, M. A. *International Journal Mineral Processing* **2011**, *100*, 51-53.